FACULTY OF SCIENCE
UNIVERSITY OF COPENHAGEN

PhD thesis

Hjalte Axel Frellesvig

Generalized Unitarity Cuts and Integrand Reduction at Higher Loop Orders

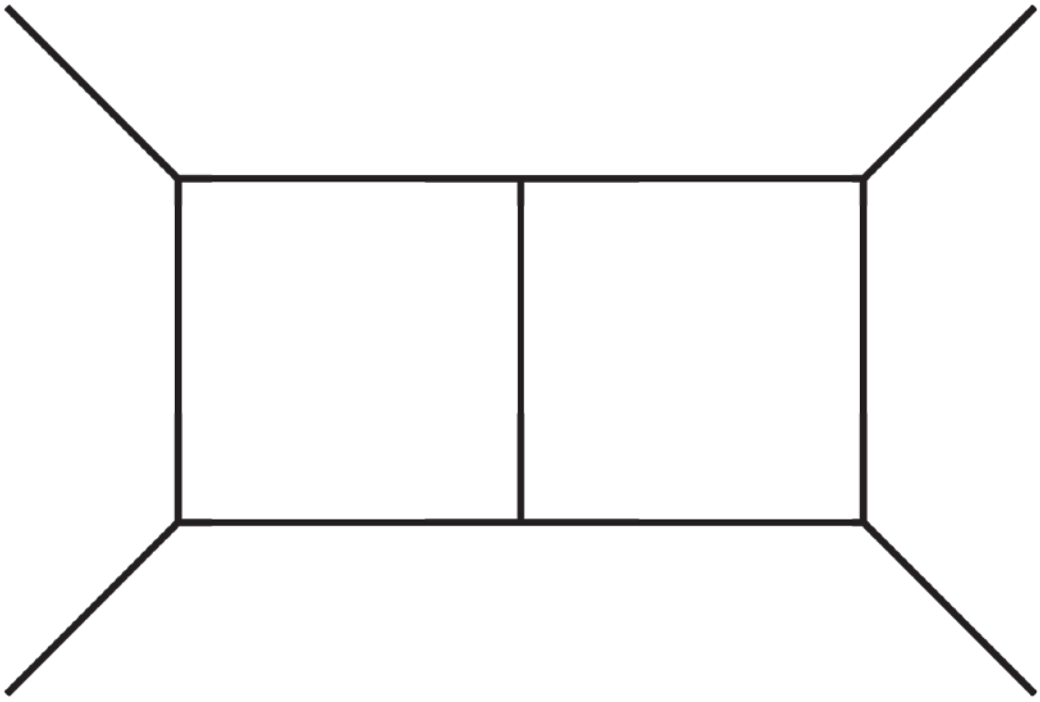

Academic advisors: Poul Henrik Damgaard and Simon David Badger

Submitted: 01/09/14

Declarations

This document is the PhD thesis of Hjalte Axel Frellesvig.

It has been submitted on the first of September 2014 in candidacy of the PhD degree, to the Niels Bohr Institute at the University of Copenhagen, and since then minor correctons of typos and formulations have been added for the online version.

It is based on the peer-reviewed articles

[1] *Hepta-Cuts of Two-Loop Scattering Amplitudes*

[2] *An Integrand Reconstruction Method for Three-Loop Amplitudes*

[3] *A Two-Loop Five-Gluon Helicity Amplitude in QCD*

and on the conference proceedings

[4] *Multi-loop Integrand Reduction with Computational Algebraic Geometry*

[5] *Multi-loop Integrand Reduction Techniques*

all by Simon Badger, Yang Zhang, and the present author.

All the text of this thesis is original.

Acknowledgements

My uttermost thanks go to my PhD advisor Simon Badger. Simon introduced me to the world of unitarity cuts and to many other aspects of amplitudes and high energy physics. Simon's door was always open, and he showed a great patience with my numerous questions which he answered with knowledge and enthusiasm. Without Simon the work presented in this thesis would not have been what it is.

I will also thank my primary advisor Poul Henrik Damgaard, whose particle physics course made me choose the path of high energy physics, a choice I have not regretted. Poul Henrik has been of great help with all administrative issues, and also as a provider of pep-talks when they were most needed.

My thanks also go to my friend and collaborator Yang Zhang. Yang's mathematical insights have been enlightening our work, and I believe that it is his kind of approach which makes physics progress.

Additional thanks go to Vittorio del Duca for hiring me for nine month in Rome. My stay at La Sapienza was a great experience which helped me expand my horizons intellectually as well as culturally.

I too am thankful to Thomas Gehrmann and the University of Zürich for hosting me for three months during the completion of parts of the work in this thesis.

My thanks also go to Johannes Henn and Vladimir Smirnov. Their extreme brilliance and knowledge has been both a help and a source of inspiration, and it is a privilege to collaborate with them.

I will also thank Donal O'Connell for discussions on the six-dimensional spinor-helicity formalism (and beer).

My thanks go to Claude Duhr, Pierpaolo Mastrolia, David Kosower, Zvi Bern, Bo Feng, Rutger Boels, Henrik Johansson, Nigel Glover, Nima Arkani-Hamed, David Gross, and many more, for providing educational talks and/or discussions.

My thanks go to my Roman friends, colleagues, and collaborators Ömer Gürdoğan, Francesco Moriello, Øyvind Almelid, Roberto Bonciani, Giuseppe Bevilacqua, and Leandro Cieri for making my stay in Rome worthwhile.

My thanks go to my fellow amplitude-PhD students at the NBI, Thomas Søndergaard, Rijun Huang, and Mads Søgaard for interesting discussions and company during long hours in the basement.

My thanks go to Tristan Dennen, Valery Yundin, Alberto Guffanti, Ricardo Monteiro, Simon Caron-Huot, Emil Bjerrum-Bohr, Florian Löbbert, Guido Macorini, Jacob Bourjaily, Ciaran Williams, Guido Festuccia, Andrew Jackson, and the rest of the people at the NBIA and in the Discovery Center, and to Kim Splittorff, Costas Zoubos, Joyce Myers, Niels Obers, Charlotte Kristjansen, Jan Ambjørn, Holger Bech Nielsen and the rest of the theory group, for all being exemplary physicists.

My thanks go to Helle Kiilerich, Anna Maria Rey, and Björn Nilsson for helping me ease the administrative burdens.

My thanks go to my fellow PhD students Pawel Caputa, Sabir Ramazanov, Christine Hartmann, Laura Jenniches, Lisa Glaser, Jakob Gath, Agnese Bissi, Andreas Vigand, Anne Mette Frejsel, Ara Martirosyan, Asger Ipsen, Alexander Karlberg, Jeppe Trøst Nielsen, and anyone else I might have forgot, for sharing this journey with me.

My thanks go to Costas Papadopoulos, NCSR Demokritos, and the HiggsTools Network for hiring me, allowing me to continue my career under warmer skies.

I also want to thank my friends and family for showing interest and support for my work, and for giving me the diversions necessary to keep my spirits up.

Finally I will thank my parents Lise Brüel and Kjeld Frellesvig. They have provided me all kinds of support and help during my studies and throughout my life, including a read-through of this thesis in its unfinished stages. It is true in the most literal sense, that had it not been for them I would not have been where I am today.

Summary

The huge amounts of data on particle scattering which have been collected by the LHC in the recent years, has enabled the investigation of interactions and other effects which so far have been too minuscule to be observed. A perfect example of this is the recent discovery of the Higgs particle.

The large amount of background to such processes has caused an ever increasing need for precise predictions by the fundamental theory. For most collision processes the leading contribution comes from QCD, the theory of the strong interactions, which is the main focus of this thesis. In practice the required precision corresponds to the next to next to leading order in the perturbative expansion of the cross section, which requires the calculation of Feynman diagrams with two or more loops.

For one-loop diagrams the corresponding problem has been solved to the extent that almost all one-loop amplitudes of physical interest are known, and their calculation automated. This is mainly due to the technique of generalized unitarity cuts combined with integrand reduction into what is known as the OPP method. This method is sufficiently easy and fast that the one-loop contributions can be incorporated into event-generation software on equal footing with the tree contributions.

More specifically, the OPP method calculates individually each topology in the expansion given by the integrand reduction. First it calculates the topologies with the most propagators, and when they are known one may calculate the lower topologies using the higher ones as subtraction terms. Combined with specialized methods to find the rational term, the OPP method provides a complete procedure for finding the one-loop corrections to any amplitude.

In this thesis we will develop a method to extend the OPP method to two loops and beyond. It is based on a categorization of the integrand using algebraic geometry, in which the set of propagators corresponding to each topology is identified with an algebraic ideal I. This allows for the identification of the set of terms which are allowed in the numerator corresponding to each topology, with those of the members of the quotient ring R/I which lives up to a set of renormalization constraints. The method works in both four and d space-time dimensions.

We start the thesis with an introduction to QCD, amplitudes, and unitarity cuts. Then we do a number of four-dimensional examples of our form of the OPP method in the context of the process $gg \to gg$. We calculate the one-loop contribution in significant detail, the three two-loop, seven-propagator topologies called the double-box, the crossed box, and the pentagon-triangle, and finally we calculate the triple-box three-loop topology. We also take a brief look at another three-loop topology, the tennis court.

By the additional calculation of a number of six-propagator two-loop topologies, we illustrate two problems with our method in its four-dimensional version. The first is *the minor problem* in which a unitarity cut solutions for a topology coincide with a cut solution for one of its parent topologies causing infinities to appear in the calculation. The other is denoted *the major problem*, and is characterized by the existence of terms which vanish on the cut without being a sum of terms

proportional to products of the propagators. These terms may be identified with members of $\sqrt{I}/I$.

It turns out that both of these problems can be solved by going to d dimensions. We illustrate the d-dimensional method by repeating part of the one-loop $gg \to gg$ calculation, showing how the higher dimensional contributions give rise to the rational term of the amplitude.

For doing d-dimensional two-loop calculations, we describe how to embed the higher-dimensional parts of the loop-momenta, denoted ρ-parameters, into two extra dimensions, and we describe how to do calculations in these dimensions using the six-dimensional spinor-helicity formalism. As an example we calculate the planar two-loop contribution to $gg \to gg$ for the case where all external gluons have the same helicity, and we get agreement with the known result.

The main calculation of this thesis is that of the planar part of $gg \to ggg$ for the mentioned helicity configuration. There are eight topologies contributing to the amplitude and we find that the result agrees with numerical checks. We find a curious relation between the result and the MHV result for $\mathcal{N} = 4$ SYM, similar to a known relation at one-loop. We also calculate a few non-planar contributions to the amplitude.

We end the thesis by comparing the method to a number of alternative methods proposed by other groups, and by a number of appendices. Primary among the appendices are a detailed introduction to the six-dimensional spinor-helicity formalism, and a derivation of the method used to perform integrals over the higher dimensional ρ-parameters.

Resumé

De enorme mængder partikelspredningsdata, som er blevet indsamlet af LHC i de senest år, har muliggjort udforskningen af vekselvirkninger og andre effekter, der indtil nu har været for små til at kunne ses. Et perfekt eksempel på dette er den nylige opdagelse af Higgspartiklen.

Den store mængde baggrund til sådanne processer gør, at behovet for præcise forudsigelser fra den fundamentale teori bestandigt vokser. For de fleste kollisionsprocesser vil det dominerende bidrag komme fra QCD, teorien om de stærke vekselvirkninger, som er det primære fokus for denne afhandling. I praksis svarer den nødvendige præcision til tredjelaveste orden i den perturbative udvikling af spredningstværsnittet, hvilket kræver en udregning af Feynmandiagrammer med to eller flere loops.

For enkeltloopdiagrammer er det tilsvarende problem blevet løst i en sådan grad, at så godt som alle enkeltloopamplituder af fysisk interesse er kendte, og udregningen af disse er blevet automatiseret. Dette skyldes primært den generaliserede unitaritetssnitsteknik, som kombineret med integrandreduktion giver, hvad der kendes som OPP-metoden. Denne metode er tilpas hurtig og let at automatisere, til at enkeltloopbidrag kan inkorporeres i eventgenereringssoftware på lige fod med træniveaubidragene.

Mere specifikt så udregner OPP-metoden hver enkelt topologi i den ekspansion, der fås fra integrandreduktionen. Først udregner den de topologier, der har de fleste propagatorer, og når de er kendte, kan man udregne de lavere topologier ved at bruge de højere som subtraktionsled. Kombineret med specifikke metoder til at finde det rationelle bidrag, giver OPP-metoden en komplet procedure til at finde enkeltloopbidragene til en vilkårlig amplitude.

I denne afhandling vil vi udvikle en metode der generaliserer OPP-metoden til to og flere loops. Den er baseret på en kategorisering af integranden ved hjælp af algebraisk geometri, idet mængden af propagatorer bliver identificeret med et algebraisk ideal I for hver enkelt topologi. Dette muliggør en identifikation af det sæt led, som er tilladt i tælleren for den enkelte topologi, med de elementer af kvotientringen R/I, som opfylder et sæt renormaliseringsbetingelser. Metoden virker både for fire og d rumtidsdimensioner.

Vi starter afhandlingen med en introduktion til QCD, amplituder og unitaritetssnit. Dernæst vil vi gennemgå et antal eksempler for vores udgave af OPP-metoden illustreret ved processen $gg \to gg$. Vi udregner enkeltloopbidraget i nogen detalje, de tre syvpropagatortopologier for treloopbidraget kaldet dobbeltboksen, krydsboksen, og femkantstrekanten, og tilslut udregner vi trelooptopologien tripelboksen. Vi tager også et hurtigt kik på en anden trelooptopologi, tennisbanen.

Ved den yderligere udregning af et antal tolooptopologier med seks propagatorer, illustrerer vi to problemer med vor metode i dens firdimensionale udgave. Det første er *det mindre problem* i hvilket en unitaritetssnitløsning for en topologi sammenfalder med en snitløsning for en modertopologi, hvilket får uendeligheder til at dukke op i udregningen. Det andet kalder vi *det større problem*, og det er

karakteriseret ved eksistensen af led, som forvinder efter snittet uden at være en sum af led proportionale med produkter af propagatorer. Disse led kan identificeres med elementer i $\sqrt{I}/I$.

Det viser sig, at begge disse problemer kan løses ved at gå til d dimensioner. Vi illustrerer den d-dimensionale metode ved at gentage dele af enkeltloopudregningen for $gg \to gg$, hvilket viser hvorledes de højeredimensionale dele tilsvarer det rationelle bidrag.

Med de d-dimensionale toloopudregninger for øje, viser vi, hvordan man kan indeslutte de højeredimensionale dele af loopimpulserne, kaldet ρ-parametre, i to ekstra dimensioner, og vi beskriver, hvordan man kan lave udregninger i disse dimensioner ved hjælp af den seksdimensionale spinorhelicitetsformalisme. Som et eksempel udregner vi toloopbidraget til $gg \to gg$ for det tilfælde, hvor alle de eksterne gluoner har den samme helicitet, og vi finder overensstemmelse med det kendte resultat.

Den primære udregning i afhandlingen er for den planære del af processen $gg \to ggg$ i den ovennævnte helicitetskonfiguration. Der er otte topologier der bidrager, og vi finder, at resultatet passer med numeriske beregninger. Vi finder en spøjs relation mellem vores resultat og MHV-resultatet for $\mathcal{N} = 4$ SYM, som svarer til en kendt enkeltlooprelation. Vi udregner også et par ikke-planære bidrag

Vi slutter afhandlingen med at sammenligne metoden med alternative metoder, fremlagt af andre forskningsgrupper, og med et antal appendices af hvilke de primære indeholder en detaljeret introduktion til den seksdimensionale spinorhelicitetsformalisme og en udledning af den metode, vi benytter til at beregne integraler over de højeredimensionale ρ-parametre.

Contents

Chapter 1

Introduction

Ever since the dawn of civilization, mankind has shown an interest in understanding and explaining the phenomena of nature. The philosophical tradition arising out of ancient Greece, is perhaps the first of the attempts at systematizing the inquiries of nature which have survived to this day. The axiomatic geometry of Euclid is a precedent of modern mathematics, and the theory of the classical elements[1] which was accepted and developed by philosophers such as Aristotle, survived all the way into the middle ages.

Theories such as that of the four elements may be seen as attempts at describing all phenomena in terms of the behaviour of a few "ontologically basic" substances. The atoms of the early atomic theory is a newer example of such a theory, and so is the Standard Model of particle physics which, to the best our current knowledge, in principle describes the behaviour of everything in our universe, with the exception[2] of gravity.

As the inquiry of nature moved from the realm of philosophy to the realm of science, the mathematical complexity of the theories grew. The Greek philosopher Pythagoras whose candidate "ontologically basic substance" was "mathematics", did in a sense turn out to be right, as no serious proposals for new physical theories are formulated in a language other than the mathematical. The Standard Model of particle physics is described using group theory, Hilbert spaces, non-Euclidean geometry, and complex analysis, mathematical tools and concepts which were unknown 200 years ago.

What is perhaps the main result of this thesis is given by eq. (12.33) on page 110, and admittedly that result is rather far from anything a philosopher like Aristotle would have acknowledged as describing nature in any way. In a sense this is perhaps regrettable, but it is more than justified by the fact that where the theories of Aristotle and his contemporaries were of a purely qualitative nature, the current theories describe nature quantitatively, in the best cases with the deviation between theory end experiment being less than a factor of 10^{-9}.

[1] In the Greek and western tradition, these are the four elements fire, air, water, and earth, with a fifth, the aether, occasionally added to explain the heavenly bodies.

[2] And also with the exception of dark matter, dark energy, massive neutrinos, baryogenesis, etc.

Thus the remainder of this thesis will be written in the language of modern physics, with little further mention of Greek philosophers.

The Standard Model of particle physics describes everything in nature as made of quantized fields interacting under the gauge group

$$SU(3) \times SU(2) \times U(1) \tag{1.1}$$

with the $SU(2) \times U(1)$-part being broken by the Higgs mechanism. The focus of this thesis will be on the $SU(3)$-part, which in its physical realization is denoted quantum chromo dynamics, or QCD.

QCD is the theory of the strong nuclear interactions which is one of four fundamental forces of nature, alongside electromagnetism, the weak nuclear interactions, and gravity. It is responsible for keeping the nucleons and the nuclei stable, so matter as we know it could not exist without the strong force.

As the the name suggests, the strong nuclear interaction is by far the strongest of the four fundamental forces, so when doing a scattering experiment with particles that interact strongly, as it happens in the LHC, it is QCD which is responsible for the dominant contributions. If the goal of the experiment is to investigate another part of the standard model, like the Higgs couplings or the weak sector, or perhaps to search for new physics like supersymmetry, QCD contributions will make a background to the signal of the process which will have to be subtracted rather precisely in other to see the potential new signal.

The LHC which has been running since 2008, has been collecting huge amounts of data with immense precision. The primary result of this so far, has been the discovery of the Higgs boson in 2012 [6], which until then was the only unobserved particle predicted by the standard model. The amount of data is high enough to allow the discovery of effects small enough to make the second-order corrections to the QCD amplitudes necessary for a proper background subtraction. Second order corrections to an amplitude will have contributions from Feynman diagrams containing two (and in some cases more) loops, and the main purpose of this thesis is the development of a method to perform (parts of) the calculation of such higher loop contributions.

At one-loop the corresponding problem has not only been solved, but solved in a way that allows for fast, numerical calculations of the involved amplitudes. Most of these numerical implementations have been done using generalized unitarity cuts [7–13], and it is that fact which inspires the attempts made in this thesis and elsewhere [14–16] to extend the generalized unitarity-cut method, and for this thesis specifically the OPP method of [9], to two loops and beyond.

Another motivation for the work done in this thesis, is that innumerable structures, some of which are rather unexpected from a traditional Feynman-diagrammatic point of view, have been uncovered in scattering amplitudes during the recent two decades. Most of these structures are to be found in unphysical theories like $\mathcal{N} = 4$ SYM [17–22], but also in QCD have such structures been appearing [23–27]. In

order to discover and to check such relations, and perhaps to cast some further light on their origin, it is convenient with a large "data-set" of known amplitudes. It is the hope that the calculations described in the present document will provide a few extra data-points to this set, and that the methods developed will help with further discoveries in the future.

So to summarize: The goal of this thesis is to derive an extension and generalization of the OPP method which is applicable to higher-loop cases, and to use it to derive a number of new results for such higher-loop topologies, with the hope that both the method and the specific results will be of interest for future experimentalist and theorists alike.

1.1 Notation

In this thesis, we will use the standard QFT unit convention which has $\hbar = c = 1$ such that the units of any quantity is some power of the unit of momentum. We will use the "mostly negative" space-time metric such that

$$g^{\mu\nu} = \text{diag}(1, -1, -1, \ldots) \tag{1.2}$$

For momenta we will denote external momenta as p_i^μ, loop-momenta as k_i^μ, and propagating momenta as l_i^μ. The Feynman slash-notation $\not{p}$ will denote contractions with the gamma-matrices or with the Pauli matrices depending on context.

Our spinor-helicity convention is such that

$$\langle ij\rangle[ji] \;=\; (p_i + p_j)^2 \;=\; s_{ij} \tag{1.3}$$

and for further details on the spinor-helicity, see section 3.2 or appendix A. We will also encounter a six-dimensional version of the spinor-helicity formalism, and for that case the conventions are listed in section 11.2 and in appendix B.

For four-point kinematics we will use the traditional names for the Mandelstam parameters defined as

$$s = (p_1 + p_2)^2 \qquad t = (p_1 + p_4)^2 \qquad u = (p_1 + p_3)^2 \tag{1.4}$$

in the case where all the momenta are out-going, which is our main convention in this thesis.

For five-point kinematics we will mainly use the cyclic Mandelstam variables $s_{i,i+1} = (p_1 + p_{i+1})^2$, and additionally we will encounter the quantity tr_5 defined as

$$\begin{aligned}\text{tr}_5 &\equiv \text{tr}(\gamma_5 \not{p}_1 \not{p}_2 \not{p}_3 \not{p}_4) \\ &= -4i\varepsilon_{\mu_1\mu_2\mu_3\mu_4} p_1^{\mu_1} p_2^{\mu_2} p_3^{\mu_3} p_4^{\mu_4} \\ &= [12]\langle 23\rangle[34]\langle 41\rangle - \langle 12\rangle[23]\langle 34\rangle[41]\end{aligned} \tag{1.5}$$

and the related quantities $\mathrm{tr}_\pm(abcd)$ defined as

$$\begin{aligned}\mathrm{tr}_+(abcd) &\equiv \tfrac{1}{2}\mathrm{tr}\big((1+\gamma_5)\not{p}_a\not{p}_b\not{p}_c\not{p}_d\big)\\ &= [ab]\langle bc\rangle[cd]\langle da\rangle\\ \mathrm{tr}_-(abcd) &\equiv \tfrac{1}{2}\mathrm{tr}\big((1-\gamma_5)\not{p}_a\not{p}_b\not{p}_c\not{p}_d\big)\\ &= \langle ab\rangle[bc]\langle cd\rangle[da]\end{aligned} \tag{1.6}$$

For more discussion of such kinematical quantities, see appendix C.1.

The colour-algebraic conventions are given by eqs. (3.2) and (3.3), but note that these convention are not followed in chapter 2.

Scattering amplitudes are denoted A, partial amplitudes $\mathcal{A}$, and primitive amplitudes $A^{[P]}$. Loop-level quantities are denoted with the number of loops in brackets, i.e. $A^{(2)}$, while the number of dimensions is in a square bracket, i.e. $A^{[4]}$.

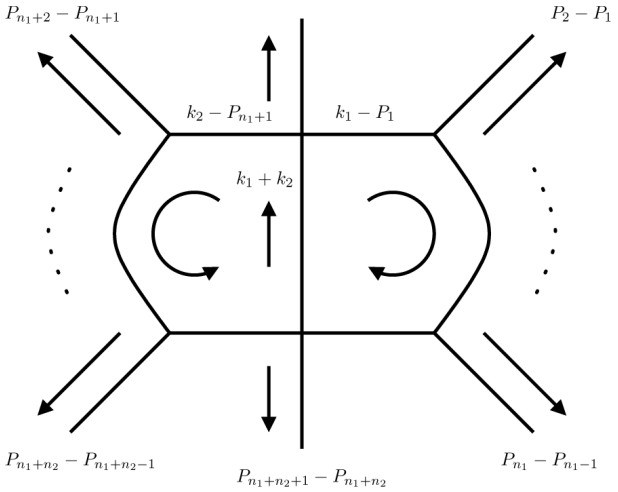

Figure 1.1: This figure shows a two-loop topology which would be referred to as $(tn_1n_21;\mathcal{P})$.

In this thesis we will encounter a number of two-loop topologies. To name them we will use a semi-systematic[3] notation in which a two-loop topology will be denoted $(tabc;\mathcal{P})$. Here t is an actual t and is short for "topology", the a, b, and c denotes the number of propagators along the three branches of the topology, and the $\mathcal{P}$ denotes any additional labels necessary to identify the topology which will be determined on a case-by-case basis and left out when superfluous. For a general planar example, see fig. 1.1.

If a topology y corresponds to a set of propagators which is a subset of the propagators for another topology x, y will be denoted a daughter topology of x, while x is a parent topology of y.

[3]It is possible to define a completely systematic notation at the cost of clarity, see [1].

1.2 Structure

The structure of this thesis is as follows:

In chapter 2 we will take a look at the theory of QCD, including the formal definition of the theory, properties such as asymptotic freedom and confinement, and a description of how to relate the theory to experimental results.

In chapter 3 we will describe scattering amplitudes, discussing Feynman diagrams, colour ordering, the spinor-helicity formalism, and Feynman rules. We will also take a look at some n-point tree-level amplitudes, and discuss their mutual relations including the BCFW recursion relation. At the end of the chapter we will discuss the amplitudes of theories other than QCD, such as QED and $\mathcal{N} = 4$ SYM.

In chapter 4 we will describe loop-level properties and effects. First we will describe the issues of regularization, renormalization, and infrared divergences. Then we we will discuss integrand reduction and evaluation of Feynman integrals using Feynman-parameters, IBP identities, and differential equations. In the last sections we will introduce the ideas of unitarity, generalized unitarity cuts and the OPP method, which we in this thesis will try to extend to multi-loop cases.

In chapter 5 we will do a one-loop example of (our approach to) the OPP method, illustrated by the process $gg \to gg$ in pure four dimensions. We will do the complete calculation of the box-coefficients for arbitrary helicities and particle content, and sketch the corresponding calculation for the triangles and the bubbles.

In chapter 6, which is based on [1], we will present the first real results, a calculation of the four-dimensional part of the three seven-propagator topologies contributing to $gg \to gg$ at two-loops. These are the double-box ($t331$), the crossed box ($t322$), and the pentagon-triangle ($t421$). We will also discuss some simplifications that occur for supersymmetric theories.

In chapter 7 we will, based on [2], calculate the three-loop triple-box contribution to $gg \to gg$ to illustrate that our method is not limited to two-loop. We will also show that our method is applicable to another three-loop topology, the tennis-court.

In chapter 8 we will discuss three four-dimensional six-propagator two-loop topologies, the three box-triangles ($t321; \mathcal{P}$). The purpose of this is to expose two problems with the four-dimensional version of our method: *the minor problem* which occurs whenever a cut-solution for a topology is identical to a cut-solution of a parent diagram of the topology, and *the major problem* which occurs whenever a part of the irreducible numerator for a topology cannot be found from generalized unitarity cuts.

In chapter 9 we will discuss the central role of algebraic geometry in the method developed in this thesis, including the use of Gröbner bases and multivariate polynomial division to find the irreducible numerator, and the use of primary decomposition to identify the individual cut solutions. We will look at both the four-dimensional and the d-dimensional case, and show that both the minor and the major problem gets solved by going to d dimensions.

In chapter 10 we will take another look at the one-loop contribution to $gg \to gg$, but this time with the full dimensional dependence. We show how to embed the

extra-dimensional momenta in a fifth dimension, and show how to regulate the polarizations of internal gluons using a scalar loop.

In chapter 11, which is based on the first half of [3], we take a look at the behaviour of two-loop amplitudes in d dimensions. We show how the extra-dimensional loop-momenta can be embedded in two extra dimensions, and we introduce the six-dimensional spinor-helicity formalism which may be used to perform calculations for such embeddings. As an example we look at the $gg \to gg$ process for the case where all the external particles have helicity plus.

In chapter 12, which is based on the second half of [3], we calculate the planar two-loop contribution to $gg \to ggg$ in pure Yang-Mills theory, for the case where all the external particles have helicity plus. Eight different topologies contribute to the process, and we find a curious relation...

In chapter 13, which is based on results from [5], we calculate two non-planar contributions to $gg \to ggg$.

In chapter 14 we sum up and conclude the thesis, and attempt to outline some directions this line of work could take in the future.

We end the thesis by a number of appendices:

In appendix A we derive and list our conventions for the four-dimensional spinor-helicity formalism in detail.

In appendix B we derive and list our conventions for the six-dimensional spinor-helicity formalism. We derive expressions for spinors for six-dimensional space-time and we show how to use them to form spinor-products, vector-products, and polarization vectors as it is done in four dimensions. We also show how to relate a set of six-dimensional spinors to two four-dimensional ones. We end the appendix by listing the gluonic three-point amplitudes in six dimensions.

In appendix C we discuss how to parametrize results for amplitudes with different kinds of kinematics, either using Mandelstam variables and epsilon contractions, or using momentum twistor variables.

In appendix D we discuss how to evaluate Feynman integrals which are a function of the higher-dimensional ρ-variables. We first introduce the concept of Schwinger parameters, and then show how to use them to evaluate the ρ-integrals by relating them to integrals in higher dimensions. We go through cases at both one and two loops.

In appendix E we list and explain a number of concepts from algebraic geometry, and provide examples of their use.

In appendix F we collect a number of minor appendices. One on flattened vectors, one on spurious vectors, one on spurious integrals, one on discrete Fourier sums, and one on PLU decomposition.

In appendix G we list a number of (one-loop) Feynman integrals which are of frequent use in this thesis. We list the general expressions, and their ϵ-expansions in four, six, and eight dimensions.

In appendix H we list the Feynman rules for SYM theories which we use in this thesis.

Chapter 2

QCD

QCD is defined as a Yang-Mills theory with gauge group $SU(3)$ coupling to six massive quarks, denoted down, up, strange, charm, bottom, and top, and their corresponding anti-quarks. The properties of the quarks are are

symbol	charge	mass
d	$(-1/3)e$	4.9 MeV
s	$(-1/3)e$	100 MeV
b	$(-1/3)e$	4200 MeV

symbol	charge	mass
u	$(2/3)e$	2.4 MeV
c	$(2/3)e$	1290 MeV
t	$(2/3)e$	173000 MeV

where the masses have been listed as their central value only. Additionally does the gauge-group give each of the quarks an extra quantum number called "colour" which can take values from one to three, thereby metaphorically corresponding to the primary colours red, green, and blue. The anti-quarks have a corresponding anti-colour[1]. The particles carrying the colour-force are denoted gluons, and they too are coloured, with one colour and one anti-colour[2]. The coloured particles, i.e. the quarks and the gluons, are collectively known as partons.

Observable particles do never have a colour, they can only be colour neutral, or "white", so the partons can only appear in colour neutral combinations, called hadrons. Two types of hadrons are by far the most common. These are the mesons, which can be obtained from combining a quark and an anti-quark, and the (anti)baryons, which are formed from three (anti)quarks, one in each (anti)colour. The proton, which is the particle type collided at the LHC, is a baryon made of two up-quarks and a down-quark.

2.1 The theory of QCD

QCD is defined by the Lagrangian density

$$\mathcal{L} = -\frac{1}{4}F_a^{\mu\nu}F_{a\mu\nu} + \bar{\psi}\big(i\not{D} - m\big)\psi \tag{2.1}$$

[1] The anti-colours are often illustrated as cyan, magenta, and yellow.

[2] One might imagine that this would lead to nine different gluons. In fact there are only eight, due to the S in the $SU(3)$ gauge group. See any introduction to QCD, such as [28,29].

where the first term describes the Yang-Mills theory, and the second term contains the interaction with the quark fields ψ and $\bar{\psi}$. The flavour, colour, and spinor indices for the quarks have been suppressed. D^μ is the covariant derivative

$$D^\mu \equiv \partial^\mu - ig_s A_a^\mu T_a \tag{2.2}$$

and $F_a^{\mu\nu}$ is the field strength tensor

$$F_a^{\mu\nu} \equiv \partial^\mu A_a^\nu - \partial^\nu A_a^\mu + g_s f_{abc} A_b^\mu A_c^\nu \tag{2.3}$$

which both are given in terms of the gauge field (or gluon field) A_a^μ.

Even though QCD has the gauge group $SU(3)$, we will in all of the following work with $SU(N_c)$, with N_c as a free variable. The gauge group makes its appearance through the generators T_a, as a general member of the gauge-group can may be written as an exponentiation of the generators as

$$U(x) = \exp\left(iT_a\phi_a(x)\right) \tag{2.4}$$

where the a-indices are known as adjoint indices and run from 1 to $N_c^2 - 1$ which is the number of generators of the gauge group. The colour index of the quarks is a fundamental index, and it runs from 1 to N_c. The structure constants f_{abc} which are defining for the algebra of the group are related to the generators, the relation being

$$[T_a, T_b] = if_{abc}T_c \tag{2.5}$$

A general gauge-transformation works on the fields as

$$\psi \to U\psi \qquad \bar{\psi} \to \bar{\psi}U^{-1} \qquad A^\mu \to U\left(A^\mu - \frac{i}{g_s}U^{-1}\partial^\mu U\right)U^{-1} \tag{2.6}$$

where $A^\mu \equiv A_a^\mu T_a$, and we see[3] that this transformation leaves the Lagrangian of eq. (2.1) invariant, thus justifying the name gauge theory.

2.2 Regimes of QCD

There are no known, exact, analytical solutions for the eigenstates of QCD or Yang-Mills theory. One approach to finding approximate solutions is perturbation theory, in which one finds the exact solution for the free theory (with $g_s = 0$), and then treats the full theory as a perturbation around the free state. This approach will yield valid solutions if $g_s \ll 1$, or rather if $\alpha_s \ll 1$ where

$$\alpha_s \equiv \frac{g_s^2}{4\pi} \tag{2.7}$$

[3]To see this, it is helpful to use that the first term in the Lagrangian may be written as $-\frac{1}{2}\mathrm{tr}(F^{\mu\nu}F_{\mu\nu})$.

But is that inequality true? It turns out that quantum effects makes the physical value of α_s dependent on the characteristic energy scale for the process μ through the beta function

$$\beta(\alpha_s) \equiv \frac{d\alpha_s}{d\log(\mu^2)} \tag{2.8}$$

where the beta function for QCD may be calculated[4] to

$$\beta(\alpha_s) = -\frac{1}{3}\Big(11N_c - 2n_q\Big)\frac{\alpha_s^2}{2\pi} + \mathcal{O}(\alpha_s^3) \tag{2.9}$$

where n_q is the number of quarks in the theory.

As β is negative, we realize that the solution for $\alpha_s(\mu)$ is a decreasing function that asymptotically will go to zero as the energy scale goes to infinity, an effect known as asymptotic freedom. This effect makes the perturbative approach more and more correct in that limit. The critical energy scale below which the perturbative approach no longer yields useful results, is that for which $\alpha_s(\mu) \approx 1$. That value is denoted Λ_{QCD} and has the value of approximately 250MeV [30]. This value may be compared with the energy scales of current particle physics experiments which go into the TeV regime corresponding to $\alpha_s < 0.1$, so we see that the perturbative approach is justified for our use.

In the other regime where $\mu \ll \Lambda_{\text{QCD}}$ we find that free quarks and gluons are by no means a good approximation, and it is also here we find the quarks and gluons bound inside hadrons like protons, neutrons, and pions, and the nucleons bound in nuclei. This tendency for the coloured particles to bind together to form colourless states is known as confinement[5].

In the rest of this thesis we will work solely within the perturbative approach in the high energy regime. We will go on to describe the details of the perturbative approach in higher detail, but let us first make an attempt to connect the rather abstract theory described by eq. (2.1) with the experimental reality.

2.3 Measurements in QCD

As we have seen, is an experimentalist going to encounter the gluonic and fermionic fields of eq. (2.1) as quantized particles known as gluons and quarks. The way to

[4]This expression is the result of the one-loop calculation only. Each extra loop-order will give another term in the α_s expansion.

[5]There is no method as elegant and systematic as perturbative QCD to describe the confined regime, but it is still worth to take an ultra-brief look at some of the methods one might use in that case. One is the flux-tube model in which one regards the individual particles as bound by strings, called flux-tubes, where it is the tension in those strings that keeps the partons bound. Another is lattice-QCD in which one performs calculations on a lattice of a theory described by a discretized version of the Lagrangian of eq. (2.1), in a way that allows for a consistent continuum limit at the end of the calculation. A third method is the ADS/CFT correspondence in which one utilizes the duality between certain quantum field theories in the weak coupling limit, and certain gravitational theories in the strong coupling limit which may be solved approximately using methods developed for the study of black holes.

investigate the behaviour of these particles is to make them interact with each other and study the results of the interactions. In practice this is done by colliding the particles at high energies and observe the results in a detector. Due to the probabilistic nature of quantum theories, repeating an experiment is not guarantied to repeat the result, the correct quantum mechanical description assigns a probability $\mathcal{P}$ to each final state $|f\rangle$ given an initial state $|i\rangle$, that is

$$\mathcal{P} = |\langle f|\mathcal{S}|i\rangle|^2 \tag{2.10}$$

where the matrix $\mathcal{S}$, known as the S-matrix, describes the spatiotemporal evolution between the states[6]. As the by far most common result of a scattering experiment is $|f\rangle = |i\rangle$, we chose to write the S-matrix as

$$\mathcal{S} = I + i\mathcal{T} \tag{2.11}$$

where $\mathcal{T}$, known as the T-matrix, contains all the interactions. Each state is characterized by its quantum numbers such as the flavour, colour, helicity, and momentum of the involved particles. As the momenta are continuous, the probabilities of eq. (2.10) are best described as a distribution

$$P(\{\bar{p}_f\}) = \frac{1}{\prod_f (2E_f)}(2\pi)^4 \delta^{[4]}\Big(p_1 + p_2 - \sum_f p_f\Big)|A(p_1, \ldots, p_n)|^2 \tag{2.12}$$

of the (three-)momenta of the final states, with the momenta of the initial states being fixed. E_f denotes the energies of the states. The quantity A is the scattering amplitude, which is defined as

$$A \equiv \langle p_{f1}, \ldots, p_{fn}|i\mathcal{T}|p_{i1}, \ldots, p_{in}\rangle \tag{2.13}$$

- an object of such importance that most of the remainder of this thesis will be devoted to (a part of) their calculation.

Often a description in terms of a cross section σ, defined as the effective target area corresponding to the probability distribution for a classical scattering process, is preferred. An expression for σ may be derived from eq. (2.12), see for instance [28] for many more details.

Naively one might hope that eq. (2.12) was the end of the story, and that accurate and frequent enough measurements would enable one to deduce the particle distribution, calculate (the square of) the amplitude using (2.12), and compare this with the theoretical prediction. But nature is not that kind, at least not for the case of QCD. The scattering one may investigate using the basic theory for the elementary partons, is called the hard scattering. But due to the colour-confinement neither the particles which are collided, nor the ones that are measured, are partons, rather

[6] In non-relativistic quantum mechanics it would be given as $\mathcal{S} = \exp(-iHt)$.

the collided particles (at the LHC) are protons, and the measured ones may be any hadron[7] with a life-time long enough to reach the detector.

Let us start by investigating the initial state. A proton is usually said to be made of two up-quarks and a down-quark bound together by gluons, but for high energy protons, quantum fluctuations may create anti-quarks or higher generational quarks complicating the picture further. Which fraction of the total momentum of the proton is carried by which of the individual constituents is indeterministic, and described by a function called the parton distribution function (or PDF). It is necessary to know this distribution to be able to deduce the (squared) scattering amplitude from an experiment, but as the interior of the proton is beyond the perturbative regime, the PDFs have to be calculated using a non-perturbative approach, usually combined with a fit to experimental data.

In the final state matters are just as involved. As the final state (off-shell) partons move away from the interaction point they will begin a process of parton showering whereby each parton will "branch", creating a large number of gluons and quark-antiquark pairs in its wake. This happens due to the colour-force between the partons, which makes it energetically favourable to form such particle-pairs out of the vacuum. In principle there is no physical distinction between the hard scattering process and the showering process, the separation is made due to calculational convenience. Eventually the showering partons will bind together to form the hadrons that are observed in the detector - a process known as hadronization. The hadrons will come in clusters corresponding to the initial hard partons, these clusters are known as jets. The parton showering is usually treated using statistical Monte Carlo methods, and the hadronization takes place outside the regime and has to be treated accordingly.

All of these issues, along with imprecisions in the detectors, statistical uncertainties in the data sampling, and several other issues [29], lie between the experimental observables and the hard scattering process. With this in mind we will ignore these issues completely in the following, were we will investigate the central mathematical object of the hard process, the scattering amplitude.

[7] This is in QCD only. In general one may also measure leptons, photons, etc.

Chapter 3

Amplitudes

In this chapter we will develop the basic theory for scattering amplitudes and mention some more advanced developments.

3.1 Feynman diagrams and colour ordering

From a careful quantization[1] of the theory given by the Lagrangian of eq. (2.1), or indeed of any quantum field theory, one arrives at the surprising result that any scattering amplitude may be written as a sum of objects known as Feynman diagrams

$$A(p_1, \ldots, p_n) = \sum_{\text{order}} \sum_{\text{graphs}} \text{diagram}(\text{order}, \text{graph}, p_1, \ldots, p_n) \tag{3.1}$$

where 'order', refers to the order in the perturbative expansion in the coupling constant. Each order has a number of contributions known as Feynman graphs, so called as they correspond exactly to the different connected graphs one may draw which join the initial and the final particles. The vertices of the graphs describe the interactions of the theory, and expanding eq. (2.1) will give three kinds of interaction terms[2], terms with three gluonic fields, a term with four gluonic field, and a term with a gluonic field along with a quark and an antiquark. This corresponds exactly to the three kinds of vertices allowed by the Feynman rules of QCD: a three-point gluon vertex, a four-point gluon vertex, and a $\bar{q}gq$ vertex. Each order corresponds to a number of loops in the graphs. The lowest order[3] has zero loops, and is therefore denoted tree-level, the next order has one loop, the next two, etc.

Eq. (3.1) made no mention of which of the external particles were in the initial, and which the final state. That is because of a property called "crossing symmetry" which relates the amplitude of a configuration which has a particle with momentum

[1] See [28] or any other book on quantum field theories.

[2] that is terms with at least one power of the interaction constant.

[3] Usually one uses a convention in which lowest order means lowest non-zero order, making this statement false in cases where the tree-diagrams vanish.

p in the initial state, to the amplitude of the configuration in which the same particle is in the final state with momentum $-p$. For this reason we will not discriminate between initial and final states in the following, and our convention will be that all particles are out-going.

We will not use the traditional Feynman rules in this thesis, but rather an updated version known as the colour ordered Feynman rules. Colour ordering uses the fact that a scattering process of n_g gluons and n_q quarks will have n_g adjoint indices and n_q fundamental indices, and that the Feynman rules ensure that they in the final amplitude will appear as factors of T^a_{ij} or f^{abc}. But as f^{abc} may be written as[4]

$$f^{abc} = \frac{-i}{\sqrt{2}}\Big(\mathrm{tr}\big(T^aT^bT^c\big) - \mathrm{tr}\big(T^aT^cT^b\big)\Big) \tag{3.2}$$

we see that all colour dependence may be written in terms of T^a only, and using the additional rules of colour algebra

$$T^a_{ij}T^a_{kl} = \delta_{il}\delta_{kj} - \frac{1}{N_c}\delta_{ij}\delta_{kl} \qquad \mathrm{tr}\big(T^aT^b\big) = \delta^{ab}$$

$$\mathrm{tr}\big(T^a\big) = 0 \qquad \delta_{ii} = N_c \qquad \delta^{aa} = N_c^2 - 1 \tag{3.3}$$

we realize that the colour dependence may be split completely from the rest of the amplitude. This allows us to write the amplitude as

$$A(\{p\},\{h\},\{a\},\{i\}) = g_s^{n-2+2L}\sum_t t(\{a\},\{i\}) \times \mathcal{A}_t(\{p\},\{h\}) \tag{3.4}$$

where the factor t denotes a colour factor made of factors of T^a, with only those free indices $\{a\}$ and $\{i\}$ that correspond to the external particles, and where $\mathcal{A}_t$, denoted the partial amplitude, contains all the kinematic factors. The coupling constant g_s to a total power which is a function of the number of external legs n and the number of loops L have been taken outside the sum.

The colour algebra defined by eq. (3.2) and eqs. (3.3), may be performed systematically, using a diagrammatic formalism known as the double line notation. As we will not do much colour algebra in this thesis, those rules will not be described here, see [31] for a review.

At tree level, the partial amplitudes may be calculated directly from an alternative set of Feynman rules, called the colour ordered Feynman rules [23, 31]. When mentioning Feynman rules in the rest of this thesis, this is what will be referred to. Before presenting these rules, let us first make a brief discussion of some properties of the colour ordering.

[4] If one tried to derive this from eq. (2.5), one would get a factor of 2 instead of $1/\sqrt{2}$. That is because this chapter and the rest of the thesis uses a different normalization of the T^a and f^{abc} than was used in chapter 2. The present normalization is most suited for the colour ordered formalism.

In the ordinary Feynman rules one has to sum over different configurations of the external particles as their position in the diagram does not have a physical meaning. But in the sum of eq. (3.4) the different configurations are summed over, giving each partial amplitude a specific ordering. This makes the number of terms contributing to each (partial) amplitude significantly smaller than it would have become by using the ordinary Feynman rules.

For loop-level amplitudes, there is not a one-to-one correspondence between the partial amplitudes, and the results which one obtains from the colour ordered Feynman rules. In such cases the result of the colour ordered Feynman rules will be denoted primitive amplitudes $A^{[P]}$, and the relation between the primitive and the partial amplitudes has to be computed on a case-by-case basis [23, 32–34]. One feature, however, is recurrent. For purely gluonic amplitudes[5], eq. (3.4) will contain terms of the form $N_c^L \mathrm{tr}(T^a \cdots T^n)$, and no other terms having N_c raised to that high a power. Those terms give the leading order (in N_c) contribution, which is defined as

$$A_{\mathrm{LC}}(p_1, \ldots, p_n) = g_s^{n-2+2L} N_c^L \sum_{\sigma \in S_n/Z_n} \mathrm{tr}\big(T^{a_{\sigma(1)}} \cdots T^{a_{\sigma(n)}}\big) \times \mathcal{A}_{\mathrm{LC}}(p_{\sigma(1)}, \ldots, p_{\sigma(n)}) \tag{3.5}$$

where $\mathcal{A}_{\mathrm{LC}}$ gets contributions only from the planar primitive amplitudes

$$\mathcal{A}_{\mathrm{LC}}(p_1, \ldots, p_n) = \sum_{\mathrm{planar}} A^{[P]}(p_1, \ldots, p_n) \tag{3.6}$$

Before we can look at the colour ordered Feynman rules and some actual amplitudes, we have to present some new notation: the spinor-helicity formalism.

3.2 The spinor-helicity formalism

The spinor-helicity formalism is the natural notation for amplitudes, as it enables a joint description of all particles, vector-bosons, quarks, scalars using the same language. The formalism is particularly suited for massless particles, which is all we will consider in the following[6]. This section will omit some explicit expressions, a more thorough but also more brief summary of the formalism is given in appendix A.

For all four-momenta we may contract with the vector of Pauli matrices as

$$p_{\alpha\dot{\beta}} \equiv p_\mu \sigma^\mu_{\alpha\dot{\beta}} = \begin{bmatrix} p_- & -p_-^\perp \\ -p_+^\perp & p_+ \end{bmatrix} \tag{3.7}$$

[5] or in general, for amplitudes for particles which all transform under the adjoint representation of the gauge group.

[6] This is not a fundamental limitation. See [35] for the use of spinor-helicity for massive particles.

with

$$p_{\pm} \equiv p_0 \pm p_3 \qquad\qquad p_{\pm}^{\perp} \equiv p_1 \pm i p_2 \tag{3.8}$$

For massless momenta, this matrix will have determinant zero, implying that its rank is one. Thus we know that we may write it as an outer product of two two-vectors. These vectors will be the spinors λ_α and $\tilde{\lambda}_{\dot{\beta}}$ which are respectively denoted holomorphic and anti-holomorphic, that is

$$p_{\alpha\dot{\beta}} = \lambda_\alpha \tilde{\lambda}_{\dot{\beta}} \tag{3.9}$$

One representation of the spinors is

$$\lambda_\alpha \equiv \begin{pmatrix} -z p_-^{\perp}/\sqrt{p_+} \\ z\sqrt{p_+} \end{pmatrix} \qquad \tilde{\lambda}_{\dot{\beta}} \equiv \begin{pmatrix} -p_+^{\perp}/(z\sqrt{p_+}) \,, & \sqrt{p_+}/z \end{pmatrix} \tag{3.10}$$

where z is a degree of freedom in the definition. If one imposes that $\lambda^\dagger = \tilde{\lambda}$ as it is custom, at least for real momenta, this freedom becomes restricted to a phase $\exp(i\theta/2)$ that reflects the little group[7] freedom for massless particles.

Manipulating the spinor indices using the Levi-Civita symbol as $\lambda^\alpha = \epsilon^{\alpha\beta}\lambda_\beta$ and similarly for the anti-holomorphic spinors, we may define the abbreviated notation

$$\langle i| \equiv \lambda^\alpha(p_i) \qquad |i\rangle \equiv \lambda_\alpha(p_i) \qquad [i| \equiv \tilde{\lambda}_{\dot{\alpha}}(p_i) \qquad |i] \equiv \tilde{\lambda}^{\dot{\alpha}}(p_i) \tag{3.11}$$

which essentially defines the spinor helicity formalism. We see that this gives

$$p^{\alpha\dot{\beta}} \;=\; p \cdot \bar{\sigma}^{\alpha\dot{\beta}} \qquad \text{with} \qquad \bar{\sigma} \;\equiv\; (\sigma_0, -\sigma_1, -\sigma_2, -\sigma_3) \tag{3.12}$$

We may define spinor products as

$$\langle ab\rangle \equiv \lambda^\alpha(p_a)\lambda_\alpha(p_b) \qquad\qquad [ab] \equiv \tilde{\lambda}_{\dot{\alpha}}(p_a)\tilde{\lambda}^{\dot{\alpha}}(p_b) \tag{3.13}$$

These products have the properties of anti-symmetry $\langle ab\rangle = -\langle ba\rangle$, $[ab] = -[ba]$, and additionally they obey the relation

$$\langle ab\rangle[ba] = 2p_a \cdot p_b \;=\; s_{ab} \tag{3.14}$$

By contraction with the Pauli-matrices, one may also form a vector-product of the spinors, $\langle a|\sigma^\mu|b]$. This vector is perpendicular to p_a and p_b, and if the two momenta are identical, one recovers the momentum through

$$p_a^\mu = \frac{\langle a|\sigma^\mu|a]}{2} \tag{3.15}$$

The spinors, spinor products and vector products, fulfill many additional identities. Some of those are listed in appendix A, and for a more thorough list see [31,36]. We should note that the spinor-helicity formalism as described here is limited to the case of four-dimensional space. It is possible to construct similar notations for other dimensions, and the special case of $d = 6$, as summarized in section 11.2 and in appendix B, will play an important role later in the thesis.

[7] The little group is the subgroup of the Poincaré group that leaves the momenta invariant. For massless particles in four dimensions that group is $SO(2) \approx U(1) \approx$ phase.

3.3 Feynman rules

At this point we are ready to write down the colour ordered Feynman rules for massless QCD. The rules of this section are consistent with those listed in [31].

Let us start by considering the gluons. Two types of purely gluonic vertices are allowed, a three-point and a four-point as given by

$$\begin{aligned} V_{ggg}^{\mu_1\mu_2\mu_3} &= \frac{i}{\sqrt{2}}\Big(g^{\mu_2\mu_3}(p_2-p_3)^{\mu_1} + g^{\mu_3\mu_1}(p_3-p_1)^{\mu_2} + g^{\mu_1\mu_2}(p_1-p_2)^{\mu_3}\Big) \\ V_{gggg}^{\mu_1\mu_2\mu_3\mu_4} &= ig^{\mu_1\mu_3}g^{\mu_2\mu_4} - \frac{i}{2}\big(g^{\mu_1\mu_2}g^{\mu_3\mu_4} + g^{\mu_2\mu_3}g^{\mu_4\mu_1}\big) \end{aligned} \tag{3.16}$$

The gluonic propagator (for gluons with momentum p) is usually given as

$$\text{prop}_g^{\mu\nu} \;=\; \frac{-ig^{\mu\nu}}{p^2} \tag{3.17}$$

which is the expression in Feynman gauge, but in this thesis we will mostly use axial gauge[8] where the result is

$$\text{prop}_g^{\mu\nu} \;=\; \frac{i}{p^2}\left(-g^{\mu\nu} + \frac{p^\mu q^\nu + q^\mu p^\nu}{p\cdot q}\right) \tag{3.18}$$

where q^μ is the axial vector defined so $A\cdot q = 0$. External gluons with helicity $\pm$ may be written using the polarization vectors

$$\varepsilon_+^\mu(p,q) = \frac{\langle q\,\sigma^\mu\,p]}{\sqrt{2}\,\langle qp\rangle} \qquad\qquad \varepsilon_-^\mu(p,q) = \frac{\langle p\,\sigma^\mu\,q]}{\sqrt{2}\,[pq]} \tag{3.19}$$

in axial gauge. These polarization vectors obey the expected relations

$$\varepsilon_\pm(p,q)\cdot\varepsilon_\pm(p,q) = 0 \qquad\qquad \varepsilon_\pm(p,q)\cdot\varepsilon_\mp(p,q) = -1 \tag{3.20}$$

and

$$\varepsilon_+^\mu(p,q)\varepsilon_-^\nu(p,q) + \varepsilon_-^\mu(p,q)\varepsilon_+^\nu(p,q) = -g^{\mu\nu} + \frac{p^\mu q^\nu + q^\mu p^\nu}{p\cdot q} \tag{3.21}$$

which we see to correspond to the expression in eq. (3.18) as expected. No expressions similar to eqs. (3.19) exist for Feynman gauge, which is part of the reason for the use of the axial gauge in this thesis.

Physical massless quarks and antiquarks are usually given by Dirac spinors u and $\bar{u}$. In that case the Feynman rules are given by the vertices

$$V_{qg\bar{q}}^\mu = \frac{i}{\sqrt{2}}\gamma^\mu \qquad\qquad V_{\bar{q}gq}^\mu = \frac{-i}{\sqrt{2}}\gamma^\mu \tag{3.22}$$

[8] Axial gauge is also known as Arnowitt-Fickler gauge.

and the propagator

$$\text{prop}_q = \frac{i\not{p}}{p^2} \tag{3.23}$$

The massless Dirac spinors may be written as

$$\begin{aligned} u^+ &= \begin{pmatrix} \lambda^\alpha \\ 0 \end{pmatrix} & u^- &= \begin{pmatrix} 0 \\ \tilde{\lambda}_{\dot{\alpha}} \end{pmatrix} \\ \bar{u}^+ &= \begin{pmatrix} 0\,, & \tilde{\lambda}^{\dot{\alpha}} \end{pmatrix} & \bar{u}^- &= \begin{pmatrix} \lambda_\alpha\,, & 0 \end{pmatrix} \end{aligned} \tag{3.24}$$

in terms of two Weyl spinors, and we see them to obey the helicity sum

$$u^+\bar{u}^- + u^-\bar{u}^+ = \not{p} \tag{3.25}$$

where we have used eqs. (3.7) and (3.12).

A theory with Weyl-fermions f (with positive chirality) instead of Dirac fermions will the give the Feynman rules

$$V^\mu_{fg\bar{f}} = \frac{i}{\sqrt{2}}\sigma^\mu \qquad\qquad V^\mu_{\bar{f}gf} = \frac{-i}{\sqrt{2}}\sigma^\mu \tag{3.26}$$

and the propagator

$$\text{prop}_f = \frac{i\not{p}}{p^2} \tag{3.27}$$

with $\not{p} \equiv \sigma \cdot p$ for this case. We see that the rules are effectively the same for the two cases of Dirac and Weyl.

For each loop in the diagrams, there will be a free momentum k. That momentum has to be integrated over using the d-fold[9] integral

$$\int \frac{\mathrm{d}^d k}{(2\pi)^d} \tag{3.28}$$

where d denotes the number of space-time dimensions. Additionally each loop containing a fermion has to get multiplied with a factor of -1.

The propagators of eqs. (3.17), (3.18), and (3.23), are occasionally written with

$$\frac{1}{p^2} \to \frac{1}{p^2 + i\tilde{\epsilon}} \tag{3.29}$$

to ensure picking up the physical branch of phase-space and loop integrals. As we will not evaluate any such integrals explicitly in this thesis we will in general not include that factor explicitly, we will however see it again in the next chapter.

Often a 'ghost'-particle has to be introduced to regularize the propagators in gluonic loops [28], but in the axial gauge, the coupling between the ghosts and the

[9] See section 4.1

remaining particles is zero [31], allowing us to ignore the ghosts for the remainder of this thesis.

This should summarize the colour ordered Feynman rules for massless QCD. The rules are also[10] listed in appendix H along with the rules for massless scalars.

3.4 Amplitudes

In this section we will list some properties of amplitudes in massless QCD, and the relations between them. Most of the content of this section is described in higher detail in [31, 36].

The study of scattering amplitudes and their properties has been a swiftly growing field for the last perhaps twenty years. Before then, most introductory text-books on quantum field theory (like [28]), showed result for the cross-sections only, in which the spin or helicity of the external particles has been summed over or averaged out. The introduction of the spinor-helicity formalism helped to remedy this, and the first major result for a tree-level scattering amplitude is the Parke-Taylor [37] amplitude

$$\mathcal{A}\left(p_1^+, .^+., p_i^-, .^+., p_j^-, .^+., p_n^+\right) = i\frac{\langle ij\rangle^4}{\langle 12\rangle\langle 23\rangle\cdots\langle n-1\,n\rangle\langle n1\rangle} \tag{3.30}$$

for n-point gluon scattering (with all particles outgoing), in the case where all the particles have helicity plus, except particles i and j which have helicity minus. The helicity-configurations described by eq. (3.30) are known as MHV, or maximally helicity violating.

The corresponding amplitudes for configurations with one or zero particles with helicity minus are identically zero

$$\mathcal{A}\left(p_1^\pm, p_2^+, .^+., p_n^+\right) = 0 \tag{3.31}$$

and the opposite configuration with $n-2$ particles of helicity minus and 2 with helicity plus, can be obtained from eq. (3.30) using parity symmetry, with the result

$$\mathcal{A}\left(p_1^-, .^-., p_i^+, .^-., p_j^+, .^-., p_n^-\right) = (-1)^n i\frac{[ij]^4}{[12][23]\cdots[n-1\,n][n1]} \tag{3.32}$$

The Parke-Taylor formulae allow us to calculate all tree-level gluonic amplitudes up to 5-point, and quite a few at higher points as well. Configurations with 3 gluons of one helicity, and $n-3$ of the other are known as NMHV (next-to MHV), and for these cases the corresponding expression will have more than one term, but still be much simpler than would be expected from the number of Feynman diagrams contributing to the processes.

[10] Feynman rules are of such importance that they belong both in the main text and in an appendix.

For processes with external massless quarks, there exists similar expressions. For one configuration the result is [36]

$$\mathcal{A}\left(p_1^-, \bar{q}_2^-, q_3^+, p_4^+, .^+., p_n^+\right) = i\frac{\langle 12\rangle^3\langle 13\rangle}{\langle 12\rangle\langle 23\rangle\cdots\langle n-1\, n\rangle\langle n1\rangle} \tag{3.33}$$

From eq. (3.30) we see that the amplitude has a cyclical symmetry $A(p_1, p_2, \ldots, p_n) = A(p_2, \ldots, p_n, p_1)$ and a reflection symmetry $A(p_1, \ldots, p_n) = (-1)^n A(p_n, \ldots, p_1)$, giving us that for a n-point configuration, only $(n-1)!/2$ different primitive amplitudes would contribute. But actually the number is lower than that due to the linear Kleiss-Kuijf relations [38] which brings the number down to $(n-2)!$, and the more involved BCJ relations [27] which brings the number further down to $(n-3)!$ different primitive tree-level amplitudes contributing to each process. We will not make use of such relations in this thesis, see [36] for a review.

Equations such as eq. (3.30) can not be derived from Feynman diagrams alone as they are true for any number of external particles, clearly a recursion relation is needed. Several such relations exist[11], but the one we shall present here is the most impressive.

The BCFW [25, 26] recursion relation is[12]

$$A_n = \sum_{i=2}^{n-1}\sum_h \frac{A^{L\,-h}_{\ \ i} A^{R\,h}_{\ \ i}}{P_i^2} \tag{3.34}$$

where

$$\begin{aligned} A^L{}_i &= A\Big(p_1 + z_i\eta, p_2, \ldots, p_i, -P_i - z_i\eta\Big) \\ A^R{}_i &= A\Big(P_i + z_i\eta, p_{i+1}, \ldots, p_{n-1}, p_n - z_i\eta\Big) \end{aligned} \tag{3.35}$$

with

$$P_i = \sum_{j=1}^{i} p_j \qquad \eta = \frac{\langle p_1|\sigma^\mu|p_n]}{2} \qquad z_i = \frac{P_i^2}{2P_i\cdot\eta} \tag{3.36}$$

so we see that an n-point tree-level amplitude A can be written as a sum of products of lower-point amplitudes with a shifted momentum $p \to p + z\eta$, allowing for the evaluation of a tree-level amplitude without referencing any off-shell quantities. For the elegant proof of the BCFW relation, see [26]. The success of BCFW has been so immense that all tree-level amplitudes is QCD and related theories are considered known [39–41].

[11] Other recursion relations for tree-level amplitudes are the Berends-Giele off-shell recursion relation, and the CSW relations [24].

[12] There is a little more to the BCFW relation than what is presented here. The shift presented here does not work for all configurations of the external helicities, for others one may use $\eta = \frac{\langle p_n|\sigma^\mu|p_1]}{2}$. See [25, 36].

One might say that the BCFW recursion relation provides a more physical method to evaluate an amplitude than the traditional Feynman diagrammatic method, if it was not for the fact that it introduces complex momenta in the intermediate steps as the vector η is complex (see eq. (A.14)). This trade-off, on-shellness for complexness, is one we will meet again later in this thesis.

Thus we see that amplitudes may be evaluated without any references to Feynman rules, except that one has to know the three-point tree-amplitudes. But we see from the Feynman rules, and also from the resulting amplitudes like eqs. (3.30), (3.32), and (3.33), that if we count the powers of the little group phase z of the spinors of eqs. (3.10), external negative-helicity gluons will get 2 powers, negative-helicity quarks will get 1 power, positive-helicity quarks will get -1 power and positive-helicity gluons will get -2 such powers. No other powers will come from anywhere. This makes it possible to deduce the results for the three-point amplitudes in any theory, and using BCFW one may thus obtain expressions for any tree-level amplitudes without reference to Lagrangians or Feynman rules at all!

This discussion should have given a hint about the developments in the amplitudes field, which hold true even in completely physical theories such as QCD. For more such developments, see [42, 43].

3.5 Other theories

In this section we will take a look at some other theories, of no less physical or theoretical interest that QCD.

QED

QED, or quantum electro dynamics, is the quantum theory of electromagnetism. It was the first theory to be formulated as a quantum field theory, and it is also the QFT which has been tested experimentally to the highest precision, as theory and experiment agrees to a factor of 10^{-8} [28]. The Lagrangian for QED looks similar to eq. (2.1), but as the gauge group for electromagnetism is the Abelian $U(1)$, the structure constants f^{abc} vanish along with the gauge boson self interactions. This means that QED only allows for one kind of vertex, $\bar{l}\gamma l$, where l denotes the charged leptons (electrons, muons, and tau-particles), and γ denotes the photon, the gauge boson of QED.

As QED has no concept of colour, it is not possible to split QED amplitudes into ordered partial amplitudes as we did for QCD in eq. (3.4). Thus the expression for amplitudes in QED cannot have the cyclic structure we see from eq. (3.30). In the MHV case, the amplitude is [44]

$$A\left(p_q^-, p_{\bar{q}}^+, p_1^-, p_2^+, .^+., p_n^+\right) = i\frac{\langle q\bar{q}\rangle^{n-2}\langle 1q\rangle^2}{\prod_{\alpha=2}^{n}\langle q\alpha\rangle\langle\bar{q}\alpha\rangle} \tag{3.37}$$

with a more involved expression known as the Kleiss-Stirling formula [44] existing for the general case.

Due to good properties of the theory, QED allows for [45] an improved version of the BCFW relation which has even less terms in the sum than eq. (3.34), allowing for a highly computationally efficient calculation of amplitudes in that theory: Using the fact [46] that no triangle and bubbles (see chapter 5) exist for photon amplitudes in QED for $n \geq 6$, a one-loop amplitude may be calculated using the generalized unitarity cuts of section 4.5 using quadruple-cuts only, from tree-amplitudes calculated using eq. (3.37) or the improved BCFW formula. Such a calculation yields a computational speed-up of 1.5 orders of magnitude compared to the use of the general Kleiss-Stirling formula, and the result may be checked by the vanishing of the ϵ-poles in the resulting amplitude.

The weak sector

All the parts of the Standard Model which are not QED or QCD belong to the weak sector as it is the weak nuclear force that is responsible for the remaining interactions. The gauge group of the weak sector is $SU(2) \times U(1)$, but the gauge symmetry is broken due to the Higgs mechanism, yielding QED, three massive vector bosons called $W_{\pm}$ and Z_0, and the Higgs particle H. The weak interactions are the only part of the standard model capable of mixing quark or lepton flavours, and as such it is the weak interactions which are responsible for beta-decays $n \to p_+ + e_- + \bar{\nu}_e$. It is also the weak interactions that are responsible for all interactions of the charge- and colourless neutrinos. It is in the week sector that by far the most exotic effects of the Standard Model are to be found, as the interactions break parity-symmetry maximally, and also CP-breaking effects are to be found in the week sector.

The exact nature of the breaking of the gauge symmetry was controversial until the Higgs particle was finally found in 2012 [6], completing the discovery of all the particles predicted by the Standard model and further grounding it as the best candidate to a theory of the elementary particles found in nature.

As it is the Higgs mechanism that is responsible for giving mass the the elementary particles, the Higgs particle couples only to particles with mass with a coupling strength proportional to that mass. So in order to calculate the QCD corrections to Higgs production, one has to use diagrams in which a massive (top) quark runs in a loop, coupling to both the gluons and the Higgs boson. Such calculations may be troublesome, so frequently the $m_t \to \infty$ limit is used, which corresponds to an effective model in which the Higgs particle couples to an effective vertex which allows it to interact directly with the massless gluons.

Supersymmetry and super Yang-Mills

Supersymmetry is a proposed symmetry relating fermions and bosons. It was originally proposed to explain various otherwise unexplained features of the Standard Model and of the universe, such as dark matter, grand unification, and the hierarchy problem. A minimal supersymmetric model is the MSSM (minimally supersymmetric standard model) in which each of the fermions in the SM are given a scalar

super-partner, and each of the gauge bosons of the theory are given a (spin $\frac{1}{2}$) fermionic partner. None of these superpartners have however been found in nature, but this has not stopped the study of supersymmetry as supersymmetric theories are interesting also for their own sake.

For that reason we will not focus on the the full supersymmetric Standard Model, but only on supersymmetric extensions of Yang-Mills theory, called super Yang-Mills or SYM. In the minimal SYM the gluon has as fermionic partner galled the gluino, which interacts in a way similar to the quarks of QCD, except that they transform under the adjoint representation of the gauge group like the gluons.

It is possible to introduce more than one supersymmetry into the theory, a number denoted by $\mathcal{N}$, with the minimal SYM being $\mathcal{N} = 1$. In the complete quantum mechanical formulation of supersymmetry which will not be described here, each supersymmetry corresponds to a supersymmetric generator with is defined to lower the helicity of a particle in the state with $\frac{1}{2}$. So starting from a theory with a positive-helicity gluon we see that having $\mathcal{N} > 4$ will introduce states with $h < -1$, in which case we leave the domain of Yang-Mills theory. Therefore SYM theories have $\mathcal{N} \leq 4$.

The particle contents of the various SYMs are

$\mathcal{N}$	n_f	n_s
0	0	0
1	1	0
2	2	1
4	4	3

(3.38)

where n_f denotes the number of chiral gluinos, and n_s the number of complex scalars. The case of $\mathcal{N} = 3$ has been omitted as it is identical to $\mathcal{N} = 4$. The scalars present for $\mathcal{N} \geq 2$ are new to SYM, the Feynman rules for them are listed in appendix H.

One reason to study supersymmetry is that at tree-level the amplitudes of Yang-Mills theory are identical[13] to those of supersymmetric Yang-Mills, so relations between the tree-level amplitudes which may be found using the supersymmetries will also apply to pure YM. An example of this is the supersymmetric Ward identities which allows the creation of relations between amplitudes containing particles of different species, see [23] for an introduction.

It is possible to make fully supersymmetric expressions for the full amplitudes as well [47], quantities known as superamplitudes, and it is possible to define a BCFW recursion relation for these superamplitudes [19] allowing the simultaneous calculation of all the amplitudes in a supermultiplet. In this thesis we will do calculations in SYM theories, but not with these methods as the goal is to develop a method which applies directly to physical theories.

[13] This is also true for massless QCD, at least if the number of quark pairs is ≤ 4 [40].

$\mathcal{N} = 4$ SYM

The theory of $\mathcal{N} = 4$ SYM, also known as maximally supersymmetric Yang-Mills or MSYM, is the beloved theory of many theorists.

The original reason for this was that it was the theory that naturally came out of the low energy limit of superstring theory upon compactification down to four dimensions, and correspondingly out of ten-dimensional $\mathcal{N} = 1$ SYM after dimensional reduction. Yet since then the theory has become the subject of interest in its own right. A reason for this is that a large number of simplifications, some of which were extremely surprising, are present in the theory, making it a close second for the title of "the simplest quantum field theory" [19].

Imposing the four supersymmetries on YM, forces the Poincaré symmetry group of space-time to "grow" into a larger group, the (super)conformal group, making $\mathcal{N} = 4$ a (super)conformal field theory. Conformal field theories have a number of remarkable properties, for instance is the beta function for such a theory guarantied to vanish.

The conformal symmetry of $\mathcal{N} = 4$ SYM has been known since it was first studied. This is unlike a corresponding symmetry known as dual-conformal symmetry which was discovered in 2006 [17], and appears as a conformal symmetry in a new set of variables called dual coordinates y, defined cyclically so that $y_i - y_{i+1} = p_i$. These developments inspired the introduction of a new set of variables called momentum twistors [48], which, however, are also of use in theories without dual-conformal symmetry. We will use the momentum twistors in this thesis to simplify some analytical expressions, which is why they will be (partially) introduced in appendix C.2.

Another peculiarity of $\mathcal{N} = 4$ worth mentioning is the "no-triangle"-property [19, 49, 50] which says that loop-contributions which contain sub-diagrams that are triangles or bubbles (see chapter 5) vanish along with the rational terms (see chapter 10). This may be seen as one source of the simplifications happening in loop-amplitudes of $\mathcal{N} = 4$.

Many further more or less expected properties of $\mathcal{N} = 4$ are the subjects of ongoing research. Primary are the ADS/CFT correspondence [51], the amplitude/Wilson-loop duality [18, 52], a complete reformulation of the theory involving "Grassmanian polytopes" [22, 48, 53, 54], and much more [20, 55], none of which will be expanded upon further in this thesis. For a review of some of these properties, see [47].

Gravity and SuGra

The fourth fundamental force, that of gravity, is not a part of the Standard Model. The reason for this is that attempts at quantizing general relativity, the classical theory of gravity, yields an unrenormalizable theory. But despite of this fact, it is possible to make a perturbative, quantum field theoretical formulation of the theory with a set of Feynman rules, even if those rules are much more involved than those of gauge theories.

It is possible to build supersymmetric extensions of gravity, called supergravity

or SuGra. The force carrying particle of gravity, the graviton, is a spin 2 particle, so the same counting as we did for SYM, shows that the maximally supersymmetric gravity theory is $\mathcal{N} = 8$ SuGra. Adding supersymmetries make the ultraviolet divergences less severe than for pure gravity, and there are signs [56] that $\mathcal{N} = 8$ SuGra is going to be finite at all loop orders.

One interesting and highly unexpected aspect of quantum gravity theories, is that the tree-level gravity amplitudes, and for loop-diagrams the numerators, turn out to be related to the product of two of the corresponding quantity in colour ordered amplitudes Yang-Mills theory. This is known as the KLT relations [57]. The relations are such that a product of two pure YM quantities yields (almost) pure gravity, a product of two $\mathcal{N} = 4$ SYM gives $\mathcal{N} = 8$ SuGra, etc. For more on KLT, see [58, 59] or the review [47].

Presumably there would be no problem in applying the methods developed in this thesis to quantum gravity, other than the fact that the renormalization constraints mentioned in in the next chapter in the context of eq. (4.11) would have to be loosened to take the unrenormalizability into account. But due the KLT relations, this is probably not of any practical use.

Chapter 4

Loops and unitarity cuts

In this chapter we will discuss some aspects of loop calculations, culminating in the description of the generalized unitarity cuts to which the remainder of this thesis is devoted.

4.1 Regularization and renormalization

For loop diagrams, the momentum circling the loops is a free parameter k in the sense that it is not fixed by momentum conservation. To get a result for the loop-amplitude we have to integrate over the loop-momenta according to eq. (3.28).

$$\int \frac{\mathrm{d}^d k}{(2\pi)^d} \tag{4.1}$$

and we see that the integration is done in d dimensions, where d is taken to be a free variable.

To see why that is necessary, let us look at the result for perhaps the simplest example imaginable, a one-loop bubble integral with a massive incoming and outgoing momentum p. In that case the integral evaluates to (see appendix G, or textbooks like [28, 60])

$$I_{\text{bubble}} \equiv \int \frac{\mathrm{d}^d k}{\pi^{d/2}} \frac{1}{k^2(k-p)^2} = \frac{\Gamma^2\left(\frac{d}{2}-1\right)\Gamma\left(2-\frac{d}{2}\right)}{\Gamma(d-2)(-p^2)^{2-\frac{d}{2}}} \tag{4.2}$$

Inserting $d = 4$ gives

$$I_{\text{bubble}}|_{d=4} = \Gamma(0) = \infty \tag{4.3}$$

As the result of our calculations has to be physical, such infinities can not show up in the result, and therefore we know that they will have to cancel between the individual diagrammatical contributions. An infinity as the one in eq. (4.3) is not sufficiently well-defined mathematically to be made to cancel with anything, and therefore the loop integral has to be regulated in a way that controls these infinities.

The method that we will use in this thesis is called dimensional regularization[1], and consists of letting the dimension be taken slightly away from four, as

$$d = 4 - 2\epsilon \tag{4.4}$$

Inserting this into eq. (4.2) and expanding in ϵ, gives the result

$$I_{\text{bubble}} = (-p^2)^{-\epsilon} e^{-\epsilon\gamma_E} \left(\frac{1}{\epsilon} + 2 + \left(4 - \tfrac{\pi^2}{12}\right)\epsilon + \left(8 - \tfrac{\pi^2}{6} - \tfrac{7\zeta_3}{3}\right)\epsilon^2 + \mathcal{O}(\epsilon^3) \right) \tag{4.5}$$

and we see the infinity as the first term in the expansion.

Dimensional regularization come in various flavours. In traditional dimensional regularization one takes all parts of the amplitude to be d-dimensional, but in this thesis we will like to keep the external particles four-dimensional, in order for them to have the same quantum numbers as physical particles. This means that only the internal particles will be taken as d-dimensional. Allowing an internal gluon to move in d dimensions, is not the same as allowing it to be polarized into the d (or rather $d-2$) dimensions too. Whether or not this is allowed for distinguishes the four-dimensional helicity, or FDH-scheme, which restricts the internal gluons to four polarization directions, from the 't Hooft-Veltman scheme which allows d-dimensional polarization [61]. In this thesis we will do both, and keep the number of polarization directions of the internal gluons as a free parameter D_s.

If one calculates an amplitude naively using dimensional regularization, one will get an infinite result. There are two kinds of such divergences, those that show up in the limit where $p \to 0$ which are called infrared divergences, and those that come from the limit $p \to \infty$ which are called ultraviolet divergences.

Let us start by regarding the ultraviolet divergences. In QCD ultraviolet divergences show up only for diagrams with have a loop-containing subgraph containing four or fewer external particles. There are five[2] such divergent combinations: Loop-corrections to the gluonic propagator, to the fermionic propagator, to the ggg vertex, to the $gggg$ vertex, and to the $\bar{q}gq$ vertex. These divergences may, at each loop order, be absorbed into the fields and the constants of the Lagrangian of eq. (2.1), A^μ, ψ, g_s, and m, yielding a renormalized Lagrangian which in addition to the Feynman rules of section 3.3, has rules for a number of counter terms which will cancel the divergences. It is further considerations on these rescalings that yield the running of the coupling constant given by eq. (2.8). At a given loop-order, the diagrams containing the counter terms will always be proportional to the lower loop orders,

[1] One may also use other regularization methods. The most famous is the dimensional cut-off in which one lets the momentum integral of eq. (4.1) have an upper limit such that $k_0^2 < \Lambda$ with Λ being the regularization scale. This method can be seen to break Lorentz invariance, so another method is the Pauli-Villars regularization in which one replaces a propagator as $1/l^2 \to 1/l^2 - 1/(l^2 - \Lambda)$. This method breaks gauge invariance instead, leaving us dimensional regularization.

[2] We are discussing QCD in a no-ghost gauge, like the axial gauge. If one were including ghosts χ, also the ghost propagator and the $\chi g \chi$ vertex would be divergent and require renormalization.

and therefore we will mostly ignore the issue of counter terms for the rest of this thesis.

The infrared divergences is another story. If one considers an amplitude, as the one given by eq. (3.30), we see that it may have a divergence in soft or collinear limits, that is limits where one of the gluons have zero momenta or where two of the gluons become parallel. Experimentally such cases can never be observed, as no detector can detect a zero energy particle, or distinguish two particles hitting the detector simultaneously in the same point, but theoretically this might anyway be a source of worrying as such detector limitations should not be what prevents us from observing infinite quantities. The solution turns out to be that this infinity will cancel with the infrared divergences, not on the level of the amplitude but only in the final probability (or cross section) of eq. (2.12), such that for instance the soft and collinear limits of a tree-level contribution to the cross section, will cancel with the infrared divergence of the 1-loop contribution for one particle less[3]. As this subtraction can be performed only at the level of the cross-section, it will not concern us more in this thesis either.

4.2 Integrand reduction

For each (colour ordered) diagram contributing to an L-loop amplitude, one gets an expression like

$$\text{diagram} = \int \left(\prod_{i=1}^{L} \frac{\mathrm{d}^d k_i}{(2\pi)^d} \right) \frac{N(k_1, \ldots, k_L)}{l_1^2 \cdots l_P^2} \tag{4.6}$$

where the momenta $l_1, \ldots, l_P$ are those of the propagators which are a function of at least one of the loop-momenta k_i. The remaining propagators are considered a part of N. As N is a scalar, its functional dependence of the loop-momenta k_i has to be through scalar products of the k_i with each other, with the external momenta for the particles p_i, or with vectors of the form $\langle p_i|\sigma^\mu|p_j]$ which are the only additional vectors one might get from the Feynman rules[4]. For d-dimensional amplitudes it is desirable to write the squared loop-momentum as

$$k^2 = (k^{[4]})^2 - \rho \tag{4.7}$$

where ρ contains the information about the d-dimensional part of k (see section 9.2), and this rewriting introduces ρ as effectively an extra scalar product for such cases.

[3] If there are more loops, one has to also account for double-soft limits at $L-2$ loops etc.

[4] One source of this is the external polarization vectors, which have this factor explicitly. Another is the external quarks where the quark set will end up sandwiching a string of Pauli matrices $\langle p_i|\sigma^{\mu_1} \cdots |p_j]$ giving the term. (This is also true in cases of massive particles, even if it may be harder to see in such cases.) From the Pauli-strings one might also get terms like $\langle p_i|\not{k}_1\not{k}_2|p_j\rangle$ but such terms are reducible to the other kinds.

Occasionally a factor in one of the terms in N will coincide with one of the propagators l_i^2, making the two cancel. If for instance a diagram has the two propagators $l_1 = k_i$ and $l_2 = k_i - p_j$, we may write the two corresponding scalar products as

$$k_i^2 = l_1^2 \qquad\qquad k_i \cdot p_j = \left(l_1^2 - l_2^2\right)/2 \tag{4.8}$$

showing how both of these scalar products can be made to cancel with the propagators for such configurations. The scalar products that can be made to cancel in such a fashion are called reducible scalar products (RSPs), and the remaining ones are called irreducible scalar products (ISPs). This cancellation can be done systematically using methods based on algebraic geometry, as described in later chapters, particularly in chapter 9. Doing the reduction allows us to write the diagram as

$$\text{diagram} = \int \left(\prod_{i=1}^{L} \frac{\mathrm{d}^d k_i}{(2\pi)^d} \right) \sum_{\sigma \in \text{subsets}} \frac{\tilde{N}_\sigma(\text{ISPs})}{\prod_{j \in \sigma} l_j^2} \tag{4.9}$$

where the sum goes over the various subsets of the original set of numerators for the diagram. The numerators $\tilde{N}$ denote the part of the numerator which is left after the reduction, and which can be a function of the k_i only through the ISPs corresponding to the subset σ.

We may do this reduction for any diagram contributing to a primitive amplitude, allowing us to write the whole L-loop amplitude as

$$A^{[P]} = \int \left(\prod_{i=1}^{L} \frac{\mathrm{d}^d k_i}{(2\pi)^d} \right) \sum_{\sigma \in \text{subsets}} \frac{\Delta_\sigma(k_1, \ldots, k_L)}{\prod_{j \in \sigma} l_j^2} \tag{4.10}$$

where the subsets here refer to subsets of the complete set of propagators present for the amplitude. The individual terms in the sum are known as topologies[5], and the numerators Δ are called the irreducible numerator of the corresponding topology. The procedure of writing an integral on the form given by eq. (4.10) is known as integrand reduction.

The functional dependence of Δ on the ISPs x_i for given topology with ν ISPs is in general

$$\Delta = \sum_{i_1, \ldots, i_\nu} c_{i_1, \ldots, i_\nu} x_1^{i_1} \cdots x_\nu^{i_\nu} \tag{4.11}$$

Each of the sums start from zero, as the only poles in the amplitude can come from the propagators l_i^2 which are not considered part of Δ. For renormalizable gauge theories, the upper limit for each ISP is no higher that the number of propagators containing the corresponding loop-momentum k_i.

There will in most cases be further constraints on the number of terms in the irreducible numerator. In principle such identities may all be generated by relations

[5]This use of the word "topology" is different from the use in mathematics.

imposed by the vanishing of Gram determinants of sets of five four-momenta [62]. There is for instance the relation

$$\det G \begin{pmatrix} k_i & \beta_1 & \beta_2 & \beta_3 & \beta_4 \\ k_j & \beta_1 & \beta_2 & \beta_3 & \beta_4 \end{pmatrix} = 0 \tag{4.12}$$

where the β_i denote a linearly independent set of momenta of the form p_i or $\langle i\sigma^\mu j]$, which in four dimensions will impose the relation that the scalar product $k_i \cdot k_j$ may be written as a combination of the products $k_i \cdot \beta_j$, showing that one can pick the set of ISPs to never contain scalar products of the form $k_i \cdot k_j$. In practice we will not use Gram-matrix relations directly other than for simple examples, but rather use the more advanced approach involving algebraic geometry, which will be described in detail in chapter 9.

In principle one may obtain the value of N, and thus for each Δ, directly from Feynman diagrams. In this thesis we will mostly use another approach, but let us first take a look at how to actually evaluate a Feynman integral.

4.3 Evaluating Feynman integrals

In this section we will describe a number of methods which may be used to evaluate a Feynman integral. Most of these methods are described in detail in [60].

Feynman integrals are the kind of integrals that show up in loop-calculations in quantum field theory. They are defined as integrals of the form

$$I = \int \left(\prod_{i=1}^{L} \frac{\mathrm{d}^d k_i}{(2\pi)^d} \right) \frac{N(k_1, \ldots, k_L)}{D_1 \cdots D_P} \tag{4.13}$$

where the integral $\int \mathrm{d}^d k_i$ means that each of the d components of k_i has to be integrated along the real axis. The denominator components D_i are quadratic functions of the k_i variables, as one will get for the denominators of the propagators in the Feynman rules.

Before describing the methods which one may use to evaluate the Feynman integrals, let us diminish the problem by reducing to a minimal independent set. It has been conjectured that such a minimal set can be obtained by the application of integration-by-parts (IBP) identities, which use the fact that an integral of a total derivative vanish, that is

$$\int \frac{\mathrm{d}^d k}{\pi^{d/2}} \frac{\partial}{\partial k^\mu} \frac{q^\mu N}{D_1 \cdots D_P} = 0 \tag{4.14}$$

where q is some momentum, loop or external, occurring in the problem. (See also [63,64]). By performing the derivative under the integral sign, we see that the result will be that some linear combination of Feynman integrals with a subset of the propagators of eq. (4.14) will sum to zero, which we may use to solve for the most

complicated one. By repeating the procedure twice, we might for instance obtain the famous relation between the one-mass triangle and bubble integrals:

$$I_{\text{triangle}}(s) = \frac{(d-3)}{s\left(\frac{d}{2}-2\right)} I_{\text{bubble}}(s) \tag{4.15}$$

with

$$\begin{aligned} I_{\text{triangle}}(s) &\equiv \int \frac{\mathrm{d}^d k}{\pi^{d/2}} \frac{1}{k^2(k-p_1)^2(k-p_1-p_2)^2} \\ I_{\text{bubble}}(s) &\equiv \int \frac{\mathrm{d}^d k}{\pi^{d/2}} \frac{1}{k^2(k-p_1-p_2)^2} \end{aligned} \tag{4.16}$$

As there is some freedom in choosing the set of propagators and the momentum q in eq. (4.14), it may seem hard to know whether one knows all available IBP identities for a given integral, but there exist an algorithm, the Laporta algorithm [65], which allows one to find all the identities in a systematic way, thereby allowing a reduction to a minimal set of integrals, called master integrals. There is a freedom in choosing the set of master integrals, but conventionally one chooses a set with as few propagators, and then with as small a numerator, as possible.

A number of computer programs exist which implements the Laporta algorithm. In this thesis we have used the programs FIRE [66, 67] and Reduze2 [68].

Let us now take a brief look at some methods to evaluate Feynman integrals, like the master integrals found by the IBP method, from scratch. The traditional method to calculate such integrals is the method of Feynman parametrization. We will not go through the detail of the method here[6] as we will not be evaluation any integrals in this thesis, only say that the method shifts the problem from evaluating the momentum integral, to evaluating P ordinary integrals over a set of parameters called Feynman parameters.

Another, related method is that of Schwinger parametrization which is a different parametrization performing the same duty. Schwinger parametrization is not as suited as Feynman parametrization for actual integral evaluations (as it has one integral more to be done in the end), but it is more suited for other tasks including the task of making sense of integrals with an insertion of the higher-dimensional ρ-parameters mentioned in the previous section, which is why they will be introduced in appendix D.

There are other methods which too can be used to perform Feynman integrals directly, but let us instead describe another approach, that of relating Feynman integrals to simpler ones using differential equations.

At loop-order two or higher it is often necessary to calculate Feynman integrals indirectly, i.e. by relating them simpler integrals rather than calculating the from

[6] A short, concise description of the method is given in the fabulous appendix of [28], with the proofs in the main text.

scratch, and one highly successful method is that of differential equations (see i.e. [69]). The idea is to apply differential operators of the form

$$\frac{\partial}{\partial p_i^\mu} p_j^\mu \tag{4.17}$$

to the Feynman integral one wants to solve, relate the results to derivatives with respect to the Mandelstam variables s_{ij} (and masses m_i), and use the resulting differential equations to get an expression for the integral. As the equations are first order differential equations they may be solved in general provided that one knows a boundary condition, but these conditions can usually be found, either by identifying the boundary value as a simpler integral, or by using the vanishing of unphysical poles. In some cases (like the double-box solved in [70]) there are however more than one unknown master integral, and then the differential equations will in general couple, making the evaluation much harder.

This issue was solved by a recent development[7] by Henn [72] which suggested to use a basis of integrals with the property of "uniform transcendentality" [73]. In that case the differential equations may be written

$$d\bar{f} = \epsilon d\tilde{A}\bar{f} \tag{4.18}$$

where $\bar{f}$ is a vector containing the master integrals, and $\tilde{A}$ a matrix containing all the relations. As the ϵ goes outside the equation, we do not have to worry about coupling of the equations, as we may solve the system order by order in its ϵ-expansion, and express the result in terms of a set of functions called Goncharov polylogarithms defined [73, 74] recursively as

$$G(a_1, \ldots, a_n; z) = \int_0^z \frac{\mathrm{d}t}{t - a_1} G(a_2, \ldots, a_n; t) \tag{4.19}$$

with $G(;z) = 1$. The Goncharov polylogarithms generalize logarithms and Euler polylogarithms $\big(\mathrm{Li}_n(z)\big)$, yet not all Feynman integrals may be written on this form [75].

Much more could be said about these issues[8], but as integral evaluation is not the purpose of this thesis, this is not the place.

4.4 Unitarity cuts

In this section we will explain and derive the Cutkosky rules [77] for finding the discontinuities of a Feynman amplitude. The S-matrix as defined by eq. (2.10) is

[7] For another recent development of the differential equation method in a different direction, see [71]

[8] And also about how to simplify integral expressions using symbols [74] and co-products [76], and about how to get the symbol directly from the differential equation.

necessarily unitary, $\mathcal{S}^\dagger\mathcal{S} = 1$. This imposes on the T-matrix as it is given by eq. (2.11):

$$\mathcal{S} = I + i\mathcal{T} \tag{4.20}$$

that

$$-i\big(\mathcal{T} - \mathcal{T}^\dagger\big) = \mathcal{T}^\dagger\mathcal{T} \tag{4.21}$$

Contacting each side with an initial state $|i\rangle$ and[9] a final state $\langle f|$, and inserting[10]

$$\sum\!\!\!\!\!\!\int_x |x\rangle\langle x| = 1 \tag{4.22}$$

we get that

$$\big(A_{i\to f}(s) - A_{i\to f}(s^*)\big) = \sum\!\!\!\!\!\!\int_x A_{i\to x}(s)A_{x\to f}(s^*) \tag{4.23}$$

where we have been using the crossing symmetry of the amplitudes $A^*_{a\to b}(s) = -A_{b\to a}(s^*)$, where s collectively denotes all the variables on which the amplitude depend.

Physically the s parameters will all be real, but if we reintroduce the fact from eq. (3.29) that the propagators of our theories actually have a tiny imaginary part in the numerators $(k^2 + i\tilde{\epsilon})$, corresponding to the replacement $s \to s + i\tilde{\epsilon}$, we see that the LHS of eq. (4.23) only will give a contribution in the case where s is just on top of a branch-cut. Such branch-cuts may only come from the logarithms or polylogarithms in loop-integrals and thus not for tree-amplitudes, so in that case the LHS of (4.23) will equal the discontinuity, denoted 'disc', over that branch cut.

The states x on the RHS of (4.23), have to be physical as $A_{i\to x}$ is not defined otherwise, and thus the integral is limited to on-shell states. Therefore it is impossible, due to momentum conservation, for x to consist of 1 or 0 particles. If x contains two particles, a counting of powers of the coupling constants on each side of eq. (4.23) will show that the sum of the loops in the amplitudes on the RHS must be one smaller than the number of loops in the amplitude on the LHS. If x has three members, the sum of the loops must be smaller by two, etc. This means that we may rewrite eq. (4.23) as

$$\mathrm{disc}\big(A^{(L)}_{n_i\to n_f}(s)\big) = \sum_{l=0}\sum_{n_x=2}\int \mathrm{d}\Phi A^{(l)}_{n_i\to n_x}(s)\, A^{(L-l-n_x+1)}_{n_x\to n_f}(s^*) \tag{4.24}$$

where the $\mathrm{d}\Phi$ denotes the phase-space integrals over the particles in x including a sum over flavours and helicities, and the superscripts denote the number of loops.

[9] We are now for a moment back to the quantum mechanical notation of section 2.3, so $|\cdot\rangle$ does not denote a spinor.

[10] This integral is the same as the integral over the distribution of eq. (2.12).

As an example, the discontinuity of a two-loop $2 \to 3$ amplitude will contain three terms (each with a phase-space integral):

$$\text{disc}\big(A^{(2)}_{2\to3}\big) = A^{(0)}_{2\to2}A^{(1)}_{2\to3} + A^{(1)}_{2\to2}A^{(0)}_{2\to3} + A^{(0)}_{2\to3}A^{(0)}_{3\to3} \tag{4.25}$$

For each individual term on the RHS of eq. (4.24), way may write the amplitude on the LHS in a way that mirrors the structure of that term:

$$A_{n_i\to n_f} = \sum_{\substack{\text{flavours}\\\text{helicities}}} \int \left(\prod_{i=1}^{n_x-1} \frac{\mathrm{d}^d k_{xi}}{(2\pi)^d}\right) i^{n_x} \frac{\tilde{A}_{n_i\to n_x}\tilde{A}_{n_x\to n_f}}{\prod_{j=1}^{n_x}(k_{xj}^2 - m_j^2)} \tag{4.26}$$

where the tildes on the RHS denote the fact that the x-states in the corresponding amplitude are off shell. So we see that if we define an operation called a unitarity cut, as[11]

$$\frac{1}{D} \to 2\pi i \delta(D) \tag{4.27}$$

we may write eq. (4.24) as

$$\text{disc}\big(A^{[L]}_{n_i\to n_f}\big) = \sum_{\substack{\text{flavours}\\\text{helicities}}} \sum_{\text{cuts}} A^{[L]}_{n_i\to n_f} \tag{4.28}$$

where the 'cuts' refer to cuts in the channel $i \to f$. This is the Cutkosky rule.

After having been largely unused for a number of decades, the Cutkosky rules were resurrected in the 1990s [7, 78], where they were used to find a number of one-loop amplitudes. The method used an integral reduction for one-loop amplitudes[12]

$$A^{[P]}_{1-\text{loop}} = \sum_i d_i I_{\text{box},i} + \sum_i c_i I_{\text{triangle},i} + \sum_i b_i I_{\text{bubble},i} + \sum_i a_i I_{\text{tadpole},i} + \mathcal{R} \tag{4.29}$$

where I_{box}, I_{triangle}, I_{bubble}, and I_{tadpole}, denote four-dimensional integrals which 4, 3, 2, or 1 propagator. $\mathcal{R}$ is denoted the rational term, and contains terms that cannot be obtained directly from the cuts in four dimensions (see chapter 10).

Each of the integrals in eq. (4.29) have their own characteristic discontinuities due to the different combinations of logarithms which appear in the results, so a cut in each channel of the amplitude allows one to construct a set of equations capable of identifying the coefficients of eq. (4.29). Expressions derived by supersymmetry allows one to also identify the rational term, and thus it becomes possible to find the whole one-loop amplitude.

[11] In fact the operation is more complicated, as the cut defined like this does not account for the complex conjugation on the RHS of eq. (4.24). This is however not important if we assume the terms on the RHS to be away from branch cuts.

[12] which is similar to the integrand reduction which we will see in eq. (5.3).

4.5 Generalized unitarity cuts

The success in the use of unitarity cuts led to the idea of generalizing them beyond the cuts of eq. (4.28) [8], which after all only discusses cuts in a single channel, that of $i \to f$. We will describe the concept of a generalized unitarity cut[13] by an example, the one-loop four-dimensional box-integral defined as

$$I_{\text{box}} = \int \frac{\mathrm{d}^4 k}{(2\pi)^4} \frac{N(k)}{(k+p_1)^2\, k^2\, (k-p_2)^2\, (k+p_1+p_4)^2} \tag{4.30}$$

Let us first make a variable change from the $\mathrm{d}^4 k$-integral, to an integral over four parameters x such that

$$k^\mu = x_1 p_1^\mu + x_2 p_2^\mu + x_3 \frac{\langle 1|\sigma^\mu|2]}{2} + x_4 \frac{\langle 2|\sigma^\mu|1]}{2} \tag{4.31}$$

This gives

$$I_{\text{box}} = \frac{is^2}{4} \int \frac{\mathrm{d}^4 \bar{x}}{(2\pi)^4} \frac{N(\bar{x})}{(k+p_1)^2\, k^2\, (k-p_2)^2\, (k+p_1+p_4)^2} \tag{4.32}$$

where the $is^2/4$ is the Jacobi-determinant of the variable change.

If we try to do the quadruple-cut naively as

$$\begin{aligned} I_{\text{box}}|_{\text{cut}} = \frac{is^2}{4} \int \frac{\mathrm{d}^4 \bar{x}}{(2\pi)^4} (2\pi i)^3 N(\bar{x})\, \delta\Big(s\big((x_1+1)x_2 - x_3 x_4\big)\Big) \\ \times \delta\Big(s\big(x_1 x_2 - x_3 x_4\big)\Big)\, \delta\Big(s\big(x_1(x_2-1) - x_3 x_4\big)\Big) \\ \times \delta\Big(s\big((x_1+1)x_2 - x_3 x_4\big) + \big((x_1+1)t + x_2 u + x_3 \langle 14\rangle[42] + x_4 \langle 24\rangle[41]\big)\Big) \end{aligned} \tag{4.33}$$

we get that the cut-constraints have two different solutions

$$k = \frac{\langle 23\rangle}{\langle 13\rangle} \frac{\langle 1|\sigma^\mu|2]}{2} \quad \text{and} \quad k = \frac{[23]}{[13]} \frac{\langle 2|\sigma^\mu|1]}{2} \tag{4.34}$$

But looking at eqs. (A.11) and (A.14), we see that these vectors are complex and therefore outside the original integration domain! A quadruple cut done using the real delta-functions of eq. (4.27) would have no solution.

The solution to this, which is the main difference between generalized unitarity cuts and the Cutkosky cut of eq. (4.27), is that the cut should be defined not as a delta function insertion but rather as a deformation of the integration contour from

[13] "Generalized unitarity cut" is a tricky expression. One could be tempted to interpret it as a cut done using "generalized unitarity", but that would be incorrect as there is no such thing as "generalized unitarity". Rather, as explained in the main text, it refers to a unitarity cut which has been generalized. It is tempting to try to find another word, as there is quite far from $\mathcal{S}^\dagger \mathcal{S} = I$ to expressions like eq. (4.28), but the name has stuck.

the real axis to a circle, or in the complex case a torus, around the pole of the cut propagator

$$\int_{-\infty}^{\infty} \frac{1}{D} \to \oint \frac{1}{D} \tag{4.35}$$

The residue theorem takes care of the $2\pi i$ making this definition in a sense more natural than eq. (4.27). Let us see what we get for the cut of eq. (4.32). There will still the two results to the cut constraints which are given by eqs. (4.34), or correspondingly by

$$\{x_1, x_2, x_3, x_4\} = \left\{0, 0, \tfrac{\langle 23\rangle}{\langle 13\rangle}, 0\right\} \quad \text{or} \quad \{x_1, x_2, x_3, x_4\} = \left\{0, 0, 0, \tfrac{[23]}{[13]}\right\} \tag{4.36}$$

The Jacobian determinant corresponding to the collective contour deformation is given as

$$\mathcal{J} = s^3\big(\langle 24\rangle[41]x_4 - \langle 14\rangle[42]x_3\big) \tag{4.37}$$

so for the two solutions, the results for the quadruple cuts are

$$I_{\text{box}}|_{\text{cut sol 1}} = \frac{i}{4st} \qquad\qquad I_{\text{box}}|_{\text{cut sol 2}} = \frac{-i}{4st} \tag{4.38}$$

We see that generalized unitarity cuts are a relative to the BCFW recursion relations mentioned in section 3.4, as both methods express an amplitude by referring only to on-shell states at the cost of introducing complex momenta. Historically the connection is also present as unitarity methods were the original justification for the validity of BCFW [25]. It further considerations along these lines which lie behind many of the other developments in the field of amplitudes [22, 24]

A lot of work was done at one-loop using the generalized unitarity cuts [8–11, 79], enough to make a complete automation of the one-loop calculations possible [12, 13, 80–85]. It is that success that inspires the work in this thesis which is an attempt to generalize these techniques to two loops and beyond.

The combination of generalized unitarity cuts with the integrand reduction of section 4.2 which will be used in this thesis, is denoted the OPP method after Ossola, Papadopoulos, and Pittau, the authors of [9]. It consists of writing the integrand as an expansion in topologies, as by eq. (4.10), and then extracting each term in the expansion using the corresponding cut. For topologies with less than the highest number of propagators, a cut will not completely isolate one term, and will therefore have to be combined with a number of subtraction terms coming from higher-point cuts. As the whole of the next chapter consists of a one-loop example, we will not go into further details here, but just remark that since the cuts are made on both sides of eq. 4.2 the two Jacobians and details about the contour will drop out, and therefore they will not feature very prominently in the remainder of this thesis, even when they are technically there.

This thesis and the works [1–3] on which it is based are not the only attempts to extending the OPP method to higher loops, other contributions are [15, 16, 86–90].

There is also another direction [14, 91–97] in the attempts to extend the generalized unitarity cuts to higher loops. In this approach the leading singularity is extracted using a maximal cut, which for a four-dimensional L-loop diagram means $4L$ cuts. If the diagram does not have this number of propagators, the remaining cuts will be of the poles introduced by the Jacobian corresponding to eq. (4.37) in our example. The resulting cut solutions are then combined according to some physical constraints[14], and rather than fitting coefficients to the full integrand basis the fit is made to a smaller basis, that of the master integrals mentioned in section 4.3.

The two methods each have their upsides and downsides, for a comparison see the perspectives of chapter 14.

[14] The vanishing of spurious terms of the kind mentioned in appendix F.3.

Chapter 5

Example: one loop

Let us as an example of the use of our version of the OPP method, calculate parts of the irreducible numerator for the one-loop four-point primitive amplitude in four dimensions.

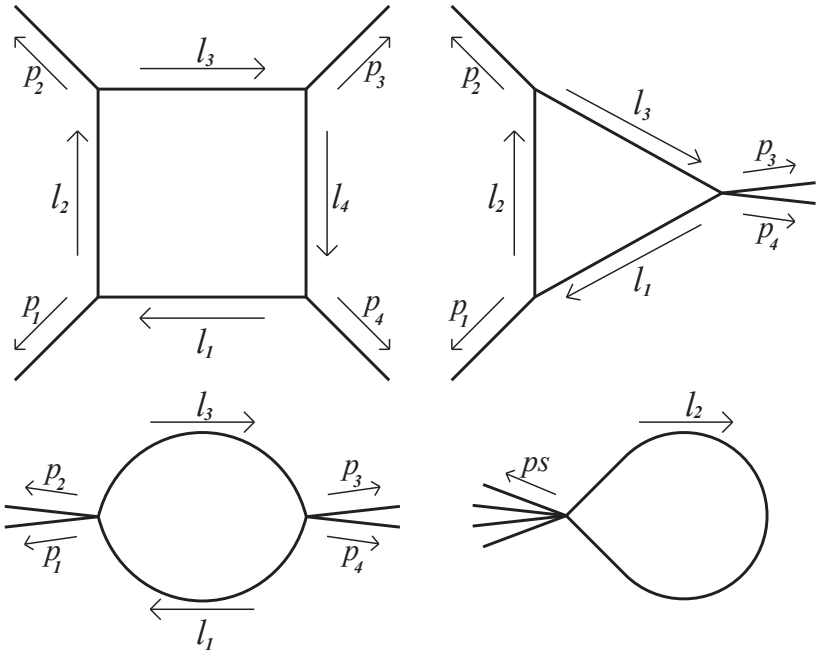

Figure 5.1: This figure shows the four types of contributions to eq. (5.3), the box, the triangle, the bubble, and the tadpole, with the rooting corresponding to Δ_{box}, $\Delta_{\text{tri},123}$, $\Delta_{\text{bubble},13}$, and $\Delta_{\text{tadpole},2}$ - the examples calculated in this chapter.

That amplitude is given as

$$A^{(1)} = \int \frac{\mathrm{d}^d k}{(2\pi)^d} \frac{N^{(1)}}{l_1^2\, l_2^2\, l_3^2\, l_4^2} \tag{5.1}$$

where N is a numerator which will depend on the theory and on the helicity configuration under consideration, and where l_1 to l_4 are the propagators

$$l_1 = k + p_1 \qquad l_2 = k \qquad l_3 = k - p_2 \qquad l_4 = k + p_1 + p_4 \tag{5.2}$$

We may write the numerator N as a sum of topologies corresponding to each subset of $\{l_1, l_2, l_3, l_4\}$ as described in the previous chapter. The topology with four propagators is called the box contribution, those with three are called triangles, those with two, bubbles, and those with one are called tadpoles, as seen on fig. 5.1. That is

$$\frac{N^{(1)}}{l_1^2\, l_2^2\, l_3^2\, l_4^2} = \frac{\Delta_{\text{box}}}{l_1^2\, l_2^2\, l_3^2\, l_4^2} + \sum_{x<y<z} \frac{\Delta_{\text{triangle},xyz}}{l_x^2\, l_y^2\, l_z^2} + \sum_{x<y} \frac{\Delta_{\text{bubble},xy}}{l_x^2\, l_y^2} + \sum_{x} \frac{\Delta_{\text{tadpole},x}}{l_x^2} \tag{5.3}$$

From combinatorics we see that there will be one box, four triangles, six bubbles, and four tadpoles. Eq. (5.3) features no rational term of the kind we saw in eq. (4.29), as (5.3) is purely four-dimensional and $\mathcal{R}$ comes solely from the higher-dimensional parts.

5.1 The box coefficient

Let us start by regarding the box-coefficient Δ_{box}. As it is a scalar quantity, it may be a function of k only through contractions with itself, p_i^μ, or $\omega^\mu \propto \varepsilon^{\mu\nu_1\nu_2\nu_3} p_{1\nu_1} p_{2\nu_2} p_{4\nu_3}$ - that is

$$\Delta_{\text{box}} = \sum_{i_1 i_2 i_3 i_4 i_5} c_{i_1 i_2 i_3 i_4 i_5} (k^2)^{i_1} (k \cdot p_1)^{i_2} (k \cdot p_2)^{i_3} (k \cdot p_4)^{i_4} (k \cdot \omega)^{i_5} \tag{5.4}$$

where each sum starts from zero, as all the poles of the integrand are in the propagators. That expressions does, however, turn out to be too general. k^2 is identical to one of the propagators, so if such a term were present it would cancel with the propagator and contribute to the corresponding triangle term instead. Similarly may all of the $k \cdot p_i$ terms be written in terms of constants and propagators

$$k^2 = l_2^2 \quad k \cdot p_1 = (l_1^2 - l_2^2)/2 \quad k \cdot p_2 = (l_2^2 - l_3^2)/2 \quad k \cdot p_4 = (l_4^2 - l_1^2 - t)/2 \tag{5.5}$$

meaning that they too will contribute only at lower point cuts.

$k \cdot \omega$ has no such property, and therefore it is a Irreducible Scalar Product (ISP). This means that the box-coefficient Δ_{box} can be written

$$\Delta_{\text{box}} = \sum_i c_i (k \cdot \omega)^i \tag{5.6}$$

From renormalizability we know that the power of k in the numerator cannot be bigger than the the power in the denominator, and therefore we get that $c_{i>4} = 0$

putting an upper limit on the sum. But in fact the limit is even lower than that. As $\{p_1, p_2, p_4, \omega\}$ spans the four-dimensional space, we know that

$$\det G\begin{pmatrix} k & p_1 & p_2 & p_4 & \omega \\ k & p_1 & p_2 & p_4 & \omega \end{pmatrix} = 0 \tag{5.7}$$

as the Gram determinant of a linearly independent set of vectors will vanish [62]. Using the specific expression

$$\omega^\mu = \frac{\langle 231]}{s}\frac{\langle 1|\sigma^\mu|2]}{2} - \frac{\langle 132]}{s}\frac{\langle 2|\sigma^\mu|1]}{2} \tag{5.8}$$

with the property $\omega^2 = \frac{tu}{s}$, eq. (5.7) is equivalent to

$$\begin{aligned}(k\cdot\omega)^2 = \frac{1}{s^2}\Big((k\cdot p_1)^2u^2 - 2tu(k\cdot p_1)(k\cdot p_2) - 2su(k\cdot p_1)(k\cdot p_4) \\ + t^2(k\cdot p_2)^2 - 2st(k\cdot p_2)(k\cdot p_4) + s^2(k\cdot p_4)^2 + stuk^2\Big)\end{aligned} \tag{5.9}$$

showing that $(k\cdot\omega)^2$ can be expressed solely in terms of RSPs and constants, which means that it too is reducible. This means that our final result for the general expression for Δ_{box} is

$$\Delta_{\text{box}} = c_0 + c_1(k\cdot\omega) \tag{5.10}$$

The $(k\cdot\omega)$-term is denoted a spurious term as it will integrate to zero as shown in appendix F.3, but we will calculate it anyway as it is needed for the subtractions.

In order to find the values of c_0 and c_1, we will use generalized unitarity cuts. We see that performing a quadruple-cut on eq. (5.3) will isolate Δ_{box} as cutting a non-existing propagator yields zero, giving

$$N^{(1)}|_{4\times\text{cut}} = \Delta_{\text{box}}|_{4\times\text{cut}}. \tag{5.11}$$

Parametrizing the loop momentum k as

$$k = x_1p_1 + x_2p_2 + x_3\frac{\langle 24\rangle}{\langle 14\rangle}\frac{\langle 1|\sigma^\mu|2]}{2} + x_4\frac{[24]}{[14]}\frac{\langle 2|\sigma^\mu|1]}{2} \tag{5.12}$$

the quadruple cut equations

$$l_1^2 = l_2^2 = l_3^2 = l_4^2 = 0 \tag{5.13}$$

have two solutions

	x_1	x_2	x_3	x_4
1	0	0	$-\frac{t}{u}$	0
2	0	0	0	$-\frac{t}{u}$

(5.14)

and we see that the two solutions are each others complex conjugates.

On these two cuts, Δ_{box} has the general values

$$\Delta_{\text{box}}|_{4\times\text{cut, sol 1}} \equiv d_1 \qquad\qquad \Delta_{\text{box}}|_{4\times\text{cut, sol 2}} \equiv d_2 \tag{5.15}$$

so inserting the values of $(k\cdot\omega)$ on the cuts ($t/2$ and $-t/2$ respectively), we get that

$$\bar{d} = M\bar{c} \tag{5.16}$$

with

$$\bar{d} \equiv \begin{pmatrix} d_1 \\ d_2 \end{pmatrix}, \qquad \bar{c} \equiv \begin{pmatrix} c_0 \\ c_1 \end{pmatrix}, \qquad M = \begin{bmatrix} 1 & t/2 \\ 1 & -t/2 \end{bmatrix}, \tag{5.17}$$

which may be inverted to

$$\bar{c} = M^{-1}\bar{d} \tag{5.18}$$

where

$$M^{-1} = \begin{bmatrix} 1/2 & 1/2 \\ 1/t & -1/t \end{bmatrix} \tag{5.19}$$

In order to find the values for d_i we need to find the value of $N^{(1)}|_{\text{cut}}$, the LHS of eq. (5.11). That value will in general depend on the theory under consideration. Let us in the following consider the case where all the external particles are gluons, and regard the various flavour-options for the propagating particles individually.

The gluonic contribution

Let us start by regarding the case where all the internal particles are gluons too.

Thinking in terms of Feynman diagrams, only diagrams which has all four of the cut propagators will survive the quadruple-cut. From the relations eqs. (3.18) and (3.21), we get

$$\text{prop}^{\mu\nu}_{\text{gluon}} = i\frac{\sum_h \varepsilon^{\mu}_h(k)\varepsilon^{\nu}_{-h}(k)}{k^2} \tag{5.20}$$

and we see that cutting a gluonic propagator is equivalent to replacing it by (i times) the helicity sum of products of polarization vectors carrying the on-shell cut momentum k, and thus the result of cutting all propagators in a loop diagram is equivalent to the helicity sum of the product of the tree level amplitudes corresponding to the vertices of the diagram.

For the gluonic box in question, we get that

$$\Delta_{\text{box,g}}|_{\text{cut}} = i^4 \sum_{\{h_1,\ldots,h_4\}} \mathcal{A}(-l_1^{-h_1}p_1^{a_1}l_2^{h_2})\mathcal{A}(-l_2^{-h_2}p_2^{a_2}l_3^{h_3})\mathcal{A}(-l_3^{-h_3}p_3^{a_3}l_4^{h_4})\mathcal{A}(-l_4^{-h_4}p_4^{a_4}l_1^{h_1}) \tag{5.21}$$

where $\{a_1, \ldots, a_4\}$ denotes the helicities of the external gluons.

Using the well-known Parke-Taylor expressions for tree-level three-point gluonic amplitudes

$$\mathcal{A}(1^-2^-3^+) = i\frac{\langle 12\rangle^3}{\langle 23\rangle\langle 31\rangle} \qquad \mathcal{A}(1^+2^+3^-) = -i\frac{[12]^3}{[23][31]} \tag{5.22}$$

we can calculate each of the 16 terms in eq. (5.21), to get their sum $\Delta_{\text{box}}|_{\text{cut}}$. The result is only vanishing for MHV helicity-configurations, that is configurations for which two of the external particles have helicity plus and the other two helicity minus. There are six of such configurations,

$$(--++) \quad (-+-+) \quad (-++-) \quad (+--+) \quad (+-+-) \quad (++--) \tag{5.23}$$

but only two, say $(--++)$ and $(-+-+)$ are truly independent, as the others are related through cyclic permutations of the legs.

For the the adjacent helicity configuration $(--++)$, the value of the helicity sum is the same at the two solutions, that is

$$d_1^{--++} \;=\; d_2^{--++} \;=\; \frac{\langle 12\rangle^3}{\langle 23\rangle\langle 34\rangle\langle 41\rangle}\big(-st\big) \tag{5.24}$$

where we see the tree-amplitude factor out of the result. Solving for the c-coefficients of eq. (5.10), we get that

$$\tilde{c}_0^{--++} = -st \qquad \tilde{c}_1^{--++} = 0 \tag{5.25}$$

where we have defined the tilded variables as $\tilde{c}_j \equiv ic_j/\mathcal{A}_{\text{tree}}$, that is as the corresponding c-coefficient without the tree-factor.

For the non-adjacent helicity configuration the result is somewhat more complicated. Defining the tilded d-coefficients correspondingly as $\tilde{d}_j \equiv id_j/\mathcal{A}_{\text{tree}}$, we get that the $\tilde{d}$-coefficients become

$$\tilde{d}_1^{-+-+} = \big(-st\big) \qquad \tilde{d}_2^{-+-+} = \frac{-st\big(s^4+t^4\big)}{u^4} \tag{5.26}$$

which corresponds to the c-coefficients

$$\tilde{c}_0^{-+-+} = \frac{-st\big(s^2+t^2+st\big)^2}{u^4}\,, \qquad \tilde{c}_1^{-+-+} = \frac{-2s^2t\big(2s^2+2t^2+3st\big)}{u^4}\,. \tag{5.27}$$

The fermionic contribution

Let us now regard the case where all the internal particles are fermions. The fermionic propagator is given by eq. (3.23) as

$$\text{prop}_{\text{fermion}} = i\frac{\not{k}}{k^2} \tag{5.28}$$

and for Dirac spinors we have that

$$\not{k} \;=\; u^+\bar{u}^- + u^-\bar{u}^+ \;=\; |k\rangle[k| + |k]\langle k| \tag{5.29}$$

This shows that cutting a fermionic line is equivalent to replacing it with a sum over the two helicity-states of the fermion, just as in the gluonic case.

After the quadruple-cut we therefore get

$$\Delta_{\text{box,f}}|_{\text{cut}} = -1\times\sum_{h\in\{+,-\}}\mathcal{A}_{fgf}(-l_1^{-h}p_1^{a_1}l_2^h)\mathcal{A}_{fgf}(-l_2^{-h}p_2^{a_2}l_3^h)\mathcal{A}_{fgf}(-l_3^{-h}p_3^{a_3}l_4^h)\mathcal{A}_{fgf}(-l_4^{-h}p_4^{a_4}l_1^h) \tag{5.30}$$

where the over-all minus comes from the Feynman-rule of eq. (H.12), telling us to multiply each independent fermion-loop with such a factor. We have limited the sum to two states, due to the fact that amplitudes of gluons with massless fermions with the same helicity, always vanish. Had we considered Weyl-spinors rather than Dirac-spinors, the result would have been the same and the two states in the sum of eq. (5.30) would come from the two independent chiral and anti-chiral contributions.

The fermionic tree-amplitudes used in eq. (5.30) are given as

$$\mathcal{A}_{fgf}(1^-2^-3^+) = i\frac{\langle 12\rangle^2}{\langle 31\rangle} \qquad\qquad \mathcal{A}_{fgf}(1^+2^-3^-) = -i\frac{\langle 23\rangle^2}{\langle 31\rangle} \tag{5.31}$$

and their complex conjugates. As in the gluonic case, there are only two independent contributions which correspond to the external gluons having the helicities $(--++)$ and $(-+-+)$.

For the $(--++)$ contribution the result is

$$\tilde{c}_{f0}^{--++} \;=\; \tilde{c}_{f1}^{--++} \;=\; 0 \tag{5.32}$$

as both of the terms in the helicity sum vanishes identically, and where the subscribed f refers to fermions. For the $(-+-+)$ contribution the result is given as

$$\tilde{c}_{f,0}^{-+-+} = \frac{-s^2t^2\big(s^2+t^2\big)}{2u^4}\,, \qquad\qquad \tilde{c}_{f,1}^{-+-+} = \frac{s^2t\big(s^2+t^2\big)}{u^4}\,. \tag{5.33}$$

The scalar contribution

The scalar propagator is given by eq. (H.2) as

$$\text{prop}_{\text{scalar}} = \frac{i}{k^2} \tag{5.34}$$

which shows that a cut only leaves a factor of i, but no sum. This means that the tree-product will be given as

$$\Delta_{\text{box,s}}|_{\text{cut}} = 2\times\mathcal{A}_{sgs}(-l_1p_1^{a_1}l_2)\mathcal{A}_{sgs}(-l_2p_2^{a_2}l_3)\mathcal{A}_{sgs}(-l_3p_3^{a_3}l_4)\mathcal{A}_{sgs}(-l_4p_4^{a_4}l_1) \tag{5.35}$$

where the factor of two comes from the fact that we use complex scalars which have two non-coupling but otherwise identical degrees of freedom. The result is purely zero for the adjacent helicity configuration $(--++)$, and for $(-+-+)$ the result is

$$\tilde{c}_{s,0}^{-+-+} = \frac{-s^3t^3}{u^4}\,, \qquad\qquad \tilde{c}_{s,1}^{-+-+} = \frac{2s^3t^2}{u^4}\,. \tag{5.36}$$

The total box-contribution

Let us regard a theory with n_f fermions and n_s complex scalars. Combining the result from the previous subsections as

$$\Delta = \Delta_g + n_f\Delta_f + n_s\Delta_s \tag{5.37}$$

we may obtain the result for Δ_{box} in such a general theory. The combinations give

$$\begin{aligned}
\Delta_{\text{box}}^{--++} &= \frac{\langle 12\rangle^3}{\langle 23\rangle\langle 34\rangle\langle 41\rangle}\,(-st)\,, \\
\Delta_{\text{box}}^{-+-+} &= \frac{\langle 13\rangle^4}{\langle 12\rangle\langle 23\rangle\langle 34\rangle\langle 41\rangle}\times \\
&\quad (-st)\bigg(1+\frac{s}{u^4}\Big((s^2+t^2)(4-n_f)+2st(3-n_s)\Big)\Big((k\cdot\omega)-t/2\Big)\bigg)
\end{aligned} \tag{5.38}$$

We see that both results reduces to the known result

$$\Delta_{\text{box}}^{\mathcal{N}=4} = i\mathcal{A}^{(0)}st \tag{5.39}$$

for the $\mathcal{N}=4$ theory, as it has $n_f=4$ and $n_s=3$ which we see by the table of eq. (3.38).

5.2 The triangle coefficients

Four triangle coefficients contribute to the $gg\to gg$ process, $\Delta_{\text{tri},ijk}$ where $\{i,j,k\}$ is a subset of $\{1,2,3,4\}$. Let us in the following focus on $\Delta_{\text{tri},123}$ which corresponds to the three propagators

$$l_1 = k+p_1 \qquad\qquad l_2 = k \qquad\qquad l_3 = k-p_2 \tag{5.40}$$

One propagator less means one less reducible scalar product, and one possible choice for ISPs is $\{(k\cdot p_4),(k\cdot\omega)\}$. But as p_4 does not appear at all in the topology, a better choice is $\{(k\cdot\omega_+),(k\cdot\omega_-)\}$ where

$$\omega_\pm^\mu \equiv \frac{\langle 1|\sigma^\mu|2]}{2} \pm \frac{\langle 2|\sigma^\mu|1]}{2} \tag{5.41}$$

is defined such that $\omega_\pm$ are perpendicular to p_1, p_2, and to each other. This means that the general expression for the irreducible numerator (corresponding to eq. (5.6) for the box case) can be written as a monomial sum as

$$\Delta_{\text{tri}} = \sum_{ij} c_{ij} (k \cdot \omega_+)^i (k \cdot \omega_-)^j \tag{5.42}$$

Renormalizability imposes the criterion that $i + j \leq 3$, but just like for the box-coefficient there are further constraints to be found. In principle this too could be done using Gram matrix relations (see [1, 62]) but finding the right relations gets tedious quickly, so we will call in some more heavy machinery.

For any topology, the set of propagators generates what is mathematically called an ideal, i.e. a subset of the full set of possible numerators N, consisting of polynomials of the RSPs with kinematic coefficients. As an ideal, it has the properties of closure under addition and multiplication. Let us call this ideal I. Any ideal can be spanned by a basis, and for I, one such basis is the set of propagators, but another basis with useful properties is the Gröbner basis G. To see this, let us make a new parametrization of k

$$k = x_1 p_1 + x_2 p_2 + x_3 \frac{\langle 1|\sigma^\mu|2]}{2} + x_4 \frac{\langle 2|\sigma^\mu|1]}{2} \tag{5.43}$$

for use in the triangle case. For this parametrization, the three propagators are

$$l_1^2 = s(x_1 x_2 - x_3^2 + x_4^2 + x_2) \quad l_2^2 = s(x_1 x_2 - x_3^2 + x_4^2) \quad l_3^2 = s(x_1 x_2 - x_3^2 + x_4^2 - x_1) \tag{5.44}$$

and these three form a basis for the ideal I. In this case the Gröbner basis for I (for the DegreeLexicographic[1] ordering) is simpler, as it is given by

$$G = \{x_2,\ x_1,\ x_4^2 - x_3^2\} \tag{5.45}$$

which means that any sum of products of the three propagators can be written as a sum of products of the elements of G with kinematic coefficients.

The first two elements of G corresponds to our RSPs, $x_1 = 2(k \cdot p_2)/s$ and $x_2 = 2(k \cdot p_1)/s$, but the third element is less trivial

$$x_4^2 - x_3^2 = \big((k \cdot \omega_-)^2 - (k \cdot \omega_+)^2\big)/s^2 \tag{5.46}$$

indicating that that particular combination of ISPs is reducible after all. This means that all terms involving (say) $(k \cdot \omega_+)^2$ can be recast as terms involving $(k \cdot \omega_-)^2$ instead, making the basis

$$\begin{aligned}\Delta_{\text{tri}} = \tilde{c}_{00} &+ \tilde{c}_{01}(k \cdot \omega_-) + \tilde{c}_{02}(k \cdot \omega_-)^2 + \tilde{c}_{03}(k \cdot \omega_-)^3 + \tilde{c}_{10}(k \cdot \omega_+) \\ &+ \tilde{c}_{11}(k \cdot \omega_+)(k \cdot \omega_-) + \tilde{c}_{12}(k \cdot \omega_+)(k \cdot \omega_-)^2\end{aligned} \tag{5.47}$$

[1] See chapter 9.

which is the minimal basis we were looking for - corresponding to eq. (5.10) for the case of the box. In more complicated cases where the Gröbner basis will have more non-trivial elements, this reduction can be performed systematically by a multivariate polynomial division with the elements of G as implemented by Zhang as the code BASISDET. See [16] and chapter 9.

Even though this basis is minimal and correct, and has only two non-spurious terms, $\tilde{c}_{00}$, and $\tilde{c}_{02}$, it does, however, turn out that it is possible to pick an alternate basis in which there only is one non-spurious term and a higher degree of symmetry. That basis is

$$\begin{aligned}\Delta_{\text{tri}} = c_{00} + c_{01}(k\cdot\omega_-) + c_{10}(k\cdot\omega_+) + c_{11}(k\cdot\omega_+)(k\cdot\omega_-) + c_{12}(k\cdot\omega_+)(k\cdot\omega_-)^2 \\ + c_{21}(k\cdot\omega_+)^2(k\cdot\omega_-) + c_{02/20}\big((k\cdot\omega_-)^2 + (k\cdot\omega_+)^2\big)\end{aligned} \tag{5.48}$$

which we will use in the following.

Just like for the box-case, we will try to find the c_i-coefficients using generalized unitarity cuts. The three cut equations

$$l_1^2 = l_2^2 = l_3^2 = 0 \tag{5.49}$$

have the two solutions

	x_1	x_2	x_3	x_4
1	0	0	τ	0
2	0	0	0	τ

(5.50)

τ is a free parameter which reflects the fact that three constraints cannot fix a four dimensional momentum completely, so after the cut Δ has a remaining degree of freedom, which is parametrized by τ. The two ISPs are linear functions[2] of τ, so as the maximum total power of ISPs appearing in eq. (5.48) is three, Δ will be given as

$$\Delta_{\text{tri}}|_{\text{cut } s} = \sum_{j=0}^{3} d_{sj}\tau^j \tag{5.51}$$

on each cut solution s, making the topology completely characterized by the the eight d_{sj} coefficients. By inserting the specific values for Δ_{tri} on the cuts, we may relate the seven c_i coefficients of (5.48) to the d_{sj} coefficients by a linear relation:

$$\bar{d} = M\bar{c} \tag{5.52}$$

with

$$\bar{d} = (d_{10}, d_{11}, d_{12}, d_{13}, d_{20}, d_{21}, d_{22}, d_{23})^T \quad \bar{c} = (c_{00}, c_{01}, c_{10}, c_{11}, c_{12}, c_{21}, c_{02/20})^T \tag{5.53}$$

[2] On solution 1, $(k\cdot\omega_\pm) = \mp s\tau/2$. On solution 2, $(k\cdot\omega_\pm) = -s\tau/2$

and

$$M = \begin{bmatrix} 1 & 0 & 0 & 0 & 0 & 0 & 0 \\ 0 & \frac{s}{2} & -\frac{s}{2} & 0 & 0 & 0 & 0 \\ 0 & 0 & 0 & -\frac{s^2}{4} & 0 & 0 & \frac{s^2}{2} \\ 0 & 0 & 0 & 0 & -\frac{s^3}{8} & \frac{s^3}{8} & 0 \\ 1 & 0 & 0 & 0 & 0 & 0 & 0 \\ 0 & -\frac{s}{2} & -\frac{s}{2} & 0 & 0 & 0 & 0 \\ 0 & 0 & 0 & \frac{s^2}{4} & 0 & 0 & \frac{s^2}{2} \\ 0 & 0 & 0 & 0 & -\frac{s^3}{8} & -\frac{s^3}{8} & 0 \end{bmatrix} \tag{5.54}$$

That M is non-square, or correspondingly that eq. (5.52) has more equations than unknowns, shows that the system of ds is over-determined. This means that a solution of $\bar{c}$ in terms of $\bar{d}$ exists[3] but that additional $n_d - n_c$ relations are imposed between the d-coefficients corresponding to the null-space of the equation set (5.52).

Mathematically this redundancy may be described as M not having an inverse in the usual sense, but for our purpose it is enough to find a "pseudo-inverse" W with the property that $WM = I$ such that eq. (5.52) becomes $\bar{c} = W\bar{d}$. This can for instance be done using PLU decomposition as described in appendix F.5. One such pseudo-inverse is[4]

$$W = \begin{bmatrix} 1 & 0 & 0 & 0 & 0 & 0 & 0 & 0 \\ 0 & \frac{1}{s} & 0 & 0 & 0 & -\frac{1}{s} & 0 & 0 \\ 0 & -\frac{1}{s} & 0 & 0 & 0 & -\frac{1}{s} & 0 & 0 \\ 0 & 0 & -\frac{2}{s^2} & 0 & 0 & 0 & \frac{2}{s^2} & 0 \\ 0 & 0 & 0 & -\frac{4}{s^3} & 0 & 0 & 0 & -\frac{4}{s^3} \\ 0 & 0 & 0 & \frac{4}{s^3} & 0 & 0 & 0 & -\frac{4}{s^3} \\ 0 & 0 & \frac{1}{s^2} & 0 & 0 & 0 & \frac{1}{s^2} & 0 \end{bmatrix} \tag{5.55}$$

with the additional null-space constraint that $d_{10} = d_{20}$.

The next step is to attempt to find the value for the triangle contribution using generalized unitarity cuts. Performing the triple-cut of the propagators l_1, l_2, l_3 on both sides of eq. (5.3), will allow us to identify the LHS with a product of trees as for the box contribution, except that one of the trees will now be four-point. On the RHS of eq. (5.3), the triple-cut will not isolate the triangle contribution $\Delta_{\text{tri},123}$, as we will get a contribution from the box-coefficient too, but we know that coefficient as we calculated it in the previous section. So for the gluonic loop we may isolate $\Delta_{\text{tri},g}$ as

$$\Delta_{\text{tri}}|_{3\times\text{cut}} = i^3 \sum_{h_1,h_2,h_3} \mathcal{A}(-l_1^{-h_1} p_1^{a_1} l_2^{h_2}) \mathcal{A}(-l_2^{-h_2} p_2^{a_2} l_3^{h_3}) \mathcal{A}_4(-l_3^{-h_3} p_3^{a_3} p_4^{a_4} l_1^{h_1}) - \frac{\Delta_{\text{box}}|_{3\times\text{cut}}}{l_4^2} \tag{5.56}$$

[3] Mathematically this is not always true (i.e. if $\text{rank}(M) < \min(n_d, n_c)$) as we see in section 8.3, but it is true in this case.

[4] This is the last time in this thesis, such a matrix will be written out in full.

where the Δ_{box}-term is denoted a subtraction term or a OPP subtraction term after [9].

As the triangle has lost some of the symmetry of the box, there are more substantially different helicity configurations contribution than in that case. There will be three such contributions, $(--++)$, $(-+-+)$, and $(-+-+)$, where the remaining MHV-contributions will be non-vanishing too, but related to these three by parity.

We will not list the results here, only note that the $(--++)$-contribution vanishes, and that the remaining ones are proportional to $4-n_f$ or $1-n_f+n_s$ of which the latter vanishes in all supersymmetric theories and the former in $\mathcal{N}=4$ in accordance with the no-triangle theorem mentioned in section 3.5.

5.3 The bubble coefficients

In this section we will take a look at the bubble coefficients.

There are six different bubbles contributing to eq. (5.3) which are of two different kinds. There are four for which the two propagators are adjacent on the box (i.e. $\Delta_{\text{bubble},\,i\,i+1}$), and two for which they are not (i.e. $\Delta_{\text{bubble},\,i\,i+2}$). Let us start by regarding the four adjacent bubbles. For those cases the corresponding bubble integral will be given as

$$I_{\text{bubble, adjacent}} = \int \frac{\mathrm{d}^d\tilde{k}}{(2\pi)^d} \frac{1}{\tilde{k}^2\,(\tilde{k}-p)^2} \tag{5.57}$$

where p is one of the four external momenta, and $\tilde{k}$ may be linearly shifted compared to the k of eqs. (5.2). As that integral is scalar it may only depend on scalar combinations of the external momenta in the expression, and as the only such momentum is p which squares to zero, zero is the only value that integral may possible have, and by regarding the general expression given by eq. (4.5) we see that this indeed is correct. This means that the values of the four coefficients multiplying the zero-mass bubbles are unimportant as they will multiply zero.

Thus we may concentrate on the non-adjacent bubbles, exemplified by

$$I_{\text{bubble,13}} = \int \frac{\mathrm{d}^d\tilde{k}}{(2\pi)^d} \frac{1}{\tilde{k}^2\,(\tilde{k}-P)^2}, \tag{5.58}$$

where $\tilde{k}=k+p_1$ and $P=p_1+p_2$ compared to eqs. (5.2).

The problem will have three ISPs, which we take to be $(k\cdot\omega_1)$, $(k\cdot\omega_2)$, $(k\cdot\omega_3)$, with[5]

$$\omega_1 = \frac{\langle 1|\sigma^\mu|2]}{2} - \frac{\langle 2|\sigma^\mu|1]}{2} \qquad \omega_2 = \frac{\langle 1|\sigma^\mu|2]}{2} + \frac{\langle 2|\sigma^\mu|1]}{2} \qquad \omega_3 = p_1 - p_2 \tag{5.59}$$

[5]Here we refer to momenta p_1 and p_2 even though they do not occur in the problem. It is possible to pick a basis based directly on P, see appendix F.2.

which all are perpendicular to P^μ and to each other. BasisDet gives that a general basis will contain nine terms, which we choose as

$$\begin{aligned}\Delta_{\text{bubble}} = {} & c_1 + c_2(k\cdot\omega_1) + c_3(k\cdot\omega_2) + c_4(k\cdot\omega_3) \\ & + c_5(k\cdot\omega_1)(k\cdot\omega_2) + c_6(k\cdot\omega_2)(k\cdot\omega_3) + c_7(k\cdot\omega_1)(k\cdot\omega_3) \\ & + c_8\big((k\cdot\omega_1)^2 + (k\cdot\omega_2)^2\big) + c_9\big((k\cdot\omega_1)^2 - (k\cdot\omega_2)^2 + 2(k\cdot\omega_3)^2\big)\end{aligned} \tag{5.60}$$

where we see that only the first term is non-spurious.

The double-cut has only one solution:

$$\tilde{k} = \tau_1 p_1 + (1-\tau_1)p_2 + \tau_2\frac{\langle 1|\sigma^\mu|2]}{2} + \frac{\tau_1(1-\tau_1)}{\tau_2}\frac{\langle 2|\sigma^\mu|1]}{2} \tag{5.61}$$

and inserting this into eq. (5.60), allows us to write the $\Delta_{\text{bubble}}|_{\text{cut}}$ as a Laurent polynomial in τ_1 and τ_2 with a total of 25 terms, with the relation being

$$\bar{d} = M\bar{c} \tag{5.62}$$

where M is a 25×9 matrix with full rank.

The tree-product will be given as

$$\begin{aligned}\Delta_{\text{box;13}}|_{2\times\text{cut}} = {} & i^2\sum_{h_1,h_3}\mathcal{A}_4(-l_1^{-h_1}p_1^{a_1}p_2^{a_2}l_3^{h_3})\mathcal{A}_4(-l_3^{-h_3}p_3^{a_3}p_4^{a_4}l_1^{h_1}) \\ & - \frac{\Delta_{\text{tri;123}}|_{2\times\text{cut}}}{l_2^2} - \frac{\Delta_{\text{tri;134}}|_{2\times\text{cut}}}{l_4^2} - \frac{\Delta_{\text{box}}|_{2\times\text{cut}}}{l_2^2\,l_4^2}\end{aligned} \tag{5.63}$$

where we see that three subtraction terms are necessary, two from the two triangles which contain both l_1 and l_3, and one from the box.

Like for the triangle-case we will not list the results here, just note that there are three different helicity configurations $(--++)$, $(-+-+)$, and $(-+-+)$, of which $(--++)$ vanishes identically, and the other two vanish in $\mathcal{N}=4$ SYM as expected.

5.4 The tadpole coefficients

The tadpole integrals

$$I_{\text{tadpole}} = \int\frac{\mathrm{d}^d\tilde{k}}{(2\pi)^d}\frac{1}{\tilde{k}^2} \tag{5.64}$$

all vanish for the same reason as the adjacent bubbles of eq. (5.57), and thus evaluating the corresponding irreducible numerators Δ_{tadpole} is physically irrelevant and will not be pursued here.

Chapter 6

Two-loop cases

In this chapter we will calculate the three two-loop seven-propagator contributions to $2 \to 2$ scattering in Yang-Mills theories in four dimensions. The results of this chapter are based on [1].

6.1 The double-box ($t331$)

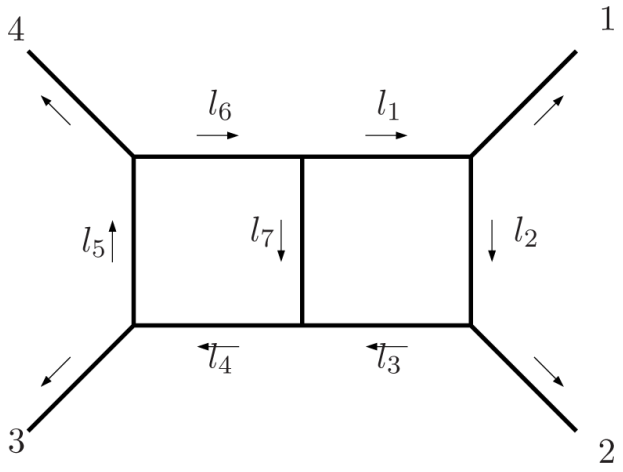

Figure 6.1: The double-box topology ($t331$) with the loop-momenta of eq. (6.2) shown.

The double-box contribution to the four-point amplitude is defined as

$$A_{331} = \int \frac{\mathrm{d}^d k_1}{(2\pi)^d} \int \frac{\mathrm{d}^d k_2}{(2\pi)^d} \frac{\Delta_{331}}{\prod_{i=1}^{7} l_i^2} \tag{6.1}$$

where we will parametrize the seven loop momenta as

$$\begin{aligned} &l_1 = k_1, && l_2 = k_1 - p_1, && l_3 = k_1 - p_1 - p_2, && l_4 = p_3 + p_4 - k_2, \\ &l_5 = p_4 - k_2, && l_6 = -k_2, && l_7 = -k_1 - k_2, \end{aligned} \tag{6.2}$$

as shown on fig. 6.1.

We will abbreviate the double-box as $(t331)$, referring to the number of propagators along each of the three branches as described in section 1.1. We choose to describe the system using a basis of four vectors $\beta = \{p_1, p_2, p_4, \omega\}$, with ω as in eq. (5.8)

$$\omega^\mu \equiv \frac{\langle 231]}{s}\frac{\langle 1|\sigma^\mu|2]}{2} - \frac{\langle 132]}{s}\frac{\langle 2|\sigma^\mu|1]}{2} \tag{6.3}$$

The system has four ISPs, with a natural choice being the set

$$(k_1 \cdot p_4),\ (k_2 \cdot p_1),\ (k_1 \cdot \omega),\ (k_2 \cdot \omega) \tag{6.4}$$

making the expression for Δ_{331} have the form

$$\Delta_{331} = \sum_{i_1 i_2 i_3 i_4} c_{i_1 i_2 i_3 i_4} (k_1 \cdot p_4)^{i_1} (k_2 \cdot p_1)^{i_2} (k_1 \cdot \omega)^{i_3} (k_2 \cdot \omega)^{i_4} \tag{6.5}$$

Performing the division towards the Gröbner basis of the ideal formed by the seven propagators as described in the previous chapters and in chapter 9, we find the most general basis to contain 32 terms, which can be chosen as the set corresponding to the coefficients

$$\begin{aligned}\{&c_{0000}, c_{0100}, c_{1000}, c_{0200}, c_{1100}, c_{2000}, c_{0300}, c_{1200}, c_{2100}, c_{3000}, c_{0400},\\ &c_{1300}, c_{3100}, c_{4000}, c_{1400}, c_{4100}, c_{0010}, c_{0110}, c_{1010}, c_{1110}, c_{2010}, c_{2110},\\ &c_{3010}, c_{3110}, c_{0001}, c_{0101}, c_{1001}, c_{0201}, c_{1101}, c_{0301}, c_{1201}, c_{1301}\}\end{aligned} \tag{6.6}$$

where only the first 16 coefficients are non-spurious.

As in the one-loop cases, we want to find the coefficients of Δ_{331} using unitarity cuts. After the hepta-cut we may identify Δ_{331} as the helicity-sum of the products of the six trees obtained from the cuts, i.e.

$$\begin{aligned}\Delta_{331}|_{7\times\text{cut}} = i^7 \sum_f \sum_{h\in\pm} &\mathcal{A}(-l_1^{-h_1}, p_1^{a_1}, l_2^{h_2})\mathcal{A}(-l_2^{-h_2}, p_2^{a_2}, l_3^{h_3})\mathcal{A}(-l_3^{-h_3}, -l_7^{-h_7}, l_4^{h_4})\\ &\times \mathcal{A}(-l_4^{-h_4}, p_3^{a_3}, l_5^{h_5})\mathcal{A}(-l_5^{-h_5}, p_4^{a_4}, l_6^{h_6})\mathcal{A}(-l_6^{-h_6}, l_1^{h_1}, l_7^{h_7})\end{aligned} \tag{6.7}$$

where the h_i denote the helicities internal to the sum, the a_i denote the helicities of the external particles, and the f the flavours of the internal particles.

The hepta-cut equations have six solutions. Parametrizing as

$$\begin{aligned}k_1^\mu &= x_1 p_1^\mu + x_2 p_2^\mu + x_3 \frac{\langle 23\rangle}{\langle 13\rangle}\frac{\langle 1|\sigma^\mu|2]}{2} + x_4 \frac{[23]}{[13]}\frac{\langle 2|\sigma^\mu|1]}{2}\\ k_2^\mu &= y_1 p_3^\mu + y_2 p_4^\mu + y_3 \frac{\langle 41\rangle}{\langle 31\rangle}\frac{\langle 3|\sigma^\mu|4]}{2} + y_4 \frac{[41]}{[31]}\frac{\langle 4|\sigma^\mu|3]}{2}\end{aligned} \tag{6.8}$$

the solutions are given as[1]

Solution	x_1	x_2	x_3	x_4	y_1	y_2	y_3	y_4
1	1	0	1	0	0	1	τ	0
2	1	0	0	1	0	1	0	τ
3	1	0	τ	0	0	1	-1	0
4	1	0	0	τ	0	1	0	-1
5	1	0	0	$\frac{s-u\tau}{t\tau}$	0	1	$\frac{u}{t}(1+\tau)$	0
6	1	0	$\frac{s-u\tau}{t\tau}$	0	0	1	0	$\frac{u}{t}(1+\tau)$

(6.9)

and we notice[2] that the solutions come in complex conjugated pairs.

Inserting one of the first four solutions into eq. (6.5), will give powers of τ going from zero to four, while inserting solutions five or six will give powers going from -4 to 4, that is

$$\Delta_{331}|_{\text{cut } s} = \begin{cases} \sum_{i=0}^{4} d_{si}\tau^i & s \in \{1,2,3,4\} \\ \sum_{i=-4}^{4} d_{si}\tau^i & s \in \{5,6\} \end{cases} \tag{6.10}$$

which has 38 terms in total.

Again we may relate the coefficients of eqs. (6.5) and (6.10) as

$$\bar{d} = M\bar{c} \tag{6.11}$$

where M is a 38×32 matrix, for which me may find a pseudo-inverse (using the method of appendix F.5) that uniquely identifies the cs.

The non-spurious integrals corresponding to the first 16 terms of eq. (6.6) are not independent but are related through a number of IBP-identities as described in section 4.3. In fact there are only two independent integrals (master integrals) which can be chosen as those corresponding to the numerators 1 and $(k\cdot p_4)$ meaning that the integral of the double-box topology can be written as

$$A_{331} = \int \frac{\mathrm{d}^4k_1}{(2\pi)^4} \int \frac{\mathrm{d}^4k_2}{(2\pi)^4} \frac{C_1 + C_2(k_1\cdot p_4)}{l_1^2\, l_2^2\, l_3^2\, l_4^2\, l_5^2\, l_6^2\, l_7^2} + \dots \tag{6.12}$$

where the ellipses cover terms with correspond to lower topologies, that is to topologies with less then seven propagators. C_1 and C_2 are related to the coefficients of

[1] The parametrization is different from what we used in [1], but the ordering of the solutions is the same.

[2] Another thing which one might notice is the one-to-one correspondence between these solutions and the non-vanishing combinations of MHV and MHV-bar trees in the sum of eq. (6.7). Such a correspondence exists for all the four-dimensionally cut diagrams in this thesis. We will not say anything more about this, see for instance [14].

eq. (6.5) through

$$C_1 = c_{000} + \frac{s_{12}s_{14}}{8}c_{1100} - \frac{s_{12}^2 s_{14}}{16}(c_{1200} + c_{2100}) + \frac{s_{12}^3 s_{14}}{32}(c_{1300} + c_{3100}) - \frac{s_{12}^4 s_{14}}{64}(c_{1400} + c_{4100}), \tag{6.13}$$

$$C_2 = c_{1000} + c_{0100} - \frac{3s_{12}}{4}c_{1100} + \frac{s_{14}}{2}(c_{0200} + c_{2000}) + \frac{3s_{12}^2}{8}(c_{1200} + c_{2100}) + \frac{s_{14}^2}{4}(c_{0300} + c_{3000}) - \frac{3s_{12}^3}{16}(c_{1300} + c_{3100}) + \frac{s_{14}^3}{8}(c_{0400} + c_{4000}) + \frac{3s_{12}^4}{32}(c_{1400} + c_{4100}). \tag{6.14}$$

6.2 The crossed box $(t322)$

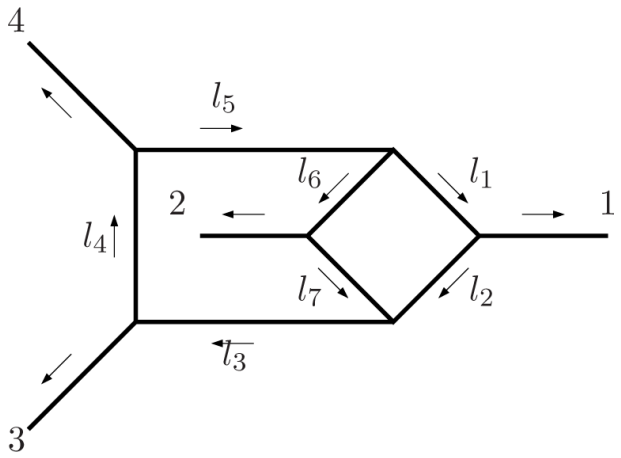

Figure 6.2: The crossed box topology $(t322)$.

The only non-planar seven-propagator contribution at two-loop four-point, is the crossed box, $(t322)$, which is shown on fig. 6.2. We will choose to parametrize it in terms of

$$\begin{aligned} l_1 &= k_1 + p_1 & l_2 &= k_1 & l_3 &= k_2 + p_3 & l_4 &= k_2 \\ l_5 &= k_2 - p_4 & l_6 &= k_2 - k_1 + p_2 + p_3 & l_7 &= k_2 - k_1 + p_3 \end{aligned} \tag{6.15}$$

As for the double-box there are four ISPs, and we pick the set

$$(k_1 \cdot p_3),\ (k_2 \cdot p_2),\ (k_1 \cdot \omega),\ (k_2 \cdot \omega), \tag{6.16}$$

with ω defined by eq. (6.3) as for the double-box case. This makes the general expression for the irreducible numerator

$$\Delta_{322} = \sum_{i_1 i_2 i_3 i_4} c_{i_1 i_2 i_3 i_4} (k_1 \cdot p_3)^{i_1} (k_2 \cdot p_2)^{i_2} (k_1 \cdot \omega)^{i_3} (k_2 \cdot \omega)^{i_4} \tag{6.17}$$

with 38 terms remaining in R/I after the polynomial division, namely those given by the list

$$\begin{aligned}\{&c_{0000}, c_{0100}, c_{1000}, c_{0200}, c_{1100}, c_{2000}, c_{0300}, c_{1200}, c_{2100}, c_{3000}, c_{0400},\\ &c_{2200}, c_{3100}, c_{4000}, c_{0500}, c_{3200}, c_{4100}, c_{0600}, c_{4200}, c_{0010}, c_{0110}, c_{1010},\\ &c_{1110}, c_{2010}, c_{2110}, c_{3010}, c_{3110}, c_{0001}, c_{0101}, c_{1001}, c_{0201}, c_{1101}, c_{0301},\\ &c_{1201}, c_{0401}, c_{1301}, c_{0501}, c_{1401}\}\end{aligned} \tag{6.18}$$

where the first 19 coefficients are non-spurious, and the remaining 19 are spurious.

Like before we want to find these coefficients by performing a hepta-cut. On the cut solutions, Δ_{322} will be given as a product of trees:

$$\begin{aligned}\Delta_{322}|_{7\times\text{cut}} = i^7 \sum_{h\in\pm} &\mathcal{A}(-l_1^{-h_1}, p_1^{a_1}, l_2^{h_2})\mathcal{A}(-l_2^{-h_2}, l_3^{h_3}, -l_7^{-h_7})\mathcal{A}(-l_3^{-h_3}, p_3^{a_3}, l_4^{h_4})\\ &\times \mathcal{A}(-l_4^{-h_4}, p_4^{a_4}, l_5^{h_5})\mathcal{A}(-l_5^{-h_5}, l_1^{h_1}, l_6^{h_6})\mathcal{A}(-l_6^{-h_6}, l_7^{h_7}, p_2^{a2})\end{aligned} \tag{6.19}$$

and parametrizing as before

$$\begin{aligned}k_1^\mu &= x_1 p_1^\mu + x_2 p_2^\mu + x_3 \frac{\langle 23\rangle}{\langle 13\rangle}\frac{\langle 1|\sigma^\mu|2]}{2} + x_4 \frac{[23]}{[13]}\frac{\langle 2|\sigma^\mu|1]}{2}\\ k_2^\mu &= y_1 p_3^\mu + y_2 p_4^\mu + y_3 \frac{\langle 41\rangle}{\langle 31\rangle}\frac{\langle 3|\sigma^\mu|4]}{2} + y_4 \frac{[41]}{[31]}\frac{\langle 4|\sigma^\mu|3]}{2}\end{aligned} \tag{6.20}$$

we find eight solutions to the hepta-cut equations, specified by

Solution	x_1	x_2	x_3	x_4	y_1	y_2	y_3	y_4
1	$\frac{t}{s}(1-\tau)$	0	$-\frac{u+t\tau}{s}$	0	0	0	τ	0
2	$\frac{t}{s}(1-\tau)$	0	0	$-\frac{u+t\tau}{s}$	0	0	0	τ
3	0	0	τ	0	0	0	1	0
4	0	0	0	τ	0	0	0	1
5	$\frac{t}{s}(1-\tau)$	0	0	$\frac{u}{s}(\tau-1)$	0	0	τ	0
6	$\frac{t}{s}(1-\tau)$	0	$\frac{u}{s}(\tau-1)$	0	0	0	0	τ
7	-1	0	0	τ	0	0	$-\frac{u}{t}$	0
8	-1	0	τ	0	0	0	0	$-\frac{u}{t}$

(6.21)

which again is parametrized by τ, the one remaining degree of freedom.

For the different cut-solutions different powers of τ may appear, the expansion is given by

$$\Delta_{322}|_{\text{cut } s} = \begin{cases} \sum_{i=0}^{6} d_{si}\tau^i & s \in \{1,2,5,6\} \\ \sum_{i=0}^{4} d_{si}\tau^i & s \in \{3,4,7,8\} \end{cases} \tag{6.22}$$

giving 48 d-coefficients in total. This makes the relation between the coefficients

$$\bar{d} = M\bar{c} \tag{6.23}$$

where M is a 48×38 for this case.

Like for the case of the double-box, there are relations between the 19 non-spurious coefficients of eq. (6.18). There are also two independent contributions for this topology, which we may chose as the integrals with numerator 1 and $(k_1 \cdot p_3)$. In that case the relation to the coefficients of eq. (6.17) is

$$\begin{aligned}
C_1 = & c_{0000} + \frac{1}{16} s_{14} s_{13} (c_{2000} - c_{1100} + 2c_{0200}) \\
& + \frac{1}{32} s_{14} s_{13} (s_{14} - s_{13}) (c_{3000} - c_{2100} + c_{1200} - 2c_{0300}) \\
& + \frac{1}{16^2} (3(s_{14} - s_{13})^2 + s_{12}^2) s_{14} s_{13} (c_{4000} - c_{3100} + c_{2200} + 2c_{0400}) \\
& + \frac{1}{16^2} ((s_{14} - s_{13})^2 + s_{12}^2) s_{14} s_{13} (s_{14} - s_{13}) (c_{3200} - c_{4100} - 2c_{0500}) \\
& + \frac{1}{16^3} (5(s_{14} - s_{13})^4 + 10 s_{12}^2 (s_{14} - s_{13})^2 + s_{12}^4) s_{14} s_{13} (c_{4200} + 2c_{0600}) \,, \\
C_2 = & c_{1000} - 2c_{0100} + \frac{3}{8} (s_{14} - s_{13}) (c_{2000} - c_{1100} + 2c_{0200}) \\
& + \frac{1}{16} (2(s_{14} - s_{13})^2 + s_{12}^2) (c_{3000} - c_{2100} + c_{1200} - 2c_{0300}) \\
& + \frac{2}{16^2} (5(s_{14} - s_{13})^2 + 7 s_{12}^2) (s_{14} - s_{13}) (c_{4000} - c_{3100} + c_{2200} + 2c_{0400}) \\
& + \frac{1}{16^2} (3(s_{14} - s_{13})^4 + 8 s_{12}^2 (s_{14} - s_{13})^2 + s_{12}^4) (c_{3200} - c_{4100} - 2c_{0500}) \\
& + \frac{2}{16^3} \left(7(s_{14} - s_{13})^4 + 30 s_{12}^2 (s_{14} - s_{13})^2 + 11 s_{12}^4\right) (s_{14} - s_{13}) (c_{4200} + 2c_{0600}) \,.
\end{aligned} \tag{6.24, 6.25}$$

6.3 The pentagon-triangle $(t421)$

The pentagon-triangle $(t421)$, which is shown in fig. 6.3, is the last seven-propagator topology at four-point two-loop. It may be parametrized by the seven loop-momenta

$$\begin{aligned}
& l_1 = k_2 - k_1 - p_4 \quad && l_2 = k_2 - k_1 + p_2 + p_3 \quad && l_3 = k_2 + p_2 + p_3 \quad && l_4 = k_2 + p_3 \\
& l_5 = k_2 && l_6 = k_2 - p_4 && l_7 = k_1
\end{aligned} \tag{6.26}$$

Naively it will have four ISPs like the other two topologies, one might for instance pick the set $\{(k_1 \cdot p_2), (k_1 \cdot p_4), (k_1 \cdot \omega), (k_2 \cdot \omega)\}$. But it turns out that one of the four $\big((k_1 \cdot \omega)\big)$ appears linearly in the Gröbner basis, making it reducible after all, so the general form of the integrand will be

$$\Delta_{421} = \sum_{i_1 i_2 i_3} c_{i_1 i_2 i_3} (k_1 \cdot p_2)^{i_1} (k_1 \cdot p_4)^{i_2} (k_2 \cdot \omega)^{i_3} \tag{6.27}$$

with the 20 coefficients

$$\begin{aligned}
\{ & c_{000}, c_{100}, c_{010}, c_{020}, c_{110}, c_{200}, c_{030}, c_{120}, c_{210}, c_{300}, \\
& c_{001}, c_{101}, c_{011}, c_{021}, c_{111}, c_{201}, c_{031}, c_{121}, c_{211}, c_{301} \}
\end{aligned} \tag{6.28}$$

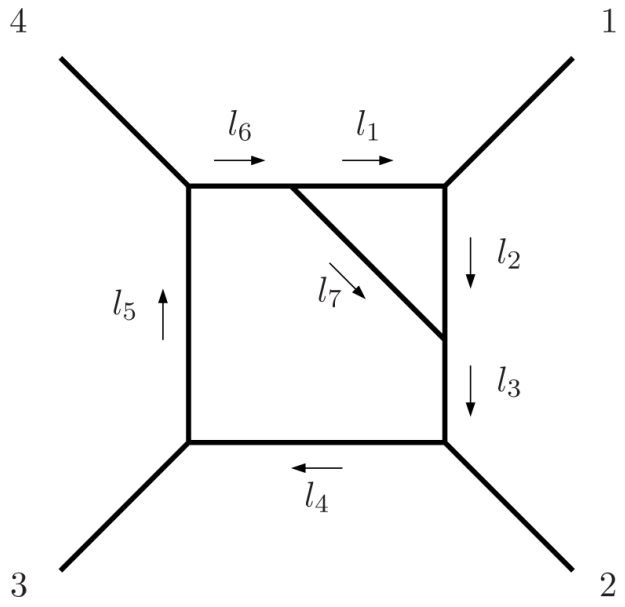

Figure 6.3: The pentagon-triangle topology ($t421$).

half of which are spurious.

The cut-solutions turn out to be redundant too, and after taking the redundancy into account there are two solutions to the hepta-cut equations

Solution	x_1	x_2	x_3	x_4	y_1	y_2	y_3	y_4
1	τ_1	0	τ_2	0	0	0	1	0
2	τ_1	0	0	τ_2	0	0	0	1

(6.29)

which due to the redundancy need two free parameters (τ_1 and τ_2) for a complete characterization.

Inserting the solutions into eq. (6.27), gives that each solution has ten different combinations of the τ-variables

$$\Delta_{421}|_{\text{cut } s} = \sum_{i,j=0}^{i+j\leq 3} d_{sij}\tau_1^i\tau_2^j \tag{6.30}$$

making the equation relating the coefficients

$$\bar{d} = M\bar{c} \tag{6.31}$$

a 20×20 linear system[3].

Applying IBP identities to each term of eq. (6.27) yields the result that all coefficients for the pentagon-triangle topology are reducible to topologies with fewer propagators.

[3]For the pentagon-triangle there is a particularly pretty closed form for this relation. See [1].

6.4 Results in Yang-Mills theories

Everything in the first parts of this chapter holds true for any renormalizable theory of massless particles. In this section we will look particularly at the results in a theory with a gluon, n_f fermions (gluinos), and n_s complex scalars, all transforming under the adjoint representation of the gauge group, but with the external particles all being gluons. The matter can flow in the loops in ten different ways, as shown in fig. 6.4 where the multiplicative flavour factor each contribution gets is listed too.

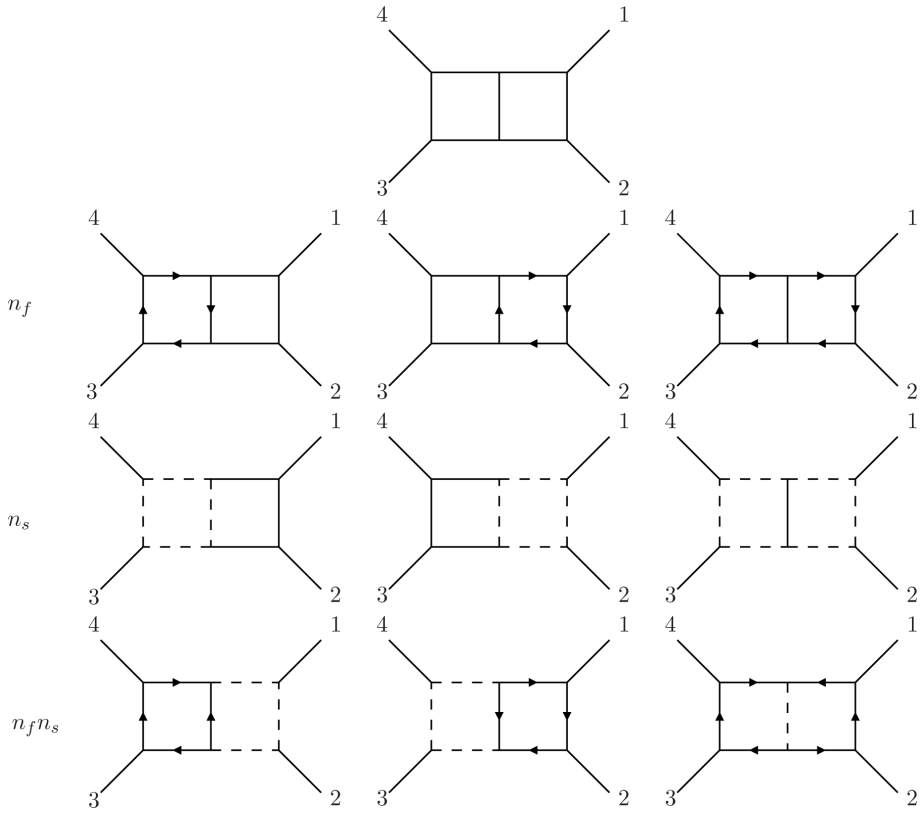

Figure 6.4: The ten flavour contributions to $gg \to gg$ at two-loop, exemplified by the ($t331$) topology. The corresponding flavour factors are also shown.

Pure Yang-Mills theory and all its super-symmetric extensions fall in the category of theories covered, where for each value of $\mathcal{N}$ the matter content is given as

$\mathcal{N}$	n_f	n_s
0	0	0
1	1	0
2	2	1
4	4	3

(6.32)

as we saw in section 3.5.

The double-box ($t331$)

For the double-box ($t331$), there are three fundamentally different, non-vanishing configurations of the helicities of the external particles[4], $(--++)$, $(-+-+)$, and $(-++-)$. The opposite helicity configurations are non-vanishing too, and can be obtained by complex conjugation.

For the configuration $(--++)$, the value of Δ_{331} is

$$\Delta_{331}^{--++} = -s_{12}^2 s_{14} \mathcal{A}^{(0)}{}_{331}^{--++} \tag{6.33}$$

that is only the c_{0000}-coefficient has a non-zero value, and that too is zero for both the fermionic and the scalar contribution. In terms of the coefficients of the two master integrals of eqs. (6.13) and (6.14) which Δ_{331} may be reduced to, the result is (obviously)

$$C_1^{--++} = -s_{12}^2 s_{14} \mathcal{A}^{(0)}{}_{331}^{--++} \tag{6.34}$$

$$C_2^{--++} = 0 \tag{6.35}$$

For the configuration $(-+-+)$, the result is

$$\begin{aligned}
\Delta_{331}^{-+-+} = \mathcal{A}^{(0)}{}_{331}^{-+-+} \Big[& - s_{14} {s_{12}}^2 \\
& - \frac{(4-n_f)(3-n_s) s_{14} {s_{12}}^2}{{s_{13}}^3} ((k_1\cdot p_4) + (k_2\cdot p_1)) \left(2(k_1\cdot p_4)\left(2(k_2\cdot p_1) + s_{12}\right) + s_{12}\left(2(k_2\cdot p_1) - s_{14}\right)\right) \\
& + \frac{s_{14} {s_{12}}^2 (1-n_f+n_s)}{{s_{13}}^4} \Big(16(k_1\cdot p_4)^3 \left(2(k_2\cdot p_1) + s_{14}\right) + 4(k_1\cdot p_4)^2 \left(6 s_{12}(k_2\cdot p_1) + (2 s_{12} - s_{14}) s_{14}\right) \\
& + 4(k_1\cdot p_4)\left(6 s_{12}(k_2\cdot p_1)^2 + s_{12}\left(2 s_{12} - s_{14}\right)(k_2\cdot p_1) + 8(k_2\cdot p_1)^3 - s_{12} {s_{14}}^2\right) \\
& - 16(k_1\cdot p_4)^4 - \left(s_{14}\left(2(k_2\cdot p_1) + s_{12}\right) - 4(k_2\cdot p_1)^2\right)^2 \Big) \\
& + \frac{(4-n_f) s_{14} {s_{12}}^2}{2 {s_{13}}^3} \Big(4(k_1\cdot p_4)^2 \left(4(k_2\cdot p_1) + 3 s_{12} + s_{14}\right) + 2(k_1\cdot p_4)\left(2(k_2\cdot p_1) - s_{14}\right)\left(4(k_2\cdot p_1) + 3 s_{12} + s_{14}\right) \\
& + 4\left(3 s_{12} + s_{14}\right)(k_2\cdot p_1)^2 - 2 s_{14}\left(3 s_{12} + s_{14}\right)(k_2\cdot p_1) + s_{12} s_{13} s_{14} \\
& + \frac{2(4-n_f)(3-n_s) s_{14} {s_{12}}^2}{{s_{13}}^3} \left((k_2\cdot p_1)\left(2(k_1\cdot p_4) + s_{12}\right)(k_2\cdot\omega) - (k_1\cdot p_4)(k_1\cdot\omega)\left(2(k_2\cdot p_1) + s_{12}\right)\right) \\
& + \frac{s_{14} {s_{12}}^2 (1-n_f+n_s)}{{s_{13}}^4} \Big(\\
& (k_1\cdot\omega)\Big(8(k_1\cdot p_4)^2\left(4(k_2\cdot p_1) + s_{14}\right) + 8(k_1\cdot p_4)\left(3 s_{12}(k_2\cdot p_1) + s_{14}\left(2(k_2\cdot p_1) + s_{12}\right)\right) \\
& - 16(k_1\cdot p_4)^3 + {s_{12}}^2\left(2(k_2\cdot p_1) + s_{14}\right)\Big) \\
& + (k_2\cdot\omega)\Big(- 2(k_1\cdot p_4)\left(4\left(3 s_{12} + 2 s_{14}\right)(k_2\cdot p_1) + 16(k_2\cdot p_1)^2 + {s_{12}}^2\right) \\
& - s_{14}\left(8 s_{12}(k_2\cdot p_1) + 8(k_2\cdot p_1)^2 + {s_{12}}^2\right) + 16(k_2\cdot p_1)^3\Big)\Big) \\
& + \frac{(4-n_f) {s_{12}}^2}{2 {s_{13}}^3} \Big(s_{12} s_{13}(-(k_1\cdot\omega))\left(2(k_2\cdot p_1) + s_{14}\right) \\
& + 2(k_1\cdot p_4)\left(2 s_{14}(k_1\cdot\omega)\left(4(k_2\cdot p_1) + 3 s_{12} + s_{14}\right) + \left(s_{12} s_{13} - 8 s_{14}(k_2\cdot p_1)\right)(k_2\cdot\omega)\right) \\
& + s_{14}\left(s_{12} s_{13} - 4\left(3 s_{12} + s_{14}\right)(k_2\cdot p_1)\right)(k_2\cdot\omega)\Big)\Big]
\end{aligned} \tag{6.36}$$

[4] that is (a_1, a_2, a_3, a_4) in the notation of eq. (6.7).

and the corresponding master integral coefficients are

$$C_1^{-+-+} = \frac{1}{4}{s_{12}}^2 s_{14}\mathcal{A}^{(0)}{}_{331}^{-+-+}\left(-\frac{6{s_{12}}^2{s_{14}}^2(1-n_f+n_s)}{{s_{13}}^4}+\frac{3(4-n_f)s_{12}s_{14}}{{s_{13}}^2}-4\right) \tag{6.37}$$

$$C_2^{-+-+} = \frac{3{s_{12}}^3 s_{14}}{2{s_{13}}^4}\mathcal{A}^{(0)}{}_{331}^{-+-+}\left(2s_{12}s_{14}(1-n_f+n_s)-(4-n_f){s_{13}}^2\right) \tag{6.38}$$

For the $(-++-)$ configuration the integrand is:

$$\begin{aligned}
\Delta_{331}^{-++-} = \mathcal{A}^{(0)}{}_{331}^{-++-}\Big[& -s_{14}{s_{12}}^2 \\
& -\frac{4{s_{12}}^2(1-n_f+n_s)}{{s_{14}}^3}\Big((k_1\cdot p_4)^3\left(8(k_2\cdot p_1)-4s_{14}\right)+(k_1\cdot p_4)^2\left({s_{14}}^2-2\left(3s_{12}+4s_{14}\right)(k_2\cdot p_1)\right) \\
& +(k_1\cdot p_4)(k_2\cdot p_1)\left(4(k_2\cdot p_1)-3s_{12}-2s_{14}\right)\left(2(k_2\cdot p_1)-s_{14}\right)+4(k_1\cdot p_4)^4+(k_2\cdot p_1)^2\left(s_{14}-2(k_2\cdot p_1)\right)^2\Big) \\
& +\frac{2(4-n_f)(3-n_s){s_{12}}^2}{{s_{14}}^2}(k_1\cdot p_4)(k_2\cdot p_1)\left(2((k_1\cdot p_4)+(k_2\cdot p_1))-s_{14}\right) \\
& +\frac{(4-n_f){s_{12}}^2}{{s_{14}}^2}\Big({s_{14}}^2((k_1\cdot p_4)+(k_2\cdot p_1))-2s_{14}\left(-(k_1\cdot p_4)(k_2\cdot p_1)+(k_1\cdot p_4)^2+(k_2\cdot p_1)^2\right) \\
& -8(k_1\cdot p_4)(k_2\cdot p_1)((k_1\cdot p_4)+(k_2\cdot p_1))\Big) \\
& +\frac{(4-n_f)(3-n_s){s_{12}}^2}{2s_{13}{s_{14}}^2}\Big(s_{12}{s_{14}}^2((k_1\cdot\omega)+(k_2\cdot\omega))-2s_{12}s_{14}((k_1\cdot p_4)(k_2\cdot\omega)+(k_2\cdot p_1)(k_1\cdot\omega)) \\
& +8s_{13}(k_1\cdot p_4)(k_2\cdot p_1)((k_1\cdot\omega)+(k_2\cdot\omega))\Big) \\
& +\frac{{s_{12}}^2(1-n_f+n_s)}{s_{13}{s_{14}}^3}\Big(2s_{12}{s_{14}}^3((k_1\cdot\omega)+(k_2\cdot\omega)) \\
& +s_{12}{s_{14}}^2\left(3s_{12}((k_1\cdot\omega)+(k_2\cdot\omega))-4(k_1\cdot p_4)(k_2\cdot\omega)-4(k_2\cdot p_1)(k_1\cdot\omega)\right) \\
& +2s_{14}\Big(4s_{13}\left(2(k_1\cdot p_4)(k_2\cdot p_1)((k_1\cdot\omega)+(k_2\cdot\omega))+(k_1\cdot p_4)^2(k_1\cdot\omega)+(k_2\cdot p_1)^2(k_2\cdot\omega)\right) \\
& -3{s_{12}}^2((k_1\cdot p_4)(k_2\cdot\omega)+(k_2\cdot p_1)(k_1\cdot\omega))\Big)-8s_{13}\Big(-3s_{12}(k_1\cdot p_4)(k_2\cdot p_1)((k_1\cdot\omega)+(k_2\cdot\omega)) \\
& +2\left((k_1\cdot p_4)^2((k_1\cdot p_4)+2(k_2\cdot p_1))(k_1\cdot\omega)+(k_2\cdot p_1)^2(2(k_1\cdot p_4)+(k_2\cdot p_1))(k_2\cdot\omega)\right)\Big)\Big) \\
& +\frac{(4-n_f){s_{12}}^2}{2s_{13}{s_{14}}^2}\Big(-3s_{12}{s_{14}}^2((k_1\cdot\omega)+(k_2\cdot\omega))-16s_{13}(k_1\cdot p_4)(k_2\cdot p_1)((k_1\cdot\omega)+(k_2\cdot\omega)) \\
& +2s_{14}\left(3s_{12}((k_1\cdot p_4)(k_2\cdot\omega)+(k_2\cdot p_1)(k_1\cdot\omega))-2s_{13}((k_1\cdot p_4)(k_1\cdot\omega)+(k_2\cdot p_1)(k_2\cdot\omega))\right)\Big)\Big]
\end{aligned} \tag{6.39}$$

and the master integral coefficients are

$$\begin{aligned}
C_1^{-++-} = & -\frac{{s_{12}}^2}{4{s_{14}}^2}\mathcal{A}^{(0)}{}_{331}^{-++-}\left(2s_{12}\left(10{s_{12}}^2+11s_{14}s_{12}+2{s_{14}}^2\right)(1-n_f+n_s)\right. \\
& \left.+s_{14}\left((4-n_f)(3-n_s)s_{12}\left(2s_{12}+s_{14}\right)-(4-n_f)s_{12}\left(4s_{12}+s_{14}\right)+4{s_{14}}^2\right)\right)
\end{aligned} \tag{6.40}$$

$$\begin{aligned}
C_2^{-++-} = & \frac{3{s_{12}}^3}{2{s_{14}}^3}\mathcal{A}^{(0)}{}_{331}^{-++-}\Big(\left(20{s_{12}}^2+22s_{14}s_{12}+4{s_{14}}^2\right)(1-n_f+n_s) \\
& +s_{14}\left((4-n_f)(3-n_s)\left(2s_{12}+s_{14}\right)-(4-n_f)\left(4s_{12}+s_{14}\right)\right)\Big)
\end{aligned} \tag{6.41}$$

We notice that the flavour factors always factorize out as $(4-n_f)$, $(3-n_s)$, and $(1-n_f+n_s)$. All of these factors vanish in $\mathcal{N}=4$, and additionally does $(1-n_f+n_s)$ vanish in all supersymmetric theories.

The crossed box ($t322$)

The crossed box too is non-vanishing only for the configurations $(--++)$, $(-+-+)$, and $(-++-)$, and their opposites.

For $(--++)$ the numerator is

$$
\begin{aligned}
\Delta_{322}^{--++} = \mathcal{A}^{(0)}{}_{322}^{--++} \Big[& - s_{14} {s_{12}}^2 \\
& + \frac{1}{2}(4-n_f) s_{14} \left(-2\left(s_{12}+2s_{14}\right)(k_2\cdot p_2) - 4(k_2\cdot p_2)^2 + s_{13}s_{14}\right) \\
& + \frac{s_{14}(1-n_f+n_s)}{{s_{12}}^2}\Big(- 4(k_2\cdot p_2)^2 \left(2(k_2\cdot p_2)+s_{12}\right)^2 - {s_{14}}^2\left(-8s_{13}(k_2\cdot p_2) + 24(k_2\cdot p_2)^2 + {s_{13}}^2\right) \\
& + 4s_{14}(k_2\cdot p_2)\left(-6s_{12}(k_2\cdot p_2) - 8(k_2\cdot p_2)^2 + s_{12}s_{13}\right)\Big) \\
& - \frac{(4-n_f)s_{12}}{2s_{13}}\left((k_2\cdot\omega)\left(s_{13}\left(2(k_2\cdot p_2)+s_{14}\right) - 2s_{12}(k_1\cdot p_3)\right) + 2(k_1\cdot\omega)\left(\left(s_{12}+2s_{14}\right)(k_2\cdot p_2) - s_{13}s_{14}\right)\right) \\
& + \frac{s_{14}(1-n_f+n_s)}{{s_{12}}^2}\Big(2(k_2\cdot p_2)\left({s_{12}}^2(3(k_1\cdot\omega)-(k_2\cdot\omega)) + 3s_{14}s_{12}(2(k_1\cdot\omega)+(k_2\cdot\omega)) + 6{s_{14}}^2(k_2\cdot\omega)\right) \\
& + 16\left(s_{12}+2s_{14}\right)(k_2\cdot p_2)^2(k_2\cdot\omega) + 16(k_2\cdot p_2)^3(k_2\cdot\omega) + s_{12}s_{13}s_{14}((k_2\cdot\omega)-2(k_1\cdot\omega)) \\
& + 2(k_1\cdot p_3)\left(16\left(s_{12}+2s_{14}\right)(k_2\cdot p_2) + 16(k_2\cdot p_2)^2 + {s_{12}}^2 + 12{s_{14}}^2 + 12s_{12}s_{14}\right)(k_2\cdot\omega)\Big)\Big]
\end{aligned}
\tag{6.42}
$$

and after applying the IBPs, this corresponds to the two master integral coefficients being

$$
C_1^{--++} = \mathcal{A}^{(0)}{}_{322}^{--++} \frac{1}{4} s_{14}\left(-\frac{2{s_{13}}^2{s_{14}}^2(1-n_f+n_s)}{{s_{12}}^2} + (4-n_f)s_{13}s_{14} - 4{s_{12}}^2\right) \tag{6.43}
$$

$$
C_2^{--++} = \mathcal{A}^{(0)}{}_{322}^{--++} \frac{-s_{14}}{2{s_{12}}^2}\left(s_{13}-s_{14}\right)\left((4-n_f){s_{12}}^2 - 2s_{13}s_{14}(1-n_f+n_s)\right) \tag{6.44}
$$

For the $(-+-+)$ configuration, the integrand is:

$$
\begin{aligned}
\Delta_{322}^{-+-+} &= \mathcal{A}^{(0)}{}_{322}^{-+-+}\Big[- s_{14}{s_{12}}^2 \\
&+ \frac{(4-n_f)s_{14}{s_{12}}^2}{{s_{13}}^3}\Big(- 2s_{13}\left(3(k_1\cdot p_3)(k_2\cdot p_2) + 3(k_1\cdot p_3)^2 + (k_2\cdot p_2)^2\right) \\
&+ 8(k_1\cdot p_3)(k_2\cdot p_2)((k_1\cdot p_3)+(k_2\cdot p_2)) + {s_{13}}^2(k_2\cdot p_2)\Big) \\
&- \frac{2(4-n_f)(3-n_s)s_{14}{s_{12}}^2}{{s_{13}}^3}(k_1\cdot p_3)((k_1\cdot p_3)+(k_2\cdot p_2))\left(2(k_2\cdot p_2)-s_{13}\right) \\
&+ \frac{4s_{14}{s_{12}}^2(1-n_f+n_s)}{{s_{13}}^4}\Big(2s_{14}(k_1\cdot p_3)((k_1\cdot p_3)+(k_2\cdot p_2))\left(2(k_2\cdot p_2)-s_{13}\right) - 8(k_1\cdot p_3)^3(k_2\cdot p_2) \\
&- 4(k_1\cdot p_3)^2(k_2\cdot p_2)^2 - 4(k_1\cdot p_3)^4 - {s_{13}}^2(k_2\cdot p_2)^2 + 4s_{13}(k_2\cdot p_2)^3 - 4(k_2\cdot p_2)^4\Big) \\
&+ \frac{(4-n_f)s_{12}s_{14}}{2{s_{13}}^3}\Big(2s_{12}(k_1\cdot\omega)\left(3s_{13}(2(k_1\cdot p_3)+(k_2\cdot p_2)) - 8(k_1\cdot p_3)(k_2\cdot p_2)\right) \\
&+ (k_2\cdot\omega)\left(2s_{12}s_{13}\left(-3(k_1\cdot p_3) - 5(k_2\cdot p_2) + s_{13}\right) + s_{14}\left(8(k_1\cdot p_3)+3s_{13}\right)\left(s_{13}-2(k_2\cdot p_2)\right)\right)\Big) \\
&- \frac{(4-n_f)(3-n_s)s_{12}s_{14}}{2{s_{13}}^3}\Big(2s_{12}(k_1\cdot\omega)\left(s_{13}(2(k_1\cdot p_3)+(k_2\cdot p_2)) - 4(k_1\cdot p_3)(k_2\cdot p_2)\right) \\
&+ (k_2\cdot\omega)\left(2(k_1\cdot p_3)\left(2s_{14}\left(s_{13}-2(k_2\cdot p_2)\right) - s_{12}s_{13}\right) + {s_{13}}^2\left(2(k_2\cdot p_2)+s_{14}\right)\right)\Big) \\
&+ \frac{s_{14}(1-n_f+n_s)}{{s_{13}}^4}\Big(2s_{12}(k_1\cdot\omega)\Big(8s_{12}(k_1\cdot p_3)^2((k_1\cdot p_3)+(k_2\cdot p_2)) \\
&+ {s_{14}}^2\left(4(k_1\cdot p_3)(k_2\cdot p_2) - s_{13}(2(k_1\cdot p_3)+(k_2\cdot p_2))\right) \\
&+ 2s_{14}\left(s_{13}\left(s_{12}(2(k_1\cdot p_3)+(k_2\cdot p_2)) + 2(k_1\cdot p_3)^2\right) - 4(k_1\cdot p_3)(k_2\cdot p_2)\left((k_1\cdot p_3)+s_{12}\right)\right) \\
&+ (k_2\cdot\omega)\Big({s_{14}}^3\left(-\left(8(k_1\cdot p_3)\left(s_{13}-3(k_2\cdot p_2)\right) + {s_{13}}^2\right)\right) \\
&+ 2{s_{14}}^2\left((k_1\cdot p_3)\left(8(k_2\cdot p_2)^2 + 3s_{12}s_{13}\right) + {s_{13}}^2\left(s_{12}-(k_2\cdot p_2)\right)\right) \\
&+ 4s_{12}s_{13}s_{14}\left(s_{13}(k_2\cdot p_2) - s_{12}(k_1\cdot p_3)\right) - 4{s_{12}}^2(k_2\cdot p_2)\left(s_{13}-2(k_2\cdot p_2)\right)^2\Big)\Big)\Big]
\end{aligned}
\tag{6.45}
$$

with the master integral coefficients being,

$$
C_1^{-+-+} = \mathcal{A}^{(0)}{}_{322}^{-+-+}\frac{{s_{12}}^2 s_{14}}{4{s_{13}}^3}\left(2s_{12}{s_{14}}^2(1-n_f+n_s) - (4-n_f)s_{14}{s_{13}}^2 - 4{s_{13}}^3\right) \tag{6.46}
$$

$$
C_2^{-+-+} = \mathcal{A}^{(0)}{}_{322}^{-+-+}\frac{{s_{12}}^2 s_{14}}{2{s_{13}}^4}\left(s_{13}+3s_{14}\right)\left(2s_{12}s_{14}(1-n_f+n_s) - (4-n_f){s_{13}}^2\right) \tag{6.47}
$$

And finally for the $(-++-)$-configuration the integrand is:

$$
\begin{aligned}
\Delta_{322}^{-++-} &= \mathcal{A}^{(0)}{}_{322}^{-++-}\Big[- s_{14}{s_{12}}^2 \\
&\frac{2(4-n_f)(3-n_s){s_{12}}^2}{{s_{14}}^2}(k_1\cdot p_3)((k_1\cdot p_3)+(k_2\cdot p_2))\,(2(k_2\cdot p_2)+s_{14}) \\
&- \frac{4{s_{12}}^2(1-n_f+n_s)}{{s_{14}}^3}\Big(2(k_1\cdot p_3)^2\,((k_2\cdot p_2)\,((k_2\cdot p_2)+s_{13})+s_{13}s_{14}) \\
&+ 2s_{13}(k_1\cdot p_3)(k_2\cdot p_2)\,(2(k_2\cdot p_2)+s_{14})+8(k_1\cdot p_3)^3(k_2\cdot p_2)+4(k_1\cdot p_3)^4+(k_2\cdot p_2)^2\,(2(k_2\cdot p_2)+s_{14})^{\,2}\Big) \\
&- \frac{(4-n_f){s_{12}}^2}{{s_{14}}^2}\Big(2s_{14}\left(3(k_1\cdot p_3)(k_2\cdot p_2)+3(k_1\cdot p_3)^2+(k_2\cdot p_2)^2\right) \\
&+ 8(k_1\cdot p_3)(k_2\cdot p_2)((k_1\cdot p_3)+(k_2\cdot p_2))+{s_{14}}^2(k_2\cdot p_2)\Big) \\
&+ \frac{(1-n_f+n_s)}{{s_{14}}^3}\Big(2s_{12}(k_1\cdot\omega)\big({s_{14}}^2\,(4(k_1\cdot p_3)(k_2\cdot p_2)-s_{13}(2(k_1\cdot p_3)+(k_2\cdot p_2)))\big) \\
&+ 2s_{14}\left(s_{13}\left(s_{12}(2(k_1\cdot p_3)+(k_2\cdot p_2))+2(k_1\cdot p_3)^2\right)-4(k_1\cdot p_3)(k_2\cdot p_2)\,((k_1\cdot p_3)+s_{12})\right) \\
&+ 8s_{12}(k_1\cdot p_3)\,((k_1\cdot p_3)((k_1\cdot p_3)+(k_2\cdot p_2))-s_{12}(k_2\cdot p_2))\,\big) \\
&+ (k_2\cdot\omega)\big({s_{14}}^3\left(8(k_1\cdot p_3)\,(3(k_2\cdot p_2)-s_{13})-{s_{13}}^2\right) \\
&+ 2{s_{14}}^2\left((k_1\cdot p_3)\left(8(k_2\cdot p_2)^2+3s_{12}s_{13}\right)+s_{12}\left(5s_{12}(k_2\cdot p_2)+{s_{13}}^2\right)\right) \\
&+ 4{s_{12}}^2s_{14}\,((k_2\cdot p_2)\,(-4(k_1\cdot p_3)+4(k_2\cdot p_2)+s_{12})+s_{13}(k_1\cdot p_3))-2{s_{14}}^4(k_2\cdot p_2)+16{s_{12}}^2(k_2\cdot p_2)^3)\Big) \\
&- \frac{(4-n_f)(3-n_s)s_{12}}{2{s_{14}}^2}\Big(2s_{12}(k_1\cdot\omega)\,(s_{14}(2(k_1\cdot p_3)+(k_2\cdot p_2))+4(k_1\cdot p_3)(k_2\cdot p_2)) \\
&+ s_{14}(k_2\cdot\omega)\,(2(k_1\cdot p_3)\,(4(k_2\cdot p_2)+s_{12}+2s_{14})+s_{13}\,(2(k_2\cdot p_2)+s_{14}))\,\Big) \\
&+ \frac{(4-n_f)s_{12}}{2{s_{14}}^2}\Big(2s_{12}(k_1\cdot\omega)\,(3s_{14}(2(k_1\cdot p_3)+(k_2\cdot p_2))+8(k_1\cdot p_3)(k_2\cdot p_2)) \qquad (6.48)\\
&- s_{14}(k_2\cdot\omega)\,((s_{12}+3s_{14})\,(2(k_2\cdot p_2)+s_{14})-2(k_1\cdot p_3)\,(8(k_2\cdot p_2)+s_{12}+4s_{14}))\Big)\Big]
\end{aligned}
$$

which lead to coefficients of the master integrals of,

$$C_1^{-++-} = \mathcal{A}^{(0)}{}_{322}^{-++-}\,\frac{{s_{12}}^2}{4{s_{14}}^2}\left(2s_{12}{s_{13}}^2(1-n_f+n_s)-{s_{14}}^2\left((4-n_f)s_{13}+4s_{14}\right)\right) \tag{6.49}$$

$$C_2^{-++-} = \mathcal{A}^{(0)}{}_{322}^{-++-}\,\frac{{s_{12}}^2}{2{s_{14}}^3}\,(3s_{13}+s_{14})\left((4-n_f){s_{14}}^2-2s_{12}s_{13}(1-n_f+n_s)\right) \tag{6.50}$$

The pentagon-triangle ($t421$)

Unlike the two topologies we have looked at so far, the pentagon-triangle topology ($t421$) is non-vanishing only for the configurations $(-+--)$, $(--+-)$, and their opposites, which all vanish at tree level.

For the $(-+--)$ configuration, the integrand is

$$\begin{aligned}\Delta^{-+--}_{421} = 4i(1-n_f+n_s)\frac{\langle 13\rangle^2\langle 14\rangle^2 s_{12}^3}{\langle 12\rangle^2 s_{13}^2 s_{14}}\Bigg((k_1\cdot p_2)(k_1\cdot p_4) \\ -\frac{2}{s_{12}}(k_1\cdot p_2)^2(k_1\cdot p_4)+\frac{2}{s_{14}}(k_1\cdot p_2)(k_1\cdot p_4)^2\Bigg) \\ -8i(1-n_f+n_s)\frac{\langle 13\rangle^2\langle 14\rangle^2 s_{12}^3}{\langle 12\rangle^2 s_{13}^2 s_{14}^2}\Bigg((k_1\cdot p_2)(k_1\cdot p_4) \\ -\frac{2}{s_{12}}(k_1\cdot p_2)^2(k_1\cdot p_4)+\frac{2}{s_{14}}(k_1\cdot p_2)(k_1\cdot p_4)^2\Bigg)(k_2\cdot\omega)\end{aligned} \tag{6.51}$$

and for the $(--+-)$ configuration it is

$$\begin{aligned}\Delta^{--+-}_{421} = 4i(1-n_f+n_s)\frac{\langle 12\rangle^2\langle 14\rangle^2 s_{13}^2}{\langle 13\rangle^2 s_{12} s_{14}}\Bigg((k_1\cdot p_2)(k_1\cdot p_4) \\ -\frac{2}{s_{12}}(k_1\cdot p_2)^2(k_1\cdot p_4)+\frac{2}{s_{14}}(k_1\cdot p_2)(k_1\cdot p_4)^2\Bigg) \\ -8i(1-n_f+n_s)\frac{\langle 12\rangle^2\langle 14\rangle^2 s_{13}^2}{\langle 13\rangle^2 s_{12} s_{14}^2}\Bigg((k_1\cdot p_2)(k_1\cdot p_4) \\ -\frac{2}{s_{12}}(k_1\cdot p_2)^2(k_1\cdot p_4)+\frac{2}{s_{14}}(k_1\cdot p_2)(k_1\cdot p_4)^2\Bigg)(k_2\cdot\omega)\end{aligned} \tag{6.52}$$

Discussion

We have compared the results to the known results from [14,98] and found complete agreement.

There is a couple of issues worth noticing. For $(t331)$ and $(t322)$ the results were always proportional to the tree-level amplitudes. This is not surprising, as that factor is more or less fixed by the little group weights corresponding to the helicities of the external particles as described in section 3.4. What is more surprising is that $(t421)$ vanishes for the MHV cases and only has a non-zero value for cases with three identical helicities[5]. Additionally we see $(t421)$ to vanish for all supersymmetric theories.

Another thing worth noticing is that[6] no terms with a total monomial power of five or higher appear, neither for $(t331)$ nor for $(t322)$, even though such terms are present in eqs. (6.6) and (6.18). The source of this is not completely clear as no restrictions, neither from the renormalization constraints nor from the Gram matrix identities, appear to rule out their presence.

[5] This is sometimes called UHV (ultra helicity violating) configurations.

[6] even though it is hard to see from the form of the equations as they are written here.

Chapter 7

Three-loop cases

Nothing in the methods described in the previous chapters restricts the integrand reduction procedure to two-loop (or one-loop) cases. In this section we will present the full result for the three-loop triple-box topology, based on the calculation done in [2], and additionally we will solve the on-shell constraints for an additional topology - the tennis court.

7.1 The triple-box

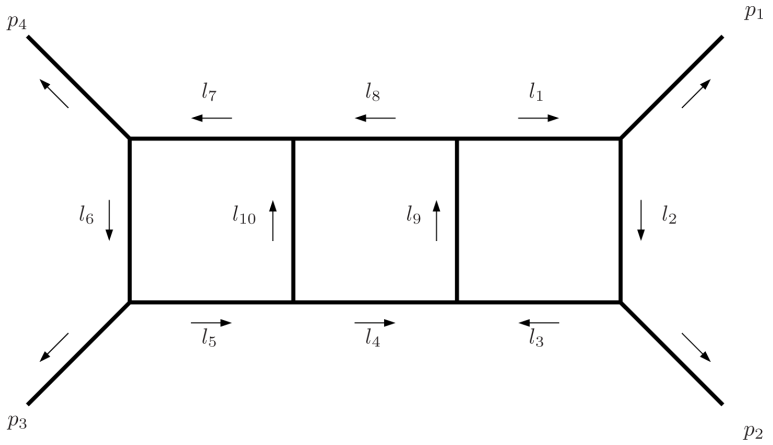

Figure 7.1: The triple-box topology with the loop-momenta shown.

The triple-box integral is defined as

$$A_{\text{triplebox}} = \int \frac{\mathrm{d}^d k_1}{(2\pi)^d} \int \frac{\mathrm{d}^d k_2}{(2\pi)^d} \int \frac{\mathrm{d}^d k_3}{(2\pi)^d} \frac{\Delta_{\text{triplebox}}}{\prod_{i=1}^{10} l_i^2}, \tag{7.1}$$

where we parametrize the ten propagating momenta as

$$\begin{aligned}
&l_1 = k_1, && l_2 = k_1 - p_1, && l_3 = k_1 - p_1 - p_2, && l_4 = k_3 + p_1 + p_2, \\
&l_5 = k_2 + p_1 + p_2, && l_6 = k_2 - p_4, && l_7 = k_2, && l_8 = k_3, \\
&l_9 = k_1 + k_3, && l_{10} = k_2 - k_3, &&&&
\end{aligned} \tag{7.2}$$

as shown on fig. 7.1.

Solution of on-shell constraints

The irreducible numerator $\Delta_{\text{triplebox}}$ of the triple-box topology, may be written in terms of monomials in seven ISPs, as

$$\begin{aligned}
\Delta_{\text{triplebox}} = \sum_{i_1 \cdots i_7} & c_{i_1 \cdots i_7} (k_1 \cdot p_4)^{i_1} (k_2 \cdot p_1)^{i_2} (k_3 \cdot p_4)^{i_3} (k_3 \cdot p_1)^{i_4} \\
& \times (k_1 \cdot \omega)^{i_5} (k_2 \cdot \omega)^{i_6} (k_3 \cdot \omega)^{i_7}
\end{aligned} \tag{7.3}$$

where a systematic approach using the multivariate polynomial division method described in the previous chapters will show that the maximal number of non-zero c-coefficients which may appear for any renormalizable theory is 398, for which half, 199, are spurious and the other half non-spurious.

We wish to identify the values of the coefficients of eq. (7.3) using generalized unitarity cuts as in the two- and one-loop cases. The deca-cut which cuts all the ten propagators of eqs. (7.2), turns out[1] to have 14 solutions which come in seven complex conjugate pairs, that we number 1-7 and 1′-7′.

Using the parametrization

$$\begin{aligned}
l_2 &= x_1 p_1 + x_2 p_2 + x_3 \frac{\langle 23 \rangle}{\langle 13 \rangle} \frac{\langle p_1 | \sigma^\mu | p_2]}{2} + x_4 \frac{\langle 13 \rangle}{\langle 23 \rangle} \frac{\langle p_2 | \sigma^\mu | p_1]}{2}, \\
-l_6 &= y_1 p_3 + y_2 p_4 + y_3 \frac{\langle 41 \rangle}{\langle 31 \rangle} \frac{\langle p_3 | \sigma^\mu | p_4]}{2} + y_4 \frac{\langle 31 \rangle}{\langle 41 \rangle} \frac{\langle p_4 | \sigma^\mu | p_3]}{2}, \\
-l_4 &= z_1 p_2 + z_2 p_3 + z_3 \frac{\langle 34 \rangle}{\langle 24 \rangle} \frac{\langle p_2 | \sigma^\mu | p_3]}{2} + z_4 \frac{\langle 24 \rangle}{\langle 34 \rangle} \frac{\langle p_2 | \sigma^\mu | p_3]}{2},
\end{aligned} \tag{7.4}$$

we get that each solution may be parametrized in terms of two free parameters which we name τ_1 and τ_2.

[1] For three-loop cases it is not trivial (though it can be done) to solve the generalized unitarity cut constraints by hand. It is useful to have a systematic algebraic method, and such a method which uses primary decomposition of the ideal formed by the ten propagators, is described in chapter 9.

The solutions 1-7 are given by

	x_1	x_2	x_3	x_4	y_1	y_2	y_3	y_4
1	0	0	$1-\frac{s}{t}\frac{1+\tau_1}{\tau_2}$	0	0	0	$1+\tau_2$	0
2	0	0	$-\frac{u}{t}(1+\tau_1)$	0	0	0	0	$-1+\frac{s}{u}\frac{1}{\tau_1}$
3	0	0	τ_2	0	0	0	0	$-1-\tau_1$
4	0	0	$-\frac{u}{t}(1+\tau_1)$	0	0	0	0	τ_2
5	0	0	τ_2	0	0	0	1	0
6	0	0	1	0	0	0	τ_2	0
7	0	0	τ_1	0	0	0	τ_2	0

	z_1	z_2	z_3	z_4
1	$\frac{s}{t}\left(1+\frac{1}{\tau_1}\right)\left(1+\frac{1}{\tau_2}\right)$	$-\frac{s}{t}\left(1+\frac{1}{\tau_1}\right)+\frac{\tau_2}{\tau_1}$	$-\frac{u}{t}\left(1+\frac{1}{\tau_1}\right)$	Z_{41}
2	$\frac{s}{t}\left(1+\tau_2\right)\left(1-\frac{u}{s}\tau_1\right)$	$\frac{s}{t}\left(1+\frac{1}{\tau_1}\right)\tau_2$	$\left(\frac{u}{t}-\frac{s}{t}\frac{1}{\tau_1}\right)\tau_2$	$-\frac{s}{t}(1+\tau_1)(1+\tau_2)$
3	$\frac{s}{t}\left(1+\frac{1}{\tau_1}\right)$	0	0	$\frac{s}{t}\left(\frac{s}{u}\frac{1}{\tau_1}-1\right)$
4	0	$-\frac{s}{t}\left(1+\frac{1}{\tau_1}\right)$	$\frac{s}{t}\frac{1}{\tau_1}-\frac{u}{t}$	0
5	τ_1	0	0	$\frac{s}{u}(1+\tau_1)$
6	0	τ_1	0	$\frac{s}{u}(1-\tau_1)$
7	0	0	0	$\frac{s}{u}$

with

$$Z_{41} \equiv \frac{s^2}{ut}\left(1+\frac{1}{\tau_1}\right)\left(1+\frac{1}{\tau_2}\right)-\frac{s}{u}\frac{1+\tau_2}{\tau_1} \tag{7.5}$$

The values for the solutions $1'$-$7'$ may be obtained by the the conjugation property.

Inserting the solutions into eq. (7.3), we get that $\Delta_{\text{triplebox}}$ on cut-solution s can be written as as a Laurent polynomial in τ_1 and τ_2, that is

$$\Delta_{\text{triplebox}}|_{\text{s}} = \sum_{ij} d_{sij}\tau_1^i\tau_2^j \tag{7.6}$$

with 622 different d-coefficients being present in total.

The coefficients of eqs. (7.3) and (7.6) are related through the linear relation

$$\bar{d} = M\bar{c} \tag{7.7}$$

where M is a 622×398 matrix.

Inverting the linear system given by eq. (7.7) analytically can be done in principle, yielding a pseudo inverse and a null-space. In practice however the system is too big to make the use of current algebraic computer systems[2] practical, but there is a method which allows us to split the problem in two.

[2]We tried Maple and Mathematica.

We note that the values of the ISPs on the cut-solutions have the property that

$$k_i \cdot p_j|_s = k_i \cdot p_j|_{s'} \qquad\qquad k_i \cdot \omega|_s = -k_i \cdot \omega|_{s'} \tag{7.8}$$

due to the conjugation property. Therefore we get that if we write the irreducible numerator $\Delta_{\text{triplebox}}$ as

$$\Delta = \Delta^{\text{spurious}} + \Delta^{\text{non-spurious}} \tag{7.9}$$

we see that

$$\Delta|_s + \Delta|_{s'} = 2\Delta^{\text{non-spurious}}|_s \qquad\qquad \Delta|_s - \Delta|_{s'} = 2\Delta^{\text{spurious}}|_s \tag{7.10}$$

as all the spurious terms contains an odd number of factors of $k_i \cdot \omega$, and vice versa.

Thus we get that $\Delta^{\text{non-spurious}}$ and Δ^{spurious} each form their own independent system of the form of eq. (7.7), that is

$$\bar{d}^+ = M^+ \bar{c}_{\text{non-spurious}} \qquad\qquad \bar{d}^- = M^- \bar{c}_{\text{spurious}} \tag{7.11}$$

with

$$d^{\pm}_{sij} = \frac{d_{sij} \pm d_{s'ij}}{2} \tag{7.12}$$

which can be treated and pseudo-inverted separately. Each matrix of eqs. (7.11) is 311×199 which is half the size of the original system, making it within the reach of our algebraic programs.

Some of the non-spurious terms have a factor of $(k_1 \cdot \omega)(k_2 \cdot \omega)$. The presence of the spurious vector ω makes such factors harder to evaluate and to subject to IBP identities, and thus it is advantageous to rewrite them in terms of terms without that factor, but which instead contain a factor of $(k_1 \cdot k_2)$, which normally is not taken to be among the ISPs. That can be done using the Gram-matrix identity

$$\det \begin{pmatrix} k_1 & 1 & 2 & 4 & \omega \\ k_2 & 1 & 2 & 4 & \omega \end{pmatrix} = 0, \tag{7.13}$$

which on the cut is equivalent to

$$(k_1 \cdot \omega)(k_2 \cdot \omega) = -\frac{t^2}{4} + \frac{t}{2}\big((k_1 \cdot 4) + (k_2 \cdot 1)\big) + \frac{tu}{s}(k_1 \cdot k_2) + \frac{s+2t}{s}(k_1 \cdot 4)(k_2 \cdot 1)\,. \tag{7.14}$$

Results for gluon scattering

Let us look at the result for the triple-box topology for $gg \to gg$ scattering in Yang-Mills theory or one of its supersymmetric extensions. Like we did for the the two-loop cases we may write $\Delta_{\text{triplebox}}|_{\text{cut}}$ as a product of trees:

$$\begin{aligned}\Delta_{\text{triplebox}}|_{10\times\text{cut}} = i^{10} \sum_f \sum_{h_i} \; & \mathcal{A}(-l_1^{-h_1}, p_1^{a_1}, l_2^{h_2})\, \mathcal{A}(-l_2^{-h_2}, p_2^{a_2}, l_3^{h_3}) \\ & \times \mathcal{A}(-l_3^{-h_3}, -l_4^{-h_4}, l_9^{h_9})\, \mathcal{A}(l_4^{h_4}, -l_5^{-h_5}, l_{10}^{h_{10}})\, \mathcal{A}(l_5^{h_5}, p_3^{a_3}, -l_6^{-h_6}) \\ & \times \mathcal{A}(l_6^{h_6}, p_4^{a_4}, -l_7^{-h_7})\, \mathcal{A}(l_7^{h_7}, -l_8^{-h_8}, -l_{10}^{-h_{10}})\, \mathcal{A}(l_8^{h_8}, l_1^{h_1}, -l_9^{-h_9})\end{aligned} \tag{7.15}$$

where again h_i denotes the helicities of the internal particles, a_j the helicities of the external particles, and f the flavours of the internal particles. For each fermionic loop we must additionally remember to multiply by the factor of -1 from the Feynman rules, and for each closed scalar loop with a factor of 2 to account for the conjugates.

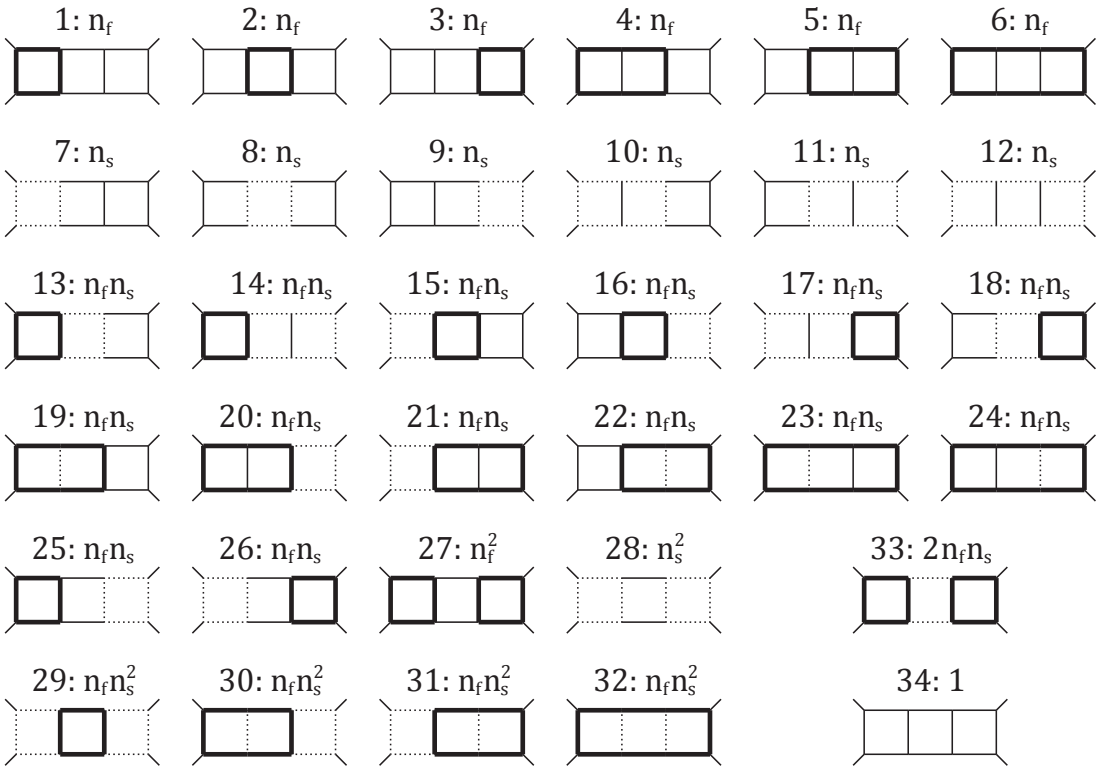

Figure 7.2: The 34 flavour combinations appearing for the triple-box topology in $gg \to gg$ scattering, along with their multiplicities in a theory with n_f fermions and n_s complex scalars. The normal lines denote gluons, the dashed lines scalars, and the bold lines fermions.

There are in total 34 different combinations of flavours contributing for theories with both fermions and scalars. The combinations are shown of fig. 7.2, along with the number of times they will appear[3] in a theory with n_f fermions and n_s complex scalars.

There are three independent helicity combinations of the external gluons which give a non-zero result. They are all MHV configurations, and the same configurations which appear for the two-loop double-box and crossed box in section 6.4, namely

[3]This number can be obtained by counting the number of continuous lines with each flavour, for all combination except the one labeled '33' which one naively would expect to carry a factor of $n_f^2 n_s^2$. To obtain the right number one has to look at the details of the super-symmetries which are the origin of the flavours in our examples.

$(--++)$, $(-+\,+-)$, and $(-+\,-+)$. The opposite helicity configurations are also non-zero, but are related through complex conjugation.

The full expressions for $\Delta_{\text{triplebox}}$, corresponding to for instance eq. (6.36) for the double-box case, are very tedious, but as for the two-loop cases the result may be simplified by reducing the result to master integrals using IBP relations. The triple-box topology has three master integrals which we will take to correspond to the numerators 1, $(k_1+p_4)^2$, and $(k_3-p_4)^2$. Factoring out the tree-level amplitude and a constant factor of s^3t, we get that

$$A_{\text{triplebox}} = s^3 t A^{(0)} I_{10}\Big(C_1 + C_2(k_1+p_4)^2 + C_3(k_3-p_4)^2\Big) + \dots \tag{7.16}$$

where I_{10} refers to the triple-box integral-part of eq. (7.1), and the ellipses to terms with fewer than ten propagators.

For the $(--++)$ configuration the result is

$$\begin{aligned} C_1^{--++} &= -1, \\ C_2^{--++} &= 0, \\ C_3^{--++} &= 0. \end{aligned} \tag{7.17}$$

For the $(-+\,+-)$ configuration the result is

$$\begin{aligned} C_1^{-+\,+-} &= -1 - (1+n_s-n_f)\frac{s}{t^3}\left(2t^2+11st+10s^2\right) \\ &\quad - (4-n_f)(3-n_s)\frac{s(t+2s)}{2t^2} + (4-n_f)\frac{s(t+4s)}{2t^2}, \\ C_2^{-+\,+-} &= \frac{2}{t}\left(1 - C_1^{-+\,+-}\right), \\ C_3^{-+\,+-} &= 0. \end{aligned} \tag{7.18}$$

And for the $(-+\,-+)$ configuration the result is

$$\begin{aligned} C_1^{-+\,-+} &= -1 + (4-n_f)\frac{st}{u^2} - 2(1+n_s-n_f)\frac{s^2t^2}{u^4} \\ &\quad + \big(2(1-2n_s)+n_f\big)(4-n_f)\frac{s^2t(2t-s)}{4u^4} \\ &\quad - \big(n_f(3-n_s)^2 - 2(4-n_f)^2\big)\frac{st(t^2-4st+s^2)}{8u^4}, \\ C_2^{-+\,-+} &= -(4-n_f)\frac{s}{u^2} + 2(1+n_s-n_f)\frac{s^2t}{u^4} \\ &\quad - \big(2(1-2n_s)+n_f\big)(4-n_f)\frac{s^2(2t-s)}{u^4} \\ &\quad + \big(n_f(3-n_s)^2 - 2(4-n_f)^2\big)\frac{s(t^2-4st+s^2)}{2u^4}, \\ C_3^{-+\,-+} &= \big(2(1-2n_s)+n_f\big)(4-n_f)\frac{3s^2(2t-s)}{2u^4} \\ &\quad - \big(n_f(3-n_s)^2 - 2(4-n_f)^2\big)\frac{3s(t^2-4st+s^2)}{4u^4}. \end{aligned} \tag{7.19}$$

Discussion

The results of this section have been compared with those for the $\mathcal{N} = 4$ case calculated in [99], with full agreement. An additional check is that two-particle cuts make the result factor into two-loop times tree, as expected.

The results for the triple-box have a lot of structure in common with the double-box case. The $(- + -+)$ configuration is the most complicated, the $(- + +-)$ configuration is simpler, and the $(- - ++)$ configuration is trivial. Like for the two-loop case the flavour factors $(4 - n_f)$, $(3 - n_s)$ and $(1 - n_f + n_s)$ appear, which all vanish for[4] $\mathcal{N} = 4$ SYM, and of which $(1-n_f+n_s)$ vanish in all super-symmetric theories. They are however joined by two new flavour factors $\big(2(1-2n_s)+n_f\big)(4-n_f)$ and $\big(n_f(3-n_s)^2 - 2(4-n_f)^2\big)$ which appear in the $(- + -+)$ configuration only, and which vanish for $\mathcal{N} = 4$ and $\mathcal{N} = 2$, but not for $\mathcal{N} = 1$, which makes the results progressively simpler with the number of super-symmetries. This is a new feature at three-loops.

Like we saw for the two-loop cases, the results for the triple-box are more constrained than suggested by eq. (7.3). This manifests as the maximal power appearing in the Laurent expansion eq. (7.6) being 4, rather than 6 which eq. (7.3) allows for some terms.

7.2 The tennis court

For the $\mathcal{N} = 4$ supersymmetric theory, there are only two planar three-loop topologies contributing to $2 \to 2$ scattering, due to the no-triangle property of that theory. One is the triple-box described in the previous section, the other is the tennis court topology shown at fig. 7.3.

We will not here complete the calculation for the tennis court, but in order to show that our method is applicable in this case too, we will solve the on-shell constraints and see that a Laurent-polynomial form for $\Delta_{\text{tenniscourt}}|_s$ at the cut solutions similar to eq. (7.6) is possible. The ten propagators may be parametrized as

$$\begin{aligned}
&l_1 = k_1 + p_1, \qquad &&l_2 = k_1, \qquad &&l_3 = k_1 - p_2, \qquad &&l_4 = k_2 + p_3, \\
&l_5 = k_2, \qquad &&l_6 = k_3, \qquad &&l_7 = k_3 - p_4, \qquad &&l_8 = k_3 - k_1 - p_1 - p_4, \\
&l_9 = k_3 - k_2, \qquad &&l_{10} = k_2 - k_1 + p_2 + p_3,
\end{aligned} \tag{7.20}$$

and we will further parametrize the three loop momenta as

$$\begin{aligned}
k_1 &= x_1 p_1 + x_2 p_2 + x_3 \frac{\langle 23\rangle}{\langle 13\rangle} \frac{\langle p_1|\sigma^\mu|p_2]}{2} + x_4 \frac{[23]}{[13]} \frac{\langle p_2|\sigma^\mu|p_1]}{2}, \\
k_2 &= y_1 p_3 + y_2 p_4 + y_3 \frac{\langle 41\rangle}{\langle 31\rangle} \frac{\langle p_3|\sigma^\mu|p_4]}{2} + y_4 \frac{[41]}{[31]} \frac{\langle p_4|\sigma^\mu|p_3]}{2}, \\
k_3 &= z_1 p_3 + z_2 p_4 + z_3 \frac{\langle 41\rangle}{\langle 31\rangle} \frac{\langle p_3|\sigma^\mu|p_4]}{2} + z_4 \frac{[41]}{[31]} \frac{\langle p_4|\sigma^\mu|p_3]}{2}.
\end{aligned} \tag{7.21}$$

[4] n_f and n_s as a function of $\mathcal{N}$ is given by the table eq. (3.38).

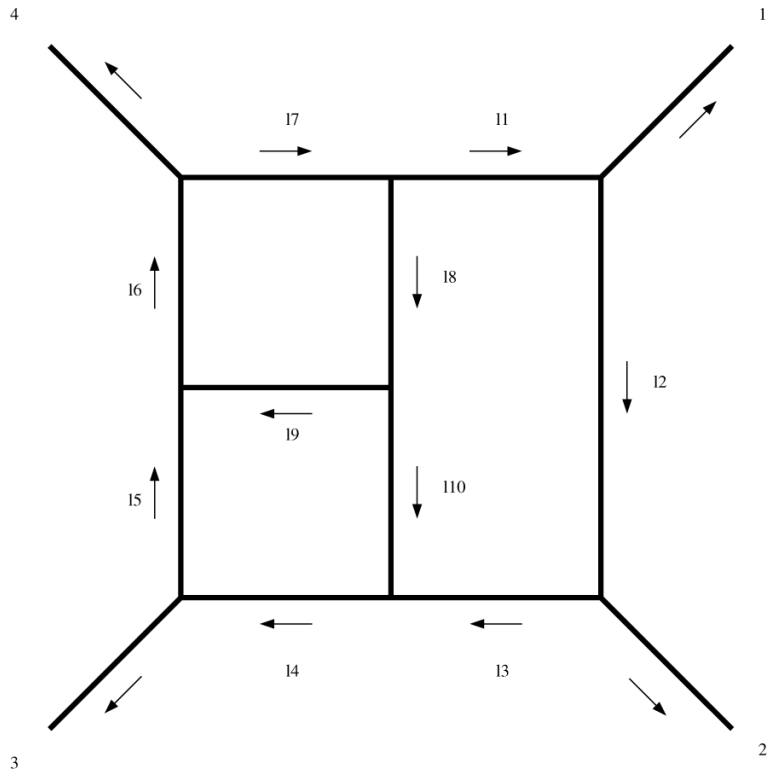

Figure 7.3: The tennis court topology as parametrized by eqs. (7.20).

The deca-cut equations have 16 solutions, which come in conjugate pairs denoted 1-8 and $1'$-$8'$. All the solutions have $x_1 = x_2 = y_2 = z_1 = 0$ and defining the non-primed solutions as the set which additionally has $x_4 = 0$, the solutions are given by

	x_3	y_1	y_3	y_4
1	1	0	τ_1	0
2	1	τ_1	τ_2	0
3	$(\chi+1)(\tau_1+1)$	0	0	$\frac{\chi}{\tau_1}+\chi+1$
4	τ_1	0	1	0
5	$(\chi+1)(\tau_1+1)$	τ_2	0	$\frac{(\tau_1\chi+\chi+\tau_1)(\tau_2+1)}{\tau_1}$
6	τ_1	τ_2	τ_2+1	0
7	τ_1	$\frac{-\tau_1+\tau_2+1}{\chi}$	$\frac{\chi-\tau_1+\tau_2+1}{\chi}$	0
8	$\chi+1-\chi\tau_1$	$-\frac{(\chi+1)(\tau_1-1)+\tau_1\tau_2}{\chi+1}$	0	$(\tau_1-1)(\chi+\tau_2-1)$

(7.22)

	z_2	z_3	z_4
1	τ_2	τ_3	0
2	0	τ_3	0
3	τ_2	0	$-\frac{(\tau_1\chi+\chi+\tau_1)(\tau_2-1)}{\tau_1}$
4	τ_2	$1-\tau_2$	0
5	0	0	$\frac{\chi}{\tau_1}+\chi+1$
6	0	1	0
7	$\frac{(\tau_1-1)(\chi-\tau_1+\tau_2+1)}{\chi\tau_2}$	0	$\frac{(\chi+1)(\tau_1-1)(\tau_1-\tau_2-1)}{\chi\tau_2}$
8	$\frac{(1-\tau_1)(\chi+\tau_2+1)}{\tau_2}$	$\frac{(\chi+1)(\tau_1-1)+\tau_1\tau_2}{\tau_2}$	0

(7.23)

with $\chi = s/t$. We notice that two of the solution pairs (nr. 1 and 2) have three degrees of freedom rather than two, and thus the parametrization is in terms of three free variables. We see all of the solutions to be comparable with a Laurent-polynomial form.

Applying the multivariate polynomial division as implemented by BasisDet, gives that $\Delta_{\text{tenniscourt}}$ may be parametrized in terms of eight ISPs as

$$\begin{aligned}\Delta_{\text{tenniscourt}} = \sum_{i_1\cdots i_8} c_{i_1\cdots i_8}&(k_1\cdot p_4)^{i_1}(k_2\cdot p_2)^{i_2}(k_3\cdot p_2)^{i_3}(k_2\cdot p_1)^{i_4}(k_3\cdot p_1)^{i_5}\\ &\times(k_1\cdot\omega)^{i_6}(k_2\cdot\omega)^{i_7}(k_3\cdot\omega)^{i_8}\end{aligned} \tag{7.24}$$

with 642 terms appearing in the sum, of which 323 are non-spurious and the remaining 319 are spurious.

Chapter 8

Further two-loop examples

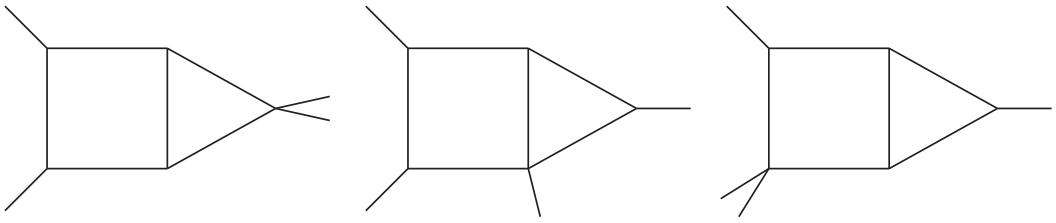

Figure 8.1: The three box-triangle topologies $(t321; M_1)$, $(t321; 4L)$, and $(t321; M_2)$.

In this chapter we will return to two-loop and look at some further examples in four dimensions, the three different box-triangle topologies which will show up in $2 \to 2$ scattering. As box-triangle topologies all are called $(t321)$ in our short-hand notation, more information is needed in order to distinguish them, we will name them $(t321; M_1)$, $(t321; 4L)$, and $(t321; M_2)$ as shown on fig. 8.1. The purpose of this is not to complete the full $2 \to 2$ calculation, but to show, and later solve, some problems with our method which do not appear for the maximum cuts.

8.1 The box-triangle topology $(t321; M_1)$

The topology $(t321; M_1)$ - so called as it has a mass $(p_1 + p_2)^2$ on the first leg - is characterized by the six loop-momenta

$$\begin{aligned} l_1 &= k_1 - p_4 & l_2 &= k_1 + p_3 & l_3 &= k_2 + p_3 \\ l_4 &= k_2 & l_5 &= k_2 - p_4 & l_6 &= k_1 - k_2 \end{aligned} \tag{8.1}$$

Using BasisDet, we find the general expression for the irreducible numerator for the topology to be

$$\Delta_{321;M_1} = \sum_{i_1 \ldots i_5} c_{i_1 \ldots i_5} (k_1 \cdot p_4)^{i_1} (k_1 \cdot \omega_+)^{i_2} (k_2 \cdot \omega_+)^{i_3} (k_1 \cdot \omega_-)^{i_4} (k_2 \cdot \omega_-)^{i_5} \tag{8.2}$$

where $\omega_\pm$ is defined analogously to the one-loop triangle case given by eqs. (5.41):

$$\omega_\pm = \frac{\langle p_3|\sigma^\mu|p_4]}{2} \pm \frac{\langle p_4|\sigma^\mu|p_3]}{2} \tag{8.3}$$

The sum of eq. (8.2) contains 69 terms of which only 19 are naively non-spurious.

To solve for $\Delta_{321;M_1}$ using generalized unitarity cuts, we will use the parametrization

$$\begin{aligned} k_1 &= x_1 p_3 + x_2 p_4 + x_3 \frac{\langle p_3|\sigma^\mu|p_4]}{2} + x_4 \frac{\langle p_4|\sigma^\mu|p_3]}{2}, \\ k_2 &= y_1 p_3 + y_2 p_4 + y_3 \frac{\langle p_3|\sigma^\mu|p_4]}{2} + y_4 \frac{\langle p_4|\sigma^\mu|p_3]}{2}. \end{aligned} \tag{8.4}$$

where it is the three-point kinematics of the problem that allows us to use this somewhat simpler parametrization. The hexa-cut equations have four solutions given by

	x_1	x_2	x_3	x_4	y_1	y_2	y_3	y_4
1	0	0	τ_1	0	0	0	0	τ_2
2	0	0	0	τ_1	0	0	τ_2	0
3	$-\tau_1$	τ_1	τ_1/τ_2	$(1-\tau_1)\tau_2$	0	0	0	τ_2
4	$-\tau_1$	τ_1	$(1-\tau_1)\tau_2$	τ_1/τ_2	0	0	τ_2	0

(8.5)

As the topology is not a maximum cut, it may not be directly identified with a product of trees, but will require a OPP subtraction term as we saw for the one-loop triangle in eq. (5.56). This will come from the double-box topology ($t331$) which is characterized by the extra propagator $l_7 = k_1$. This means that

$$\begin{aligned} \Delta_{321;M_1}|_{6\times\text{cut}} = i^6 \sum_{h_1\ldots h_6} &\mathcal{A}_4(-l_1^{-h_1}, p_1^{a_1}, p_2^{a_2}, l_2^{h_2})\mathcal{A}(-l_2^{-h_2}, l_3^{h_3}, l_6^{h_6})\mathcal{A}(-l_3^{-h_3}, p_3^{a_3}, l_4^{h_4}) \\ &\times \mathcal{A}(-l_4^{-h_4}, p_4^{a_4}, l_5^{h_5})\mathcal{A}(-l_5^{-h_5}, l_1^{h_1}, -l_6^{-h_6}) - \frac{\Delta_{331}|_{6\times\text{cut}}}{l_7^2} \end{aligned} \tag{8.6}$$

This we may identify as a Laurent polynomial on each solution

$$\Delta_{321;M_1}|_{6\times\text{cut,sol } s} = \sum_{i,j} d_{sij} \tau_1^i \tau_2^j \tag{8.7}$$

and identify the coefficients of eq. (8.7) with those of eq. (8.2) using

$$\bar{d} = M\bar{c} \tag{8.8}$$

where the matrix has rank 69 and thus it may be inverted in the usual fashion yielding expressions for the coefficients of eq. (8.2) for each helicity configuration and each flavour content. Thus we saw no problems in the calculation of $(t321; M_1)$.

8.2 The box-triangle topology $(t321; 4L)$

This topology, which has got its name from the presence of a fourth leg, may be parametrized by the six propagating momenta

$$\begin{aligned} l_1 &= k_1 + p_1 & l_2 &= k_1 & l_3 &= k_2 + p_3 \\ l_4 &= k_2 & l_5 &= k_2 - p_4 & l_6 &= k_1 - k_2 + p_1 + p_4 \end{aligned} \tag{8.9}$$

With ω defined as in eq. (6.3), the irreducible numerator is given as

$$\Delta_{321;4L} = \sum_{i_1 \ldots i_5} c_{i_1 \ldots i_5} (k_1 \cdot p_4)^{i_1} (k_1 \cdot p_3)^{i_2} (k_2 \cdot p_1)^{i_3} (k_1 \cdot \omega)^{i_4} (k_2 \cdot \omega)^{i_5} \tag{8.10}$$

which like the previous case has 69 terms, but in this case 35 turn out to be non-spurious.

We find that the hexa-cut equations have six solutions which can be parametrized as

$$\begin{aligned} k_1 &= x_1 p_1 + x_2 p_2 + x_3 \frac{\langle 23 \rangle}{\langle 13 \rangle} \frac{\langle p_1 | \sigma^\mu | p_2]}{2} + x_4 \frac{\langle 13 \rangle}{\langle 23 \rangle} \frac{\langle p_2 | \sigma^\mu | p_1]}{2} \\ k_2 &= y_1 p_3 + y_2 p_4 + y_3 \frac{\langle 41 \rangle}{\langle 31 \rangle} \frac{\langle p_3 | \sigma^\mu | p_4]}{2} + y_4 \frac{\langle 31 \rangle}{\langle 41 \rangle} \frac{\langle p_4 | \sigma^\mu | p_3]}{2} \end{aligned} \tag{8.11}$$

where

	x_1	x_2	x_3	x_4	y_1	y_2	y_3	y_4
1	$\tau_1 - 1$	0	τ_1	0	0	0	τ_2	0
2	$\tau_1 - 1$	0	0	τ_1	0	0	0	τ_2
3	τ_1	0	τ_2	0	0	0	1	0
4	τ_1	0	0	τ_2	0	0	0	1
5	$\tau_1 - 1$	0	$\tau_1 + \frac{s}{t}\frac{\tau_1(\tau_2-1)}{\tau_2}$	0	0	0	0	$\frac{u}{t}(\tau_2 - 1)$
6	$\tau_1 - 1$	0	0	$\tau_1 + \frac{s}{t}\frac{\tau_1(\tau_2-1)}{\tau_2}$	0	0	$\frac{u}{t}(\tau_2 - 1)$	0

(8.12)

Topology $(t321; 4L)$ requires two subtraction terms, one from the pentagon-triangle $(t421)$ and one from the double-box $(t331)$ which have the extra propagators $l_7 = k_2 + p_2 + p_3$ and $l_8 = k_1 - p_2$ respectively, so that is

$$\begin{aligned} \Delta_{321;4L}|_{6\times\text{cut}} = i^6 \sum_{h_1 \ldots h_6} & \mathcal{A}(-l_1^{-h_1}, p_1^{a_1}, l_2^{h_2}) \mathcal{A}_4(-l_2^{-h_2}, p_2^{a_2}, l_3^{h_3}, l_6^{h_6}) \mathcal{A}(-l_3^{-h_3}, p_3^{a_3}, l_4^{h_4}) \\ & \times \mathcal{A}(-l_4^{-h_4}, p_4^{a_4}, l_5^{h_5}) \mathcal{A}(-l_5^{-h_5}, l_1^{h_1}, -l_6^{-h_6}) - \frac{\Delta_{421}|_{6\times\text{cut}}}{l_7^2} - \frac{\Delta_{331}|_{6\times\text{cut}}}{l_8^2} \end{aligned} \tag{8.13}$$

But when evaluating eq. (8.13) we notice something bad: For two of the cut solutions, nr. 3 and 4, the tree-product diverges on the cut! This is due to the four-point tree of eq. (8.13) which has a contribution from a Feynman diagram in

which $l_7 = l_3 + p_2$ appears as a propagator, and it turns out that l_7 squares to identically zero for those two solutions. Comparing with the pentagon-triangle case of section 6.3 we see indeed that solutions 3 and 4 coincide exactly with the two solutions of $(t421)$, meaning that at those solutions it is impossible to perform the hexa-cut without also cutting the seventh propagator, making the cut effectively a hepta-cut. Whenever such a coincidence happens this problem occurs!

Foreshadowing what happens for the final box-triangle topology, we will name this issue *the minor problem*, as it can be solved by a careful analytical treatment since the unwanted pole will cancel with the corresponding explicit pole from the $(t421)$ subtraction term. But for a numerical approach the minor problem is a major obstacle. There is a general solution to the minor problem based on algebraic geometry which we shall see in the next chapter, but let us first proceed to the last of the box-triangle topologies.

8.3 The box-triangle topology $(t321; M_2)$

The final of the independent box-triangle topologies contributing to $2 \to 2$ processes is $(t321; M_2)$, so named due to the mass on the second leg. It may be parametrized by the six propagating momenta

$$\begin{aligned} l_1 &= k_1 + p_1 & l_2 &= k_1 & l_3 &= k_2 + p_2 + p_3 \\ l_4 &= k_2 & l_5 &= k_2 - p_4 & l_6 &= k_1 - k_2 + p_1 + p_4 \end{aligned} \tag{8.14}$$

BasisDet gives that the form of the irreducible numerator for the topology is

$$\Delta_{321;M_1} = \sum_{i_1 \ldots i_5} c_{i_1 \ldots i_5} (k_1 \cdot p_4)^{i_1} (k_1 \cdot \omega_+)^{i_2} (k_2 \cdot \omega_+)^{i_3} (k_1 \cdot \omega_-)^{i_4} (k_2 \cdot \omega_-)^{i_5} \tag{8.15}$$

where $\omega_\pm$ is defined to be perpendicular to p_1, p_4 and to each other, in a way similar to eq. (8.3). The sum has 63 terms, with 19 being naively non-spurious.

There are two solutions to the hexa-cut equations, and for the parametrization

$$\begin{aligned} k_1 &= x_1 p_1 + x_2 p_4 + x_3 \frac{\langle p_1 | \sigma^\mu | p_4]}{2} + x_4 \frac{\langle p_4 | \sigma^\mu | p_1]}{2} \\ k_2 &= y_1 p_1 + y_2 p_4 + y_3 \frac{\langle p_1 | \sigma^\mu | p_4]}{2} + y_4 \frac{\langle p_4 | \sigma^\mu | p_1]}{2} \end{aligned} \tag{8.16}$$

they are

	x_1	x_2	x_3	x_4	y_1	y_2	y_3	y_4
1	τ_1	0	τ_2	0	0	1	τ_3	0
2	τ_1	0	0	τ_2	0	1	0	τ_3

(8.17)

which we see to have one more degree of freedom than naively expected, like we saw for the pentagon-triangle in section 6.3.

Only one subtraction term is needed for $(t321; M_2)$, that of the pentagon-triangle, so we get as the full expression

$$\Delta_{321;M_2}|_{6\times\text{cut}} = i^6 \sum_{h_1\ldots h_6} \mathcal{A}(-l_1^{-h_1}, p_1^{a_1}, l_2^{h_2})\mathcal{A}(-l_2^{-h_2}, l_3^{h_3}, l_6^{h_6})\mathcal{A}_4(-l_3^{-h_3}, p_2^{a_2}, p_3^{a_3}, l_4^{h_4}) \\ \times \mathcal{A}(-l_4^{-h_4}, p_4^{a_4}, l_5^{h_5})\mathcal{A}(-l_5^{-h_5}, l_1^{h_1}, -l_6^{-h_6}) - \frac{\Delta_{421}|_{6\times\text{cut}}}{l_7^2} \tag{8.18}$$

with the propagator of the subtraction term being $l_7 = k_2 + p_3$.

Inserting the cut solutions into eq. (8.15) yields a polynomial in the three free parameters

$$\Delta_{321;M_2}|_{6\times\text{cut, sol } s} = \sum_{i_1 i_2 i_3} d_{s i_1 i_2 i_3} \tau_1^{i_1} \tau_2^{i_2} \tau_3^{i_3} \tag{8.19}$$

where the two solutions together contain 74 different terms. This allows us to relate the coefficients of eq. (8.15) with those of eq. (8.19) in the usual fashion as

$$\bar{d} = M\bar{c} \tag{8.20}$$

where M is a 74×63 matrix. It turns out, however, that the rank of M is only 62 making the system uninvertible in any way that allows us to extract the values of all the c-coefficients of eq. (8.15)!

Looking closer, it turns out that the problem lies with the two monomials

$$(k_1 \cdot \omega_-)(k_2 \cdot \omega_+) \qquad \text{and} \qquad (k_1 \cdot \omega_+)(k_2 \cdot \omega_-) \tag{8.21}$$

which turn out to evaluate to the same as each other on both of the solutions (namely $-s_{14}^2/4$ on solution 1 and $s_{14}^2/4$ on solution 2), making it impossible to extract the values of the corresponding c-coefficients separately. It may seem surprising that such a thing can happen after the division with the ideal of the propagators, as that procedure accounts for all relations between the monomials, yet this issue turn out to be a loophole in the procedure.

After dividing by the linear part of the ideal, which removes all the RSPs, the remaining ideal $I_{\text{non-linear}}$ may be spanned by the three quadratic propagators

$$\frac{s_{14}}{2}\left\{k_1^2, k_2^2, \left((k_1 - k_2 + p_1 + p_4)^2 - k_1^2 - k_2^2\right)/2\right\} = \{I_1, I_2, I_3\} \tag{8.22}$$
$$= \left\{(k_1\cdot\omega_-)^2 - (k_1\cdot\omega_+)^2\,,\ (k_2\cdot\omega_-)^2 - (k_2\cdot\omega_+)^2\,,\ (k_1\cdot\omega_+)(k_2\cdot\omega_+) - (k_1\cdot\omega_-)(k_2\cdot\omega_-)\right\}$$

The difference between the two problematic monomials square to

$$(k_1\cdot\omega_-)^2(k_2\cdot\omega_+)^2 + (k_1\cdot\omega_+)^2(k_2\cdot\omega_-)^2 - 2(k_1\cdot\omega_-)(k_2\cdot\omega_-)(k_1\cdot\omega_+)(k_2\cdot\omega_+) \tag{8.23}$$

and we see that it is in the ideal as it is given by

$$(k_2\cdot\omega_+)^2 I_1 + (k_1\cdot\omega_+)^2 I_2 + 2(k_1\cdot\omega_+)(k_2\cdot\omega_+) I_3 \tag{8.24}$$

The same is not the case for the non-squared difference

$$\delta = (k_1 \cdot \omega_-)(k_2 \cdot \omega_+) - (k_1 \cdot \omega_+)(k_2 \cdot \omega_-) \tag{8.25}$$

which therefore is not in the ideal, but as we see it will still vanish on the cut, since the square vanishes due to it being a member of the ideal. This means that the set of quantities that vanish on the cut is bigger in general than the set spanned by the propagators. Therefore may the coefficients of the monomials related to the quantities in the difference of these two sets not be fixed using generalized unitarity cuts! We will call this issue *the major problem.*

The major problem can be formulated mathematically by identifying the quantities that vanish on the cut with members of the radical of the ideal I, which we will denote $\sqrt{I}$. A radical of an ideal is defined as the set of quantities for which some power is a member of I, and we see exactly that the monomial difference δ of eq. (8.25), is member of $\sqrt{I}$ but not of I. Thus the major problem will occur in cases[1] where $I \neq \sqrt{I}$, that is cases where I isn't radical, where a radical ideal is defined as an ideal for which $I = \sqrt{I}$.

Both the major and the minor problem can be solved by going to d dimensions as we will see in the following chapter.

[1] And where additionally $\sqrt{I}/I$ has members that fulfill the renormalization constraints.

Chapter 9

The use of algebraic geometry

In the previous chapters we saw the use of algebraic geometry-based methods in finding a minimal basis of ISPs for the irreducible numerator Δ for the various topologies under consideration. But that was for specific examples, here the method will be described in its generality, first for the case of four dimensions, and later in the d-dimensional case. The d-dimensional discussion will also address and solve the minor and the major problem of the previous chapter. The four-dimensional part is based on [16] and [86], and the d-dimensional part additionally on [3]. For a list of terms and definitions of use in algebraic geometry, see appendix E.

9.1 The four-dimensional case

The scalar numerator of a given diagram with L loops will always be a function of a limited number of scalar products, the products of the L loop-momenta with the 4 members of a basis[1] β spanning the space of the external momenta. For four-point or lower it is not possible to pick a β containing only external momenta, in that case it will have to be supplemented by spurious "ω"-vectors, which can be defined as in eqs. (5.8) or (5.41) (see in general the discussion in appendix F.2). This means that each k may be parametrized as

$$k_i = \sum_{j=1}^{4} x_{ij}\beta_j \tag{9.1}$$

For each k_i there will be a linear relation between x_{ij} and the four $k_i \cdot \beta_j$ given by the inverse Gram matrix of the basis

$$x_{ij} = G^{-1}\begin{pmatrix} \beta_1 & \beta_2 & \beta_3 & \beta_4 \\ \beta_1 & \beta_2 & \beta_3 & \beta_4 \end{pmatrix}_{jh} (k_i \cdot \beta_h) \tag{9.2}$$

so fixing the members of one of the sets is equivalent to fixing the members of the other set with no ambiguities.

[1] It is possible, and sometimes (as in the cases of two-loop butterfly-type topologies) desirable, to define different βs for each loop, but that subtlety has no impact on our discussion.

In addition to products of the form $k_i \cdot \beta_j$, products of the form $k_i \cdot k_j$ may also appear in diagrammatic numerators, but from eqs. (9.1) and (9.2) (see also the discussion in section 4.2) we see that they may be expressed completely in terms of the $k_i \cdot \beta_j$ products, although by potentially quadratic relations. And thus we get the result that any imaginable (scalar) integrand numerator is a sum of products of the scalar products mentioned above, with rational coefficients.

This makes Δ a member of the *ring* R generated by the scalar products. The set of propagators P generates a subset of that ring, which is closed under multiplication and addition, making it an *ideal* I of the ring.

Thus when we write a general numerator for a P-propagator topology

$$N = \Delta + \sum_i \kappa_i D_1^{a_{1,i}} \cdots D_P^{a_{P,i}} \tag{9.3}$$

we may identify the terms in the sum with the members of the ideal I, and Δ with those of the remaining members of R, which lives up to the renormalization constraints as described in section 4.2.

While I can be generated by the propagators, another basis is the *Gröbner basis* G. From the properties of the Gröbner basis we get that the remainder Δ may be generated in a systematic way using repeated multivariate polynomial division (see appendix E) of the members of R with the members of G. If G is generated using the monomial ordering DegreeLexicographic[2] all the leading terms in G will be linear in (at most one of) the scalar products, while the remaining terms will contain higher powers.

The ideal I_{linear} which is generated by the linear subset G_{linear} of G, will contain all monomials containing RSPs. This means that the naive basis for Δ is those of the elements of the *quotient ring* R/I_{linear} which one obtains from the remainders after polynomial division of R with the basis G_{linear} (or, as G_{linear} is linear, by putting the members of G_{linear} to zero directly). The scalar products still present in R/I_{linear} are the ISPs. The actual Δ will of course only contain elements of R/I_{linear} which additionally fulfill the renormalizability constraints.

But if one instead regards the quotient ring which one obtains from multivariate polynomial division towards the full ideal, i.e. R/I, no relations relating its members to the members of I can exist, meaning that Δ is spanned by those of the monomials in R/I which fulfill the renormalization constraints, that is

$$\Delta \in R/I \tag{9.4}$$

But as non-linear relations relate the monomials of R/I to others in R, it is easiest to impose the renormalization constraints on the members of R (or[3] R/I_{linear}), and

[2]DegreeLexicographic is defined to first pick the elements with the lowest (linear) total power of scalar products, going upwards order by order (thus the name Degree) and within each order it sorts the elements according to a fixed (potentially alphabetic) ordering (thus the Lexicographic).

[3]In Zhang's program BasisDet, the reduction is happening in two steps first by division with respect to I_{linear} leaving the ISPs, and then fining a new, potentially nicer Gröbner basis for $I_{\text{non-linear}}$ - the remaining members of I. In this case the renormalization constraints are imposed between the two divisions.

then reduce each of those elements individually letting Δ be spanned by the union of the remainders. For further details on this algorithm, and its analytical implementation by Zhang as the Mathematica package BasisDet, see [16].

By the *Lasker-Noether Theorem*, the ring R may be written as the intersection of a set of *primary ideals*, i.e.

$$I = \bigcap_{i=1}^{s} I_i \tag{9.5}$$

where none of the primary factors will be equivalent in any way. Taking the *zero locus*[4] of eq. (9.5), we obtain

$$\mathcal{Z}(I) = \bigcup_{i=1}^{s} \mathcal{Z}(I)_i \tag{9.6}$$

which is the decomposition of the total subset of R which solves the combined cut-constraints, into the individual cut solutions. As such we may identify each of the primary ideals of eq. (9.5) with a specific cut solution, allowing for an alternate way to characterize the full set of solutions to the constraints imposed by the generalized unitarity cuts. To perform the primary decompositions in practice, one may use the code Macaulay2 (see [100]) and the Mathematica package MathematicaM2 by Zhang[5] which calls the code from Mathematica.

9.2 The d-dimensional case

In the d-dimensional case things are similar but with important simplifications, and it is these simplifications which allows us to solve the minor and the major problems of sections 8.2 and 8.3.

In the forms of dimensional regularization which we will use in this thesis, only the loop-momenta are taken to be d dimensional, while the external momenta are kept in four dimensions as also described in section 4.1. This allows us to write each of the loop-momenta as

$$k_i = \bar{k}_i + k_i^{[-2\epsilon]} \tag{9.7}$$

where $\bar{k}$ denotes the four-dimensional part. As the external momenta have no higher-dimensional component, all dependence on $k^{[-2\epsilon]}$ must be through scalar products of the loop-momenta with each other. This means that in addition to the $4L$ scalar

[4] The zero locus of an ideal is the set of points for which all members of the ideal evaluate to zero. In our case this corresponds to the space of cut solutions, as this is where all the members of I, i.e. the propagators and combinations thereof, vanishes. See also appendix E.

[5] This package may be obtained at Zhang's personal website `http://www.nbi.dk/~zhang/`, along with the BasisDet package.

products $\{x\}$ which were necessary in order to characterize the set of loop-momenta in the four-dimensional case, the total set of quantities necessary for a full description is supplemented by $L(L+1)/2$ ρ-parameters defined by[6]

$$\rho_i = -k_i^{[-2\epsilon]2} \qquad\qquad \rho_{ij} = -2k_i^{[-2\epsilon]} \cdot k_j^{[-2\epsilon]} \tag{9.8}$$

where the minus signs are there to compensate for the minus in the spatial part of the metric, giving a total of $L(L+9)/2$ variables to describe a general uncut numerator. The Gram-matrix relations which in the four-dimensional case imposed non-linear relations between the members of $\{x\}$, will in this case impose linear relations between each member of $\{\rho\}$ and the members of $\{x\}$, as the cut-constraints impose[7] the linear relations $\rho_i = \bar{k}_i^2$, where $\bar{k}_i^2$ will inherit the non-linear relations from the four-dimensional case. This means that the generalized unitarity cuts impose only linear constraints, and therefore each cut can be made to fix exactly one degree of freedom of the k_i. Thus P cuts will always leave

$$L(L+9)/2 - P \tag{9.9}$$

degrees of freedom, making that number the *dimension*[8] of the cut solutions. As a diagram and its parent diagrams will have different values of P, eq. (9.9) shows that the dimensions of their cut-solutions too will be different. But we saw in section 8.2 that the minor problem showed up in cases where a diagram and one of its parent diagrams have identical cut solutions, which implies identical dimensions of those solutions, so therefore we see that the minor problem will never occur in d-dimensional cases.

Due to this linearity, one can show that the ideal I will be a *prime ideal*, which is defined as an ideal for which $ab \in I \Rightarrow a \in I \vee b \in I$. This implies two useful properties: As a prime ideal is primary, the primary decomposition of eq. (9.5) will have only one term, meaning that the cut-equations will have a unique solution, relieving us from the multiplicity of solution which showed up in the four-dimensional cases. And as a prime ideal is radical[9] the major problem is avoided too, as it occurred when there were terms in Δ which were members of $\sqrt{I}$, something which is impossible when $I = \sqrt{I}$ as we saw in section 8.3.

In the remaining parts of this thesis, we will utilize these properties to calculate a number of topologies in d dimensions.

[6] Elsewhere the notations $\mu_{ii} = \rho_i$ and $\mu_{ij} = \rho_{ij}$ or $\mu_i \cdot \mu_j = \rho_{ij}$ have been used.

[7] For butterfly-type topologies (or for that matter the triple-box) this is not true for all the ρ_{ij}. But in these cases there are no cut-constraints limiting their values, so the following holds in these cases too. See [3].

[8] If one perceives the zero-locus of the ideal as a manifold in the $L(L+9)/2$-dimensional space of possible loop-momentum configurations, eq. (9.9) gives exactly the dimension of that manifold.

[9] As defined in section 8.3 and in appendix E, a radical ideal is an ideal for which $I = \sqrt{I}$.

Chapter 10

One-loop in d dimensions

Let us take a look at the same $2 \to 2$ scattering problem which we considered in chapter 5, but this time in d dimensions.

10.1 d-dimensional integrand reduction

The integral that we want to consider, is that of one-loop $gg \to gg$ scattering in pure Yang-Mills theory

$$A^{(1)} = \int \frac{\mathrm{d}^d k}{(2\pi)^d} \frac{N}{l_1^2\, l_2^2\, l_3^2\, l_4^2} \tag{10.1}$$

where l_1 to l_4 are the propagators.

$$l_1 = k + p_1 \qquad l_2 = k \qquad l_3 = k - p_2 \qquad l_4 = k + p_1 + p_4 \tag{10.2}$$

After the integrand reduction, the integral becomes[1]

$$A^{(1)} = \int \frac{\mathrm{d}^d k}{(2\pi)^d} \left(\frac{\Delta^{[d]}_{\text{box}}}{l_1^2\, l_2^2\, l_3^2\, l_4^2} + \sum_{x<y<z} \frac{\Delta^{[d]}_{\text{triangle},xyz}}{l_x^2\, l_y^2\, l_z^2} + \sum_{x<y} \frac{\Delta^{[d]}_{\text{bubble},xy}}{l_x^2\, l_y^2} \right) \tag{10.3}$$

where the difference from eq. (5.3) is that the Δs are taken to be in d dimensions.

As described in the previous chapter, we will write the d-dimensional loop-momentum as

$$k = \bar{k} + k^{[-2\epsilon]} \tag{10.4}$$

where $\bar{k}$ denotes the four-dimensional part of the momentum. This four-dimensional part can be parametrized in the usual way

$$\bar{k}^\mu = x_1 p_1^\mu + x_2 p_2^\mu + x_3 \frac{\langle p_1 | \sigma^\mu | p_2]}{2} + x_4 \frac{\langle p_2 | \sigma^\mu | p_1]}{2} \tag{10.5}$$

[1] We do not include the tadpoles, as they vanish like in the four-dimensional case of section 5.4.

The remaining part of k may only appear in the results through its square, which we define to be

$$\rho \equiv -k^{[-2\epsilon]^2} \tag{10.6}$$

Let us start by considering the box coefficients $\Delta^{[d]}_{\text{box}}$. As the loop momenta have a degree of freedom more than they had in the four-dimensional case, there will naturally be two ISPs. We pick $(k \cdot \omega)$ and ρ, where ω is defined as

$$\omega^\mu = \frac{\langle 231]}{s}\frac{\langle 1|\sigma^\mu|2]}{2} - \frac{\langle 132]}{s}\frac{\langle 2|\sigma^\mu|1]}{2} \tag{10.7}$$

as in eq. (5.8).

This makes the expression for $\Delta^{[d]}_{\text{box}}$

$$\Delta^{[d]}_{\text{box}} = \sum_{ij} c_{ij}(k \cdot \omega)^i \rho^j \tag{10.8}$$

The by-now standard method of multivariate polynomial division, leaves five coefficients in the basis:

$$\{c_{00}, c_{01}, c_{02}, c_{10}, c_{11}\} \tag{10.9}$$

We see that the terms 1 and $(k \cdot \omega)$ corresponds to the two terms which we had in the four-dimensional expression eq. (5.10), but with the terms ρ, ρ^2 and $(k \cdot \omega)\,\rho$ being new. How do we make sense of such expressions? $(k \cdot \omega)\,\rho$ will integrate to zero for the usual reason as described in appendix F.3, and the other two may be related to "ordinary" Feynman integrals through the dimensional shift relations

$$\begin{aligned}
\int \frac{\mathrm{d}^d k}{\pi^{d/2}} \frac{\rho}{D_1 \cdots D_n} &= \epsilon \int \frac{\mathrm{d}^{d+2} k}{\pi^{(d+2)/2}} \frac{1}{D_1 \cdots D_n} \\
\int \frac{\mathrm{d}^d k}{\pi^{d/2}} \frac{\rho^2}{D_1 \cdots D_n} &= \epsilon(\epsilon - 1) \int \frac{\mathrm{d}^{d+4} k}{\pi^{(d+4)/2}} \frac{1}{D_1 \cdots D_n}
\end{aligned} \tag{10.10}$$

also given by eqs. (D.23) and (D.25), as shown in appendix D. From eqs. (G.7) in appendix G, we see that the results will be

$$I^{[4-2\epsilon]}_{\text{box}}(\rho) = 0 + \mathcal{O}(\epsilon) \qquad\qquad I^{[4-2\epsilon]}_{\text{box}}(\rho^2) = -\frac{1}{6} + \mathcal{O}(\epsilon) \tag{10.11}$$

meaning that the only contribution from the higher-dimensional parts of the integral is finite.

The same thing will happen for the triangle and the bubble contributions, which allows us to write eq. (10.3) as

$$A^{(1)} = \int \frac{\mathrm{d}^4 k}{(2\pi)^4} \left(\frac{\Delta^{[4]}_{\text{box}}}{l_1^2\, l_2^2\, l_3^2\, l_4^2} + \sum_{x<y<z} \frac{\Delta^{[4]}_{\text{triangle},xyz}}{l_x^2\, l_y^2\, l_z^2} + \sum_{x<y} \frac{\Delta^{[4]}_{\text{bubble},xy}}{l_x^2\, l_y^2} \right) + \mathcal{R} \tag{10.12}$$

where $\mathcal{R}$ is denoted the rational term and contains all the contributions from the -2ϵ-dimensional parts of the integrals.

There are methods to find the rational term $\mathcal{R}$ separately from the rest of the amplitude (see [11, 101]), but as most of these methods do not generalize to higher loops in any obvious way they will not be described here. Let us instead focus on a way of identifying the full set of the coefficients of eq. (10.9), independently of whether or not they contain factors of ρ.

One obvious approach is to try to identify the cut $\Delta^{[d]}_{\text{box}}$ as a product of tree-level amplitudes, as we did in the four dimensional cases. But in this case the trees will in general have to be of particles in d dimensions, which may not be well-defined generally. The solution is to embed the $4-2\epsilon$ dimensions into an integer number of dimensions, and at one loop that number can be chosen as five, with the fifth component of the loop-momentum being

$$k_5 = \sqrt{-\rho} \tag{10.13}$$

We see that this factor will only appear squared, making it similar to a four-dimensional momentum with a mass $m^2 = \rho$ [11, 102].

The quadruple-cut imposes four constraints on the loop-momentum k, giving

$$\bar{k}^\mu|_{4\times\text{cut}} = \tau\frac{\langle 23\rangle}{\langle 13\rangle}\frac{\langle 1|\sigma^\mu|2]}{2} + (1-\tau)\frac{[23]}{[13]}\frac{\langle 2|\sigma^\mu|1]}{2} \tag{10.14}$$

with the additional constraint

$$\rho = \bar{k}^2 \tag{10.15}$$

This solution is unique, in agreement with the result of the previous chapter.

If one carries on naively with this unitarity-based approach, another problem turns up. The helicity-sum over the cut propagators will now be over three[2] helicity-states rather than two, so to get the correct limit back to $d = 4$ these extra states will have to be removed, and just removing them from the helicity sum by force is not an option as it will break gauge invariance. The solution is to notice from the Feynman rules (see appendix H), that a higher dimensional vector boson behaves just like a scalar of the type known from $\mathcal{N} = 4$ SYM [61, 79]. Thus we get that removing the higher dimensional helicity component from the helicity sum, corresponds to subtracting a scalar loop. For different regularization schemes we may want different values[3] for the number of polarization directions of the gluons D_s, as described in section 4.1. This gives

$$\Delta^{[d]}_{\text{g}} = \Delta^{[5]}_{\text{g}} + (D_s - 5)\Delta^{[5]}_{\text{s}} \tag{10.16}$$

[2]If one interprets the massless five-dimensional particles as massive four-dimensional ones, and if one does that the third polarization direction will correspond to the longitudinal.

[3]As described in section 4.1, this could be the FDH scheme which has $D_s = 4$, or the 't Hooft-Veltman scheme in which $D_s = d$.

where the subscribed g denotes a gluon circling the loop, and a subscribed s denotes a scalar. That is

$$\Delta_{\rm g}^{[5]} = \sum_{\{h_1,\ldots,h_4\}}^{[5]} \mathcal{A}_{ggg}(-l_1^{-h_1} p_1^{a_1} l_2^{h_2}) \mathcal{A}_{ggg}(-l_2^{-h_2} p_2^{a_2} l_3^{h_3}) \mathcal{A}_{ggg}(-l_3^{-h_3} p_3^{a_3} l_4^{h_4}) \mathcal{A}_{ggg}(-l_4^{-h_4} p_4^{a_4} l_1^{h_1})$$
$$\Delta_{\rm s}^{[5]} = \mathcal{A}_{sgs}(-l_1 p_1^{a_1} l_2) \mathcal{A}_{sgs}(-l_2 p_2^{a_2} l_3) \mathcal{A}_{sgs}(-l_3 p_3^{a_3} l_4) \mathcal{A}_{sgs}(-l_4 p_4^{a_4} l_1) \tag{10.17}$$

just like in the four-dimensional case of eq. (5.21).

Using eq. (10.16), we may combine the two contributions, and we see from the form of eq. (10.8), that the expression for the cut irreducible numerator will be

$$\Delta_{\rm box}|_{\rm cut} = \sum_{i=0}^{4} d_i \tau^i \tag{10.18}$$

where the terms may be related as

$$\bar{d} = M \bar{c} \tag{10.19}$$

where M is quadratic as it will be in most d-dimensional cases, and easily invertible.

10.2 Results for the one-loop box

In d dimensions all helicity configurations of the external gluons give a non-vanishing result. This means that there are four structurally different configurations $(--++)$, $(-+-+)$, $(-+++)$, and $(++++)$, where the two last are new to the d-dimensional case.

Let us start by regarding the helicity configuration $(--++)$. In this case we get on the cut, the expressions

$$\Delta_{\rm g}^{--++}|_{\rm cut} = \frac{\langle 12\rangle^3}{\langle 23\rangle\langle 34\rangle\langle 41\rangle} st \left(-1 - 4\frac{t}{u}\tau + \frac{t}{u^2}(4u-3t)\tau^2 + 6\frac{t^2}{u^2}\tau^3 - 3\frac{t^2}{u^2}\tau^4\right)$$
$$\Delta_{\rm s}^{--++}|_{\rm cut} = \frac{\langle 12\rangle^3}{\langle 23\rangle\langle 34\rangle\langle 41\rangle} \frac{-st^3}{u^2}\tau^2 \tag{10.20}$$

which, after combining according to eq. (10.16) and inverting using eq. (10.19), gives the result

$$\Delta_{\rm box}^{--++} = \frac{\langle 12\rangle^3}{\langle 23\rangle\langle 34\rangle\langle 41\rangle} \left(-st + 4t\rho - (D_s - 2)\frac{t}{s}\rho^2\right) \tag{10.21}$$

Following the same procedure for the other configurations we get

$$\begin{aligned}
\Delta^{-+-+}_{\text{box}} &= \frac{\langle 13\rangle^4}{\langle 12\rangle\langle 23\rangle\langle 34\rangle\langle 41\rangle}(-st)\bigg(\Big(s^2+t^2-4u\rho+4s(k\cdot\omega)\Big)\frac{1}{u^2} \\
&\quad + \Big(s^2t^2/2+2stu\rho+u^2\rho^2-s(st+2u\rho)(k\cdot\omega)\Big)\frac{(D_s-2)}{u^4}\bigg) \\
\Delta^{-+++}_{\text{box}} &= \frac{\langle 12\rangle^2[23]}{\langle 42\rangle^2\langle 23\rangle}\left(\frac{st}{2u}\rho-\frac{s}{u}(k\cdot\omega)\rho+\rho^2\right)(D_s-2) \\
\Delta^{++++}_{\text{box}} &= \frac{st}{\langle 12\rangle\langle 23\rangle\langle 34\rangle\langle 41\rangle}\rho^2(D_s-2)
\end{aligned} \tag{10.22}$$

If we take the four-dimensional limits $D_s \to 4$ and $\rho \to 0$, we obtain

$$\begin{aligned}
&\tilde{\Delta}^{--++}_{\text{box}[4]} = -st \qquad \tilde{\Delta}^{-+++}_{\text{box}[4]} = 0 \qquad \tilde{\Delta}^{++++}_{\text{box}[4]} = 0 \\
&\tilde{\Delta}^{-+-+}_{\text{box}[4]} = \frac{-st}{u^4}\Big((s^2+t^2+st)^2+2s(2s^2+2t^2+3st)(k\cdot\omega)\Big)
\end{aligned} \tag{10.23}$$

with the tree left out, and we see this to agree with the gluonic[4] part of eqs. (5.38).

From the results of eqs. (10.22), we may now obtain the box-contribution to the rational terms for the various helicity configurations using eqs. (10.11), and the results are

$$\begin{aligned}
\tilde{\mathcal{R}}^{--++}_{\text{box}} &= \frac{D_s-2}{6}\frac{t}{s} & \tilde{\mathcal{R}}^{-+-+}_{\text{box}} &= \frac{D_s-2}{6}\frac{st}{u^2} \\
\tilde{\mathcal{R}}^{-+++}_{\text{box}} &= -\frac{D_s-2}{6} & \tilde{\mathcal{R}}^{++++}_{\text{box}} &= -\frac{D_s-2}{6}
\end{aligned} \tag{10.24}$$

We could go ahead and finish the one-loop calculation with the triangles, the bubbles, and the other flavours, but let us instead move on to more loops, and look at two-loop topologies in d dimensions.

[4] As the D_s contribution has been calculated using the scalar amplitudes, we could have recovered the scalar part of eqs. (5.38) too, by the substitution $D_s \to 4+2n_s$.

Chapter 11

Two-loops in d dimensions

In this chapter we will describe how to perform integrand reduction for two-loop amplitudes in d dimensions, in a way compatible with generalized unitarity cuts. We will need this for the calculation of the penta-box in the next chapter, which is arguably the most important result of the thesis. First we will describe in general how to treat the d-dimensional two-loop case, then we will describe the six-dimensional spinor-helicity formalism of [103] which we will use in the calculation of the tree-level amplitudes, and finally we will do an example of $2 \to 2$ gluon scattering in the all-plus helicity configuration. This chapter is largely based of the first half of [3].

11.1 Treatment of two loops

At the two-loop order the set of ISPs is supplemented by three ρ-parameters of the type defined in eq. (9.8):

$$\rho_1 = -\left(k_1^{[-2\epsilon]}\right)^2 \qquad \rho_2 = -\left(k_2^{[-2\epsilon]}\right)^2 \qquad \rho_{12} = -2k_1^{[-2\epsilon]} \cdot k_2^{[-2\epsilon]} \tag{11.1}$$

As in the one-loop case we need to embed the d-dimensional loop-momenta in an integer-dimensional space in order to make full sense of the tree-level amplitudes and the cuts. To contain the three ρ-parameters we need to embed in at least $\mathcal{D} = 6$ dimensions, and in that case the specific embedding is

$$k_1 \to \left(\bar{k}_1, m_1 \cos(\theta_1), m_1 \sin(\theta_1)\right), \qquad k_2 \to \left(\bar{k}_2, m_2 \cos(\theta_2), m_2 \sin(\theta_2)\right) \tag{11.2}$$

where $m_1^2 = \rho_1$, $m_2^2 = \rho_2$, and the angles θ_1 and θ_2 are related by

$$\cos(\theta_1 - \theta_2) = \frac{\rho_{12}}{2m_1 m_2} \tag{11.3}$$

This leaves one degree of freedom, say the angle θ_2, but the physicality of the resulting irreducible numerator requires it to be independent of that choice, and indeed independence from this unphysical degree of freedom can be used as a check of intermediate results.

Like we saw in the one-loop case, this embedding introduces new polarization directions for gluons circling the loops - two such new directions in this case, which we need to remove in a way compatible with gauge invariance in order to get a result which goes correctly unto the four-dimensional case in the limit. Let us keep the number of dimensions in which the gluons are allowed to be polarized as a free parameter D_s as we saw in the previous chapter and in section 4.1. In the case where $D_s > \mathcal{D}$ it is easy to see from the Feynman rules of appendix H that each extra polarization direction behaves exactly as a $\mathcal{D}$-dimensional scalar with the same interaction as the scalars known from super Yang-Mills, for which the Feynman rules too are listed in appendix H.

This gives

$$\Delta_g^{[D_s]} = \Delta_g^{[\mathcal{D}]} + (D_s - \mathcal{D})\Delta_s^{[\mathcal{D}]} + (D_s - \mathcal{D})^2\Delta_{2s}^{[\mathcal{D}]} \tag{11.4}$$

where the subscripts g, s, and $2s$ denote diagrams with pure gluons, with one scalar loop, and with two scalar loops respectively. We realize that $\Delta_{2s}^{[\mathcal{D}]}$ can exist only for butterfly-type topologies[1], as they alone allow for two independent loops. We may analytically continue eq. (11.4) to the regime where $D_s < \mathcal{D}$, with the result

$$\Delta_g^{[D_s]} = \Delta_g^{[\mathcal{D}]} - (6 - D_s)\Delta_s^{[\mathcal{D}]} + (6 - D_s)^2\Delta_{2s}^{[\mathcal{D}]} \tag{11.5}$$

where we have inserted $\mathcal{D} = 6$. This is similar to eq. (10.16) for the one-loop case. We will keep D_s as a free parameter as different schemes correspond to different values. The FDH scheme which takes only the internal momenta to be d-dimensional has $D_s = 4$, while the 't Hooft-Veltman scheme which takes all of the internal particles to be d-dimensional therefore has $D_s = d$, as described in section 4.1.

It should be noted that it is not necesary to use eq. (11.5) to obtain an amplitude with D_s-dependence. If one is satisfied with doing a purely Feynman diagrammatical calculation rather that using generalized unitarity cuts, the D_s dependence can be introduced by using

$$D_s = g^\mu_\mu \tag{11.6}$$

as the $g^{\mu\nu}$ in the propagators come from the helicity sum as seen by eq. (5.20).

11.2 The six-dimensional spinor-helicity formalism

In the one-loop case where we needed to evaluate five-dimensional tree-amplitudes, we could use the fact that a massless five-dimensional particle is similar to a four-dimensional massive one. This is unfortunately impossible for the six-dimensional case. For that case we need to treat the extra dimensions as dimensions on an equal footing with the original four, and a way to perform this is to use a six

[1] A butterfly topology is one for which no propagator is dependent on both k_1 and k_2.

dimensional spinor-helicity formalism which has been developed by Cheung and O'Connell in [103]. That formalism is described in detail in appendix B, and we will here summarize those of the results which are relevant for the present discussion. It should be noted that the idea of using the six-dimensional spinor-helicity formalism in the context of unitarity cuts origins in refs. [104, 105].

In six dimensions one may define Weyl spinors Λ^{Aa} and $\tilde{\Lambda}^{\dot{a}}_{A}$, corresponding to λ^{α} and $\tilde{\lambda}_{\dot{\alpha}}$ in four dimensions. The index A is a spinor index running from 1 to 4, and the indices a and $\dot{a}$ are indices of the little group which each run from 1 to 2. The similarity with the four-dimensional case allows us to adopt a similar notation:

$$\Lambda^{Aa} = \langle P^{a}| \,, \qquad\qquad \tilde{\Lambda}_{A\dot{a}} = [P_{\dot{a}}| \,, \tag{11.7}$$

and indeed the basic relations obeyed by the six dimensional spinors are similar too. Contracting two spinors of the same momentum, gives the momentum back

$$\Lambda^{Aa}\Lambda^{B}_{a} = P^{\mu}\tilde{\Sigma}^{AB}_{\mu} \,, \qquad\qquad \tilde{\Lambda}_{A\dot{a}}\tilde{\Lambda}^{\dot{a}}_{B} = P_{\mu}\Sigma^{\mu}_{AB} \,, \tag{11.8}$$

where we have used Σ^{μ} to denote the six-dimensional version of the Pauli matrices σ^{μ}.

By contracting the spinor indices one obtains a spinor product $\langle i_a \, j_{\dot{b}}]$ which is related to the square of the momentum as

$$\det\left(\langle i_a \, j_{\dot{b}}]\right) = (P_i + P_j)^2 \equiv S_{ij} \tag{11.9}$$

a relation which is similar to $\langle ij\rangle[ji] = s_{ij}$ in the four-dimensional case, except that we see that the little group indices allows $\langle i_a \, j_{\dot{b}}]$ to contain the information of both of the four-dimensional spinor products, making only one kind needed. We may also form two kinds of vector product of spinors $\langle P_a \Sigma^{\mu} Q^{b}\rangle$ and $[P^{\dot{a}}\tilde{\Sigma}^{\mu}Q_{\dot{b}}]$, which can be made to reproduce the original vector as

$$P^{\mu}_{i} = \frac{-1}{4}\big\langle i^{a}\Sigma^{\mu}i_{a}\big\rangle = \frac{-1}{4}\big[i_{\dot{a}}\tilde{\Sigma}^{\mu}i^{\dot{a}}\big] \,. \tag{11.10}$$

similar to eq. (3.15) in the four-dimensional case.

We may, also in six dimensions, use the vector products to form a set of polarization vectors valid in an axial gauge. With an axial direction given by the vector Q^{μ}, the result is

$$\mathcal{E}^{\mu}_{a\dot{a}}(P,Q) = \frac{-1}{\sqrt{2}}\frac{\big\langle P_a\Sigma^{\mu}Q^{b}\big\rangle\big\langle Q_b P_{\dot{a}}\big]}{2P\cdot Q} = \frac{1}{\sqrt{2}}\frac{\big\langle P_a Q_{\dot{b}}\big]\big[Q^{\dot{b}}\tilde{\Sigma}^{\mu}P_{\dot{a}}\big]}{2P\cdot Q}, \tag{11.11}$$

where the four combinations of little group indices correspond to the four polarization directions available for six-dimensional vector bosons. If the momentum and the reference momentum of the particle is limited to four dimensions, helicity $\{11\}$ corresponds to helicity $+$, $\{22\}$ corresponds to $-$, and $\{12\}$ and $\{21\}$ are then the two new polarization directions into the extra dimensions.

The polarization vectors of eq. (11.11) obey the usual rules that $P\cdot\mathcal{E} = Q\cdot\mathcal{E} = 0$, and has the inner product rules

$$\mathcal{E}_{11}\cdot\mathcal{E}_{22} = -1\,, \qquad \mathcal{E}_{12}\cdot\mathcal{E}_{21} = 1\,, \qquad \text{other combinations} = 0\,. \tag{11.12}$$

The completeness relation for the polarization vectors is given as

$$\mathcal{E}^{\mu}_{a\dot{b}}\mathcal{E}^{\nu a\dot{b}} = \mathcal{E}^{\mu}_{11}\mathcal{E}^{\nu}_{22} + \mathcal{E}^{\mu}_{22}\mathcal{E}^{\nu}_{11} - \mathcal{E}^{\mu}_{12}\mathcal{E}^{\nu}_{21} - \mathcal{E}^{\mu}_{21}\mathcal{E}^{\nu}_{12} = -g^{\mu\nu} + \frac{P^{\mu}Q^{\nu} + Q^{\mu}P^{\nu}}{P\cdot Q}\,. \tag{11.13}$$

where we note the minus on the two last terms.

11.3 Two-to-two gluon scattering

In this section we will illustrate the d-dimensional method to calculate the planar two-loop contribution to the process $gg \to gg$ in the case where all the particles have the same positive helicity. The result of this section is not new, but was first calculated in [106]. Due to the exclusive helicity configuration, only two topologies contribute to the process, the double-box ($t331$) and the double-triangle-butterfly ($t330$) as seen on fig. 11.1.

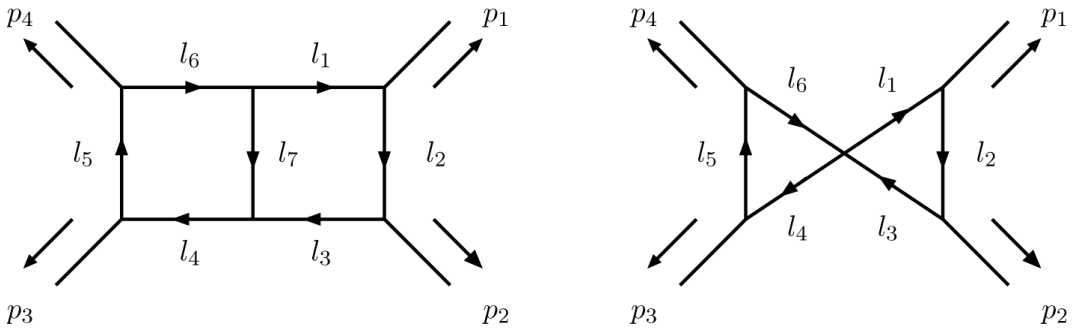

Figure 11.1: The two topologies ($t331$) and ($t330$) contributing to the all-plus helicity configuration.

The double-box ($t331$)

The double-box topology ($t331$) is given by

$$A^{[d]}_{331} = \int \frac{\mathrm{d}^d k_1}{(2\pi)^d} \int \frac{\mathrm{d}^d k_2}{(2\pi)^d} \frac{\Delta^{[d]}_{331}}{\prod_{i=1}^{7} l_i^2}, \tag{11.14}$$

where the propagating momenta will be parametrized as

$$\begin{aligned} &l_1 = k_1\,, && l_2 = k_1 - p_1\,, && l_3 = k_1 - p_1 - p_2\,, && l_4 = p_3 + p_4 - k_2\,, \\ &l_5 = p_4 - k_2\,, && l_6 = -k_2\,, && l_7 = -k_1 - k_2\,. \end{aligned} \tag{11.15}$$

which is the same parametrization as we used in section 6.1.

Using multivariate polynomial division toward the Gröbner basis for the ideal formed by the propagators of eqs. (11.15) as described in chapter 9 and implemented by BasisDet, we obtain that the irreducible numerator $\Delta^{[d]}_{331}$ may be written in terms of seven ISPs as

$$\Delta^{[d]}_{331} = \sum_{i_1 \ldots i_7} c_{i_1 \ldots i_7} (k_1 \cdot \omega)^{i_1} (k_2 \cdot \omega)^{i_2} (k_1 \cdot p_4)^{i_3} (k_2 \cdot p_1)^{i_4} \rho_1^{i_5} \rho_{12}^{i_6} \rho_2^{i_7} \tag{11.16}$$

where the sum goes over 160 distinct terms, and where ω is defined by eq. (6.3) to be perpendicular to all of the external momenta.

To account correctly for the dimensional dependence we have to use eq. (11.5), and thus we need to calculate three separate six-dimensional irreducible numerators, $\Delta^{[6]}_g$, $\Delta^{[6]}_s$, and $\Delta^{[6]}_{2s}$, which were the contribution with respectively zero, one, and two scalar loops.

To find those, we will use generalized unitarity cuts, and the hepta-cut equations $l_i^2 = 0$ have the solution

$$\begin{aligned} \bar{k}_1^\mu &= p_1^\mu + \tau_1 \frac{\langle 23 \rangle}{\langle 13 \rangle} \frac{\langle 1|\sigma^\mu|2]}{2} + \tau_2 \frac{[23]}{[13]} \frac{\langle 2|\sigma^\mu|1]}{2}, \\ \bar{k}_2^\mu &= p_4^\mu + \tau_3 \frac{\langle 41 \rangle}{\langle 31 \rangle} \frac{\langle 3|\sigma^\mu|4]}{2} + \tau_4 \frac{[41]}{[31]} \frac{\langle 4|\sigma^\mu|3]}{2}, \end{aligned} \tag{11.17}$$

along with

$$\rho_1 = \bar{k}_1^2 \,, \qquad \rho_2 = \bar{k}_2^2 \,, \qquad \rho_{12} = 2\bar{k}_1 \cdot \bar{k}_2 \,. \tag{11.18}$$

This solution is unique as it will be in all d-dimensional cases as we saw in section 9.2, and it is a function of four free parameters as predicted by eq. (9.9). Substituting the solution into eq. (11.16) yields the polynomial expression

$$\Delta_{331}|_{\text{cut}} = \sum_{j_1 \ldots j_4} d_{j_1 \ldots j_4} \tau_1^{j_1} \tau_2^{j_2} \tau_3^{j_3} \tau_4^{j_4} \tag{11.19}$$

which too has 160 terms, and relating the two expressions of eqs. (11.19) and (11.16) gives the linear relation

$$\bar{d} = M \bar{c} \tag{11.20}$$

where the matrix M is 160×160 and of full rank.

For each of the six-dimensional flavour contributions of eq. (11.5), we may calculate $\Delta|_{\text{cut}}$ as a product of trees as in all the cases in the previous sections. For the purely gluonic contribution Δ_g we have that

$$\begin{aligned} \Delta^{[6]}_{g,\,331}\big|_{\text{cut}} = \\ i^7 \times \sum_{\substack{\{h_1,\ldots,h_7\} \in \\ \{11,12,21,22\}}} \Big(& \sigma_{h_1,\ldots,h_7} \mathcal{A}(-l_1^{-h_1}, p_1^{\{11\}}, l_2^{h_2}) \mathcal{A}(-l_2^{-h_2}, p_2^{\{11\}}, l_3^{h_3}) \mathcal{A}(-l_3^{-h_3}, l_4^{h_4}, -l_7^{-h_7}) \\ & \mathcal{A}(-l_4^{-h_4}, p_3^{\{11\}}, l_5^{h_5}) \mathcal{A}(-l_5^{-h_5}, p_4^{\{11\}}, l_6^{h_6}) \mathcal{A}(-l_6^{-h_6}, l_1^{h_1}, l_7^{h_7}) \Big), \end{aligned} \tag{11.21}$$

where the little group indices $\{11\}$ correspond to helicity + in four dimensions. The σ-factor in the sum is new to the six-dimensional case. It accounts for the minus signs on the last two terms of the six-dimensional completeness relation eq. (11.13) which are needed to reproduce the metric, and it is defined as

$$\sigma_{h_1,\ldots,h_n} \equiv \prod_{i=1}^{n} (2\delta_{a_i \dot{a}_i} - 1). \tag{11.22}$$

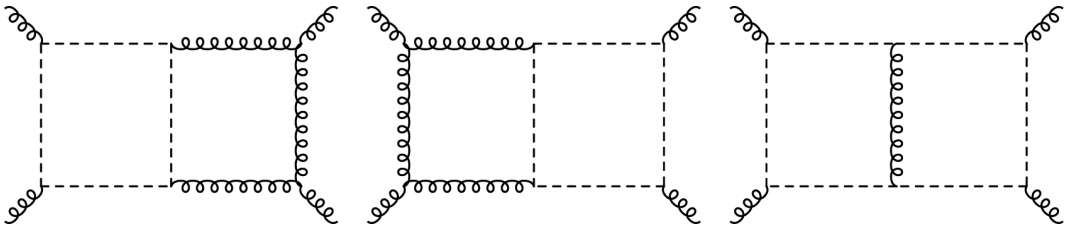

Figure 11.2: The three flavour contributions to $\Delta_{s,\,331}$.

The contribution with one scalar loop $\Delta_{s,\,331}$ have contributions from three different flavour contributions; those with the scalar loop on the left, those with the scalar loop on the right, and those for which the scalar goes all the way around as depicted on fig. 11.2. For these cases the coefficients of eq. (11.19) may be fitted from products of trees as in the purely gluonic case of eq. (11.21), but where the scalars have no σ-like coefficients and do not participate in the helicity sums.

$\Delta_{2s,\,331}$ vanishes as the $(t331)$ topology does not allow for separate scalar loops.

Combing the two coefficients according to eq. (11.5) yields the known result from [106]:

$$\Delta_{331} = \frac{-i s_{12}^2 s_{14} F_1(D_s, \rho_1, \rho_2, \rho_{12})}{\langle 12\rangle\langle 23\rangle\langle 34\rangle\langle 41\rangle}, \tag{11.23}$$

where

$$F_1(D_s, \rho_1, \rho_2, \rho_{12}) \equiv (D_s - 2)\,(\rho_1\rho_2 + \rho_1\rho_3 + \rho_2\rho_3) + 4\left(\rho_{12}^2 - 4\rho_1\rho_2\right) \tag{11.24}$$

and $\rho_3 \equiv \rho_1 + \rho_2 + \rho_{12}$.

The butterfly $(t330)$

The calculation for the butterfly topology of fig. 11.1 is very similar to that of the double-box. It may be parametrized in terms of the first six of the momenta of eqs. (11.15), and BasisDet tells us that the form of the irreducible numerator Δ_{330} is similar to the double-box case of eq. (11.16), except that the sum goes over 146 terms in general.

The solution to the hexa-cut equations is identical to that of eqs. (11.17) and (11.18), except that no cut fixes ρ_{12} making it a fifth free parameter $\rho_{12} = s_{12}\tau_5$ where

the s_{12} have been inserted to make all the τs unitless. The polynomial expansion in the five τ variables of Δ_{330} on the cut will have 146 terms, making the linear system quadratic and trivially invertible.

The value of each Δ_{330} on the cut can be fit from a product of trees, if ones removes the leading singularity coming from ($t331$) by the OPP procedure. Thus the purely gluonic contribution is given as

$$\Delta^{[6]}_{g,\,330}\big|_{\text{cut}} = i^6 \times \sum_{\{h_1,\ldots,h_6\}} \Big(\sigma_{h_1,\ldots,h_6} \mathcal{A}(-l_1^{-h_1}, p_1^{\{11\}}, l_2^{h_2}) \mathcal{A}(-l_2^{-h_2}, p_2^{\{11\}}, l_3^{h_3}) \mathcal{A}(-l_3^{-h_3}, l_4^{h_4}, -l_6^{-h_6}, l_1^{h_1}) \mathcal{A}(-l_4^{-h_4}, p_3^{\{11\}}, l_5^{h_5}) \mathcal{A}(-l_5^{-h_5}, p_4^{\{11\}}, l_6^{h_6}) \Big) - \frac{1}{(l_6 - l_1)^2} \Delta^{[6]}_{g,\,331}. \tag{11.25}$$

The Δ_s term has four contributions for the butterfly cases, as seen by fig. 11.3. Three of these are in common with the ($t331$)-case but the fourth is unique to butterflies. It has its origin in the $V_{ss's's'}$-vertex of appendix H, and can be interpreted as a scalar loop forming a figure eight.

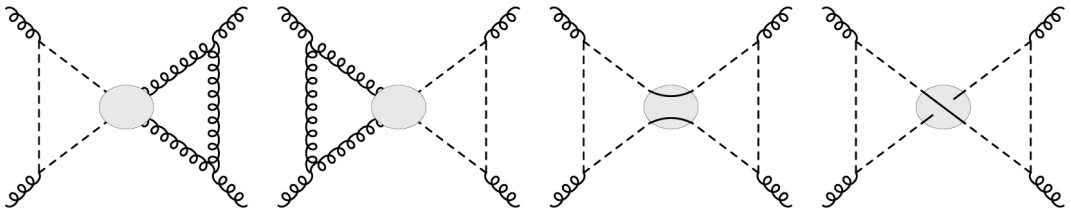

Figure 11.3: The four flavour contributions to $\Delta_{s,\,330}$

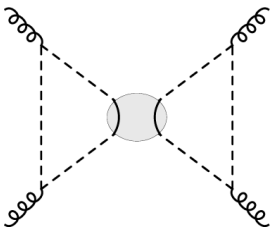

Figure 11.4: The flavour contribution to $\Delta_{2s,\,330}$

The Δ_{2s} term is non-vanishing for the butterfly case, and it is shown on fig. 11.4. Combining $\Delta_{g,\,330}$, $\Delta_{s,\,330}$, and $\Delta_{2s,\,330}$ according to eq. (11.5) gives the result

$$\Delta_{330} = \frac{-i s_{12} s_{14} \Big(2(D_s - 2)(\rho_1 + \rho_2)\rho_{12} + (D_s - 2)^2 \rho_1 \rho_2 \big((k_1 + k_2)^2 + s_{12} \big) / s_{12} \Big)}{\langle 12 \rangle \langle 23 \rangle \langle 34 \rangle \langle 41 \rangle}. \tag{11.26}$$

which too agrees with the known result from [106].

Chapter 12

Two-to-three gluon scattering

In this chapter, which is based on the second half of [3], we will develop and show the main result of this thesis, the full, d-dimensional, planar, two-loop, pure Yang-Mills contribution to the process $gg \to ggg$ in the case where all[1] the external gluons have positive helicity.

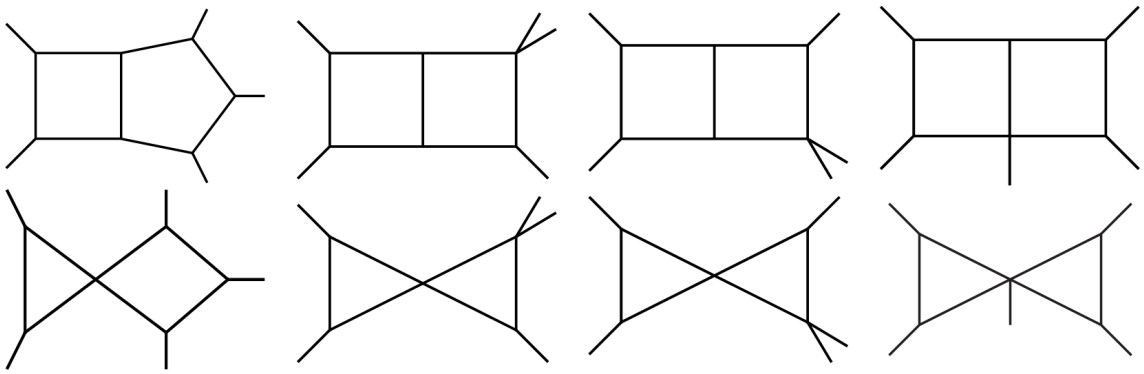

Figure 12.1: The eight topologies which contribute to the process described in this section. They are $(t431)$, $(t331; M_1)$, $(t331; M_2)$, $(t331; 5L)$, $(t430)$, $(t330; M_1)$, $(t330; M_2)$, $(t330; 5L)$ in (western) reading order.

As we saw for the similar case for $2 \to 2$ in section 11.3, the specific helicity configuration makes most of the topologies which could be contributing to the amplitude vanish, leaving only a few. For $2 \to 3$ there are eight such topologies which are shown on fig. 12.1.

All the topologies have a set of propagators, which is a subset of those of the parent topology $(t431)$ - the pentagon-box. $(t431)$ is rooted as shown on fig. 12.2,

[1] They are all positive in the case where all the gluons are perceived as out-going. If we actually regard the process as $gg \to ggg$, the two incoming gluons will have helicity minus, and the three outgoing helicity plus.

where the eight momenta are given as

$$\begin{aligned} &l_1 = k_1, && l_2 = k_1 - p_1, && l_3 = k_1 - p_1 - p_2, \\ &l_4 = k_1 - p_1 - p_2 - p_3, && l_5 = -k_2 + p_4 + p_5, && l_6 = -k_2 + p_5, \\ &l_7 = -k_2, && l_8 = -k_1 - k_2, \end{aligned} \tag{12.1}$$

We will keep this enumeration and rooting for all the topologies, even if it means ruining the consecutivity of the loop-momenta.

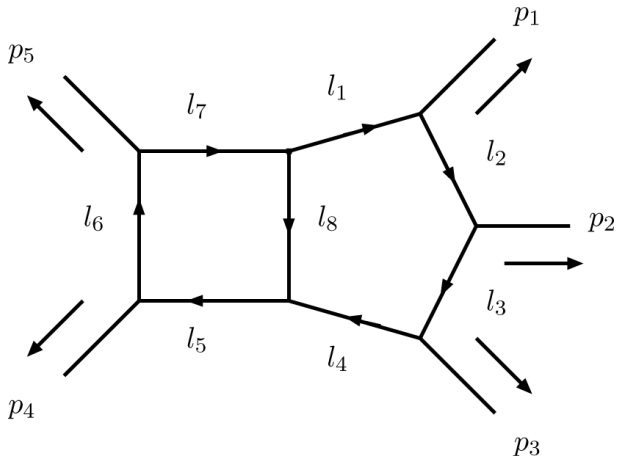

Figure 12.2: The rooting of the parent topology ($t431$).

The topologies $(t331; M_1)$ and $(t330; M_1)$ are related to the topologies $(t331; M_2)$ and $(t330; M_2)$ due to reflection symmetry, as

$$\Delta_{M_1}(k_1, k_2, p_1, p_2, p_3, p_4, p_5) = -\Delta_{M_2}(-p_{45} - k_1, p_{45} - k_2, p_3, p_2, p_1, p_5, p_4) \tag{12.2}$$

so therefore only six of the eight are independent. In the following six sections we will calculate the values of those independent topologies, in order to be able to combine and analyze the result in sections 12.7, 12.8, and 12.9.

In addition to the eight topologies of fig. 12.2, we have checked additional topologies $(t521)$, $(t421; M)$, $(t321; 5L)$, $(t420)$, $(t320; 5L)$, and $(t220; 5L)$. They all vanish when the irreducible numerators from the following sections are used as OPP subtraction terms.

We did the calculations of the following sections twice, both using a numerical implementation of the six-dimensional spinor-helicity formalism and using a Feynman diagrammatic approach with the intermediate expressions simplified using the momentum twistor variables of appendix C.2.

12.1 The pentagon-box $(t431)$

Using BasisDet, we get that the irreducible numerator Δ_{431}, may be written in terms of 79 monomials of the six ISPs

$$(k_1 \cdot p_5)\,,\ \ (k_2 \cdot p_2)\,,\ \ (k_2 \cdot p_1)\,,\ \ \rho_1\,,\ \ \rho_{12}\,,\ \ \rho_2\,, \tag{12.3}$$

where a little bit of manual rearranging of the output of BasisDet is needed in order to make the four-dimensional limit manifest[2].

The on-shell constraints have the solution

$$\begin{aligned}\bar{k}_1^\mu &= p_1^\mu + \tau_1 \frac{\langle 23\rangle}{\langle 13\rangle}\frac{\langle 1|\sigma^\mu|2]}{2} + (1-\tau_1)\frac{[23]}{[13]}\frac{\langle 2|\sigma^\mu|1]}{2} \\ \bar{k}_2^\mu &= p_5^\mu + \tau_2 \frac{\langle 51\rangle}{\langle 41\rangle}\frac{\langle 4|\sigma^\mu|5]}{2} + \tau_3 \frac{[51]}{[41]}\frac{\langle 5|\sigma^\mu|4]}{2}\end{aligned} \tag{12.4}$$

with the additional constraints

$$\rho_1 = \bar{k}_1^2 \qquad\qquad \rho_2 = \bar{k}_2^2 \qquad\qquad \rho_{12} = 2(\bar{k}_1 \cdot \bar{k}_2) \tag{12.5}$$

For the all-plus helicity configuration we may fit the cut topology from a sum over products of tree-level amplitudes as we did for the $2 \to 2$ case in eq. (11.21), and combine the six-dimensional flavour contributions according to eq. (11.5). Doing so yields the result

$$\Delta_{431} = -\frac{i\, s_{12}s_{23}s_{45}\, F_1(D_s,\rho_1,\rho_2,\rho_{12})}{\langle 12\rangle\langle 23\rangle\langle 34\rangle\langle 45\rangle\langle 51\rangle \mathrm{tr}_5}\left(\mathrm{tr}_+(1345)(k_1+p_5)^2 + s_{51}s_{34}s_{45}\right) \tag{12.6}$$

where

$$\mathrm{tr}_5 \equiv \mathrm{tr}\left(\gamma_5 \not{p}_1 \not{p}_2 \not{p}_3 \not{p}_4\right) \qquad\qquad \mathrm{tr}_\pm(abcd) \equiv \mathrm{tr}\left((1\pm\gamma_5)\not{p}_a \not{p}_b \not{p}_c \not{p}_d\right) \tag{12.7}$$

with further relations listed in section 1.1. Additionally we have that

$$F_1(D_s,\rho_1,\rho_2,\rho_{12}) \equiv (D_s-2)\left(\rho_1\rho_2 + \rho_1\rho_3 + \rho_2\rho_3\right) + 4\left(\rho_{12}^2 - 4\rho_1\rho_2\right) \tag{12.8}$$

with $\rho_3 \equiv \rho_1 + \rho_2 + \rho_{12}$, just like for the $2 \to 2$ case of eq. (11.24).

12.2 The massive double-box $(t331; M_2)$

For this topology we get that the irreducible numerator consists of 160 monomials of the ISPs

$$(k_1 \cdot \omega)\,,\ \ (k_2 \cdot \omega)\,,\ \ (k_1 \cdot p_5)\,,\ \ (k_2 \cdot p_1)\,,\ \ \rho_1\,,\ \ \rho_{12}\,,\ \ \rho_2\,, \tag{12.9}$$

[2]The limit is manifest if all the terms which appear in the four-dimensional case, are present in the d-dimensional case as well. As BasisDet uses the DegreeLexicographic ordering which prefers low powers to high powers in all cases, this will not happen automatically as it may trade some high powers of $k_i \cdot \beta_j$ for low powers of ρ.

where the vector ω is defined to be perpendicular to p_1, p_4, and p_5.

The hepta-cut equations have the solution

$$\begin{aligned}\bar{k}_1^\mu &= p_1^\mu + \tau_1 \frac{\langle \flat 4\rangle}{\langle 14\rangle}\frac{\langle 1|\sigma^\mu|\flat]}{2} + \tau_2 \frac{[\flat 4]}{[14]}\frac{\langle \flat|\sigma^\mu|1]}{2} \\ \bar{k}_2^\mu &= p_5^\mu + \tau_3 \frac{\langle 51\rangle}{\langle 41\rangle}\frac{\langle 4|\sigma^\mu|5]}{2} + \tau_4 \frac{[51]}{[41]}\frac{\langle 5|\sigma^\mu|4]}{2}\end{aligned} \tag{12.10}$$

with the additional constraints

$$\rho_1 = \bar{k}_1^2 \qquad \rho_2 = \bar{k}_2^2 \qquad \rho_{12} = 2(\bar{k}_1 \cdot \bar{k}_2) \tag{12.11}$$

Here the vector $p_\flat$ is a massless "flattened" vector defined as

$$p_\flat \equiv p_{23}^{\flat_1} = p_2 + p_3 + \frac{s_{23}}{s_{12}+s_{13}} p_1 \tag{12.12}$$

in accordance with the method described in appendix F.1.

The result for the helicity configuration is

$$\Delta_{331;M_2} = -\frac{i\, s_{51} s_{45}^2\, \mathrm{tr}_-(1234)\, F_1(D_s, \rho_1, \rho_2, \rho_{12})}{\langle 12\rangle\langle 23\rangle\langle 34\rangle\langle 45\rangle\langle 51\rangle \mathrm{tr}_5}. \tag{12.13}$$

12.3 The five-legged double-box $(t331; 5L)$

This irreducible numerator for this topology[3] can be expanded in terms of 160 monomials of the ISPs

$$(k_1 \cdot p_5)\,,\ (k_1 \cdot p_4)\,,\ (k_2 \cdot p_2)\,,\ (k_2 \cdot p_1)\,,\ \rho_1\,,\ \rho_{12}\,,\ \rho_2\,. \tag{12.14}$$

The solution to the hepta-cut equations is given by

$$\begin{aligned}\bar{k}_1^\mu &= p_1^\mu + \tau_1 \frac{\langle 23\rangle}{\langle 13\rangle}\frac{\langle 1|\sigma^\mu|2]}{2} + \tau_2 \frac{[23]}{[13]}\frac{\langle 2|\sigma^\mu|1]}{2} \\ \bar{k}_2^\mu &= p_5^\mu + \tau_3 \frac{\langle 51\rangle}{\langle 41\rangle}\frac{\langle 4|\sigma^\mu|5]}{2} + \tau_4 \frac{[51]}{[41]}\frac{\langle 5|\sigma^\mu|4]}{2}\end{aligned} \tag{12.15}$$

with the additional constraints

$$\rho_1 = \bar{k}_1^2 \qquad \rho_2 = \bar{k}_2^2 \qquad \rho_{12} = 2(\bar{k}_1 \cdot \bar{k}_2) \tag{12.16}$$

The result is

$$\Delta_{331;5L} = \frac{i\, s_{12} s_{23} s_{34} s_{45} s_{51}\, F_1(D_s, \rho_1, \rho_2, \rho_{12})}{\langle 12\rangle\langle 23\rangle\langle 34\rangle\langle 45\rangle\langle 51\rangle \mathrm{tr}_5}. \tag{12.17}$$

[3]The five-legged double-box is also sometimes called the turtle-box.

12.4 The box-triangle butterfly ($t430$)

The irreducible numerator for this topology can be expanded in 85 monomials of the ISPs

$$(k_1 \cdot \omega_{123})\,,\ (k_2 \cdot \omega_{45-})\,,\ (k_2 \cdot \omega_{45+})\,,\ \rho_1\,,\ \rho_{12}\,,\ \rho_2\,, \tag{12.18}$$

with

$$\omega^\mu_{123} \equiv \frac{\langle 23\rangle[31]}{s_{12}}\frac{\langle 1|\sigma^\mu|2]}{2} - \frac{\langle 13\rangle[32]}{s_{12}}\frac{\langle 2|\sigma^\mu|1]}{2}, \tag{12.19}$$

as in eq. (6.3), and $\omega_{45\pm}$ defined in a way that makes them perpendicular to p_4, p_5, and to each other, as was done in the triangle case by eq. (5.41).

The seven generalized unitarity cut equations have the solution

$$\begin{aligned}\bar{k}_1^\mu &= p_1^\mu + \tau_1\frac{\langle 23\rangle}{\langle 13\rangle}\frac{\langle 1|\sigma^\mu|2]}{2} + (1-\tau_1)\frac{[23]}{[13]}\frac{\langle 2|\sigma^\mu|1]}{2}\\ \bar{k}_2^\mu &= p_5^\mu + \tau_2\frac{\langle 51\rangle}{\langle 41\rangle}\frac{\langle 4|\sigma^\mu|5]}{2} + \tau_3\frac{[51]}{[41]}\frac{\langle 5|\sigma^\mu|4]}{2}\end{aligned} \tag{12.20}$$

with the additional constraints

$$\rho_1 = \bar{k}_1^2 \qquad\qquad \rho_2 = \bar{k}_2^2 \qquad\qquad \rho_{12} = s_{45}\tau_4 \tag{12.21}$$

The result is

$$\begin{aligned}\Delta_{430} = &-\frac{is_{12}\mathrm{tr}_+(1345)}{2\langle 12\rangle\langle 23\rangle\langle 34\rangle\langle 45\rangle\langle 51\rangle s_{13}}\big(2(k_1\cdot\omega_{123}) + s_{23}\big)\\ &\times\left(2(D_s-2)(\rho_1+\rho_2)\rho_{12} + (D_s-2)^2\rho_1\rho_2\frac{(k_1+k_2)^2+s_{45}}{s_{45}}\right)\end{aligned} \tag{12.22}$$

We notice a number of new features in this result. This is a case - the first which we have seen - where it is advantageous to chose a different β for each k_i, and additionally we see that the result simplifies if one uses $(k_1+k_2)^2$ as an ISP rather than ρ_{12} on the $(D_s-2)^2$ term. These two features are recurrent in the other butterfly topologies.

12.5 The massive double-triangle butterfly ($t330; M_2$)

This topology has 146 coefficients in terms of the ISPs

$$(k_1 \cdot \omega_{1\flat-})\,,\ (k_2 \cdot \omega_{45-})\,,\ (k_1 \cdot \omega_{1\flat+})\,,\ (k_2 \cdot \omega_{45+})\,,\ \rho_1\,,\ \rho_{12}\,,\ \rho_2\,, \tag{12.23}$$

where $\omega_{1\flat\pm}$ is defined to be perpendicular to[4] p_1, p_2+p_3, and to each other, while $\omega_{45\pm}$ is defined to be perpendicular to p_4, p_5, and to each other as in the case of $(t331; M_2)$.

[4] or alternatively to p_1, to $p_\flat$ as defined by eq. (12.12), and to each other.

The hexa-cut equations have the solution

$$\bar{k}_1^\mu = p_1^\mu + \tau_1 \frac{\langle \flat 4\rangle}{\langle 14\rangle}\frac{\langle 1|\sigma^\mu|\flat]}{2} + \tau_2 \frac{[\flat 4]}{[14]}\frac{\langle \flat|\sigma^\mu|1]}{2}$$
$$\bar{k}_2^\mu = p_5^\mu + \tau_3 \frac{\langle 51\rangle}{\langle 41\rangle}\frac{\langle 4|\sigma^\mu|5]}{2} + \tau_4 \frac{[51]}{[41]}\frac{\langle 5|\sigma^\mu|4]}{2} \tag{12.24}$$

with the additional constraints

$$\rho_1 = \bar{k}_1^2 \qquad \rho_2 = \bar{k}_2^2 \qquad \rho_{12} = s_{45}\tau_5 \tag{12.25}$$

where $p_\flat$ is defined as in eq. (12.12).

The result is

$$\Delta_{330;M_2} = \frac{i\,\mathrm{tr}_+(1345)}{2\langle 12\rangle\langle 23\rangle\langle 34\rangle\langle 45\rangle\langle 51\rangle}\frac{s_{23}-s_{45}}{s_{13}}$$
$$\times\left(2(D_s-2)(\rho_1+\rho_2)\rho_{12} + (D_s-2)^2\rho_1\rho_2\frac{(k_1+k_2)^2+s_{45}}{s_{45}}\right). \tag{12.26}$$

12.6 The five-legged double-triangle butterfly $(t330; 5L)$

This topology has 146 coefficients in terms of the ISPs

$$(k_1\cdot\omega_{123})\,,\ (k_1\cdot p_3)\,,\ (k_2\cdot\omega_{453})\,,\ (k_2\cdot p_3)\,,\ \rho_1\,,\ \rho_{12}\,,\ \rho_2\,, \tag{12.27}$$

with the ω-vectors defined to be perpendicular to the vectors denoted by their three indices, in analogy with eq. (12.19).

The hexa-cut equation has the solution

$$\bar{k}_1^\mu = p_1^\mu + \tau_1 \frac{\langle 23\rangle}{\langle 13\rangle}\frac{\langle 1|\sigma^\mu|2]}{2} + \tau_2 \frac{[23]}{[13]}\frac{\langle 2|\sigma^\mu|1]}{2}$$
$$\bar{k}_2^\mu = p_5^\mu + \tau_3 \frac{\langle 51\rangle}{\langle 41\rangle}\frac{\langle 4|\sigma^\mu|5]}{2} + \tau_4 \frac{[51]}{[41]}\frac{\langle 5|\sigma^\mu|4]}{2} \tag{12.28}$$

with the additional constraints

$$\rho_1 = \bar{k}_1^2 \qquad \rho_2 = \bar{k}_2^2 \qquad \rho_{12} = s_{45}\tau_5 \tag{12.29}$$

and the result for the topology is

$$\begin{aligned}
\Delta_{330;5L} \;=\; & \frac{-i}{\langle 12\rangle\langle 23\rangle\langle 34\rangle\langle 45\rangle\langle 51\rangle}\times \\
\Bigg(\frac{1}{2}\Bigg(&\mathrm{tr}_+(1245) - \frac{\mathrm{tr}_+(1345)\mathrm{tr}_+(1235)}{s_{13}s_{35}}\Bigg)\Bigg(2(D_s-2)(\rho_1+\rho_2)\rho_{12} \\
&+ (D_s-2)^2\rho_1\rho_2\frac{4(k_1\cdot p_3)(k_2\cdot p_3) + (k_1+k_2)^2(s_{12}+s_{45}) + s_{12}s_{45}}{s_{12}s_{45}}\Bigg) \\
&+ (D_s-2)^2\rho_1\rho_2\Bigg[\,(k_1+k_2)^2 s_{51} \\
&+ \mathrm{tr}_+(1235)\left(\frac{(k_1+k_2)^2}{2s_{35}} - \frac{k_1\cdot p_3}{s_{12}}\left(1 + \frac{2(k_2\cdot\omega_{453})}{s_{35}} + \frac{s_{12}-s_{45}}{s_{35}s_{45}}(k_2-p_5)^2\right)\right) \\
&+ \mathrm{tr}_+(1345)\left(\frac{(k_1+k_2)^2}{2s_{13}} - \frac{k_2\cdot p_3}{s_{45}}\left(1 + \frac{2(k_1\cdot\omega_{123})}{s_{13}} + \frac{s_{45}-s_{12}}{s_{12}s_{13}}(k_1-p_1)^2\right)\right)\Bigg]\Bigg)
\end{aligned} \tag{12.30}$$

We notice a few things about this result. The β bases have been chosen to be less spurious than could be possible, as we for instance use $(k_1\cdot\omega_{123})$ and $(k_1\cdot p_3)$ rather that $(k_1\cdot\omega_{12\pm})$. This is to make the result simplify. Additionally we see that the result includes some terms, $(k_1-p_1)^2$ and $(k_2-p_5)^2$, which vanish completely on the cut as they correspond to the two propagators l_2 and l_6 of eqs. (12.1). This is in order to prevent the terms from appearing at lower point cuts.

12.7 Result for two-to-three gluon scattering

Knowing all the planar topologies, we may now calculate the leading colour two-loop contribution to $gg\to ggg$ for the specific all-plus helicity configuration. The leading colour contribution (see eq. (3.5)) is given as

$$\begin{aligned}
&A_{\text{leading colour}} = \\
&g_s^7 N_c^2 \sum_{\sigma\in S_5} \mathrm{tr}\big(T^{a_{\sigma(1)}}T^{a_{\sigma(2)}}T^{a_{\sigma(3)}}T^{a_{\sigma(4)}}T^{a_{\sigma(5)}}\big)\mathcal{A}^{(2)}\big(\sigma(1),\sigma(2),\sigma(3),\sigma(4),\sigma(5)\big)
\end{aligned} \tag{12.31}$$

where the sum is over all the permutations of the indices. The quantity $\mathcal{A}^{(2)}$ is[5] the partial amplitude which is given as

$$\mathcal{A}^{(2)} = \sum_{\text{cyclic}} A^{[P]}(1,2,3,4,5) \;-\frac{11}{3\epsilon}\mathcal{A}^{(1)} \tag{12.32}$$

where the last term is the counter-term from the UV renormalization, and $A^{[P]}$ is the primitive amplitude which is what we get by combining the topologies which we

[5] $\mathcal{A}^{(2)}$ is what is called $A^{(2)}_{5;1,1}$ in the notation of [33, 106]

calculated in the start of this section.

Eliminating all the spurious terms which integrate to zero as described in appendix F.3, we get the result

$$
\begin{aligned}
&A^{[P]}(1,2,3,4,5) = \frac{i}{\langle 12\rangle\langle 23\rangle\langle 34\rangle\langle 45\rangle\langle 51\rangle}\Big(c^a_{431} I_{431}[F_1] \\
&+ c^b_{431} I_{431}\big[F_1\ (k_1+p_5)^2\big] + c_{331;M_1} I_{331;M_1}[F_1] + c_{331;M_2} I_{331;M_2}[F_1] + c_{331;5L} I_{331;5L}[F_1] \\
&+ c_{430}\big(s_{23} I_{430}\big[F_3\ ((k_1+k_2)^2+s_{45})\big] + I_{430}\big[F_3\ ((k_1+k_2)^2+s_{45})\ 2(k_1{\cdot}\omega_{123})\big]\ \big) \\
&+ c_{330;M_1} I_{330;M_1}\big[F_3\ ((k_1+k_2)^2+s_{45})\big] + c_{330;M_2} I_{330;M_2}\big[F_3\ ((k_1+k_2)^2+s_{45})\big] \\
&+ c^a_{330;5L} I_{330;5L}[F_3\ N_1(k_1,k_2,1,2,3,4,5)] + c^b_{330;5L} I_{330;5L}[F_3\ N_2(k_1,k_2,1,2,3,4,5)] \\
&+ c^c_{330;5L} I_{330;5L}[F_3\ N_2(k_2,k_1,5,4,3,2,1)] + c^d_{330;5L} I_{330;5L}\big[F_3\ (k_1+k_2)^2\big]\Big),
\end{aligned}
\tag{12.33}
$$

where

$$
\begin{aligned}
c^a_{431} &= -\frac{s_{12}s_{23}s_{34}s_{45}^2 s_{51}}{\mathrm{tr}_5}\,, & c^b_{431} &= -\frac{s_{12}s_{23}s_{45}\mathrm{tr}_+(1345)}{\mathrm{tr}_5}\,, \\
c_{331;M_1} &= -\frac{s_{34}s_{45}^2\mathrm{tr}_+(1235)}{\mathrm{tr}_5}\,, & c_{331;M_2} &= -\frac{s_{51}s_{45}^2\mathrm{tr}_-(1234)}{\mathrm{tr}_5}\,, \\
c_{331;5L} &= \frac{s_{12}s_{23}s_{34}s_{45}s_{51}}{\mathrm{tr}_5}\,, & c_{430} &= -\frac{s_{12}\mathrm{tr}_+(1345)}{2s_{13}s_{45}}\,, \\
c_{330;M_1} &= \frac{(s_{12}-s_{45})\mathrm{tr}_+(1345)}{2s_{13}s_{45}}\,, & c_{330;M_2} &= \frac{(s_{23}-s_{45})\mathrm{tr}_+(1345)}{2s_{13}s_{45}}\,, \\
c^b_{330;5L} &= \frac{\mathrm{tr}_+(1235)}{2s_{35}s_{12}}\,, & c^c_{330;5L} &= \frac{\mathrm{tr}_+(1345)}{2s_{13}s_{45}}\,, \\
c^a_{330;5L} &= \frac{1}{2}\left(\frac{\mathrm{tr}_+(1235)\mathrm{tr}_+(1345)}{s_{13}s_{35}} - \mathrm{tr}_+(1245)\right)\,, \\
c^d_{330;5L} &= c^a_{330;5L}\frac{s_{12}+s_{45}}{s_{12}s_{45}} - s_{12}c^b_{330;5L} - s_{45}c^c_{330;5L} - s_{51}\,,
\end{aligned}
\tag{12.34}
$$

and

$$
\begin{aligned}
F_1 &= (D_s-2)(\rho_1\rho_2+\rho_1\rho_3+\rho_2\rho_3) + 4(\rho_{12}^2 - 4\rho_1\rho_2), \\
F_3 &= (D_s-2)^2\rho_1\rho_2, \\
N_1(k_1,k_2,1,2,3,4,5) &= \frac{1}{s_{12}s_{45}}\big(4(k_1\cdot p_3)(k_2\cdot p_3) + s_{12}s_{45}\big), \\
N_2(k_1,k_2,1,2,3,4,5) &= \frac{2}{s_{45}}(k_1\cdot p_3)\big(s_{35}s_{45} + 2(s_{45}-s_{12})(k_2\cdot p_5)\big).
\end{aligned}
\tag{12.35}
$$

We see that eq. (12.33) contains a number of integrals over the ρ-parameters of eqs. (11.18). To make sense of these, we use the technique described in appendix D, which allows us to relate them to higher dimensional integrals without such

coefficients. The result as given by eqs. (D.32) is

$$\begin{aligned}
I^{[4-2\epsilon]}\big(N(\bar{k}_i)(\rho_{12}^2 - 4\rho_1\rho_2)\big) &= -2\epsilon(2\epsilon+1)I^{[6-2\epsilon]}\big(N(\bar{k}_i)\big),\\
I^{[4-2\epsilon]}\big(N(\bar{k}_i)(\rho_1\rho_2 + \rho_1\rho_3 + \rho_2\rho_3)\big) &= 3\epsilon^2 I^{[6-2\epsilon]} + 2\epsilon(\epsilon-1)\sum_{i,j\in\mathcal{P}} \mathbf{i}^+\mathbf{j}^+ I^{[8-2\epsilon]}\big(N(\bar{k}_i)\big),\\
I^{[4-2\epsilon]}_{\text{butterfly}}\big(N(\bar{k}_i)\rho_1\rho_2\big) &= \epsilon^2 I^{[6-2\epsilon]}_{\text{butterfly}}\big(N(\bar{k}_i)\big),\\
I^{[4-2\epsilon]}_{\text{butterfly}}\big(N(\bar{k}_i)(\rho_1+\rho_2)\rho_{12}\big) &= 0,
\end{aligned} \tag{12.36}$$

where the set $\mathcal{P}$ includes the three branches of the topology such that the sum goes over all possible ways to increase the power of two propagators for each of the branches, as described in appendix D. The last equation of eqs. (12.36) has been applied already in order to obtain eq. (12.33).

Three of the integrals appearing in eq. (12.33) are still unknown[6] analytically, due to their five scales, so (12.33) will have to be our final form for the amplitude. Yet we are able to test the result in two ways.

The first test is a numerical evaluation of the poles of the partial amplitude of eq. (12.32), to see if they match those of the one-loop contribution as they should to enable infrared finiteness [107]. Our result passes this test. For more information on this check, including a table of numerical values, see [3].

Another test comes from the vanishing of unphysical poles, i.e. poles in non-adjacent Mandelstam variables $s_{i,i+2}$ which appear in the intermediate results of eqs. (12.34), for some of the butterfly coefficients. To do this we will evaluate the butterfly-contribution analytically.

12.8 Analytical result for the butterfly topologies

As a butterfly-integral in any dimension is nothing but a product of one-loop integrals, we may use the known one-loop results [60] to evaluate them analytically.

We see from eq. (12.33) that all the butterfly integrals contain an insertion of the F_3 of eqs. (12.35), and we see from (12.36) that such integrals all have a ϵ^2 factoring out. And as all the six-dimensional one-loop integrals diverges as mostly $1/\epsilon$ the combined result for the butterfly integrals will have to be finite.

Let us write the butterfly contribution to the primitive amplitude of eq. (12.33) as

$$\begin{aligned}
A^{[P]}_{\text{butterfly}}(1,2,3,4,5) \;=\; & \frac{i(D_s-2)^2}{\langle 12\rangle\langle 23\rangle\langle 34\rangle\langle 45\rangle\langle 51\rangle}\times\\
\Big(& c_{430}\big(s_{23}I^a_{430} + I^b_{430}\big) + c_{330;M_1}I_{330;M_1} + c_{330;M_2}I_{330;M_2}\\
& + c^a_{330;5L}I^a_{330;5L} + c^b_{330;5L}I^b_{330;5L} + c^c_{330;5L}I^c_{330;5L} + c^d_{330;5L}I^d_{330;5L}\Big)
\end{aligned} \tag{12.37}$$

[6] I have to add that I hope to remedy this rather soon.

with the coefficients given by eqs. (12.34). In that case we may evaluate all the integrals, with the results

$$\begin{aligned}
I^a_{430} &= \frac{1}{4} + \mathcal{O}(\epsilon)\,, \\
I^b_{430} &= \frac{\mathrm{tr}_5}{36 s_{12}} + \mathcal{O}(\epsilon)\,, \\
I_{330;M_1} &= \frac{s_{34} - 2s_{12} + 5s_{45}}{36} + \mathcal{O}(\epsilon)\,, \\
I_{330;M_2} &= \frac{s_{51} - 2s_{23} + 5s_{45}}{36} + \mathcal{O}(\epsilon)\,, \\
I^a_{330;5L} &= \frac{(s_{23} - 2s_{45})(s_{34} + 2s_{45}) + s_{12}(2s_{34} + 17 s_{45} - 2s_{23} - 4s_{12})}{36 s_{12} s_{45}} + \mathcal{O}(\epsilon)\,, \\
I^b_{330;5L} &= \frac{(2s_{35} - s_{34})(2s_{13} + s_{23})}{36} + \mathcal{O}(\epsilon)\,, \\
I^c_{330;5L} &= \frac{(2s_{13} - s_{23})(2s_{35} + s_{34})}{36} + \mathcal{O}(\epsilon)\,, \\
I^d_{330;5L} &= \frac{-2s_{12} + s_{51} + s_{23} + s_{34} - 2s_{45}}{36} + \mathcal{O}(\epsilon)\,.
\end{aligned} \tag{12.38}$$

Combining it all into the partial amplitude of eq. (12.32), the result can be written as

$$\mathcal{A}^{(2)}_{\text{butterfly}} = \frac{i(D_s-2)^2}{\langle 12\rangle\langle 23\rangle\langle 34\rangle\langle 45\rangle\langle 51\rangle} \, \frac{-1}{72\; s_{12}s_{23}s_{34}s_{45}s_{51}} \sum_{\text{cyclic}} X(1,2,3,4,5) \tag{12.39}$$

with

$$\begin{aligned}
X(1,2,3,4,5) = s_{12}^2\Big(& s_{23}\big(s_{12}s_{51}s_{23}s_{34} + s_{51}s_{23}^2 s_{34} - 2s_{51}s_{23}s_{34}^2 - 2s_{12}s_{51}s_{23}s_{45} \\
& + s_{12}s_{23}^2 s_{45} + s_{51}s_{23}^2 s_{45} + s_{12}s_{23}s_{34}s_{45} + 12 s_{51}s_{23}s_{34}s_{45} - 2s_{23}^2 s_{34}s_{45} \\
& + 2s_{51}s_{34}^2 s_{45} - 2s_{23}s_{34}^2 s_{45} + 2s_{23}s_{34}s_{45}^2 + 2s_{34}^2 s_{45}^2\big) - \big(s_{23}^2 s_{45} \\
& + s_{51}s_{34}s_{45} + s_{23}s_{34}s_{45} - s_{51}s_{23}s_{34} - s_{51}s_{23}s_{45}\big)\mathrm{tr}_5\Big)
\end{aligned} \tag{12.40}$$

where the terms in the cyclic sum of eq. (12.39) have been reordered to make it simplify. We see that no non-physical poles are left in the result, which is another non-trivial passed check.

12.9 Discussion

The result of eq. (12.33) obeys a curious relation.

At one-loop, the relation [108]

$$\Delta^{(1)}_{\text{YM}}(1^+,\cdots,n^+) = \langle 12\rangle^{-4}(D_s-2)\rho^2 \Delta^{(1)}_{\mathcal{N}=4}(1^-,2^-,3^+,\cdots,n^+) \tag{12.41}$$

between the box-integrands of Yang-Mills theory for helicity configuration all-plus, and $\mathcal{N} = 4$ SYM for a MHV configuration, has been known for a while. At two-loops, the $\mathcal{N} = 4$ result is known from [109, 110], and the corresponding relation seems to be

$$\begin{aligned}\Delta^{(2)}_{\mathrm{YM}}(1^+, \cdots, n^+) = \\ F_1 \langle 12 \rangle^{-4} \Delta^{(2)}_{\mathcal{N}=4}(1^-, 2^-, 3^+, \cdots, n^+) + \text{butterfly topologies}\end{aligned} \tag{12.42}$$

which we have checked for $n \in \{4, 5\}$. This relation highlights the importance of the butterfly-contribution given by eqs. (12.39) and (12.40), as such contributions seem to be the main difference between our all-plus amplitude and $\mathcal{N} = 4$ in which they clearly vanish due to the no-triangle theorem.

Investigations into the origin eq. (12.42) might be an interesting endeavor for the future.

Chapter 13

Non-planar contributions

An obvious step after calculating the planar contribution to the $gg \to ggg$ process for the specific helicity configuration, would be the calculate the non-planar contribution too in order to get the full two-loop correction to the amplitude. Two of the non-planar topologies, those with eight propagators which will be parent-topologies for the remaining ones, will be calculated in this chapter. These results were first presented in [5].

These two topologies are denoted $(t332)$ and $(t422)$, and are shown on fig. 13.1.

13.1 The topology $(t332)$

This topology has eight propagators which we label

$$\begin{aligned} l_1 &= k_1, & l_2 &= k_1 - p_1, & l_3 &= k_1 - p_1 - p_2, & l_4 &= k_2, \\ -l_5 &= k_2 - p_4, & l_6 &= k_2 - p_3 - p_4, & l_7 &= k_1 + k_2, & l_8 &= k_1 + k_2 + p_5. \end{aligned} \quad (13.1)$$

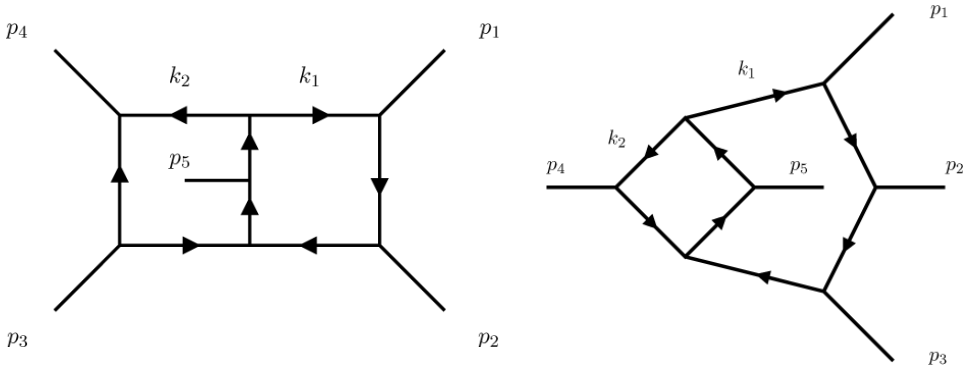

Figure 13.1: $(t332)$ and $(t422)$, the maximal non-planar topologies for five-point amplitudes.

Using BasisDet we find that the irreducible numerator of the topology can be written as 82 coefficients multiplying monomials of the six ISPs

$$(k_1 \cdot p_4)\,,\ \ (k_2 \cdot p_1)\,,\ \ (k_1 \cdot p_5)\,,\ \ \rho_1\,,\ \ \rho_{12}\,,\ \ \rho_2\,. \tag{13.2}$$

The solution to the octa-cut equations is

$$\bar{k}_1^\mu = p_1^\mu + \tau_1 \frac{[13]}{[23]} \frac{\langle 1|\sigma^\mu|2]}{2} + \tau_2 \frac{\langle 13\rangle}{\langle 23\rangle} \frac{\langle 2|\sigma^\mu|1]}{2} \tag{13.3}$$

$$\bar{k}_2^\mu = p_4^\mu + \tau_3 \frac{\langle 14\rangle}{\langle 13\rangle} \frac{\langle 3|\sigma^\mu|4]}{2} + \kappa \frac{\langle 13\rangle}{\langle 14\rangle} \frac{\langle 4|\sigma^\mu|3]}{2} \tag{13.4}$$

with the additional constraints that

$$\rho_1 = \bar{k}_1^2\,, \qquad \rho_2 = \bar{k}_2^2\,, \qquad \rho_{12} = 2\bar{k}_1 \cdot \bar{k}_2\,, \tag{13.5}$$

where

$$\kappa \equiv \frac{-s_{14}}{\mathrm{tr}_-(1354)} \left(s_{51} + s_{45} + \frac{1}{s_{23}} \big(\tau_1 \mathrm{tr}_-(1523) + \tau_2 \mathrm{tr}_+(1523)\big) + \frac{1}{s_{13}} \tau_3 \mathrm{tr}_-(1453) \right). \tag{13.6}$$

Evaluating Δ_{332} on the cut gives an expansion in the free parameters which contains 83 terms, making this topology the first example in d dimensions where the linear system is non-quadratic. Inverting it yields the result

$$\Delta_{332} = \frac{2iF_1\ s_{12}s_{34}}{\langle 12\rangle\langle 23\rangle\langle 34\rangle\langle 45\rangle\langle 51\rangle \mathrm{tr}_5} \big(c_1(k_1 \cdot p_4) + c_2(k_2 \cdot p_1) + c_3(k_1 \cdot p_5)\big), \tag{13.7}$$

with

$$c_1 = -s_{51}\mathrm{tr}_-(2345), \tag{13.8}$$

$$c_2 = s_{45}\mathrm{tr}_-(2351), \tag{13.9}$$

$$c_3 = s_{23}s_{45}s_{51} - s_{51}\mathrm{tr}_-(2345) - s_{45}\mathrm{tr}_-(2351), \tag{13.10}$$

and with F_1 defined as in eq. (12.8).

13.2 The topology $(t422)$

This topology is defined by the eight propagators

$$\begin{aligned} &l_1 = k_1, \quad && l_2 = k_1 - p_1, \quad && l_3 = k_1 - p_1 - p_2, \quad && l_4 = k_1 - p_1 - p_2 - p_3, \\ &l_5 = k_2, \quad && l_6 = k_2 - p_4, \quad && l_7 = k_1 + k_2, \quad && l_8 = k_1 + k_2 + p_5, \end{aligned} \tag{13.11}$$

and the irreducible numerator may be expressed in terms of 65 monomials of the ISPs

$$(k_2 \cdot p_2)\,,\ \ (k_2 \cdot p_1)\,,\ \ (k_2 \cdot p_5)\,,\ \ \rho_1\,,\ \ \rho_{12}\,,\ \ \rho_2\,. \tag{13.12}$$

The solution to the cut-constraints is

$$\bar{k}_1^\mu = p_1^\mu + \tau_1 \frac{\langle 23\rangle}{\langle 13\rangle}\frac{\langle 1|\sigma^\mu|2]}{2} + (1-\tau_1)\frac{[23]}{[13]}\frac{\langle 2|\sigma^\mu|1]}{2}\,, \tag{13.13}$$

$$\bar{k}_2^\mu = \kappa p_4^\mu + \tau_2 \frac{\langle 15\rangle}{\langle 14\rangle}\frac{\langle 4|\sigma^\mu|5]}{2} + \tau_3\frac{[15]}{[14]}\frac{\langle 5|\sigma^\mu|4]}{2}\,, \tag{13.14}$$

with

$$\kappa \equiv -\frac{1}{s_{45}s_{13}}\big(s_{13}s_{15} + \tau_1 \mathrm{tr}_-(1523) + (1-\tau_1)\mathrm{tr}_+(1523)\big). \tag{13.15}$$

and the additional constraints

$$\rho_1 = \bar{k}_1^2\,, \qquad \rho_2 = \bar{k}_2^2\,, \qquad \rho_{12} = 2\bar{k}_1\cdot\bar{k}_2\,. \tag{13.16}$$

As in the previous case the linear system becomes non-square, this time there are 76 terms in the τ expansion, and the result is

$$\Delta_{422} = \frac{iF_1\ s_{12}s_{23}s_{45}}{\langle 12\rangle\langle 23\rangle\langle 34\rangle\langle 45\rangle\langle 51\rangle \mathrm{tr}_5}\big(c_0 + 2c_1(k_2\cdot p_5)\big) \tag{13.17}$$

with

$$c_0 \;=\; s_{34}s_{45}s_{51}\,, \qquad c_1 \;=\; -\mathrm{tr}_+(1345)\,. \tag{13.18}$$

Chapter 14

Perspectives and conclusions

In this thesis we have shown a way to extend the OPP method beyond one loop. We have shown examples for two and three loops, with the the primary result of the thesis being the calculation of planar $gg \to ggg$ at two-loops in the case where all the external particles have the same helicity, with the result being given by eq. (12.33). For that case we found an interesting relation to the $\mathcal{N} = 4$ theory given by eq. (12.42), which is inviting to further investigations.

We also showed how a number of problems, the minor and the major problem of chapter 8, shows up for four-dimensional generalized cuts, but are avoided in the d-dimensional case for which several of the steps of the method quite counterintuitively become simpler. These simplifications are seen by the use of algebraic geometry as explained in chapter 9, and one major part of the method outlined in this thesis is exactly the central role played by algebraic geometry.

As indicated by the calculations of chapter 13, there is nothing hindering the completion of the $gg \to ggg$ calculation for our specific helicity configuration by calculating the non-planar part. One might finish this through the methods of this thesis, but another feasible way would be to relate the planar and non-planar topologies through the BCJ colour-kinematics relation, as discussed in [27, 111].

We saw no examples of the use of the techniques of this thesis on theories involving massive particles, either externally or internally. From the point of view of the particles in the tree-products this is not believed to be a fundamental hindrance [35, 112, 113], but from the point of view of the unitarity cut solutions, it might be.

The calculations in this thesis depended on the fact that it was possible to write the Δ on the cut as a Laurent-expansion in a set of free parameters

$$\Delta|_{\text{cut}} = \sum_{i_1,\ldots,i_n} d_{i_1,\ldots,i_n} \tau_1^{i_1} \cdots \tau_n^{i_n} \tag{14.1}$$

Nowhere did we prove that this is always possible, and that is because it is not.

In all the cases in this thesis, the zero-locus for each cut-equation form a higher dimensional manifold with geometric genus zero. But there are cases for which the zero-locus will have a non-zero genus, making it the equivalent of a circle or an

n-torus. An example is the double-box with six massive legs [93], and for a further investigation and classification of these genera, see [114, 115]. A high genus will make a parametrization like that of eq. (14.1) impossible, and such examples have mostly shown up for cases with either internal or external[1] masses. Presumably our method can be implemented with a different and less restrictive expansion, but this is a question for the future. As all examples of such high genera have been of cuts in four dimensions, it is also currently unknown whether the problem will show up for the case of d-dimensional cuts.

The method of this thesis may be extended to other helicity configurations, or other distributions of particle flavours internally[2] or externally. The main issue with more general helicity configurations is the treatment of diagrams with doubled propagators. At one-loop such diagrams would never show up in physical amplitudes as they are not allowed by the Feynman rules for a general momentum configuration. But at two-loops or higher they may show up, for topologies that correspond to a lower-loop topology with a bubble insertion on one of the propagators. What it means to cut such a doubled propagator is not obvious, and so far the best approach to such cases has been to perform an integrand reduction from Feynman diagrams without the use of any unitarity cuts [88]. It is however possible to make mathematical sense of such double-cuts [96], but it is not completely clear how to integrate this with the methods described in this thesis.

One main feature of the method developed in this thesis was the use of the six-dimensional spinor-helicity formalism as described in chapter 11. Where the d-dimensional dependence for one-loop amplitudes can be contained in just one ρ-parameter, the two-loop case needs three such parameters requiring a six-dimensional embedding. Where previous uses of the six-dimensional spinor-helicity in a unitarity context [104, 105] have been algebraic, we did a numerical calculation avoiding any large intermediate expressions. And even though the six-dimensional helicity sums are over more states than the corresponding four-dimensional calculation, it still scales much better with the number of loops and legs than Feynman diagrams.

One issue about the six-dimensional formalism is that is cannot generalize beyond two-loops as it cannot contain the necessary degrees of freedom[3]. One imaginable solution would be to change to the ten-dimensional spinor-helicity formalism of [116], but this somehow seems unsatisfactory. A purely four-dimensional approach to the problem of the treatment of the ρ-parameters has been proposed [117] (see also [61, 118]), but whether this method will generalize beyond one loop is currently unknown.

[1] Topologies with external masses can of course show up in massless theories as we saw examples of in chapter 12. But in such a theory the six-point massive double-box would for instance only show up at ten-point or higher, making it of no practical relevance.

[2] There may be a minor issue in the treatment of d-dimensional fermions.

[3] A three-loop topology will have six ρ-parameters, and one might imagine that they would fit into three six-dimensional loop-momenta. A detailed calculation shows this to not be the case, but perhaps it can be solved for the three-loop case using six dimensional massive particles.

Yet another issue of the method of this paper is that at two or more loops the integrand basis for the irreducible numerators Δ contain orders of magnitudes more terms that the minimal integral basis (compare for instance the 398 terms of eq. (7.3) with the three terms of eq. (7.16)). This is for sure a weakness of our method compared to the maximal unitarity method of [14] which fits only to a basis of master integrals. Obtaining a basis in terms of master integrals using the methods of this thesis, will require the reduction of integrals with numerator powers as high as allowed by the renormalization constraints, whereas the maximal unitarity method only requires knowledge of the master integrals.

On the other hand a strong point of the method of this thesis is the ease of which it generalizes to d dimensions where several aspects of the method actually simplifies as mentioned. The maximal unitarity method is able to deal with d-dimensional cuts [119], but only at the cost of considerable mathematical complications. It seems like an optimal method for performing generalized unitarity cuts for higher loops, would combine the easy handling of d-dimensional and numerical calculations of the method presented here, with a fit to basis of master integrals like the maximal unitarity method. Whether or not such a method exists is a question for the future.

The work in this thesis presented the first result for a two-loop five-point process in pure Yang-Mills theory. The methods of this thesis can probably be extended to the non-planar parts, to other helicity configurations, and to contributions involving quarks, without many extra complications. The restart of the LHC with energies up to 14 TeV which is scheduled to the spring of 2015, allows the search for even more elusive particles and interactions to continue. Identifying such effects in the flood of QCD data is a challenge, but a challenge which can be overcome using results and methods as those presented on the previous pages.

Appendices

Appendix A

Spinor-helicity formalism in four dimensions

In this appendix we shall go through definitions and identities for the spinor-helicity formalism as it looks in four dimensions. It is based on [23,31,35,120]. For further discussion, see also section 3.2.

For the four Pauli matrices we use the convention

$$\sigma^0_{\alpha\dot\beta} = \begin{bmatrix} 1 & 0 \\ 0 & 1 \end{bmatrix}, \quad \sigma^1_{\alpha\dot\beta} = \begin{bmatrix} 0 & 1 \\ 1 & 0 \end{bmatrix}, \quad \sigma^2_{\alpha\dot\beta} = \begin{bmatrix} 0 & -i \\ i & 0 \end{bmatrix}, \quad \sigma^3_{\alpha\dot\beta} = \begin{bmatrix} 1 & 0 \\ 0 & -1 \end{bmatrix}. \tag{A.1}$$

Contraction with a massless four-momentum

$$p^\mu = (p_0,\ p_1,\ p_2,\ p_3) \tag{A.2}$$

gives the matrix

$$p_{\alpha\dot\beta} \ \equiv \ p_\mu \sigma^\mu_{\alpha\dot\beta} = \begin{bmatrix} p_- & -p_-^\perp \\ -p_+^\perp & p_+ \end{bmatrix} \tag{A.3}$$

with

$$p_\pm \equiv p_0 \pm p_3 \qquad\qquad p_\pm^\perp \equiv p_1 \pm i p_2 \tag{A.4}$$

As the rank of the $p_{\alpha\dot\beta}$-matrix is one, we know that it can be written as an outer product of two two-vectors called Weyl-spinors, as

$$p_{\alpha\dot\beta} = \lambda_\alpha \tilde\lambda_{\dot\beta} \tag{A.5}$$

with

$$\lambda_\alpha \equiv \begin{pmatrix} -z p_-^\perp/\sqrt{p_+} \\ z\sqrt{p_+} \end{pmatrix} \qquad \tilde\lambda_{\dot\beta} \equiv \begin{pmatrix} -p_+^\perp/(z\sqrt{p_+}) \ , & \sqrt{p_+}/z \end{pmatrix} \tag{A.6}$$

where λ is a holomorphic and $\tilde\lambda$ is an anti-holomorphic spinor. We note that the parameter z is free in the general case, but for the case of real momenta it is restricted to a phase, $|z| = 1$.

Raising and lowering the holomorphic and anti-holomorphic spinor indices, is done as

$$\lambda^\alpha = \epsilon^{\alpha\beta}\lambda_\beta \qquad \lambda_\alpha = \epsilon_{\alpha\beta}\lambda^\beta \qquad \tilde{\lambda}^{\dot{\alpha}} = \epsilon^{\dot{\alpha}\dot{\beta}}\tilde{\lambda}_{\dot{\beta}} \qquad \tilde{\lambda}_{\dot{\alpha}} = \epsilon_{\dot{\alpha}\dot{\beta}}\lambda^{\dot{\beta}} \tag{A.7}$$

with

$$\epsilon^{\alpha\beta} \equiv \begin{bmatrix} 0 & 1 \\ -1 & 0 \end{bmatrix} \qquad \epsilon_{\alpha\beta} \equiv \begin{bmatrix} 0 & -1 \\ 1 & 0 \end{bmatrix} \tag{A.8}$$

so we get

$$\lambda^\alpha = \begin{pmatrix} z\sqrt{p_+}\,, & zp_-^\perp/\sqrt{p_+} \end{pmatrix} \qquad \tilde{\lambda}^{\dot{\beta}} = \begin{pmatrix} \sqrt{p_+}/z \\ p_+^\perp/(z\sqrt{p_+}) \end{pmatrix} \tag{A.9}$$

Defining

$$\langle i| \equiv \lambda^\alpha(p_i) \qquad |i\rangle \equiv \lambda_\alpha(p_i) \qquad [i| \equiv \tilde{\lambda}_{\dot{\alpha}}(p_i) \qquad |i] \equiv \tilde{\lambda}^{\dot{\alpha}}(p_i) \tag{A.10}$$

and using the NW-SE (north-west south-east) convention for undotted indices and the SW-NE convention for the dotted ones, we are able to contract spinors of the same holomorphicity with the result

$$\begin{aligned} \langle ab\rangle \;&\equiv\; \lambda^\alpha(p_a)\lambda_\alpha(p_b) = z_a z_b \left(\frac{\sqrt{(p_+)_b}}{\sqrt{(p_+)_a}}(p_-^\perp)_a - \frac{\sqrt{(p_+)_a}}{\sqrt{(p_+)_b}}(p_-^\perp)_b \right) \\ [ab] \;&\equiv\; \tilde{\lambda}_{\dot{\alpha}}(p_a)\tilde{\lambda}^{\dot{\alpha}}(p_b) = \frac{-1}{z_a z_b} \left(\frac{\sqrt{(p_+)_b}}{\sqrt{(p_+)_a}}(p_+^\perp)_a - \frac{\sqrt{(p_+)_a}}{\sqrt{(p_+)_b}}(p_+^\perp)_b \right) \end{aligned} \tag{A.11}$$

These spinor products have the properties that $\langle ab\rangle = -\langle ba\rangle$, $[ab] = -[ba]$, and additionally that

$$\langle ab\rangle[ba] \;=\; 2p_a \cdot p_b \;=\; s_{ab} \tag{A.12}$$

As Weyl spinors have two components, we may always write one as a linear combination of two others. This relation is known as the Schouten identity, and may we written

$$|a\rangle\langle bc\rangle = |b\rangle\langle ac\rangle + |c\rangle\langle ba\rangle \qquad |a][bc] = |b][ac] + |c][ba] \tag{A.13}$$

The Schouten identity is also often seen on a form where eqs. (A.13) are contracted with a fourth spinor.

Contracted with the vector of Pauli matrices, the Weyl spinors may also form a vector product $\langle i|\sigma^\mu|j]$. An explicit expression in terms of components is

$$\frac{\langle i|\sigma^\mu|j]}{2} \equiv \frac{\lambda_i^\alpha \sigma^\mu_{\alpha\dot{\beta}} \tilde{\lambda}_j^{\dot{\beta}}}{2} = \frac{z_i}{2z_j} \begin{pmatrix} n_i n_j + p_{i-}^\perp p_{j+}^\perp/(n_i n_j) \\ p_{i-}^\perp n_j/n_i + p_{j+}^\perp n_i/n_j \\ i\left(p_{i-}^\perp n_j/n_i - p_{j+}^\perp n_i/n_j\right) \\ n_i n_j - p_{i-}^\perp p_{j+}^\perp/(n_i n_j) \end{pmatrix} \tag{A.14}$$

where we have used the definition

$$n \equiv \sqrt{p_+} \tag{A.15}$$

The vector product has the property that it allows reforming the original four-vector, as

$$p^\mu = \frac{\langle p|\sigma^\mu|p]}{2} \tag{A.16}$$

Two vector products defined as in eq. (A.14) may be contracted with the result

$$\langle a|\sigma^\mu|b]\langle c|\sigma_\mu|d] = 2\langle ac\rangle[db] \tag{A.17}$$

a relation known as the Fierz identity.

An important use of the vector products is by their ability to form specific expressions for polarization vectors in axial gauge. If we take the direction of the "axis" to be given by the massless vector q^μ, the polarization vectors for massless particles with momentum p are

$$\varepsilon_+^\mu(p,q) = \frac{\langle q|\sigma^\mu|p]}{\sqrt{2}\,\langle qp\rangle} \qquad\qquad \varepsilon_-^\mu(p,q) = \frac{\langle p|\sigma^\mu|q]}{\sqrt{2}\,[pq]} \tag{A.18}$$

which we see to obey the relations

$$p\cdot\varepsilon_\pm(p,q) = 0, \qquad \varepsilon_\pm(p,q)\cdot\varepsilon_\pm(p,q) = 0, \qquad \varepsilon_\pm(p,q)\cdot\varepsilon_\mp(p,q) = -1, \tag{A.19}$$

and the completeness relation

$$\varepsilon_+^\mu(p,q)\varepsilon_-^\nu(p,q) + \varepsilon_-^\mu(p,q)\varepsilon_+^\nu(p,q) = -g^{\mu\nu} + \frac{p^\mu q^\nu + q^\mu p^\nu}{p\cdot q} \tag{A.20}$$

For more identities for the spinors, spinor products, and polarization vectors, see [31].

Appendix B

The six-dimensional spinor-helicity formalism

In all (even) dimensions, one can make a spinor-helicity formalism [121]. In this appendix the focus will be on the six-dimensional case as developed in [103] and further described in [104]. We will use a notation where six-dimensional objects are denoted using capital letters, corresponding to the replacements

$$\begin{array}{cccccc} p^\mu & s_{ij} & \sigma^\mu & \lambda^\alpha & \tilde{\lambda}_{\dot{\alpha}} & \varepsilon^\mu_\pm \\ P^\mu & S_{ij} & \Sigma^\mu & \Lambda^A & \tilde{\Lambda}_A & \mathcal{E}^\mu_{a\dot{a}} \end{array} \tag{B.1}$$

B.1 Six-dimensional spinors

In six dimensions the equivalent of the Pauli-matrices σ^μ in four dimensions, are the six matrices

$$\begin{array}{lll} \Sigma^0 \equiv i\sigma_1 \otimes \sigma_2, & \Sigma^1 \equiv i\sigma_2 \otimes \sigma_3, & \Sigma^2 \equiv -\sigma_2 \otimes \sigma_0, \\ \Sigma^3 \equiv -i\sigma_2 \otimes \sigma_1, & \Sigma^4 \equiv -\sigma_3 \otimes \sigma_2, & \Sigma^5 \equiv i\sigma_0 \otimes \sigma_2, \end{array} \tag{B.2}$$

that is

$$\Sigma^0_{AB} = \begin{bmatrix} 0 & 0 & 0 & 1 \\ 0 & 0 & -1 & 0 \\ 0 & 1 & 0 & 0 \\ -1 & 0 & 0 & 0 \end{bmatrix}, \quad \Sigma^1_{AB} = \begin{bmatrix} 0 & 0 & 1 & 0 \\ 0 & 0 & 0 & -1 \\ -1 & 0 & 0 & 0 \\ 0 & 1 & 0 & 0 \end{bmatrix}, \quad \Sigma^2_{AB} = \begin{bmatrix} 0 & 0 & i & 0 \\ 0 & 0 & 0 & i \\ -i & 0 & 0 & 0 \\ 0 & -i & 0 & 0 \end{bmatrix},$$
$$\Sigma^3_{AB} = \begin{bmatrix} 0 & 0 & 0 & -1 \\ 0 & 0 & -1 & 0 \\ 0 & 1 & 0 & 0 \\ 1 & 0 & 0 & 0 \end{bmatrix}, \quad \Sigma^4_{AB} = \begin{bmatrix} 0 & i & 0 & 0 \\ -i & 0 & 0 & 0 \\ 0 & 0 & 0 & -i \\ 0 & 0 & i & 0 \end{bmatrix}, \quad \Sigma^5_{AB} = \begin{bmatrix} 0 & 1 & 0 & 0 \\ -1 & 0 & 0 & 0 \\ 0 & 0 & 0 & 1 \\ 0 & 0 & -1 & 0 \end{bmatrix}. \tag{B.3}$$

Likewise the equivalent of $\tilde{\sigma}^\mu$ is

$$\tilde{\Sigma}^0 = -\Sigma^0, \quad \tilde{\Sigma}^1 = \Sigma^1, \quad \tilde{\Sigma}^2 = -\Sigma^2, \quad \tilde{\Sigma}^3 = \Sigma^3, \quad \tilde{\Sigma}^4 = -\Sigma^4, \quad \tilde{\Sigma}^5 = \Sigma^5. \tag{B.4}$$

Contracting with the six-momentum P^μ gives

$$P^\mu \Sigma_{\mu AB} = \begin{bmatrix} 0 & -P_+^3 & -P_+^2 & P_+^1 \\ P_+^3 & 0 & -P_-^1 & P_-^2 \\ P_+^2 & P_-^1 & 0 & -P_-^3 \\ -P_+^1 & -P_-^2 & P_-^3 & 0 \end{bmatrix} \quad P^\mu \tilde{\Sigma}_\mu^{AB} = \begin{bmatrix} 0 & -P_-^3 & -P_-^2 & -P_-^1 \\ P_-^3 & 0 & P_+^1 & P_+^2 \\ P_-^2 & -P_+^1 & 0 & -P_+^3 \\ P_-^1 & -P_+^2 & P_+^3 & 0 \end{bmatrix} \tag{B.5}$$

with

$$P_\pm^1 \equiv P_0 \pm P_3 \qquad P_\pm^2 \equiv P_1 \pm iP_2 \qquad P_\pm^3 \equiv P_5 \pm iP_4 \tag{B.6}$$

We want the holomorphic spinors Λ^A to fulfill a relation like $\Lambda^A\Lambda^B = P{\cdot}\tilde{\Sigma}^{AB}$ and likewise for the anti-holomorphic spinors $\tilde{\Lambda}_A$. But as $P{\cdot}\tilde{\Sigma}^{AB}$ has rank two, and not one as in the four-dimensional case, the spinors must carry an extra index, which will be the little group index a going from one to two, making their representation 4×2 matrices.

Thus the relations are

$$\epsilon^{ba}\Lambda_a^A\Lambda_b^B = P^\mu\tilde{\Sigma}_\mu^{AB} \qquad \tilde{\Lambda}_{A\dot{a}}\epsilon^{\dot{a}\dot{b}}\tilde{\Lambda}_{B\dot{b}} = P^\mu\Sigma_{\mu AB} \tag{B.7}$$

and the solutions are

$$\Lambda_a^A = \begin{bmatrix} (cP_-^3 - xP_-^2)/(zn^2) & x/z & c/z & (cP_+^2 + xP_+^3)/(zn^2) \\ z(yP_-^3 - cP_-^2)/n^2 & zc & zy & z(cP_+^3 + yP_+^2)/n^2 \end{bmatrix}_{aA} \tag{B.8}$$

$$\tilde{\Lambda}_{A\dot{a}} = \begin{bmatrix} -\tilde{x}/\tilde{z} & \tilde{z}\tilde{c} \\ (\tilde{c}P_+^3 - \tilde{x}P_-^2)/(\tilde{z}n^2) & \tilde{z}(\tilde{c}P_-^2 - \tilde{y}P_+^3)/(n^2) \\ (\tilde{c}P_+^2 + \tilde{x}P_-^3)/(\tilde{z}n^2) & -\tilde{z}(\tilde{y}P_+^2 + \tilde{c}P_-^3)/(n^2) \\ -\tilde{c}/\tilde{z} & \tilde{z}\tilde{y} \end{bmatrix}_{A\dot{a}} \tag{B.9}$$

with x, y, z, $\tilde{x}$, $\tilde{y}$, and $\tilde{z}$ being free parameters (for now) and

$$c \equiv \sqrt{n^2 + xy} \qquad \tilde{c} \equiv \sqrt{n^2 + \tilde{x}\tilde{y}} \tag{B.10}$$

where we use $n \equiv \sqrt{P_+^1}$ for six-dimensional expressions.

B.2 The four-dimensional representation

One can express Λ_a^A and $\Lambda_{A\dot{a}}$ in terms of two four-dimensional spinors λ and μ and their conjugates according to

$$\Lambda_a^A = \begin{bmatrix} -\kappa\mu_\alpha & \tilde{\lambda}^{\dot{\alpha}} \\ \lambda_\alpha & \tilde{\kappa}\tilde{\mu}^{\dot{\alpha}} \end{bmatrix}_{aA} \qquad \tilde{\Lambda}_{A\dot{a}} = \begin{bmatrix} \kappa'\mu^\alpha & \lambda^\alpha \\ -\tilde{\lambda}_{\dot{\alpha}} & \tilde{\kappa}'\tilde{\mu}_{\dot{\alpha}} \end{bmatrix}_{A\dot{a}} \tag{B.11}$$

with[1]

$$m \equiv P_-^3 \qquad \tilde{m} \equiv P_+^3 \qquad \kappa \equiv \frac{m}{\langle \mu\lambda \rangle} \qquad \tilde{\kappa} \equiv \frac{\tilde{m}}{[\lambda\mu]} \qquad \kappa' \equiv \frac{\tilde{m}}{\langle \mu\lambda \rangle} \qquad \tilde{\kappa}' \equiv \frac{m}{[\lambda\mu]} \tag{B.12}$$

This is only consistent if we impose the restrictions

$$m\tilde{x} = \tilde{m}x \qquad\qquad \tilde{m}\tilde{y} = my \qquad\qquad \tilde{z} = z \qquad\qquad \tilde{c} = c \tag{B.13}$$

where the last one follows from the first two.

The four-dimensional vectors $p^\flat$ and ξ corresponding to these sets of spinors, can be combined according to

$$p = \frac{\langle \lambda | \sigma^\mu | \lambda]}{2} + \kappa\tilde{\kappa}\frac{\langle \mu | \sigma^\mu | \mu]}{2} \equiv p^\flat + \frac{m\tilde{m}}{2p\cdot\xi}\xi \tag{B.14}$$

where p is a massive four-dimensional vector with $p^2 = m\tilde{m}$. This is exactly the expression for writing a general massive vector p in terms of a "flattened" vector $p^\flat$ and a reference vector ξ as described in appendix F.1, and it also motivates the choice for the name m for that parameter.

In this four-dimensional spinor language, the parameters x and y in eq. (B.8) reflects the freedom in choosing the reference vector ξ, and the parameter z corresponds to the little group phase freedom in four dimensions. We note from eqs. (B.8) and (B.9) that the z-scaling of the μ-spinors is opposite that of the λ-spinors.

Explicit expressions for ξ and $p^\flat$ are

$$\frac{m\tilde{m}}{2p\cdot\xi}\xi = \frac{1}{2}\begin{pmatrix} -xy + (cP_-^3 - xP_-^2)(cP_+^3 + yP_+^2)/n^4 \\ \big((cP_-^3 - xP_-^2)y - (cP_+^3 + yP_+^2)x\big)/n^2 \\ i\big((cP_-^3 - xP_-^2)y + (cP_+^3 + yP_+^2)x\big)/n^2 \\ -xy - (cP_-^3 - xP_-^2)(cP_+^3 + yP_+^2)/n^4 \end{pmatrix} \tag{B.15}$$

$$p^\flat = \frac{1}{2}\begin{pmatrix} c^2 + (cP_+^2 + xP_+^3)(cP_-^2 - yP_-^3)/n^4 \\ c(cP_+^2 + xP_+^3 + cP_-^2 - yP_-^3)/n^2 \\ -ic(cP_+^2 + xP_+^3 - cP_-^2 + yP_-^3)/n^2 \\ c^2 - (cP_+^2 + xP_+^3)(cP_-^2 - yP_-^3)/n^4 \end{pmatrix} \tag{B.16}$$

in terms of of x, y, and c, and we see that

$$p = p^\flat + \frac{m\tilde{m}}{2p\cdot\xi}\xi = (P_0, P_1, P_2, P_3) \tag{B.17}$$

In the "massless" case $m\tilde{m} = 0$ we define that $x = y = 0$ in order to obtain $p = p^\flat$ in that case.

[1] With my conventions, this has opposite signs compared to [104].

B.3 Six-dimensional spinor products

We can define a six-dimensional spinor product as

$$\begin{aligned}\langle i_a|j_{\dot b}] \equiv \Lambda^A_{ia}\tilde\Lambda^j_{A\dot b} &= \left[\begin{array}{cc} [ij]+\kappa_i\kappa'_j\langle\mu_i\mu_j\rangle & \kappa_i\langle\mu_i j\rangle - \tilde\kappa'_j[i\mu_j] \\ \tilde\kappa_i[\mu_i j]-\kappa'_j\langle i\mu_j\rangle & -\big(\langle ij\rangle+\tilde\kappa_i\tilde\kappa'_j[\mu_i\mu_j]\big)\end{array}\right]_{a\dot b} \\ &\equiv \left[\begin{array}{cc} B_{ij} & C_{ij} \\ D_{ij} & -A_{ij}\end{array}\right]_{a\dot b}\end{aligned} \tag{B.18}$$

with four-dimensional spinor products of i or μ_i defined as those based on the spinors of $p_i^\flat$ or μ_i of eqs. (B.11). It follows from eq. (B.18) that $\langle i_a|i_{\dot b}] = 0$.

Mirroring $s_{ij} = \langle ij\rangle[ji]$ in four dimensions, the six-dimensional spinor product has the property that

$$\begin{aligned}\det\big(\langle i_a|j_{\dot b}]\big) &= \langle ij\rangle[ji] + \kappa_i\tilde\kappa_i\kappa'_j\tilde\kappa'_j\langle\mu_i\mu_j\rangle[\mu_j\mu_i] + \kappa_i\tilde\kappa_i\langle j\mu_i\rangle[\mu_i j] + \kappa'_j\tilde\kappa'_j[i\mu_j]\langle\mu_j i\rangle \\ &\quad + \tilde\kappa_i\tilde\kappa'_j\Big([ij][\mu_j\mu_i] + [i\mu_j][\mu_i j]\Big) + \kappa_i\kappa'_j\Big(\langle ij\rangle\langle\mu_j\mu_i\rangle + \langle i\mu_j\rangle\langle\mu_i j\rangle\Big) \\ &= \langle ij\rangle[ji] + \frac{m_i\tilde m_i m_j\tilde m_j}{\langle i\mu_i\rangle[\mu_i i]\langle j\mu_j\rangle[\mu_j j]}\langle\mu_i\mu_j\rangle[\mu_j\mu_i] + \frac{m_i\tilde m_i}{\langle i\mu_i\rangle[\mu_i i]}\langle j\mu_i\rangle[\mu_i j] \\ &\quad + \frac{m_j\tilde m_j}{\langle j\mu_j\rangle[\mu_j j]}\langle i\mu_j\rangle[\mu_j i] - \tilde m_i m_j - m_i\tilde m_j \\ &= s_{ij} - (m_i+m_j)\,(\tilde m_i+\tilde m_j) = S_{ij}\end{aligned} \tag{B.19}$$

where the determinant is taken over the little group indices.

B.4 Vector products and polarization vectors

One can also define vector products

$$\langle i_a\Sigma^\mu j_b\rangle \qquad\qquad [i_{\dot a}\tilde\Sigma^\mu j_{\dot b}] \tag{B.20}$$

similar to $\langle i\sigma^\mu j]$ in the four-dimensional case. The result has a Lorentz-index and two little group indices, and thus it can be written as a six-vector of 2×2 matrices. The result is too complicated for us to write down here analytically, but it has the properties that

$$P^\mu = \frac{-1}{4}\langle P^a\Sigma^\mu P_a\rangle = \frac{-1}{4}[P_{\dot a}\tilde\Sigma^\mu P^{\dot a}] \tag{B.21}$$

and

$$\langle i_a\Sigma^\mu j_b\rangle\; P_{i\mu} = \langle i_a\Sigma^\mu j_b\rangle\; P_{j_\mu} = [i_{\dot a}\tilde\Sigma^\mu j_{\dot b}]\; P_{i\mu} = [i_{\dot a}\tilde\Sigma^\mu j_{\dot b}]\; P_{j_\mu} = 0 \tag{B.22}$$

all paralleling expressions in the four-dimensional case. For analytical calculations is is useful to know the property

$$\langle i_a\Sigma^\mu j_b\rangle[k_{\dot c}\tilde\Sigma_\mu l_{\dot d}] = 2\Big(\langle i_a l_{\dot d}]\langle j_b k_{\dot c}] - \langle i_a k_{\dot c}]\langle j_b l_{\dot d}]\Big) \tag{B.23}$$

similar to the four-dimensional eq. (A.17).

Expressions for the six-dimensional polarization vectors can be written in terms of the vector products, with Q as the axial reference vector:

$$\mathcal{E}^{\mu}_{a\dot{a}}(P,Q) = \frac{-1}{\sqrt{2}}\frac{\langle P_a \Sigma^{\mu} Q^b\rangle\langle Q_b P_{\dot{a}}]}{2P\cdot Q} = \frac{1}{\sqrt{2}}\frac{\langle P_a Q_{\dot{b}}][Q^{\dot{b}}\tilde{\Sigma}^{\mu} P_{\dot{a}}]}{2P\cdot Q} \tag{B.24}$$

These polarization vectors have the property that

$$\mathcal{E}_{11}\cdot\mathcal{E}_{22} = -1 \qquad \mathcal{E}_{12}\cdot\mathcal{E}_{21} = 1 \qquad \text{other combinations} = 0 \tag{B.25}$$

$$\mathcal{E}^{\mu}_{11}\mathcal{E}^{\nu}_{22} + \mathcal{E}^{\mu}_{22}\mathcal{E}^{\nu}_{11} - \mathcal{E}^{\mu}_{12}\mathcal{E}^{\nu}_{21} - \mathcal{E}^{\mu}_{21}\mathcal{E}^{\nu}_{12} = -g^{\mu\nu} + \frac{P^{\mu}Q^{\nu} + Q^{\mu}P^{\nu}}{P\cdot Q} \tag{B.26}$$

where the LHS of (B.26) corresponds to $\mathcal{E}^{\mu}_{a\dot{b}}\mathcal{E}^{\nu a\dot{b}}$.

The two little group indices of the polarization vectors of eq. (B.24) corresponds to the the polarization of the gluon, In the case where both the gluonic momentum and the reference momentum are four-dimensional, 11 corresponds to polarization $+$, 22 to polarization $-$, and 12 and 21 to the two new polarization directions into the extra dimensions.

B.5 Tree-level gluonic amplitudes in six dimensions

In six dimensions it is possible to make one unifying expression for tree-level amplitudes with any helicity-combination with a given number of external legs. For $gg \to gg$ that expression is

$$\mathcal{A}(p_i,p_j,p_k,p_l) = \frac{-i}{st}\langle i_a j_b k_c l_d\rangle[i_{\dot{a}} j_{\dot{b}} k_{\dot{c}} l_{\dot{d}}] \tag{B.27}$$

with

$$\begin{aligned}\langle i_a j_b k_c l_d\rangle &\equiv \varepsilon_{ABCD}\lambda^A_{i\,a}\,\lambda^B_{j\,b}\,\lambda^C_{k\,c}\,\lambda^D_{l\,d}\\ [i_{\dot{a}} j_{\dot{b}} k_{\dot{c}} l_{\dot{d}}] &\equiv \varepsilon^{ABCD}\lambda^i_{A\,\dot{a}}\,\lambda^j_{B\,\dot{b}}\,\lambda^k_{C\,\dot{c}}\,\lambda^l_{D\,\dot{d}}\end{aligned} \tag{B.28}$$

At three-point the corresponding identity is of similar size but requires some further notation that will not be introduced here [103], and the same is the case at higher points.

During the calculations of sections 11 and 12 we used eq. (B.27) to calculate four-point amplitudes, and used non-simplified expressions generated directly from Feynman diagrams to evaluate amplitudes at five or higher points. For the three-point amplitudes on the other hand simplified expressions are rather easy to obtain,

the results being

$$
\begin{aligned}
A\left(1_{22},2_{22},3_{11}\right) &= i\frac{\langle 12\rangle^3}{\langle 23\rangle\langle 31\rangle} \\
A\left(1_{11},2_{11},3_{22}\right) &= -i\frac{[12]^3}{[23][31]} \\
A\left(1_{22},2_{21},3_{12}\right) = A\left(1_{22},2_{12},3_{21}\right) &= i\frac{\langle 21\rangle\langle 13\rangle}{\langle 23\rangle} \\
A\left(1_{11},2_{12},3_{21}\right) = A\left(1_{11},2_{21},3_{12}\right) &= -i\frac{[21][13]}{[23]} \\
A\left(1_{22},2_{11},3_{12}\right) &= i\frac{\langle 1\xi\rangle[\xi 2]}{\langle 2\xi\rangle[\xi 1]}\frac{(p_1-p_2)\cdot\xi m_3 + p_3\cdot\xi(m_2-m_1)}{2p_3\cdot\xi} \\
A\left(1_{22},2_{11},3_{21}\right) &= -i\frac{\langle 1\xi\rangle[\xi 2]}{\langle 2\xi\rangle[\xi 1]}\frac{(p_1-p_2)\cdot\xi \tilde{m}_3 + p_3\cdot\xi(\tilde{m}_2-\tilde{m}_1)}{2p_3\cdot\xi} \\
A\left(1_{11},2_{22},3_{12}\right) &= i\frac{\langle 2\xi\rangle[\xi 1]}{\langle 1\xi\rangle[\xi 2]}\frac{(p_1-p_2)\cdot\xi m_3 + p_3\cdot\xi(m_2-m_1)}{2p_3\cdot\xi} \\
A\left(1_{11},2_{22},3_{21}\right) &= -i\frac{\langle 2\xi\rangle[\xi 1]}{\langle 1\xi\rangle[\xi 2]}\frac{(p_1-p_2)\cdot\xi \tilde{m}_3 + p_3\cdot\xi(\tilde{m}_2-\tilde{m}_1)}{2p_3\cdot\xi} \\
A\left(1_{12},2_{12},3_{21}\right) &= i\left(\frac{p_3\cdot\xi}{p_1\cdot\xi}m_1 - \frac{p_3\cdot\xi}{p_2\cdot\xi}m_2\right) \\
A\left(1_{21},2_{21},3_{12}\right) &= -i\left(\frac{p_3\cdot\xi}{p_1\cdot\xi}\tilde{m}_1 - \frac{p_3\cdot\xi}{p_2\cdot\xi}\tilde{m}_2\right)
\end{aligned}
\tag{B.29}
$$

with everything else being zero, except for the cyclic permutations.

We note that the cases with an even number of higher dimensional helicities fits perfectly with the four-dimensional expressions if one identifies the 12 and 21 helicities with four-dimensional scalars, and that all the cases fit with the expression for amplitudes for massive particles in four dimensions [122] with individual higher-dimensional polarizations corresponding to the third direction allowed in the massive case. This nice correspondence does unfortunately not carry on to higher points in all cases.

B.6 Summary

In six dimensions spinors can be defined with the property that

$$
\Lambda^{aA}\Lambda^B_a = P\cdot\tilde{\Sigma}^{AB} \qquad\qquad \tilde{\Lambda}_{A\dot{a}}\tilde{\Lambda}^{\dot{a}}_B = P\cdot\Sigma_{AB} \tag{B.30}
$$

The general expressions for the six-dimensional spinors are

$$
\Lambda^A_a = \begin{bmatrix} -\kappa\mu_\alpha & \tilde{\lambda}^{\dot{\alpha}} \\ \lambda_\alpha & \tilde{\kappa}\tilde{\mu}^{\dot{\alpha}} \end{bmatrix}_{aA} \qquad\qquad \tilde{\Lambda}_{A\dot{a}} = \begin{bmatrix} \kappa'\mu^\alpha & \lambda^\alpha \\ -\tilde{\lambda}_{\dot{\alpha}} & \tilde{\kappa}'\tilde{\mu}_{\dot{\alpha}} \end{bmatrix}_{A\dot{a}} \tag{B.31}
$$

in terms of four-dimensional spinors, with

$$m \equiv P_-^3 \quad \tilde{m} \equiv P_+^3 \quad \kappa \equiv \frac{m}{\langle \mu\lambda \rangle} \quad \tilde{\kappa} \equiv \frac{\tilde{m}}{[\lambda\mu]} \quad \kappa' \equiv \frac{\tilde{m}}{\langle \mu\lambda \rangle} \quad \tilde{\kappa}' \equiv \frac{m}{[\lambda\mu]} \tag{B.32}$$

Interpreting λ and μ as the spinors for the four-dimensional vectors $p^\flat$ and ξ, the vector

$$p = p^\flat + \frac{m\tilde{m}}{2p \cdot \xi}\xi \tag{B.33}$$

is massive with $p^2 = m\tilde{m}$, showing how the extra-dimensional components can be interpreted as mass parameters.

Six-dimensional spinors have a spinor product

$$\langle i_a | j_{\dot{b}}] = \begin{bmatrix} B_{ij} & C_{ij} \\ D_{ij} & -A_{ij} \end{bmatrix}_{a\dot{b}} \tag{B.34}$$

with

$$\begin{aligned} A_{ij} &\equiv \langle ij \rangle + \tilde{\kappa}_i \tilde{\kappa}'_j [\mu_i \mu_j] & C_{ij} &\equiv \kappa_i \langle \mu_i j \rangle - \tilde{\kappa}'_j [i \mu_j] \\ B_{ij} &\equiv [ij] + \kappa_i \kappa'_j \langle \mu_i \mu_j \rangle & D_{ij} &\equiv \tilde{\kappa}_i [\mu_i j] - \kappa'_j \langle i \mu_j \rangle \end{aligned} \tag{B.35}$$

and the property that $\det(\langle i_a | j_{\dot{b}}]) = S_{ij}$.

The six-dimensional spinors also have a vector-product $\langle i_a \Sigma^\mu j_b \rangle$, which can be used to form a six-dimensional polarization vector

$$\mathcal{E}^\mu_{a\dot{a}}(P, K) = \frac{-1}{\sqrt{2}} \frac{\langle P_a \Sigma^\mu K^b \rangle \langle K_b P_{\dot{a}}]}{2P \cdot K} \tag{B.36}$$

which obeys all the usual relations.

The six-dimensional spinor-helicity formalism may be used to generate closed expressions for tree-level scattering amplitudes which are even nicer than in the four-dimensional case.

Appendix C

Kinematics and momentum twistors

A physical scalar quantity which is a function of n external momenta summing to zero, is said to possess n-point kinematics.

In this appendix we will describe two ways of expressing quantities in n-point kinematics, using Mandelstam variables and epsilon contractions, and using momentum twistor variables.

C.1 Kinematics

Aside from an over all helicity-dependent factor, all dependence on the external momenta must (in four dimensions) come from contractions of those momenta with the Lorenz-invariant tensors $g_{\mu\nu}$ or $\varepsilon_{\mu_1\mu_2\mu_3\mu_4}$, but not all of these factors are independent. When separating the $g_{\mu\nu}$ contractions into (squared) masses and Mandelstam variables, so that our quantities are defined as

$$m_i^2 \equiv p_i^2, \qquad s_{ij} \equiv (p_i + p_j)^2, \qquad \mathrm{tr}_5(abcd) \equiv -4i\varepsilon_{\mu_a\mu_b\mu_c\mu_d} p_a^{\mu_a} p_b^{\mu_b} p_c^{\mu_c} p_d^{\mu_d}, \tag{C.1}$$

combinatorics tells us that the number of linearly independent[1] parameters is given as

$\#m_i$	$\#s_{ij}$	$\#\mathrm{tr}_5$	$\#z$
n	$n(n-3)/2$	$C(n-1,4)$	$3n-10$
3	0	0	–
4	2	0	2
5	5	1	5
6	9	5	8
7	14	15	11
8	20	35	14

(C.2)

[1] Not linearly independent in the usual sense, the meaning here is that the parameters are not related by linear relations.

for various kinematics, where $C(i,j)$ denotes the binomial coefficients

$$C(n-1,4) = \frac{(n-1)!}{(n-5)!4!} \tag{C.3}$$

For $n \geq 6$ the $n(n-3)/2$ parameters are not completely independent, but are related by relations imposed by the vanishing of the Gram determinants of any five-member subset of the momenta, and in general there will be $(n-5)(n-4)/2$ such relations leaving $3n-10$ totally independent Mandelstam variables, a number which is listed as $\#z$ in the table of eq. (C.2).

None of the tr_5 variables are completely independent, but are related to the Mandelstam variables through the kinematical Gram matrix as

$$\begin{aligned}\mathrm{tr}_5(abcd)^2 &= 16 \det G \begin{pmatrix} p_a & p_b & p_c & p_d \\ p_a & p_b & p_c & p_d \end{pmatrix} \\ &= s_{ab}^2 s_{cd}^2 + s_{ac}^2 s_{bd}^2 + s_{ad}^2 s_{bc}^2 - 2\big(s_{ac}s_{ad}s_{bc}s_{bd} + s_{ab}s_{ad}s_{bc}s_{cd} + s_{ab}s_{ac}s_{bd}s_{ad}\big)\end{aligned} \tag{C.4}$$

where the latter relation holds in the fully massless case only.

For four-point kinematics we usually chose the two independent Mandelstam variables to be $s \equiv (p_1+p_2)^2$ and $t \equiv (p_1+p_4)^2$, with the third Mandelstam variable $u \equiv (p_1+p_3)^2$ being related to the other two, the relation being $s+t+u=0$ in the massless case.

For five-point kinematics we chose to pick the five cyclic Mandelstam variables $s_{i,i+1}$ (where the sum is defined in a cyclic way), and then the non-cyclic parameters are related through the relation

$$s_{i,i+2} = s_{i+3,i+4} - s_{i,i+1} - s_{i+1,i+2} \tag{C.5}$$

in the massless case. Only one independent epsilon contraction will appear at five-point, and we take that to be $\mathrm{tr}_5(1234)$ which we also denote tr_5 due to the unambiguity.

C.2 Momentum twistors

For massless kinematics there is an alternate way to express the set of external momenta, namely as momentum twistors. Momentum twistors were introduced by Hodges in [48], based on the space-time twistors introduced in [123]. Momentum twistors have their greatest strengths for highly symmetric theories, but as we shall see they introduce simplifications in more general cases as well.

A momentum twistor is defined as

$$Z_i = \begin{pmatrix} \lambda_{i\alpha} \\ \mu_i^{\dot\beta} \end{pmatrix} \tag{C.6}$$

Where $\lambda_{i\alpha}$ is the holomorphic spinor of eq. (A.6) and $\mu_i^{\dot\beta}$ is an anti-holomorphic spinor, which is related to the the usual anti-holomorphic spinors through

$$\tilde\lambda_i^{\dot\beta} = \frac{\langle i,\, i+1\rangle \mu_{i-1}^{\dot\beta} + \langle i+1,\, i-1\rangle \mu_i^{\dot\beta} + \langle i-1,\, i\rangle \mu_{i+1}^{\dot\beta}}{\langle i,\, i+1\rangle \langle i-1,\, i\rangle} \tag{C.7}$$

The momentum twistors have manifestly a lot of the symmetries of the problem. They have the full Lorentz (or Poincaré) symmetry, and also the invariance under scaling of the holomorphic and anti-holomorphic spinors of eqs. (A.6) and other relations obeyed by the spinors like the Schouten identity. For n-point kinematics, we may write the total set of momentum twistors Z as an $4 \times n$ matrix, which in general has that number of elements. But due to the mentioned symmetries the number is reduced to $3n - 10$ which is the number listed as $\#z$ in table (C.2).

Four-point momentum twistors

At four-point a momentum twistor parametrization needs two variables, which we will call z_1 and z_2, and a good choice is

$$Z = \begin{pmatrix} 1 & 0 & -\frac{1}{z_1} & -\frac{1}{z_1} - \frac{1}{z_2} \\ 0 & 1 & 1 & 1 \\ 0 & 0 & 1 & 0 \\ 0 & 0 & 0 & 1 \end{pmatrix} \tag{C.8}$$

This corresponds to the $\tilde\lambda$-spinors

$$\tilde\lambda_1 = \begin{pmatrix} 0 \\ -1 \end{pmatrix} \qquad \tilde\lambda_2 = \begin{pmatrix} z_1 \\ 0 \end{pmatrix} \qquad \tilde\lambda_3 = \begin{pmatrix} -z_1 - z_2 \\ z_2 \end{pmatrix} \qquad \tilde\lambda_4 = \begin{pmatrix} z_2 \\ -z_2 \end{pmatrix} \tag{C.9}$$

which again correspond to the Mandelstam variables

$$s = z_1 \qquad\qquad t = z_2 \tag{C.10}$$

showing a one-to-one correspondence between the Mandelstams and the twistor variables. This is not surprising, as four-point kinematics has a none of the complicated non-linear relations which are seen at higher points.

Five-point momentum twistors

At five-point, the best parametrization of Z which we have found so far[2] is

$$Z = \begin{pmatrix} 1 & 0 & \frac{1}{z_1} & \frac{1}{z_1} + \frac{1}{z_1 z_2} & \frac{1}{z_1} + \frac{1}{z_1 z_2} + \frac{1}{z_1 z_2 z_3} \\ 0 & 1 & 1 & 1 & 1 \\ 0 & 0 & 0 & \frac{z_4}{z_2} & 1 \\ 0 & 0 & 1 & 1 & 1 - \frac{z_5}{z_4} \end{pmatrix} \tag{C.11}$$

[2]This parametrization was first presented in [5]. It is an improvement over the one we used in [3].

For this case the (cyclic) Mandelstam variables are given as

$$\begin{aligned} s_{12} &= z_1 \qquad & s_{23} &= z_1 z_4 \qquad & s_{34} &= \frac{z_1(z_2 z_3(z_5-1)+(z_3+1)z_4)}{z_2} \\ s_{45} &= z_1 z_5 \qquad & s_{51} &= z_1 z_3(z_2 - z_4 + z_5) \end{aligned} \tag{C.12}$$

and the epsilon contraction is given as

$$\mathrm{tr}_5 = \frac{z_1^2((z_2-z_4)(z_2 z_3-(z_3+1)z_4)-z_5(z_3(z_2^2+z_4)+z_4))}{z_2} \tag{C.13}$$

so we see that any rational function of five-point kinematics without an over-all helicity-dependent factor, can be written as a rational function of the five momentum twistor variables without the ambiguity introduced by potential square-roots coming from eq. (C.4). The system can be inverted to give

$$\begin{aligned} z_1 &= s_{12} & z_4 &= \frac{s_{23}}{s_{12}} & z_5 &= \frac{s_{45}}{s_{12}} \\ z_2 &= \frac{\langle 23\rangle\langle 14\rangle}{\langle 12\rangle\langle 34\rangle} & z_3 &= \frac{\langle 34\rangle\langle 15\rangle}{\langle 13\rangle\langle 45\rangle} \end{aligned} \tag{C.14}$$

expressing the momentum twistor parameters in terms of helicity independent kinematical variables.

Appendix D

Evaluation of integrals with ρ insertions

In this appendix we will derive the procedure for integrating over the higher dimensional ρ_{ij} parameters which appear in results like eqs. (11.23) and (12.33). The derivation is based on [98, 124]. As the procedure relies heavily on Schwinger parametrization, we will start by introducing that.

D.1 Schwinger parametrization

Schwinger parametrization is a method to perform Feynman integrals of the form[1]

$$I = \int \left(\prod_i \frac{\mathrm{d}^d k_i}{\pi^{d/2}} \right) \frac{1}{D_1^{a_1} \cdots D_n^{a_n}} \tag{D.1}$$

where the propagators D_i are functions of the loop-momenta k_i and the external basis β.

The central "trick" to Schwinger parametrization is to perform the transformation

$$\frac{1}{y^a} = \frac{1}{(a-1)!} \int_0^\infty \mathrm{d}x \; x^{a-1} \exp\left(-xy\right) \tag{D.2}$$

on each of the propagators in eq. (D.1), where the new x-variables are known as Schwinger parameters[2]. This transforms the integral into

$$\begin{aligned} I = \int \left(\prod_i \frac{\mathrm{d}^d k_i}{\pi^{d/2}} \right) \int \left(\prod_j \mathrm{d}x_j \frac{x_j^{a_j - 1}}{(a_j - 1)!} \right) \times \\ \exp\left(- \sum_i z_i k_i^2 - 2 \sum_{i,j \leq i} z_{ij} k_i \cdot k_j - \sum_i k_i \cdot v_i - z_0 \right) \end{aligned} \tag{D.3}$$

[1] For ease, we will restrict the discussion to the case of a numerator of 1. This restriction is not a limitation of the Schwinger parametrization method.

[2] Schwinger parameters are also known as alpha parameters [60], and in that case the parameters x_i are denoted α_i.

where the constants z_i, z_{ij}, and z_0, and the vectors v_i are functions only of kinematic variables and Schwinger parameters. A variable shift[3] from the loop momentum variables k_i to a shifted set q_i

$$q_i^\mu = k_i^\mu + \sum_{j>i} y_j k_j^\mu + w^\mu \tag{D.4}$$

where again y_j and w^μ are functions of kinematic variables only, can be made in a way that completes the square of the exponential so that the integral becomes

$$I = \int \left(\prod_j \frac{\mathrm{d}^d q_j}{\pi^{d/2}} \right) \int \left(\prod_i \mathrm{d}x_i \frac{x_i^{a_i - 1}}{(a_i - 1)!} \right) \exp\left(- \sum_i c_i q_i^2 + c_0 \right) \tag{D.5}$$

We may now perform the momentum integrations using Gaussian integration

$$\int \mathrm{d}^d y \exp(-a y^2) = \left(\frac{\pi}{a} \right)^{d/2} \tag{D.6}$$

with the result that

$$I = \int \left(\prod_j \mathrm{d}x_j \frac{x_j^{a_j - 1}}{(a_j - 1)!} \right) \exp\big(c_0(\{x\})\big) \, \Lambda^{-d/2} \tag{D.7}$$

with

$$\Lambda \equiv \prod_{i>0} c_i(\{x\}) \tag{D.8}$$

The specific expressions[4] for Λ in terms of the z_i variables from eq. (D.3) varies between different loop numbers.

At one-loop it is given by

$$\Lambda_{\text{1-loop}} \;=\; z_1 \;=\; \sum_i x_i \tag{D.9}$$

that is as the sum of all the Schwinger parameters in the problem.

At two-loop it is given by

$$\Lambda_{\text{2-loop}} \;=\; z_1 z_2 - z_{12}^2 \;=\; \kappa_1 \kappa_2 + \kappa_1 \kappa_{12} + \kappa_2 \kappa_{12} \tag{D.10}$$

where the κs denotes the sums of the Schwinger parameters for the propagators along one of the three branches of a two-loop topology, that is those corresponding

[3]The facts that k_i have prefactor one and that only k_j with $j > i$ are allowed, ensure that the Jacobian matrix will be upper triangular with only ones on the diagonal, which means that the Jacobian determinant for the variable change is 1.

[4]The specific expression for c_0 is much more involved than for Λ, but as the the goal of this section isn't to actually evaluate an integral using eq. (D.7), that will not concern us.

to propagators which are function of k_1 only, k_2 only, and $k_1 \pm k_2$ only, respectively. So for for instance the pentagon-box parametrized by

$$\begin{aligned} &l_1 = k_1 && l_2 = k_1 - p_1 && l_3 = k_1 - p_1 - p_2 && l_4 = k_1 - p_1 - p_2 - p_3 \\ &l_5 = k_2 - p_5 - p_4 && l_6 = k_2 - p_5 && l_7 = k_2 && l_8 = k_1 + k_2 \end{aligned} \tag{D.11}$$

as in eqs. (12.1), has

$$\kappa_1 = x_1 + x_2 + x_3 + x_4 \qquad \kappa_2 = x_5 + x_6 + x_7 \qquad \kappa_{12} = x_8 \tag{D.12}$$

In the three-loop case Λ is given by

$$\begin{aligned} \Lambda_{\text{3-loop}} &= z_1 z_2 z_3 - z_1 z_{23}^2 - z_2 z_{13}^2 - z_3 z_{12}^2 + 2 z_{12} z_{13} z_{23} \\ &= \kappa_1\kappa_2\kappa_3 + \kappa_1\kappa_2\kappa_{23} + \kappa_1\kappa_2\kappa_{31} + \kappa_1\kappa_3\kappa_{12} + \kappa_1\kappa_3\kappa_{23} + \kappa_2\kappa_3\kappa_{12} \\ &\quad + \kappa_2\kappa_3\kappa_{31} + \kappa_1\kappa_{12}\kappa_{23} + \kappa_1\kappa_{23}\kappa_{31} + \kappa_1\kappa_{31}\kappa_{12} + \kappa_2\kappa_{12}\kappa_{23} + \kappa_2\kappa_{23}\kappa_{31} \\ &\quad + \kappa_2\kappa_{31}\kappa_{12} + \kappa_3\kappa_{23}\kappa_{31} + \kappa_3\kappa_{12}\kappa_{23} + \kappa_3\kappa_{31}\kappa_{12} \end{aligned} \tag{D.13}$$

where again κ_i denotes the sum of the Schwinger parameters along the branches containing only k_i, and κ_{ij} denotes the sum along branches containing $k_i - k_j$.

D.2 Integrals with ρ insertions

In this section we will use the methods developed in the previous section, to perform integrals of the form

$$I = \int \left(\prod_i \frac{\mathrm{d}^d k_i}{\pi^{d/2}} \right) \frac{\rho_{ij}}{D_1^{a_1} \cdots D_n^{a_n}} \tag{D.14}$$

where we remember that

$$k_i^2 = \bar{k}_i^2 - \rho_i \qquad 2k_i \cdot k_j = 2\bar{k}_i \cdot \bar{k}_j - \rho_{ij} \tag{D.15}$$

Starting from eq. (D.3), the above replacement gives

$$\begin{aligned} I = \int \mathrm{d}\bar{\rho} \int \left(\prod_i \frac{\mathrm{d}^4 \bar{k}_i}{\pi^{4/2}} \right) \int \left(\prod_j \mathrm{d}x_j \right) \exp\left(\sum_i z_i \rho_i + \sum_{i,j<i} z_{ij} \rho_{ij} \right) \times \\ \exp\left(- \sum_i z_i \bar{k}_i^2 - 2 \sum_{i,j \le i} z_{ij} \bar{k}_i \cdot \bar{k}_j - \sum_i \bar{k}_i \cdot v_i - z_0 \right) \end{aligned} \tag{D.16}$$

in the case where all the propagators have a power of one, and where

$$\int \mathrm{d}\bar{\rho} \equiv \int \left(\prod_i \frac{\mathrm{d}^{-2\epsilon} k_i^{[-2\epsilon]}}{\pi^{-\epsilon}} \right) \tag{D.17}$$

Completing the squares and performing the Gaussian integrals on the four-dimensional part, gives

$$I = \int \mathrm{d}\bar{\rho} \int \left(\prod_j \mathrm{d}x_j \right) \exp\bigl(c_0\bigr)\, \Lambda^{-4/2} \exp\left(\sum_i z_i \rho_i + \sum_{i,j<i} z_{ij} \rho_{ij} \right) \tag{D.18}$$

and by comparing with eq. (D.7), we see that

$$\int \mathrm{d}\bar{\rho} \exp\left(\sum_i z_i \rho_i + \sum_{i,j<i} z_{ij} \rho_{ij} \right) = \Lambda^{\epsilon} \tag{D.19}$$

which at one-loop corresponds to

$$\int \mathrm{d}\bar{\rho} \exp(z\rho) = z^{\epsilon} \tag{D.20}$$

By taking a derivative with respect to z, we get

$$\int \mathrm{d}\bar{\rho}\, \rho \exp(z\rho) = \epsilon z^{\epsilon-1} \tag{D.21}$$

which is the relation we need, because if we go through the Schwinger parametrization procedure for a one-loop integral with a numerator of ρ, the result after the Gaussian integration of the four-dimensional part, is

$$\begin{aligned} I_{1-\mathrm{loop},\rho} &= \int \mathrm{d}\bar{\rho} \int \left(\prod_j \mathrm{d}x_j \right) \exp\bigl(c_0\bigr)\, \rho\, \Lambda^{-4/2} \exp(z\rho) \\ &= \epsilon \int \left(\prod_j \mathrm{d}x_j \right) \exp\bigl(c_0\bigr)\, \Lambda^{-(d+2)/2} \end{aligned} \tag{D.22}$$

which is nothing but ϵ times the integrals without the ρ in two dimensions more. So now we have the dimension shift relation for one-loop:

$$\int \frac{\mathrm{d}^d k}{\pi^{d/2}} \frac{\rho}{D_1 \cdots D_n} = \epsilon \int \frac{\mathrm{d}^{d+2} k}{\pi^{(d+2)/2}} \frac{1}{D_1 \cdots D_n} \tag{D.23}$$

We will also need the relation for two powers of ρ. Taking two derivatives of eq. (D.20), gives

$$\int \mathrm{d}\bar{\rho}\, \rho^2 \exp(z\rho) = \epsilon(\epsilon - 1) z^{\epsilon-2} \tag{D.24}$$

and going through the same steps as before, gives the relation

$$\int \frac{\mathrm{d}^d k}{\pi^{d/2}} \frac{\rho^2}{D_1 \cdots D_n} = \epsilon(\epsilon - 1) \int \frac{\mathrm{d}^{d+4} k}{\pi^{(d+4)/2}} \frac{1}{D_1 \cdots D_n} \tag{D.25}$$

for the ρ^2 case.

D.3 The two-loop case

At two loops the general principle is the same. Eq. (D.19) becomes

$$\int \mathrm{d}\bar{\rho} \exp(z_1\rho_1 + z_2\rho_2 + z_{12}\rho_{12}) = \big(z_1 z_2 - z_{12}^2\big)^{\epsilon} \tag{D.26}$$

and various combinations of derivatives with respect to z_1, z_2, and z_{12}, correspond to the rules

$$\begin{aligned}
\rho_i &\to \epsilon z_j \Lambda^{\epsilon-1} & \rho_{12} &\to -2\epsilon z_{12}\Lambda^{\epsilon-1} \\
\rho_i^2 &\to \epsilon(\epsilon-1) z_j^2 \Lambda^{\epsilon-2} & \rho_{12}^2 &\to \epsilon\left(-2\Lambda + 4(\epsilon-1)z_{12}^2\right)\Lambda^{\epsilon-2} \\
\rho_1\rho_2 &\to \epsilon\big(\Lambda + (\epsilon-1)z_1 z_2\big)\Lambda^{\epsilon-2} & \rho_i\rho_{12} &\to -2\epsilon(\epsilon-1) z_j z_{12}\Lambda^{\epsilon-2}
\end{aligned} \tag{D.27}$$

Unlike the one-loop case various factors of z_i appear in the numerator. If we recall that

$$z_1 = \kappa_1 + \kappa_{12} \qquad z_2 = \kappa_2 + \kappa_{12} \qquad z_{12} = \kappa_{12} \tag{D.28}$$

with the notation from eqs. (D.12), a z in the numerator corresponds to various sums of the Schwinger parameters, and a Schwinger parameter in the numerator correspond to a higher power of the corresponding propagator, as we see from eq. (D.3). This means that for instance

$$\begin{aligned}
\int \frac{\mathrm{d}^d k_1}{\pi^{d/2}} \int \frac{\mathrm{d}^d k_2}{\pi^{d/2}} \frac{\rho_1}{D_1 \cdots D_n} &= \epsilon \int \left(\prod_j \mathrm{d}x_j\right) (\kappa_2 + \kappa_{12}) \exp\big(c_0(\{x\})\big)\, \Lambda^{-(d+2)/2} \\
&= \epsilon \sum_{i \in \{2\}\cup\{12\}} \int \frac{\mathrm{d}^{d+2} k_1}{\pi^{(d+2)/2}} \int \frac{\mathrm{d}^{d+2} k_2}{\pi^{(d+2)/2}} \frac{1}{D_1 \cdots D_i^2 \cdots D_n}
\end{aligned} \tag{D.29}$$

where the two sets correspond to the sets of propagators for which either only k_2, or both k_1 and k_2 appear.

It is some specific combinations of ρs that tends to appear in the cases considered in this thesis, see for instance eq. (12.33), namely

$$\begin{aligned}
F_{1a} &= \rho_{12}^2 - 4\rho_1\rho_2 & F_{1b} &= \rho_1\rho_2 + \rho_1\rho_3 + \rho_2\rho_3 \\
F_2 &= (\rho_1 + \rho_2)\rho_{12} & F_3 &= \rho_1\rho_2
\end{aligned} \tag{D.30}$$

where $\rho_3 \equiv \rho_1 + \rho_2 + \rho_{12}$. The last two, F_2 and F_3, only appear for butterfly-type topologies, that is topologies for which there are no propagators that are functions of $k_1 + k_2$, corresponding to $\kappa_{12} = 0$.

Using eqs. (D.27) just like before, we get that

$$\begin{aligned}
I^{[4-2\epsilon]}\big(N(\bar{k}_i)(\rho_{12}^2 - 4\rho_1\rho_2)\big) &= -2\epsilon(2\epsilon+1) I^{[6-2\epsilon]}\big(N(\bar{k}_i)\big), \\
I^{[4-2\epsilon]}\big(N(\bar{k}_i)(\rho_1\rho_2 + \rho_1\rho_3 + \rho_2\rho_3)\big) &= 3\epsilon^2 I^{[6-2\epsilon]} + 2\epsilon(\epsilon-1) \sum_{i,j\in\mathcal{P}} \mathbf{i}^+\mathbf{j}^+ I^{[8-2\epsilon]}\big(N(\bar{k}_i)\big), \\
I^{[4-2\epsilon]}_{\text{butterfly}}\big(N(\bar{k}_i)\rho_1\rho_2\big) &= \epsilon^2 I^{[6-2\epsilon]}_{\text{butterfly}}\big(N(\bar{k}_i)\big), \\
I^{[4-2\epsilon]}_{\text{butterfly}}\big(N(\bar{k}_i)(\rho_1+\rho_2)\rho_{12}\big) &= 0,
\end{aligned} \tag{D.31}$$

where $N(\bar{k})$ denotes any numerator which is a function of the k_i only through the four-dimensional parts. The set $\mathcal{P}$ includes all possible ways to increase the power of a propagator along one of the three branches of the topology. For the double-box as parametrized by eqs. (11.15) we have for instance

$$\begin{aligned}
\sum_{i,j\in\mathcal{P}(331)} \mathbf{i}^+\mathbf{j}^+ I_{331}^{[8-2\epsilon]}(1,1,1,1,1,1,1) \;=\; & \\
I_{331}^{[8-2\epsilon]}(3,1,1,1,1,1,1) + I_{331}^{[8-2\epsilon]}(2,2,1,1,1,1,1) + I_{331}^{[8-2\epsilon]}(2,1,2,1,1,1,1) & \\
+I_{331}^{[8-2\epsilon]}(1,3,1,1,1,1,1) + I_{331}^{[8-2\epsilon]}(1,2,2,1,1,1,1) + I_{331}^{[8-2\epsilon]}(1,1,3,1,1,1,1) & \\
+I_{331}^{[8-2\epsilon]}(1,1,1,3,1,1,1) + I_{331}^{[8-2\epsilon]}(1,1,1,2,2,1,1) + I_{331}^{[8-2\epsilon]}(1,1,1,2,1,2,1) & \\
+I_{331}^{[8-2\epsilon]}(1,1,1,1,3,1,1) + I_{331}^{[8-2\epsilon]}(1,1,1,1,2,2,1) + I_{331}^{[8-2\epsilon]}(1,1,1,1,1,3,1) & \\
+I_{331}^{[8-2\epsilon]}(1,1,1,1,1,1,3). & \qquad \text{(D.32)}
\end{aligned}$$

Appendix E

Algebraic geometry

In this appendix we will review a number of concepts from algebraic geometry which we use in this thesis, and provide a few examples.

E.1 Concepts from algebraic geometry

Ring

A ring is a set which is closed under the relations of addition and multiplication. The ring is an *Abelian group* under the addition, meaning that it has a 0, a negative element for each positive one, and that the addition is commutative and associative. Additionally it is a *monoid* (a *semigroup* with an identity) under the multiplication, which means that it has a 1, and that multiplication is associative. All rings encountered in this thesis will be *commutative rings*, which means that the members commute under multiplication. Examples of rings are the sets $\mathbb{Z}$, $\mathbb{Q}$, $\mathbb{R}$, $\mathbb{C}$.

Polynomial ring

A polynomial ring is a ring consisting of polynomials in a set of free variables, with coefficients taken from another ring. The set of polynomials in n free variables is a polynomial ring with the coefficient ring (in general) being $\mathbb{C}$. Products of the variables in the set are called *monomials* of the polynomial ring.

Ideal

An ideal I of a ring R is a subset of R with the property that multiplication of any member of I with any member of R will generate a member of I. Ideals will be closed under both addition and multiplication.

Primary ideal

A primary ideal I of a (commutative) ring R is an ideal with the extra property that whenever a product of two elements of R is a member of I, then some (integer) power of one of the elements is a member of I. Primary ideals are of interest due to the *Lasker-Noether Theorem* which states that any ideal of a *Noetherian Ring* (a rather abstract property which is fulfilled by all rings that we will encounter), can be written as the intersection of a number of primary ideals, $I = \cap_i I_i$.

Radical (of an) ideal

A radical of an ideal I in a ring R, denoted $\sqrt{I}$, is the set of elements of R with the property that some integer power is a member of I. The radical of an ideal is itself an ideal, and if $I = \sqrt{I}$, the ideal is denoted radical.

Prime ideal

A prime ideal I in a ring R is an ideal with the property that if the product of any two members of R is a member of I, then at least one of the two is also a member of I. Prime ideals are both primary and radical, and the radical of a primary ideal will always be prime.

Generating set

A generating set of an ideal I in a ring R, is set members of I, such that any element of I can be written as a linear combination of the members of the minimal set, with coefficients from R

Multivariate polynomial division

Multivariate polynomial division is an algorithm to perform polynomial division for polynomials of more than one variable. It relies on a *monomial ordering* which is a way to assign an ordering to the monomials of the polynomials. In this thesis we will use the monomial ordering *DegreeLexicographic* which first orders the monomials by degree, that is after the total power of the variables, and then orders the terms with the same degree lexicographically, that according to a specific ordering of the variables which could for instance be alphabetical.

After having assigned the monomial ordering, the multivariate polynomial division procedure of polynomials f and g finds the leading order monomial m of g, and then identifies the highest order monomial of f, m' which is a multiple of m, such that $m' = qm$ where q will be the quotient of the division. In that case we may write

$$f = q_1 g + f_1 \tag{E.1}$$

where f_1 is the remainder of the (first part of the) division. Repeating this procedure gives $f_1 = q_2 g + f_2$, and the procedure can be repeated until g no longer divides any of the terms in f_i, in which case we have

$$f = qg + r \tag{E.2}$$

where q is the sum of the q_i, and r is the remainder after the final division.

If one has a set of polynomials, for instance as a generating set for an ideal, one may define *repeated polynomial division* towards the members of this set. In this procedure one starts by division with respect to the first member of this set, then with respect to the next, etc. The result of this procedure will in general be dependent on the order of the elements in the set.

Gröbner basis

A Gröbner basis G of an ideal I in a polynomial ring R, is a generating set for I with the property any member of I has a leading term which is divisible by the leading term of one of the members of G. This means that any member f of R can be reduced towards G in an unique way, by repeated division of f with a member of G which divides the leading term. It is always possible to find a Gröbner basis for an ideal generated by a finite generating set. The traditional algorithm for finding Gröbner bases is called *Buchberger's algorithm* and will not be discussed here. For practical purposes this thesis will rely on the GroebnerBasis function in Mathematica.

Quotient ring

A quotient ring R/I of a ring R with an ideal I is the ring obtained by mapping all members of I to zero in R. All members of R/I can be obtained by multivariate polynomial division of a member of R with the Gröbner basis for I.

Zero locus

In a space parametrized by a set of variables x_i, a zero locus is the subspace $Z(S)$ in which a set of polynomials S in the variables all vanish. A sub-space which is the zero locus for some S is called an *algebraic set*. A zero locus for a set S is equivalent to the zero locus of the ideal I generated by the set. A theorem named *Hilbert's Nullstellensatz* tells us that if a polynomial f vanishes on the zero locus of of an ideal I, then $f \in \sqrt{I}$.

E.2 Examples

Primary decomposition

The set of integers $\mathbb{Z}$ is a ring, and the set of multiples of some integer n, written $n\mathbb{Z}$, is an ideal of that ring. For the case of $n = 30$ we may write the ideal as the

intersections of the sets of multiples of 2, 3, and 5, the prime factors of 30, that is $30\mathbb{Z} = 2\mathbb{Z} \cap 3\mathbb{Z} \cap 5\mathbb{Z}$. This is the primary decomposition of $30\mathbb{Z}$, showing how primary decomposition of ideals correspond to prime factorization of numbers.

To see why it is called primary decomposition, rather than prime decomposition, let us look at another example in which the same prime factor occurs more than once. For $n = 45$, the prime factorization is $45 = 3 \times 3 \times 5$, but $45\mathbb{Z} \neq 3\mathbb{Z} \cap 3\mathbb{Z} \cap 5\mathbb{Z}$ as the latter set also includes for instance the number 15. Rather the correct primary decomposition is $45\mathbb{Z} = 9\mathbb{Z} \cap 5\mathbb{Z}$, where $9\mathbb{Z}$ is an example of a primary ideal which is not prime, as 9 is an integer power of a prime number without itself being prime.

Multivariate polynomial division

Let us say we have the polynomials

$$f = 2y^2x + 3yx^2 + x^3 + 4xy - 2x^2 \qquad g = 2yx + x^2 \tag{E.3}$$

and we want to find the quotient and residue of f/g. In the DegreeLexicographic ordering (with $y > x$) the leading term of g is $m = 2yx$. The leading terms of f is $2y^2x$ with we see to divide m with the quotient y. Thus we may write f as

$$f = yg + f' \qquad \text{with} \qquad f' = 2yx^2 + x^3 + 4xy - 2x^2 \tag{E.4}$$

Repeating this procedure gives

$$f' = xg + f'' \qquad \text{with} \qquad f'' = 4xy - 2x^2 \tag{E.5}$$

and repeating again gives

$$f'' = 2g + f''' \qquad \text{with} \qquad f''' = -4x^2 \tag{E.6}$$

m does not divide any terms in f''' meaning that the procedure is done, with the result

$$f = qg + r \qquad \text{with} \qquad q = (x + y + 2) \quad \text{and} \quad r = -4x^2 \tag{E.7}$$

Gröbner bases

Let us regard the ring of polynomials in $\{x, y, z\}$ with integer coefficients, and an ideal I in that ring is generated by the three polynomials in the generating set

$$S = \{xy - 4x - 2 \ , \quad z^3 + xy \ , \quad xz^2 - y^2 - z + 2\} \tag{E.8}$$

The ideal I will contain all polynomials which can be written as linear combinations of the members of S, and we want to know whether the polynomial

$$f = 2yz^3 - 2xz^3 - xy^3 + 2y^2z + 6xy^2 + x^2y + 2z^2 + 2y^2 - 4x^2 - 4z - 2x \tag{E.9}$$

is a member of I. This is very hard to determine without the application of Gröbner bases. For the DegreeLexicographic ordering (with $x < y < z$), the Gröbner basis[1] for I is

$$\begin{aligned} G = \{\ & xy - 4x - 2\ , \\ & 4x^3 + 2yz + 14xz + y^2 + 2x^2 + 9z - 2\ , \\ & y^3 - 2z^2 + yz - 4y^2 - 4z - 2y + 8\ , \\ & y^2z + z^2 + 4x^2 - 2z + 2x\ , \\ & xz^2 - y^2 - z + 2\ , \\ & z^3 + 4x + 2\ \} \end{aligned} \tag{E.10}$$

A repeated polynomial division with respect to the members of G in a way that always reduces the leading term in f (this could be in the order $g_6, g_6, g_3, g_5, g_4, g_1, g_1, g_1, g_1$ where g_i is the ith element of G), will yield the result 0, showing that f can be generated by the Gröbner basis, and that it therefore is a member of I.

To see why a Gröbner basis is necesary in order to perform such a reduction, let us take a look a the ideal generated by y^2 and $y^2 + x$. Clearly x^3 is a member of this ideal, but we see that none of the two generators divide x^3. The Gröbner basis for this ideal on the other hand is $\{x, y^2\}$ where a repeated division will give the result zero, thereby proving that $x^3 \in I$.

[1] as found using Mathematica's GroebnerBasis function.

Appendix F

Minor appendices

F.1 Flattened vectors

In some cases we want to find a set of massless Lorentz vectors spanning the space spanned by the two general Lorentz vectors p_1 and p_2. In the case where both p_1 and p_2 are massless the answer is obvious, but let us imagine the case where $p_1^2 = 0$ but $p_2^2 \neq 0$. In that case the answer is the two vectors p_1 and

$$p_2^{\flat_1} \equiv p_2 - \frac{p_2^2}{2p_1 \cdot p_2} p_1 \tag{F.1}$$

where the symbol $\flat$, known from musical notation, is denoted "flat", making $p_2^{\flat_1}$ a flattened version of the vector p_2.

In the case where both p_1 and p_2 are massive[1] we will use eq. (F.1) recursively as

$$p_1^{\flat_2} = p_1 - \frac{p_1^2}{2p_1 \cdot p_2^{\flat_1}} p_2^{\flat_1} \qquad\qquad p_2^{\flat_1} = p_2 - \frac{p_2^2}{2p_2 \cdot p_1^{\flat_2}} p_1^{\flat_2} \tag{F.2}$$

which can be solved with the result

$$p_1^{\flat_2} = \frac{p_1 - \frac{p_1^2}{\gamma_{12}} p_2}{1 - \frac{p_1^2 p_2^2}{\gamma_{12}^2}} \qquad\qquad p_2^{\flat_1} = \frac{p_2 - \frac{p_2^2}{\gamma_{12}} p_1}{1 - \frac{p_1^2 p_2^2}{\gamma_{12}^2}} \tag{F.3}$$

where

$$\gamma_{12} \equiv 2p_1^{\flat_2} \cdot p_2^{\flat_1} = p_1 \cdot p_2 + \sqrt{(p_1 \cdot p_2)^2 - p_1^2 p_2^2} \tag{F.4}$$

The system of eqs. (F.3) may be inverted with the result

$$p_1 = p_1^{\flat_2} + \frac{p_1^2}{\gamma_{12}} p_2^{\flat_1}, \qquad\qquad p_2 = p_2^{\flat_1} + \frac{p_2^2}{\gamma_{12}} p_1^{\flat_2}. \tag{F.5}$$

[1] We note that this case is not present at all in this thesis.

F.2 Spurious directions

For loop calculations with n-point kinematics, it is convenient to define a basis β spanning four-dimensional space.

In cases where $n \leq 4$, such a basis can not be constructed out of the external momenta alone, it is necessary to introduce a number of new directions, denoted spurious directions ω. It is convenient to define these directions such that each vector ω is perpendicular to all the other members of β, meaning that cases with more than one ω will have $\omega_i \cdot \omega_j \propto \delta_{ij}$. Let us go through the various kinematics case by case.

$n = 4$

For four-point kinematics we have the four external momenta p_1 to p_4 which we take to be massless. Only three of those momenta are independent, as the fourth is fixed by momentum conservation. The way to pick a momentum that is perpendicular to all four, is[2]

$$\omega^\mu \propto \varepsilon^{\mu\nu_1\nu_2\nu_3} p_{1\nu_1} p_{2\nu_2} p_{3\nu_3} \tag{F.6}$$

In this thesis we choose a normalization such that

$$\omega^\mu \equiv \frac{\langle 23\rangle[31]}{s}\frac{\langle 1|\sigma^\mu|2]}{2} - \frac{\langle 13\rangle[32]}{s}\frac{\langle 2|\sigma^\mu|1]}{2} \tag{F.7}$$

which has the convenient properties of having units of momentum like the other members of β, and that it is easy to see all four perpendicularities. This choice corresponds to

$$\omega^\mu = \frac{2i}{s}\varepsilon^{\mu\nu_1\nu_2\nu_3} p_{1\nu_1} p_{2\nu_2} p_{3\nu_3} \tag{F.8}$$

$n = 3$

For three-point kinematics we have the three massless momenta p_1, p_2, p_3, of which only two are independent. This leaves two spurious directions, which we will chose as

$$\omega_+^\mu \equiv \frac{\langle 1|\sigma^\mu|2]}{2} + \frac{\langle 2|\sigma^\mu|1]}{2} \qquad \omega_-^\mu \equiv \frac{\langle 1|\sigma^\mu|2]}{2} - \frac{\langle 2|\sigma^\mu|1]}{2} \tag{F.9}$$

In fact any combination of parameters

$$\omega_+^\mu = a\frac{\langle 1|\sigma^\mu|2]}{2} + b\frac{\langle 2|\sigma^\mu|1]}{2} \qquad \omega_-^\mu \equiv c\frac{\langle 1|\sigma^\mu|2]}{2} - d\frac{\langle 2|\sigma^\mu|1]}{2} \tag{F.10}$$

with the requirement that $ad = bc$ would have been acceptable, the definition of eqs. (F.9) was chosen for its simplicity. Another common choice which we will not use in this thesis, is $a = b = i$ and $c = d = 1$ which has the property that $\omega_+^2 = \omega_-^2$.

[2] This is completely analogous to the cross-product in three Euclidean dimensions, where $\bar{a} \times \bar{b} = \varepsilon_{ijk}\bar{a}_j\bar{b}_k$ is the unique direction perpendicular to vectors $\bar{a}$ and $\bar{b}$.

$n = 2$

For two-point kinematics there is only one independent external momentum direction P^μ, which we will take to be massive. In this case we can chose an arbitrary massless reference direction ξ^μ, and define the three spurious vectors

$$\omega_1^\mu \equiv \frac{\langle \flat|\sigma^\mu|\xi]}{2} - \frac{\langle \xi|\sigma^\mu|\flat]}{2} \quad \omega_2^\mu \equiv \frac{\langle \flat|\sigma^\mu|\xi]}{2} + \frac{\langle \xi|\sigma^\mu|\flat]}{2} \quad \omega_3^\mu \equiv P^\mu - \frac{P^2}{P\cdot\xi}\xi^\mu \tag{F.11}$$

with

$$p_\flat^\mu \equiv P^\mu - \frac{P^2}{2P\cdot\xi}\xi^\mu \tag{F.12}$$

in accordance with the philosophy of appendix F.1.

In the case we looked at in section 5.3, we used eq. (5.59):

$$\omega_1^\mu = \frac{\langle 1|\sigma^\mu|2]}{2} - \frac{\langle 2|\sigma^\mu|1]}{2} \qquad \omega_2^\mu = \frac{\langle 1|\sigma^\mu|2]}{2} + \frac{\langle 2|\sigma^\mu|1]}{2} \qquad \omega_3^\mu = p_1^\mu - p_2^\mu \tag{F.13}$$

where the external momentum P was given as $P = p_1 + p_2$. This corresponds to eqs. (F.11) for $\xi = p_2$, in which case $p_\flat = p_1$.

$n = 1$ **or** $n = 0$

We will not in this thesis look at any examples where the problem depends on no external momenta at all. Let us however for completeness list how to form a basis in that case. Picking two massless reference momenta ζ and ξ, allows us to write the four directions as

$$\begin{aligned} \omega_1^\mu &= \frac{\langle \zeta|\sigma^\mu|\xi]}{2} - \frac{\langle \xi|\sigma^\mu|\zeta]}{2} & \omega_3^\mu &= \xi^\mu - \zeta^\mu \\ \omega_2^\mu &= \frac{\langle \zeta|\sigma^\mu|\xi]}{2} + \frac{\langle \xi|\sigma^\mu|\zeta]}{2} & \omega_4^\mu &= \xi^\mu + \zeta^\mu \end{aligned} \tag{F.14}$$

which all are perpendicular to each other as required.

F.3 Spurious integrals

In this appendix we will investigate when a monomial is spurious, i.e when it will integrate to zero.

If the kinematics of a problem is four-point or lower, one needs to define at least one spurious vector ω to span the four dimensional space of the external particles as described in appendix F.2. In that case a monomial is spurious if (but, as we shall see, not only if) it contains exactly one factor of $k_i \cdot \omega$, where ω is defined to

be perpendicular to all other vectors in the basis β. To see this let us write the k_i integral as

$$I_{\text{spurious}} = \int \frac{\mathrm{d}^d k_i}{(2\pi)^d} X(\{k\}, \tilde{\beta}) \, (k_i \cdot \omega) = \omega_\mu \int \frac{\mathrm{d}^d k_i}{(2\pi)^d} X(\{k\}, \tilde{\beta}) \, {k_i}^\mu \tag{F.15}$$

where $X(\{k\}, \tilde{\beta})$ is defined to contain all the propagators and remaining parts of the monomial, and where $\tilde{\beta}$ is defined as the set of the remaining three elements of the momentum basis β. As ω is present nowhere under the integral sign, the integral will have to evaluate to a function of the members of $\tilde{\beta}$ only, that is

$$\omega_\mu \int \frac{\mathrm{d}^d k_i}{(2\pi)^d} X(\{k\}, \{\tilde{\beta}\}) \, {k_i}^\mu = \omega_\mu \left(Y_1 \beta_1^\mu + Y_2 \beta_2^\mu + Y_3 \beta_3^\mu \right) = 0 \tag{F.16}$$

where the last step is true by the definition of ω.

If there are several ωs in a basis, the above derivation still holds for each ω.

If a given ω is present in a number of factors Φ which is greater than one, but odd, they too will be spurious. We see that from the fact that

$$\int \left(\prod_j \frac{\mathrm{d}^d k_j}{(2\pi)^d} \right) X(\{k\}, \tilde{\beta}) k_{i_1}^{\mu_1} \cdots k_{i_\Phi}^{\mu_\Phi} \tag{F.17}$$

will evaluate to a sum of tensors which all will include at least one factor of $\tilde{\beta}_i^{\mu_j}$, as the only other tensors that may appear ($g^{\mu\nu}$ and potentially $\varepsilon^{\mu_1\mu_2\mu_3\mu_4}$) each have an even number of indices.

This means that a sufficient condition for a monomial to be spurious is for the following to hold:

- At least one spurious vector ω_i appears in an odd number of factors in the monomial.

There are however other ways in which a term can be spurious. One, which we saw in the the case of the one-loop triangle, is a term of the form

$$\int \frac{\mathrm{d}^d k}{(2\pi)^d} X(k, p_1, p_2) \left((k \cdot \omega_+)^2 + (k \cdot \omega_-)^2 \right) \tag{F.18}$$

where $\omega_+^2 = -\omega_-^2$. The two terms do not vanish individually, as the integral of $k^\mu k^\nu$ will contain a term proportional to $g^{\mu\nu}$ which does not vanish as the spurious vectors are massive, but their sum will vanish as the masses cancel, making the specific combination spurious.

For butterfly-type topologies there are more ways in which monomials can be spurious. We see one example in the box-triangle butterfly-topology ($t430$) considered in section 12.4. As it has five-point kinematics, it seems to have no room for a spurious ω-direction. But if one defines a separate β for each individual loop which accounts for the kinematics of that loop and not of the whole diagram, we will get

the ISPs $(k_1 \cdot \omega_{12\pm})$ and $(k_2 \cdot \omega_{345})$, as we do in section 12.4. Monomials of these ISPs will behave just as the spurious monomials at lower-point kinematics, as the integral over k_i can not give a term dependent on k_j (with $i \neq j$), as it could in the general case.

Another kind of spurious terms unique to the butterfly-type topologies, are those with one[3] factor of ρ_{12}. We see one occurrence of this in eq. (D.32), but it is a general feature. We see this from symmetry, as one of the loop-integrals for such cases will give

$$\begin{aligned}\int \frac{\mathrm{d}^d k_i}{(2\pi)^d} X(k_i, \beta)\rho_{12} &= -2k_{j\mu}^{[-2\epsilon]} \int \frac{\mathrm{d}^d k_i}{(2\pi)^d} X(k_i, \beta) k_i^\mu \\ &= -2k_{j\mu}^{[-2\epsilon]} \sum_{n=1}^{4} Y_n \beta_n^\mu \;=\; 0 \end{aligned} \tag{F.19}$$

where the last identity holds as all vectors in β are four-dimensional.

F.4 Discrete Fourier sums

Discrete Fourier sums is a method to extract the coefficients d_i of a Laurent polynomial f of the form

$$f(\tau) = \sum_{j=-a}^{b} d_j \tau^j \tag{F.20}$$

which has

$$N = a + b + 1 \tag{F.21}$$

terms in total.

The discrete Fourier sums dictate that

$$d_k = \frac{1}{N} \sum_{l=0}^{N-1} \frac{f(\tau_l)}{\tau_l^k} \tag{F.22}$$

where

$$\tau_l = r \exp\Big(i\big(2\pi l/N + \phi\big)\Big) \;=\; \tilde{r} \exp\Big(2\pi i l/N\Big) \tag{F.23}$$

such that the factor $\tilde{r}$ contains both the arbitrarily chosen radius r, and the arbitrary phase ϕ.

To prove eq. (F.22), let us insert f on the RHS, with the result

$$\sum_{j=-a}^{b} \frac{d_j}{N} \sum_{l=0}^{N-1} \frac{\tilde{r}^j \exp(2\pi i l j/N)}{\tilde{r}^k \exp(2\pi i l k/N)} \tag{F.24}$$

[3] or just an odd number of factors of ρ_{12}

Performing the inner sum gives

$$\tilde{r}^{j-k} \sum_{l=0}^{N-1} \exp\left(2\pi i(j-k)/N\right)^l = N\tilde{r}^{j-k}\delta_{jk} \tag{F.25}$$

where we have used the geometric sum

$$\sum_{l=0}^{N-1} x^l = \frac{1-x^N}{1-x} \tag{F.26}$$

and the fact that $j-k$ is an integer. Inserting this into the outer sum of eq. (F.24) gives d_k, thereby proving eq. (F.22).

F.5 Pseudo-inverse using PLU decomposition

PLU-decomposition is the decomposition of a matrix into a permutation matrix, a lower triangular matrix, and an upper triangular matrix

$$M = PLU \tag{F.27}$$

We will not here describe how to find a PLU-decomposition, only note that it can be done for any matrix of full rank, which is all we shall consider.

The goal of this section is to use the PLU decomposition to find a pseudo-inverse of the matrix M in the case where M is $n_d \times n_c$ with $n_d \geq n_c$, such that the equation system

$$\bar{d} = M\bar{c} \tag{F.28}$$

has the solution

$$\bar{c} = W\bar{d} \tag{F.29}$$

where W is the pseudo-inverse $WM = I$.

After the PLU-decomposition of M the matrices P and L will be $n_d \times n_d$, U will be $n_d \times n_c$, and all three matrices will be of full rank. This means that eq. (F.28) must imply

$$U\bar{c} = L^{-1}P^T\bar{d} \tag{F.30}$$

where we have used the fact that a permutation matrix has $P^{-1} = P^T$.

But as U is upper triangular and non square, we know that its lower $n_d - n_c$ rows must be zero, and likewise for the lower $n_d - n_c$ entries of $U\bar{c}$, so from eq. (F.30) we know that the lower $n_d - n_c$ entries of $L^{-1}P^T$ must contain the null-space condition for the vector $\bar{d}$, since $L^{-1}P^T\bar{d} = 0$ for those elements. The remaining n_c

equations will contain the relations between $\bar{c}$ and $\bar{d}$. If we let $\mathfrak{C}$ denote the operation of removing the lower $n_d - n_c$ rows of a matrix, we get from (F.30)

$$\mathfrak{C}(U)\bar{c} = \mathfrak{C}\big(L^{-1}\big)P^T\bar{d} \tag{F.31}$$

and as $\mathfrak{C}(U)$ is square and of full rank, we may now invert it giving

$$\bar{c} = \mathfrak{C}(U)^{-1}\mathfrak{C}\big(L^{-1}\big)P^T\bar{d} \tag{F.32}$$

allowing us to identify the matrix on the RHS as our pseudo-inverse W.

It should be noted that even though PLU-decomposition involves two matrix inversions, it is occasionally used for the inversion of square matrices too, as the inversion of L and $\mathfrak{C}(U)$ are much easier than the inversion of a general matrix due to the triangular properties.

Appendix G

Table of integrals

This appendix contains a (small) list of some Feynman integrals which are of use in our calculations. The expressions are adapted from [60, 69].

$$
\begin{aligned}
I_{\text{bubble}} &= \int \frac{\mathrm{d}^d k}{\pi^{d/2}} \frac{1}{k^2 (k-P)^2} \;=\; \frac{\Gamma^2\left(\frac{d}{2}-1\right)\Gamma\left(2-\frac{d}{2}\right)}{\Gamma(d-2)(-P^2)^{2-\frac{d}{2}}} \\
I_{\text{triangle}} &= \int \frac{\mathrm{d}^d k}{\pi^{d/2}} \frac{1}{(k+p_1)^2 k^2 (k-p_2)^2} \;=\; -\frac{\Gamma^2\left(\frac{d}{2}-2\right)\Gamma\left(3-\frac{d}{2}\right)}{\Gamma(d-3)(-s)^{3-\frac{d}{2}}} \\
I_{\text{box}} &= \int \frac{\mathrm{d}^d k}{\pi^{d/2}} \frac{1}{(k+p_1)^2 k^2 (k-p_2)^2 (k+p_1+p_4)} \\
&= -2\frac{\Gamma\left(\frac{d}{2}-1\right)\Gamma\left(\frac{d}{2}-2\right)\Gamma\left(2-\frac{d}{2}\right)}{st\,\Gamma(d-3)} \left(s^{\frac{d}{2}-2} H\left(d, -\tfrac{u}{t}\right) + t^{\frac{d}{2}-2} H\left(d, -\tfrac{u}{s}\right)\right)
\end{aligned}
\tag{G.1}
$$

where $H(d,x)$ is defined as the Gaussian hyper-geometric function

$$
H(d,x) = {}_2F_1\left(\tfrac{d}{2}-2\,,\ \tfrac{d}{2}-2\,;\ \tfrac{d}{2}-1\,;\ x\right) \tag{G.2}
$$

In general the ϵ-expansions are of greater use that the closed expressions above, and we will now regard the expansions in $d = 4-2\epsilon$, $d = 6-2\epsilon$, and $d = 8-2\epsilon$ dimensions.

For convenience we will factor the result as

$$
\begin{aligned}
\hat{I}_{\text{bubble}} &= \exp(\epsilon\gamma_E)(-P^2)^{2-\frac{d}{2}} I_{\text{bubble}} \\
\hat{I}_{\text{triangle}} &= \exp(\epsilon\gamma_E)(-s)^{3-\frac{d}{2}} I_{\text{triangle}} \\
\hat{I}_{\text{box}} &= \exp(\epsilon\gamma_E) Q(d) s^{\epsilon} I_{\text{box}}
\end{aligned}
\tag{G.3}
$$

where

$$
Q(4-2\epsilon) = st \qquad Q(6-2\epsilon) = s+t \qquad Q(8-2\epsilon) = 1 \tag{G.4}
$$

We get for the bubble

$$\begin{aligned}
\hat{I}^{[4-2\epsilon]}_{\text{bubble}} &= \frac{1}{\epsilon} + 2 + \mathcal{O}(\epsilon) \\
\hat{I}^{[6-2\epsilon]}_{\text{bubble}} &= \frac{-1}{6\epsilon} - \frac{4}{9} + \mathcal{O}(\epsilon) \\
\hat{I}^{[8-2\epsilon]}_{\text{bubble}} &= \frac{1}{60\epsilon} - \frac{23}{450} + \mathcal{O}(\epsilon)
\end{aligned} \tag{G.5}$$

for the triangle

$$\begin{aligned}
\hat{I}^{[4-2\epsilon]}_{\text{triangle}} &= -\frac{1}{\epsilon^2} + \frac{\pi^2}{12} + \mathcal{O}(\epsilon) \\
\hat{I}^{[6-2\epsilon]}_{\text{triangle}} &= -\frac{1}{2\epsilon} - \frac{3}{2} + \mathcal{O}(\epsilon) \\
\hat{I}^{[8-2\epsilon]}_{\text{triangle}} &= \frac{1}{24\epsilon} + \frac{19}{144} + \mathcal{O}(\epsilon)
\end{aligned} \tag{G.6}$$

and finally for the box[1]

$$\begin{aligned}
\hat{I}^{[4-2\epsilon]}_{\text{box}} &= \frac{4}{\epsilon^2} + \frac{2\log(\chi)}{\epsilon} + \left(\log^2(\chi) + 2\text{Li}_2\left(1+\tfrac{1}{\chi}\right) + 2\text{Li}_2(\chi+1) - \frac{\pi^2}{3}\right) + \mathcal{O}(\epsilon) \\
\hat{I}^{[6-2\epsilon]}_{\text{box}} &= \left(\log(-\chi)\big(\log(\chi) - \log(-\chi)\big) + \text{Li}_2\left(1+\tfrac{1}{\chi}\right) + \text{Li}_2(\chi+1)\right) + \mathcal{O}(\epsilon) \\
\hat{I}^{[8-2\epsilon]}_{\text{box}} &= \frac{1}{6\epsilon} + \left(\frac{11}{18} + \frac{1}{6(1+\chi)^2}\Bigg(- \big(\chi^2 + \chi\log(-\chi) - 1\big)\log(-\chi)\right. \\
&\quad \left. + \chi\big(\chi + \log(-\chi) + 1\big)\log(\chi) + \chi\left(\text{Li}_2(1+\chi) + \text{Li}_2\left(1+\tfrac{1}{\chi}\right)\right)\Bigg)\right) + \mathcal{O}(\epsilon)
\end{aligned} \tag{G.7}$$

where $\chi = s/t$.

[1] Thanks to Laura Jenniches for helping me expand the box of eq. (G.1) using HypExp [125].

Appendix H

Feynman rules

In this appendix we will write the colour ordered Feynman rules for massless particles, for the cases of gluons (g), Weyl-fermions (f), and complex scalars (s). The rules in this appendix are consistent with [31].

The gluonic propagator is given as either

$$\text{prop}_g^{\mu\nu} = \frac{-ig^{\mu\nu}}{p^2} \qquad \text{or} \qquad \text{prop}_g^{\mu\nu} = \frac{i}{p^2}\left(-g^{\mu\nu} + \frac{p^\mu q^\nu + q^\mu p^\nu}{p\cdot q}\right) \tag{H.1}$$

in respectively Feynman gauge, and axial gauge with reference vector q^μ. For fermions and scalars the propagators are

$$\text{prop}_f = \frac{i\not{p}}{p^2} \qquad\qquad \text{prop}_s = \frac{i}{p^2} \tag{H.2}$$

For the vertices we have the gluonic three- and four-point vertex

$$\begin{aligned} V_{ggg}^{\mu_1\mu_2\mu_3} &= \frac{i}{\sqrt{2}}\Big(g^{\mu_2\mu_3}(p_2-p_3)^{\mu_1} + g^{\mu_3\mu_1}(p_3-p_1)^{\mu_2} + g^{\mu_1\mu_2}(p_1-p_2)^{\mu_3}\Big) \\ V_{gggg}^{\mu_1\mu_2\mu_3\mu_4} &= ig^{\mu_1\mu_3}g^{\mu_2\mu_4} - \frac{i}{2}\big(g^{\mu_1\mu_2}g^{\mu_3\mu_4} + g^{\mu_2\mu_3}g^{\mu_4\mu_1}\big) \end{aligned} \tag{H.3}$$

the gluon-fermion vertices

$$V^\mu_{\alpha\dot\beta f g \bar f} = \frac{i}{\sqrt{2}}\sigma^\mu_{\alpha\dot\beta} \qquad\qquad V^\mu_{\alpha\dot\beta \bar f g f} = \frac{-i}{\sqrt{2}}\sigma^\mu_{\alpha\dot\beta} \tag{H.4}$$

the gluon-scalar vertices

$$V^\mu_{sgs} = \frac{i}{\sqrt{2}}(p_1-p_3)^\mu \qquad V^{\mu\nu}_{ggss} = \frac{i}{2}g^{\mu\nu} \qquad V^{\mu\nu}_{gsgs} = -ig^{\mu\nu} \tag{H.5}$$

the four-point scalar vertices

$$V_{sss's'} = -\frac{i}{2} \qquad\qquad V_{ss'ss'} = i \tag{H.6}$$

and finally the fermion-scalar vertices

$$V_{\alpha\beta}^{fsf} = \frac{i}{\sqrt{2}}\delta_{\alpha\beta} \qquad\qquad V_{\dot\alpha\dot\beta}^{\bar f s^* \bar f} = \frac{-i}{\sqrt{2}}\delta_{\dot\alpha\dot\beta} \tag{H.7}$$

For external particles we have for the gluons

$$\varepsilon_+^\mu(p,q) = \frac{\langle q|\sigma^\mu|p]}{\sqrt{2}\,\langle qp\rangle} \qquad\qquad \varepsilon_-^\mu(p,q) = \frac{\langle p|\sigma^\mu|q]}{\sqrt{2}\,[pq]} \tag{H.8}$$

in axial gauge, with no similar expression existing for Feynman gauge. For the fermions we have that

$$\lambda(p) = \big(\langle p|\,,\ |p]\big) \qquad\qquad \bar\lambda(p) = \big(|p\rangle\,,\ [p|\big) \tag{H.9}$$

and for the scalars we have nothing but

$$s = 1 \tag{H.10}$$

For each loop, we have to integrate over the loop momentum

$$\int \frac{\mathrm{d}^d k}{(2\pi)^d} \tag{H.11}$$

and

$$\text{for each fermion loop, multiply by } -1 \tag{H.12}$$

The rules for Dirac fermions are very similar to those for Weyl, see section 3.3.

In this appendix, like in most of the rest of the thesis, we have not written the $i\tilde\epsilon$ prescription of the propagators explicitly. See eq. (3.29).

No mention have been made of ghosts, as they vanish in axial gauge, but in Feynman gauge they behave just like the scalars in the above equations, except that they get an extra minus for each loop, like the fermions in eq. (H.12).

In the six-dimensional case everything is the same as in four dimensions, after having applied the replacements given by eqs. (B.1).

Bibliography

[1] S. Badger, H. Frellesvig, and Y. Zhang, "Hepta-Cuts of Two-Loop Scattering Amplitudes," *JHEP*, vol. 1204, p. 055, 2012.

[2] S. Badger, H. Frellesvig, and Y. Zhang, "An Integrand Reconstruction Method for Three-Loop Amplitudes," *JHEP*, vol. 1208, p. 065, 2012.

[3] S. Badger, H. Frellesvig, and Y. Zhang, "A Two-Loop Five-Gluon Helicity Amplitude in QCD," *JHEP*, vol. 1312, p. 045, 2013.

[4] S. Badger, H. Frellesvig, and Y. Zhang, "Multi-loop Integrand Reduction with Computational Algebraic Geometry," *J.Phys.Conf.Ser.*, vol. 523, p. 012061, 2014.

[5] S. Badger, H. Frellesvig, and Y. Zhang, "Multi-loop integrand reduction techniques," 2014.

[6] G. Aad *et al.*, "Observation of a new particle in the search for the Standard Model Higgs boson with the ATLAS detector at the LHC," *Phys.Lett.*, vol. B716, pp. 1–29, 2012.

[7] Z. Bern, L. J. Dixon, D. C. Dunbar, and D. A. Kosower, "Fusing gauge theory tree amplitudes into loop amplitudes," *Nucl.Phys.*, vol. B435, pp. 59–101, 1995.

[8] R. Britto, F. Cachazo, and B. Feng, "Generalized unitarity and one-loop amplitudes in N=4 super-Yang-Mills," *Nucl.Phys.*, vol. B725, pp. 275–305, 2005.

[9] G. Ossola, C. G. Papadopoulos, and R. Pittau, "Reducing full one-loop amplitudes to scalar integrals at the integrand level," *Nucl.Phys.*, vol. B763, pp. 147–169, 2007.

[10] D. Forde, "Direct extraction of one-loop integral coefficients," *Phys.Rev.*, vol. D75, p. 125019, 2007.

[11] S. Badger, "Direct Extraction Of One Loop Rational Terms," *JHEP*, vol. 0901, p. 049, 2009.

[12] C. Berger, Z. Bern, L. Dixon, F. Febres Cordero, D. Forde, *et al.*, "An Automated Implementation of On-Shell Methods for One-Loop Amplitudes," *Phys.Rev.*, vol. D78, p. 036003, 2008.

[13] G. Cullen, N. Greiner, G. Heinrich, G. Luisoni, P. Mastrolia, *et al.*, "Automated One-Loop Calculations with GoSam," *Eur.Phys.J.*, vol. C72, p. 1889, 2012.

[14] D. A. Kosower and K. J. Larsen, "Maximal Unitarity at Two Loops," *Phys.Rev.*, vol. D85, p. 045017, 2012.

[15] P. Mastrolia and G. Ossola, "On the Integrand-Reduction Method for Two-Loop Scattering Amplitudes," *JHEP*, vol. 1111, p. 014, 2011.

[16] Y. Zhang, "Integrand-Level Reduction of Loop Amplitudes by Computational Algebraic Geometry Methods," *JHEP*, vol. 1209, p. 042, 2012.

[17] J. Drummond, J. Henn, V. Smirnov, and E. Sokatchev, "Magic identities for conformal four-point integrals," *JHEP*, vol. 0701, p. 064, 2007.

[18] J. Drummond, J. Henn, G. Korchemsky, and E. Sokatchev, "On planar gluon amplitudes/Wilson loops duality," *Nucl.Phys.*, vol. B795, pp. 52–68, 2008.

[19] N. Arkani-Hamed, F. Cachazo, and J. Kaplan, "What is the Simplest Quantum Field Theory?," *JHEP*, vol. 1009, p. 016, 2010.

[20] N. Arkani-Hamed, J. L. Bourjaily, F. Cachazo, S. Caron-Huot, and J. Trnka, "The All-Loop Integrand For Scattering Amplitudes in Planar N=4 SYM," *JHEP*, vol. 1101, p. 041, 2011.

[21] S. Caron-Huot, "Superconformal symmetry and two-loop amplitudes in planar N=4 super Yang-Mills," *JHEP*, vol. 1112, p. 066, 2011.

[22] N. Arkani-Hamed, J. L. Bourjaily, F. Cachazo, A. B. Goncharov, A. Postnikov, *et al.*, "Scattering Amplitudes and the Positive Grassmannian," 2012.

[23] M. L. Mangano and S. J. Parke, "Multiparton amplitudes in gauge theories," *Phys.Rept.*, vol. 200, pp. 301–367, 1991.

[24] F. Cachazo, P. Svrcek, and E. Witten, "MHV vertices and tree amplitudes in gauge theory," *JHEP*, vol. 0409, p. 006, 2004.

[25] R. Britto, F. Cachazo, and B. Feng, "New recursion relations for tree amplitudes of gluons," *Nucl.Phys.*, vol. B715, pp. 499–522, 2005.

[26] R. Britto, F. Cachazo, B. Feng, and E. Witten, "Direct proof of tree-level recursion relation in Yang-Mills theory," *Phys.Rev.Lett.*, vol. 94, p. 181602, 2005.

[27] Z. Bern, J. Carrasco, and H. Johansson, "New Relations for Gauge-Theory Amplitudes," *Phys.Rev.*, vol. D78, p. 085011, 2008.

[28] M. Peskin and D. Schroeder, *An Introduction to Quantum Field Theory*. Advanced book classics, Addison-Wesley Publishing Company, 1995.

[29] R. Ellis, W. Stirling, and B. Webber, *QCD and Collider Physics*. Cambridge Monographs on Particle Physics, Nuclear Physics and Cosmology, Cambridge University Press, 2003.

[30] J.-L. Kneur and A. Neveu, "$Lambda^{\rm QCD}_{\rm MS}$ from Renormalization Group Optimized Perturbation," *Phys.Rev.*, vol. D85, p. 014005, 2012.

[31] L. J. Dixon, "Calculating scattering amplitudes efficiently," 1996.

[32] Z. Bern, L. J. Dixon, and D. A. Kosower, "One loop corrections to two quark three gluon amplitudes," *Nucl.Phys.*, vol. B437, pp. 259–304, 1995.

[33] Z. Bern, J. Rozowsky, and B. Yan, "Two loop four gluon amplitudes in N=4 superYang-Mills," *Phys.Lett.*, vol. B401, pp. 273–282, 1997.

[34] V. Del Duca, L. J. Dixon, and F. Maltoni, "New color decompositions for gauge amplitudes at tree and loop level," *Nucl.Phys.*, vol. B571, pp. 51–70, 2000.

[35] S. Dittmaier, "Weyl-van der Waerden formalism for helicity amplitudes of massive particles," *Phys.Rev.*, vol. D59, p. 016007, 1998.

[36] H. Elvang and Y.-t. Huang, "Scattering Amplitudes," 2013.

[37] S. J. Parke and T. R. Taylor, "Amplitude for n-gluon scattering," *Phys. Rev. Lett.*, vol. 56, pp. 2459–2460, Jun 1986.

[38] R. Kleiss and H. Kuijf, "Multi - Gluon Cross-sections and Five Jet Production at Hadron Colliders," *Nucl.Phys.*, vol. B312, p. 616, 1989.

[39] J. Drummond and J. Henn, "All tree-level amplitudes in N=4 SYM," *JHEP*, vol. 0904, p. 018, 2009.

[40] L. J. Dixon, J. M. Henn, J. Plefka, and T. Schuster, "All tree-level amplitudes in massless QCD," *JHEP*, vol. 1101, p. 035, 2011.

[41] J. L. Bourjaily, "Efficient Tree-Amplitudes in N=4: Automatic BCFW Recursion in Mathematica," 2010.

[42] N. Bjerrum-Bohr, P. H. Damgaard, R. Monteiro, and D. O'Connell, "Algebras for Amplitudes," *JHEP*, vol. 1206, p. 061, 2012.

[43] F. Cachazo, S. He, and E. Y. Yuan, "Scattering Equations and KLT Orthogonality," 2013.

[44] R. Kleiss and W. Stirling, "Cross sections for the production of an arbitrary number of photons in electron-positron annihilation," *Physics Letters B*, vol. 179, no. 1-2, pp. 159 – 163, 1986.

[45] S. D. Badger and J. M. Henn, "Compact QED Tree-Level Amplitudes From Dressed BCFW Recursion Relations," *Phys.Lett.*, vol. B692, pp. 143–151, 2010.

[46] S. Badger, N. Bjerrum-Bohr, and P. Vanhove, "Simplicity in the Structure of QED and Gravity Amplitudes," *JHEP*, vol. 0902, p. 038, 2009.

[47] H. Elvang, Y.-t. Huang, and C. Peng, "On-shell superamplitudes in N<4 SYM," *JHEP*, vol. 1109, p. 031, 2011.

[48] A. Hodges, "Eliminating spurious poles from gauge-theoretic amplitudes," *JHEP*, vol. 1305, p. 135, 2013.

[49] Z. Bern, N. Bjerrum-Bohr, and D. C. Dunbar, "Inherited twistor-space structure of gravity loop amplitudes," *JHEP*, vol. 0505, p. 056, 2005.

[50] N. Bjerrum-Bohr and P. Vanhove, "Explicit Cancellation of Triangles in One-loop Gravity Amplitudes," *JHEP*, vol. 0804, p. 065, 2008.

[51] J. M. Maldacena, "The Large N limit of superconformal field theories and supergravity," *Adv.Theor.Math.Phys.*, vol. 2, pp. 231–252, 1998.

[52] J. Drummond, G. Korchemsky, and E. Sokatchev, "Conformal properties of four-gluon planar amplitudes and Wilson loops," *Nucl.Phys.*, vol. B795, pp. 385–408, 2008.

[53] N. Arkani-Hamed, F. Cachazo, and C. Cheung, "The Grassmannian Origin Of Dual Superconformal Invariance," *JHEP*, vol. 1003, p. 036, 2010.

[54] N. Arkani-Hamed and J. Trnka, "The Amplituhedron," 2013.

[55] S. Caron-Huot and J. M. Henn, "A solvable relativistic hydrogen-like system," 2014.

[56] Z. Bern, L. J. Dixon, and R. Roiban, "Is N = 8 supergravity ultraviolet finite?," *Phys.Lett.*, vol. B644, pp. 265–271, 2007.

[57] H. Kawai, D. C. Lewellen, and S.-H. H. Tye, "Construction of fermionic string models in four dimensions," *Nuclear Physics B*, vol. 288, no. 0, pp. 1 – 76, 1987.

[58] P. H. Damgaard, R. Huang, T. Sondergaard, and Y. Zhang, "The Complete KLT-Map Between Gravity and Gauge Theories," *JHEP*, vol. 1208, p. 101, 2012.

[59] T. Sondergaard, "Perturbative Gravity and Gauge Theory Relations: A Review," *Adv.High Energy Phys.*, vol. 2012, p. 726030, 2012.

[60] V. Smirnov, *Feynman Integral Calculus*. Springer, 2006.

[61] Z. Bern, A. De Freitas, L. J. Dixon, and H. Wong, "Supersymmetric regularization, two loop QCD amplitudes and coupling shifts," *Phys.Rev.*, vol. D66, p. 085002, 2002.

[62] R. K. Ellis, W. Giele, and Z. Kunszt, "A Numerical Unitarity Formalism for Evaluating One-Loop Amplitudes," *JHEP*, vol. 0803, p. 003, 2008.

[63] J. Gluza, K. Kajda, and D. A. Kosower, "Towards a Basis for Planar Two-Loop Integrals," *Phys.Rev.*, vol. D83, p. 045012, 2011.

[64] Y. Zhang, "Integration-by-parts identities from the viewpoint of differential geometry," 2014.

[65] S. Laporta, "High precision calculation of multiloop Feynman integrals by difference equations," *Int.J.Mod.Phys.*, vol. A15, pp. 5087–5159, 2000.

[66] A. Smirnov, "Algorithm FIRE – Feynman Integral REduction," *JHEP*, vol. 0810, p. 107, 2008.

[67] A. V. Smirnov, "FIRE5: a C++ implementation of Feynman Integral REduction," 2014.

[68] A. von Manteuffel and C. Studerus, "Reduze 2 - Distributed Feynman Integral Reduction," 2012.

[69] T. Gehrmann and E. Remiddi, "Differential equations for two loop four point functions," *Nucl.Phys.*, vol. B580, pp. 485–518, 2000.

[70] T. Gehrmann and E. Remiddi, "Using differential equations to compute two loop box integrals," *Nucl.Phys.Proc.Suppl.*, vol. 89, pp. 251–255, 2000.

[71] C. G. Papadopoulos, "Simplified differential equations approach for Master Integrals," *JHEP*, vol. 1407, p. 088, 2014.

[72] J. M. Henn, "Multiloop integrals in dimensional regularization made simple," *Phys.Rev.Lett.*, vol. 110, no. 25, p. 251601, 2013.

[73] A. B. Goncharov, M. Spradlin, C. Vergu, and A. Volovich, "Classical Polylogarithms for Amplitudes and Wilson Loops," *Phys.Rev.Lett.*, vol. 105, p. 151605, 2010.

[74] A. B. Goncharov, "Multiple polylogarithms, cyclotomy and modular complexes," *ArXiv e-prints*, May 2011.

[75] S. Laporta and E. Remiddi, "Analytic treatment of the two loop equal mass sunrise graph," *Nucl.Phys.*, vol. B704, pp. 349–386, 2005.

[76] C. Duhr, "Hopf algebras, coproducts and symbols: an application to Higgs boson amplitudes," *JHEP*, vol. 1208, p. 043, 2012.

[77] R. E. Cutkosky, "Singularities and discontinuities of Feynman amplitudes," *J. Math. Phys.*, vol. 1, p. 249, 1960.

[78] Z. Bern, L. J. Dixon, D. C. Dunbar, and D. A. Kosower, "One loop n point gauge theory amplitudes, unitarity and collinear limits," *Nucl.Phys.*, vol. B425, pp. 217–260, 1994.

[79] W. T. Giele, Z. Kunszt, and K. Melnikov, "Full one-loop amplitudes from tree amplitudes," *JHEP*, vol. 0804, p. 049, 2008.

[80] P. Mastrolia, G. Ossola, T. Reiter, and F. Tramontano, "Scattering AMplitudes from Unitarity-based Reduction Algorithm at the Integrand-level," *JHEP*, vol. 1008, p. 080, 2010.

[81] G. Bevilacqua, M. Czakon, M. Garzelli, A. van Hameren, A. Kardos, *et al.*, "HELAC-NLO," *Comput.Phys.Commun.*, vol. 184, pp. 986–997, 2013.

[82] R. K. Ellis, W. Giele, Z. Kunszt, K. Melnikov, and G. Zanderighi, "One-loop amplitudes for W^+ 3 jet production in hadron collisions," *JHEP*, vol. 0901, p. 012, 2009.

[83] S. Badger, B. Biedermann, P. Uwer, and V. Yundin, "Numerical evaluation of virtual corrections to multi-jet production in massless QCD," *Comput.Phys.Commun.*, vol. 184, pp. 1981–1998, 2013.

[84] G. Ossola, C. G. Papadopoulos, and R. Pittau, "CutTools: A Program implementing the OPP reduction method to compute one-loop amplitudes," *JHEP*, vol. 0803, p. 042, 2008.

[85] G. Cullen, H. van Deurzen, N. Greiner, G. Heinrich, G. Luisoni, *et al.*, "GoSam-2.0: a tool for automated one-loop calculations within the Standard Model and beyond," 2014.

[86] P. Mastrolia, E. Mirabella, G. Ossola, and T. Peraro, "Scattering Amplitudes from Multivariate Polynomial Division," *Phys.Lett.*, vol. B718, pp. 173–177, 2012.

[87] P. Mastrolia, E. Mirabella, G. Ossola, and T. Peraro, "Integrand-Reduction for Two-Loop Scattering Amplitudes through Multivariate Polynomial Division," *Phys.Rev.*, vol. D87, no. 8, p. 085026, 2013.

[88] P. Mastrolia, E. Mirabella, G. Ossola, and T. Peraro, "Multiloop Integrand Reduction for Dimensionally Regulated Amplitudes," *Phys.Lett.*, vol. B727, pp. 532–535, 2013.

[89] R. H. Kleiss, I. Malamos, C. G. Papadopoulos, and R. Verheyen, "Counting to One: Reducibility of One- and Two-Loop Amplitudes at the Integrand Level," *JHEP*, vol. 1212, p. 038, 2012.

[90] B. Feng and R. Huang, "The classification of two-loop integrand basis in pure four-dimension," *JHEP*, vol. 1302, p. 117, 2013.

[91] H. Johansson, D. A. Kosower, and K. J. Larsen, "Two-Loop Maximal Unitarity with External Masses," *Phys.Rev.*, vol. D87, p. 025030, 2013.

[92] K. J. Larsen, "Global Poles of the Two-Loop Six-Point N=4 SYM integrand," *Phys.Rev.*, vol. D86, p. 085032, 2012.

[93] S. Caron-Huot and K. J. Larsen, "Uniqueness of two-loop master contours," *JHEP*, vol. 1210, p. 026, 2012.

[94] M. Sogaard, "Global Residues and Two-Loop Hepta-Cuts," *JHEP*, vol. 1309, p. 116, 2013.

[95] H. Johansson, D. A. Kosower, and K. J. Larsen, "Maximal Unitarity for the Four-Mass Double Box," 2013.

[96] M. Sogaard and Y. Zhang, "Unitarity Cuts of Integrals with Doubled Propagators," 2014.

[97] M. Sogaard and Y. Zhang, "Massive Nonplanar Two-Loop Maximal Unitarity," 2014.

[98] Z. Bern, A. De Freitas, and L. J. Dixon, "Two loop helicity amplitudes for gluon-gluon scattering in QCD and supersymmetric Yang-Mills theory," *JHEP*, vol. 0203, p. 018, 2002.

[99] Z. Bern, L. J. Dixon, and V. A. Smirnov, "Iteration of planar amplitudes in maximally supersymmetric Yang-Mills theory at three loops and beyond," *Phys.Rev.*, vol. D72, p. 085001, 2005.

[100] D. R. Grayson and M. E. Stillman, *Macaulay2, a software system for research in algebraic geometry.* http://www.math.uiuc.edu/Macaulay2/.

[101] Z. Bern, L. J. Dixon, and D. A. Kosower, "Bootstrapping multi-parton loop amplitudes in QCD," *Phys.Rev.*, vol. D73, p. 065013, 2006.

[102] G. Ossola, C. G. Papadopoulos, and R. Pittau, "On the Rational Terms of the one-loop amplitudes," *JHEP*, vol. 0805, p. 004, 2008.

[103] C. Cheung and D. O'Connell, "Amplitudes and Spinor-Helicity in Six Dimensions," *JHEP*, vol. 0907, p. 075, 2009.

[104] Z. Bern, J. J. Carrasco, T. Dennen, Y.-t. Huang, and H. Ita, "Generalized Unitarity and Six-Dimensional Helicity," *Phys.Rev.*, vol. D83, p. 085022, 2011.

[105] S. Davies, "One-Loop QCD and Higgs to Partons Processes Using Six-Dimensional Helicity and Generalized Unitarity," *Phys.Rev.*, vol. D84, p. 094016, 2011.

[106] Z. Bern, L. J. Dixon, and D. Kosower, "A Two loop four gluon helicity amplitude in QCD," *JHEP*, vol. 0001, p. 027, 2000.

[107] S. Catani, "The Singular behavior of QCD amplitudes at two loop order," *Phys.Lett.*, vol. B427, pp. 161–171, 1998.

[108] Z. Bern, L. J. Dixon, D. C. Dunbar, and D. A. Kosower, "One loop selfdual and N=4 superYang-Mills," *Phys.Lett.*, vol. B394, pp. 105–115, 1997.

[109] Z. Bern, M. Czakon, D. Kosower, R. Roiban, and V. Smirnov, "Two-loop iteration of five-point N=4 super-Yang-Mills amplitudes," *Phys.Rev.Lett.*, vol. 97, p. 181601, 2006.

[110] J. J. Carrasco and H. Johansson, "Five-Point Amplitudes in N=4 Super-Yang-Mills Theory and N=8 Supergravity," *Phys.Rev.*, vol. D85, p. 025006, 2012.

[111] Z. Bern, S. Davies, T. Dennen, Y.-t. Huang, and J. Nohle, "Color-Kinematics Duality for Pure Yang-Mills and Gravity at One and Two Loops," 2013.

[112] W. B. Kilgore, "One-loop Integral Coefficients from Generalized Unitarity," 2007.

[113] S. Badger, "Generalised Unitarity At One-Loop With Massive Fermions," *Nucl.Phys.Proc.Suppl.*, vol. 183, pp. 220–225, 2008.

[114] R. Huang and Y. Zhang, "On Genera of Curves from High-loop Generalized Unitarity Cuts," *JHEP*, vol. 1304, p. 080, 2013.

[115] J. D. Hauenstein, R. Huang, D. Mehta, and Y. Zhang, "Global Structure of Curves from Generalized Unitarity Cut of Three-loop Diagrams," 2014.

[116] S. Caron-Huot and D. O'Connell, "Spinor Helicity and Dual Conformal Symmetry in Ten Dimensions," *JHEP*, vol. 1108, p. 014, 2011.

[117] R. A. Fazio, P. Mastrolia, E. Mirabella, and W. J. Torres Bobadilla, "On the Four-Dimensional Formulation of Dimensionally Regulated Amplitudes," 2014.

[118] Z. Bern and A. Morgan, "Massive loop amplitudes from unitarity," *Nucl.Phys.*, vol. B467, pp. 479–509, 1996.

[119] R. Huang, D. Kosower, M. Sogaard, and Y. Zhang, "To appear," 2015.

[120] D. Maitre and P. Mastrolia, "S@M, a Mathematica Implementation of the Spinor-Helicity Formalism," *Comput.Phys.Commun.*, vol. 179, pp. 501–574, 2008.

[121] R. H. Boels and D. O'Connell, "Simple superamplitudes in higher dimensions," *JHEP*, vol. 1206, p. 163, 2012.

[122] N. Craig, H. Elvang, M. Kiermaier, and T. Slatyer, "Massive amplitudes on the Coulomb branch of N=4 SYM," *JHEP*, vol. 1112, p. 097, 2011.

[123] R. Penrose and M. MacCallum, "Twistor theory: An approach to the quantisation of fields and space-time," *Physics Reports*, vol. 6, no. 4, pp. 241 – 315, 1973.

[124] C. Anastasiou, *Two loop integrals and QCD scattering*. PhD thesis, Durham University, http://etheses.dur.ac.uk/4385/, 2001.

[125] T. Huber and D. Maitre, "HypExp: A Mathematica package for expanding hypergeometric functions around integer-valued parameters," *Comput.Phys.Commun.*, vol. 175, pp. 122–144, 2006.